NOTTINGHAM TRENT UNIVERSITY

BUILDING ENERGY INVESTIGATION FRAMEWORK

Submitted by Ahmad Said Galadanci to Nottingham Trent University in partial fulfilment of the degree of Doctor of Philosophy in Civil Engineering

2020

Copyright Statement

Dedication

To my loving parents ***Said Nasir Zubair*** and ***Prof. Hadiza S Galadanci,*** thank you for the support**.** To my loving, supporting and treasured wife, Nanono Asmau Sabo, thank you for being patient and supportive. My daughter Khadijah Ahmad and my siblings Maamun, Nasir (Don), Halimah (pes pes), thank you for being there throughout my journey.

Acknowledgement

Alhamdullilah, Alhamdulillah. All the praise be to Allah the Almighty God who has given me health, sanity, ability, patience and knowledge for completing the thesis.

I want to express my gratitude to my supervisors Professor Anton Ianakiev and Dr Rolands Kromanis for the support, guidance and invaluable advice provided throughout this journey. The motivation and the trust of Anton to take on this journey has been invaluable. The constructive criticism from Dr Rolands Kromanis have been vital for my study.

I could not have done this without the support of my friends and colleagues, Dr Misbahu Sharfuddeen, Dr Farouk Umar, Giorgio, Nader, Arijit, Sherna, George, Brendan, Dami, Abdulhakim, Said, Florence and others that I have not mentioned. I would also like to say thank you to the staff of Nottingham Trent University: Judith Kipling, James cooper and all Civil Engineering staffs for making my journey easier.

The research would not have been possible without Nottingham Trent University's Estate department, especially Joe Fallon and Scott Brooks. Furthermore, I want to express my gratitude also to the entire staff of Nottingham energy partnership and NTU Sports.

I would also like to acknowledge the care and encouragement from my guardians in the United Kingdom, C.Eng Khalifa Saeed Galadanci and Yursa Khadija Mahmoud.

Finally, to my family for their support, love and encouragement

This study was funded by Petroleum Technology Development Fund (PTDF), Nigeria and REMOURBAN project that is supported by the EU Horizon 2020 research and innovation programme under grant agreement No 646511

Abstract

Climate change has affected the lives and properties of people in the last decade with high temperature record broken eight times. This has led to a global urgency on the need to reduce carbon emissions and energy consumption. According to the United Nations Global Status Report 2017, buildings and construction together account for 36% of the global energy use and 39% of energy related carbon dioxide emissions. The building and construction industry are aiming to reduce their carbon footprint by carefully designing and constructing energy efficient buildings. However, not all buildings perform as expected or planned as some of these buildings underperform by gaining or losing more heat than needed, thereby the need for building energy assessment. Thermal bridging affects the energy performance of buildings by creating weak points within the building envelope. Researchers have stated that the impact of thermal bridging has not been considered properly. The study introduces a novel framework for investigating building energy performance.

A novel systematic framework which comprises of phases, namely thermography investigation, building energy modelling, thermal bridges characterisation and future prediction for overheating is developed. The framework is capable of assessing the effect of thermal bridges and predicts the future performance of buildings under different weather conditions. A sport changing facility, which was designed as a low energy building, serves as a demonstrator for the application of the framework.

The research contributed a novel framework for the evaluating building energy performance considering effects of thermal bridges and future predictions. Furthermore, the research addresses the risk of overheating in buildings and also the effect of building services on buildings overheating. A systematic review of thermal bridges conducted within the research and a combined classification of thermal bridges. Furthermore, the framework contributed to the monitoring intervention in practice such as the REMOURBAN projects.

Table of Contents

List of figures

List of tables

Chapter 1: Introduction

1.0 Background

Nowadays, society is aware of the urgency for low energy solutions due to the growing cost of energy and the implementation of low carbon policies (Ramallo Gonzalez et al., 2013). According to Kampf (2009), urban settlements consume about 75% of the global energy resource. The author further stressed that the need to understand how to minimise resource consumption in the urban environment as it is widely accepted that the combustion of non-renewable fossil fuels leads to climatic disorders. In the United Kingdom, the domestic sector alone accounts for 30% of the total energy demand, which is responsible for about 27% of carbon emissions (Ramallo Gonzalez et al., 2013). Clarke (2001) stated that about 50 to 75% reduction in the energy consumption of buildings could be achieved with better designs. This reduction would have a significant effect on the reduction of energy bills, contribute extensively to climate change and environmental impacts.

Buildings (old and new) are significant as they play a crucial role in the impact of energy. Government agencies such as the European Directive on Energy Performance of Buildings (EFBD) provide specifications on the energy performance of buildings. Due to impact of buildings on energy, along with rising energy cost, has increased the demand for development and usage of building simulation software, for example, EnergyPlus, Design Builder, TRNSYS and ESP-r (Kampf 2009). In the European Union, legislation requires all member states to reduce carbon dioxide emissions by 20% in 2020. However, in the United Kingdom, the Climate Change Act of 2008 requires the government to reduce the total national emissions of carbon dioxide to a level of 81% below 1990 levels by 2050. Furthermore, the London energy plans to limit further climate change by reducing carbon dioxide emissions from London. The BRE Environmental Assessment Method known as BREEAM, is assisting planners to independently measure and certify the overall potential sustainability of a masterplan proposal during the planning stage of the development control process (Kämpf, 2009).

Projects and interventions such as the REMOURBAN Project (Regeneration Model for Accelerating the Smart Urban Transformation) are created to achieve energy efficiency across different sectors. The REMOURBAN project is divided into three sections namely ,Energy: Low energy districts, Mobility: Sustainable mobility and ICT: integrating infrastructures and society

Low energy districts involve retrofitting, renewable heating and cooling distributed energy generation, monitoring tools for energy efficiency, electricity distribution and advanced building energy management systems.

In recent years, there has been much debate regarding the temperature rising in the future. These have led to researchers pondering about climate leading to the risk of overheating or hothouse effect. Climate change has been associated with extreme weather events in 2018, which have led to thousands of lives lost and damage throughout the world. Extreme weather has had an impact on sustainable development on every continent (World Metrological Organisation, 2018). These events include hurricane Florence and hurricane Michael both in the United States.

In a report by the World Metrological Organisation (WMO), the fourth warmest year on record is stipulated to be 2018. The past four years (2015-2018) are also the four warmest years in which 2018 is the coolest of the four. Furthermore, 20 warmest years were experienced within the past 22years. Record heatwaves around Europe (United Kingdom) and the world (Japan) were experienced in 2018 (McGrath, 2018a). According to the WMO report, in the late spring and summer of 2018, a considerable part of Europe encountered unprecedented heat and drought with temperatures and rainfall well above and below average, respectively.

Moreover, WMO concluded that the World is not on course to meet the climate change target due to a rise of 1°C average global temperature above pre-industrial levels. In the United Kingdom, a study by the Met Office revealed that the heatwave experienced in 2018 was made about 30 times more likely due to emissions from human activities. The odds of a United Kingdom heatwave without global warming in any given year were less than half a percent, and this has risen to 12% due to climate change (McGrath, 2018b) with WMO describing the weather between May and July exceptionally warm and dry. Not just the United Kingdom, Europe experienced the driest and warmest period in record with countries such as Finland had temperatures above 25°C and 30°C for 25 and 8 consecutive days respectively (World Metrological Organisation, 2018). Therefore, overheating risk is becoming higher as temperatures are predicted to increase further. Chattered Institute of Building Services Engineers (CIBSE) described overheating as a widely used term that is not precisely defined or understood. Furthermore, they defined overheating as the time at which

building occupants feel uncomfortably due to high temperature. Moreover, the discomfort felt by the occupants is caused by the indoor environment.

The UKCP18 and UKCP09 are based on a baseline period of 1981-2000 and 1961-1990. However, there is a considerable amount of overlap when comparing the outcomes of UKCP09 and UKCP18. The UK Climate projections 2018 (UKCP18) provides probabilistic projections overland and a set of high resolution spatially coherent future climate projections for the globe and UK at 60km and 12km scale respectively. A summary of observations from the UKCP18 is outlined below

- Greater frequency of hotter drier summers and milder wetter winters across the UK
- Further rises in sea levels around the UK coastline
- By 2070, in the high emission scenario, there is a possibility of an increase in temperature at the range 0.9°C to 5.4°C in summer and 0.7°C to 4.2°C in winter

(Lowe et al., 2018)

Building energy consumption are affected by different factors such as the level of insulation, the airtightness of the building and the heating ventilation and air conditioning units (HVAC). Mayer et al. (2014) stated that with the renewed interest of conserving energy, combined with more stern energy requirement in codes, the construction industry is focused on increased thermal insulation in wall assemblies particularly to reduce thermal bridging.

Thermal Bridging as defined by Building Research Establishment (BRE) is an area of building construction that has significantly higher heat transfer than the surrounding materials. Whale (2016) observed that in a typical newly built building, about 20 – 30% of the heat loss is caused by thermal bridges. Moreover, the author observed that thermal bridges become more significant as homes become better insulated. Mayer et al. (2014) stated that over $5.5 billion in expenditures and about 1% of all energy use represents thermal bridges. Therefore, thermal bridge materialises as a result of heat flowing around insulation and through materials with high thermal conductivity such as fasteners and metal studs (Mayer et al., 2014). Totten et al. (2008) further revealed that thermal bridging contributes to multiple problems, such as an increase in energy usage during heating and cooling periods, and also causes internal surface condensations. Moreover, the author identified that the positioning of doors, windows and window walls, curtain walls, skylights and other fenestration within the wall thickness of a wall or roof element might provide a short circuit of the thermal pathway the manufacturer intended in their design and instead provide a thermal bridge.

Ge & Baba (2015) stated that there are a finite number of studies reporting the effect of direct 2D or 3D modelling of thermal bridges on the energy performance of buildings. Furthermore, Ascione et al. (2012) proposed the use of integrated energy simulation software to examine the effect of thermal bridges on the energy performance of a whole building. Software such as ANSYS Fluent has been used as a numerical prediction tool to evaluate thermal bridging such as in Martin et al. (2011) and Ascione et al. (2012). According to Ascione et al. (2013), multi-dimensional effects and thermal bridges are neglected by building simulation programs as in most cases, and the programs consider one-dimensional heat transfer. The impact of thermal bridges in buildings energy demand is not yet properly calculated, as stated by Martin et al. (2012).

The building industry has strongly been using computer simulation and computational techniques (H. Wang & Zhai, 2016). Targets such as the reduction in energy consumption, improving indoor environmental quality and cutback of environmental impacts can be achieved using simulation-based design and optimisation techniques (H. Wang & Zhai, 2016). There have been many ways of solving heat transfer of construction elements in buildings such as; Finite Element and Finite Difference Method, Lumped Parameter Model, Conduction Transfer Function, Thermal Response Factor and Radiant Time Series Method

Numerical methods such as finite element and finite difference methods are used to solve partial differential equations that govern the conduction heat transfer through the construction elements of buildings (Rodriguez Jara et al., 2016). According to Ascione et al. (2012), ANSYS a finite element analysis software is a robust instrument used for the numerical prediction of kinetic, thermal and hygrometric fields. Rodriguez Jara et al. (2016) stated that the response factor and transfer function method are widely used in building simulation programs such as EnergyPlus and TRNSYS. Wang and Zhai (2016) also stated that DesignBuilder, Open-studio and EQuest are examples of third party modules and interfaces which make simulation programs such as EnergyPlus easier tools for engineering applications.

Building structure elements that consist of several layers of different materials have been known to have the components of both thermal capacitance and resistance; therefore, the thermal performance of buildings can be modelled using the reduced-order lumped parameter model (H. Wang & Zhai, 2016). Lumped parameter modelling also is known as “analogue circuit” models due to their connotation with electric circuits has the capability of

hourly simulation of a whole building energy consumption, but the computational intensity is much less (H. Wang & Zhai, 2016). With lumped parameter models, elements consisting of *n* layers of materials can be combined to form two lumped thermal resistances and one thermal capacity (H. Wang & Zhai, 2016). Underwood (2014) observed that the Lumped parameter modelling method to building dynamic thermal response is motivated to find simpler and hence computationally less expensive methods for the analysis of building thermal energy response.

Third-party module DesignBuilder is acknowledged as a comprehensive interface to EnergyPlus building simulator and is widely used by simulation experts and beginners. EnergyPlus has been the subject of extensive validation through an ongoing United States Department of Energy development and support program

1.1 Problem Statement

In recent years, there has been a worldwide discussion on the effect of fossil fuels and climate change on the world. This has brought about the need to have different sources of sustainable energy. Buildings account for 1/3rd of the final global energy consumption and similar levels of CO_2 emissions: hence the justification of building energy performance having increasing importance worldwide (Borgstein et al., 2016). Therefore, the need to create, design and refurbish buildings to energy-efficient standard arises. Buildings are designed to provide maximum comfort, even during extreme events such as heatwaves. Recently, there has been a global rise in temperatures with the average global temperature between 2006 and 2015 being 0.86°C while 2018 had 0.99±0.13°C above the pre-industrial baseline (1850-1900) (World Metrological Organisation, 2018).

Different studies have been done on improving the building energy performance, but only a few studies have been done on the effect of thermal bridges overall building (Ge & Baba, 2015). The impact of thermal bridges in building energy demand is not properly calculated or neglected, as stated by Martin et al. (2011). Furthermore, Martin et al. (2012) revealed that the correct implementation of thermal bridges in buildings' energy demand models means a major effort by the designer, which is not often rewarded. In a recent study by Kuusk et al. (2017), it was revealed that the energy losses as a result of thermal bridges are not taken into account sufficiently as a simplified approach or use default values in energy calculation software are adopted. Correctly implementing the effect of thermal bridges would reduce the performance gap between predicted and measured performance as De Wilde (2014) mentioned that the present gap is too wide to be acceptable.

With the trend of global warming, studies on overheating have been done over the years. These studies (Din & Brotas, 2017; Fokaides et al., 2016; Gupta & Gregg, 2018; S. Porritt et al., 2011; S. M. Porritt et al., 2012; Stazi et al., 2017) assessed the risks and mitigations of overheating in buildings under different climates. However, not all the studies consider the effect of unwanted heat gains and losses on indoor climate, which may give rise to overheating.

This study proposes an *Energy Investigation Framework* that will consider the effect of thermal bridges in overall building, thereby aiming to reduce the performance gap between the predicted and the measured performance. Furthermore, the framework would provide a platform to assess and predict building performance (such as the risk of overheating) in the future.

1.2 Aims and Objective

1.2.1 Research Aim

The research aims to create a framework for investigating the building energy performance with a focus on the effect of unwanted heat gains and losses (thermal bridges) and the risk of overheating in modern low energy buildings.

1.2.2 Objectives

The goal of this research is to use finite element analysis as a tool to investigate the thermal properties and responses of existing structures. Existing buildings provided by the Nottingham Trent University Estate Department would be investigated. Data acquired from the existing structures would then be used to verify the model and investigate the energy performance. Listed are the objective required to achieve the set aim;

- Systematic literature review on thermal bridges
- Create a framework for the overall investigation of energy performance in buildings
- Modelling and investigating the existing building structures provided using building simulation programs (DesignBuilder)
- Investigating the effect of thermal bridging on the existing structure
- Modelling of thermal bridges within the building using Finite Element Analysis software package
- Assess the overall performance and overheating risks for current and future weather in existing buildings

To achieve the aim of the research. Certain questions must be answered. These are;

- How can the energy performance of a building be fully investigated?
- With the rise in global warming awareness, how can the risk of overheating be assessed in low energy buildings?
- What is the energy performance of a low energy building?
- What is the overall effect of thermal bridging on the energy performance of buildings?

1.3 Significance of the Study

This research proposes a significant effect on the environment. The significances include;

- Providing more literature on thermal bridges effects on the energy performance of buildings as suggested by Ge and Baba (2015)
- Creating a framework for the investigation of energy and the effects of thermal bridges on the energy performance of buildings
- Improving the energy performance and consumption of building will have a significant effect in reducing the greenhouse effect or global warming
- Will lead to providing sustainable and cost-effective energy consumption buildings

1.4 Thesis Structure

This section outlines the structure of the thesis: Energy investigation framework, understanding our building from an energy perspective. The thesis is structured in the form of chapters. **Chapter 1: Introduction** is an introductory chapter that portrays the rationale or motive behind the study. It also reports the identified problem that the research aims to address together with the research methods, process, aims and objectives of the study.

Chapter 2: The Literature review describes the heat transfer mechanisms and energy analysis concerning buildings. It introduces the basic theoretical equation and describes the process of analysing heat transfer and energy in buildings. Furthermore, an extensive review of the software used in this study is discussed in the chapter. **Chapter 3: Thermal Bridges** is an extensive review of thermal bridges that discusses the definition, classification, analysis, possible solutions and the effect of thermal bridges on the energy consumption of buildings.

Chapter 4: Energy Investigation Framework deals with the research methodology used to address the identified problems in Section 1.1. This chapter discusses the energy investigation framework, together with the relevant methods and how these methods are

used concurrently to achieve the research aims and objectives. **Chapter 5: Case-study Clifton Clubhouse** in this chapter, the energy investigation framework is applied to a case-study: Clifton Clubhouse. The effect of thermal bridges, risk of overheating in the present and future weather conditions and energy performance of the clubhouse are evaluated in this chapter.

Chapter 6: Discussion is devoted to the effectiveness of the energy investigation framework and the result of its application to the case study. The implications of the results are discussed in this chapter. **Chapter 7: Conclusion and Contribution to Knowledge** is concerned primarily on the achievements, recommendations, and how the research contributes to knowledge both in the practice and research environment. The aims and objectives of the thesis are recalled and how they were achieved are discussed.

1.5 Contribution to knowledge

The contribution to the knowledge of this study is introduced in this section. Detailed explanations of the contribution to knowledge are provided in Chapter 7: Section 7.4. This study has contributed to both practice and research and is outlined below.

- **The energy investigation framework**: This framework provides the energy assessor with a platform for in-depth assessment of building energy investigation. The framework is a systematic combination of relevant methods used to assess building energy performance. Using the framework, the building performance, the effect of thermal bridges and the risk of overheating in the present and future climate can be evaluated.
- **The risk of overheating in building**: Recent weather events have raised the awareness of the overheating in buildings. The assessment of the risk of overheating is not new and is affected by different factors such as unwanted heat gains and losses. With the energy investigation framework, the risk of overheating is assessed, and the study aims at stressing the need for accurate models in other to assess the overheating risks in buildings.
- **Effect of thermal bridges**: Thermal bridging and their effects are known in the industry, but they are underestimated. A systematic review of the methods and effects of thermal bridges was achieved. Furthermore, the effect of thermal bridges using a framework (Energy investigation framework) in conjunction with other building effects was analysed.

Chapter 2: Literature review

2.1 Introduction

There has been a worldwide focus on reducing greenhouse gas emissions in which buildings play a major role. Understanding the concepts of heat transfer mechanism and energy analysis in buildings is the backbone to achieving set targets and goals such as that of the Climate Change Act and EU 2030 energy and climate goals. This chapter, therefore, aims to summarise the concept of heat transfer in application to buildings and how energy analysis in buildings. The purpose of the chapter is to give a summary of the advances and current research in the field of energy analysis in buildings.

2.2 Heat transfer

Heat is defined as thermal energy that is transferred between two systems because of the temperature difference. From the conservation of energy, which states that energy can neither be created nor destroyed during a process. Therefore, energy is transformed from one form to the other, but the total energy remains the same. Heat is known (from the second law of thermodynamics) to move naturally from a high-temperature body to a low-temperature body. Due to this, heat transfer is divided into three mechanisms, namely conduction, convection, and radiation.

A building envelope serves as an intermediary between the inner and outer environment. The building envelope also provides a passive function that imposes a bias on ambient temperature through the provision of heating or cooling. Heat and mass transfer processes that would take place in a building include

- Conduction
- Solar radiation
- Infiltration
- Heat and moisture dissipation
- Heating or cooling and humidification or dehumidification provided by the Heating Ventilation and Air Conditioning (HVAC) system

2.3 Main Modes of Heat Transfer

Heat is transferred through building elements such as walls, floors, and roofs, through a number of mechanisms within that element. Heat transfer is a vector quantity and occurs through conduction, convection, and radiation (Asadi et al., 2018). In this section, the three modes/mechanisms of heat transfer, namely convection; radiation and conduction, are reviewed concerning buildings.

2.3.1 Conduction

Conduction is a process where energy is transferred from one body to another. McMullan (2018) defined conduction as the transfer of heat energy through a material without the molecules of the material changing their basic positions. Asadi et al. (2018) mentioned that in solids, the heat transfer due to conduction is a mixture of energy transport and molecular vibrations by the free electrons. Conduction is expressed mathematically using Fourier law of heat conduction;

$$q_x = -kA\frac{dT}{dx} \qquad \textit{Equation 2-1}$$

Where k is the thermal conductivity expressed as W/mK, A is the area of heat transfer expressed as m^2, and $\frac{dT}{dx}$ is the temperature gradient.

Fourier's law of heat conduction states that the heat flow by conduction in any direction is proportional to the temperature gradient and area perpendicular to the flow direction and is in the direction of the negative gradient.

Conduction of a material is defined by thermal conductivity. Materials conduct heat at different rates due to the difference in thermal conductivity with metals having a high thermal conductivity. Thereby metals are considered as the best conductors of heat (McMullan, 2018). The rate of speed at which conduction occurs through solids, liquids, and gases varies.

2.3.2 Convection

Convection comes from two Latin verbs convector-are and conveho-vehere, which means to bring together or to carry into one place. Therefore, convection is defined as the process of heat transfer effected by the flow of fluids. This is generally the prevalent form of heat transfer in liquids and gases. Heat transfer due to convection can be expressed using Newton's law of cooling;

$$q = hA\,(T_s - T_\infty)$$ *Equation 2-2*

Where h is the convective heat transfer coefficient expressed as W/m^2K, A is the heat transfer area expressed as m^2, T_s is the surface temperature and T_∞ is the fluid temperature.

Convection is not only defined by the heat but also affected by the fluid flow. In this case, the Navier stokes equation, which is composed, of conservation of mass and momentum are required. Energy transferred by convection is through combined molecular diffusion and bulk flow. Heat flow due to convection relies upon the property of the medium (fluid). However, it is autonomous on the properties of the material of the surface (Kothandaraman, 2006).

The convective heat transfer coefficient denoted as (h) is influenced by factors such as the fluid properties (density, viscosity, specific heat, and conductivity), the flow velocity and the surface geometry. From the factors mentioned, the convective heat transfer coefficient varies from point to point as the properties mentioned above vary temperature and location.

Convection can be divided into two modes; forced and free or natural convection. Forced convection is caused when the fluid flow is induced by external means such as fans and pumps while free or natural convection is caused when the flow is as a result of buoyant forces induced by the difference in temperature in the fluid body. In buildings the two modes of convection are present.

2.3.3 Radiation

Radiation is the energy emitted irrespective of temperature by matter in the form of electromagnetic waves which is within a wave-length of 0.1 to 10µm. Radiative heat transfer occurs when the material surface is in visual contact for direct radiation transfer with no medium required (Kothandaraman, 2006). From Stefan-Boltzmann law,

"*Heat radiated is proportional to the fourth power of the absolute temperature of the surface and heat transfer rate between surfaces"*,

Hence radiation is expressed mathematically as

$$q = A\varepsilon\sigma\,({T^4}_s - {T^4}_{surr})$$ *Equation 2-3*

Where A is the area of heat transfer expressed as m^2, ε is the emissivity, σ is the Stefan-Boltzmann constant (which has a value of $5.67\,x\,10^{-8}W/m^2K^4$), T_s is the absolute temperature of the surface and T_{surr} is the absolute temperature of the surroundings.

2.4 Thermal Conductivity, Resistance and Transmittance

Thermal conductivity (*K-value*) is defined as the time rate of steady-state heat flow through a unit area of 1m thick homogeneous material in a direction perpendicular to the isothermal planes, induced by a unit temperature difference across a sample (Al-Homoud, 2005). constant of proportionality in Fourier's equation represents the coefficient of thermal conductivity (Kothandaraman, 2006) and the unit of thermal conductivity is W/mK. As mentioned by Asadi et al (2018), the energy consumption of buildings relies on the values of thermal conductivity. Furthermore, materials with low or moderate thermal conductivity (known as insulation) help to reduce the energy usage in buildings. A very important factor that affects thermal conductivity is temperature. For insulators, the thermal conductivity increases with temperature due to an increase in thermal atomic activities while in gases it also increases with temperature due to increases in the random activity of atoms and molecules (Kothandaraman, 2006).

Thermal resistance (*R-value*) is defined as a measure of the resistance of heat flow due to suppressing conduction, convection, and radiation. The thermal resistance of a material is affected by the material conductivity, material thickness and density (Al-Homoud, 2005). Mathematically, the thermal resistance can be expressed as a reciprocal of thermal conductivity and therefore can be regarded as an alternative index of conduction. The unit of thermal resistance is mK/W (McMullan, 2018).

Thermal transmittance (*U-value*) also known as the overall heat transfer coefficient is defined as the rate of heat flow through a unit surface area of a component with a unit temperature difference between the surfaces of the two sides of the component. McMullan (2018) added that the heat transfer is by all mechanisms under standard conditions through a particular section of the construction. U-values are used to predict the quantity of plane element heat loss through the external elements of a building (Marshall et al., 2017). The thermal transmittance is measured as heat flow in watts through 1 m^2 of a structure when there is a temperature difference across the structure of 1 degree ($K\ or\ °C$). Thermal transmittance is therefore the reciprocal of the sum of the resistances of all layers composing that component. The key to reducing the energy consumption of buildings is to look at how the heat is lost from the building; therefore, U-Values play a key a role in energy consumptions. Furthermore, CIBSE (2006) described the U-value as a principal factor in the determination of steady-state heat losses/gains. BS EN ISO 6946 (2007) and BRE 443 (Anderson, 2006) provide guidance on thermal resistance and transmittance calculation methods.

The thermal conductivity of a material denoted as *K* is used to define a material in a Finite Element Analysis model and also in the application of Fourier's Law. The heat flux denoted as q", of a material, defined as the rate of heat transfer per unit area can be expressed mathematically as

$$q^{"} = k\frac{(T_1 - T_2)}{L} \qquad \textit{Equation 2-4}$$

For Heat flow $q^{"}$, Equation 2-4 is multiplied by the cross-sectional area (A)

$$q^{"} = q^{"}A = kA\frac{(T_1 - T_2)}{L} \qquad \textit{Equation 2-5}$$

For a building system, were heat is transmitted only through conduction and characterized by an isotropic homogeneous material; the thermal resistance of the material R is given by

$$R = \frac{L}{K} \qquad \textit{Equation 2-6}$$

Therefore, the thermal transmittance U is given by

$$U = \frac{1}{R} \qquad \textit{Equation 2-7}$$

Where $q^{"}$is the heat flow, k is the thermal conductivity (W/mK) , $T_1 - T_2$ is the temperature difference between the external and internal environment $(°C)$, L is the thickness of the layer (m), A is the cross-sectional area (m^2), R is the thermal resistivity (mK/W) and U is the thermal transmittance (W/m^2K) .

In some cases, the thermal resistance of a material (in this case a non-homogeneous material) may not be proportional to the thickness and Equation 2-6 does not apply. This occurs in the case of materials of low density where the radiant heat transfer is significant (CIBSE, 2006). Furthermore, CIBSE (2006) revealed manufacturers define the thermal properties of non-homogeneous materials (insulating materials) by means of thermal resistance. However, it should be noted that the value of thermal resistivity applies to a particular thickness of the material and hence cannot be extrapolated for other thicknesses.

2.5 Building heating model

Buildings lose heat primarily by two mechanisms- conduction through the building envelope and convective loss due to ventilation (Green et al., 2015). According to the traditional heat transfer model, the total heat demand in a room is given by the relationship between the index temperature T_i , ambient temperature T_e, heat loss through conduction $\sum AU$ through the building fabric and ventilation heat loss V as shown in Equation 2-8

$$Q = (T_i - T_e)\left(V + \sum AU\right) \qquad \textit{Equation 2-8}$$

Where $(V + \sum AU)$ is the known as the heat loss factor or loss coefficient and $(T_i - T_e)$ is the temperature difference between the indoor and outdoor environments.

In a steady-state analysis, the room index temperature T_i acts as the indicator that influences the heat loss to ambient temperature T_e by conduction and ventilation, and temperature at which heat from other sources and heating appliances are delivered.

The CIBSE guide A, the entire building is defined by a coefficient of transmission heat loss denoted as H_t, which is given as

$$H_t = \sum(AU) + \sum(L\Psi) \qquad \textit{Equation 2-9}$$

Where H_t is the coefficient of transmission heat loss , $\sum(AU)$ is sum over all the components of the building of the product of the area of each component and its U-value and $\sum(L\Psi)$ is the sum over all thermal bridges and the product of the length of each thermal bridge and its linear thermal transmittance (discussed in detail in chapter 3).

According to Chatterton 2008, the heat loss in buildings is caused by the convection and radiation mechanisms from external part of the building and by outdoor air infiltration. As a result of the heating equipment is sized based on the steady state heat flow through the building envelope, together with estimates of the structure's thermal storages capacity, gains from the occupants, lights, heating systems and machines. Therefore, the steady-state heat loss through the building fabric is given by

$$Q = \sum(UA)\,(T_{ei} - T_{ao}) \qquad \textit{Equation 2-10}$$

Where:$\sum(UA)$ is the sum of the products of the area and thermal transmittance of each room surface

The European EN ISO 13790 standard defines the building energy demand which is given in Equation 2-11 below.

$$Q_{HEATING} = (Q_{H.trans} + Q_{H.vent}) - (Q_{H.int} + Q_{H.sol}).\eta_{H.gn}$$

Equation 2-11

$$Q_{trans} = H_D.(T_{int} - T_{ext}).\theta$$

For heat loss as a result of ventilation, this is caused by warm air being replaced by a colder air which must be heated. Therefore, the rate of heat loss due to ventilation or infiltration can be expressed as

$$P_v = \frac{C_v N V \Delta t}{3600}$$

Equation 2-12

Where P_v is the rate of ventilation heat loss, C_v is the volumetric specific heat capacity of air, N is the air infiltration rate for the room in air changes per hour, V is the volume of the room and Δt is the difference in temperature between the indoor and outdoor environment.

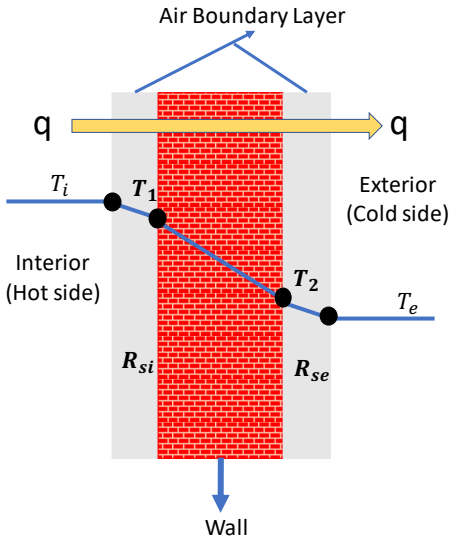

Figure 2-1: Heat transfer through walls

From Figure 2-1, the total resistance through the wall is given by

$$R_t = (1/h_{si}) + \sum(L/k) + R_a + 1/h_{so} = \frac{1}{U} \quad m^2K/W$$

Equation 2-13

The reciprocal of the surface conductance h_{si} and h_{so} on the internal and external surfaces is given by

$$R_{si} = 1/h_{si} \text{ And } R_{so} = 1/h_{so}$$

Equation 2-14

From which the U-value (thermal transmittance) for the composite structure which includes surface film resistance is calculated. Therefore, the intensity of heat flow (heat flux) is given by

$$q = U.(t_i - t_o) W/m^2 \quad \textit{Equation 2-15}$$

Therefore, Equation 2-15 can be written as

$$q = \frac{dt}{R_t} W/m^2 \quad \textit{Equation 2-16}$$

Note: if the indoor and outdoor temperature difference dt is steady, the heat flux *I* will be steady, therefore

$$dt \propto R_t \text{ and } \frac{dt_1}{R_1} = \frac{dt_2}{R_2} \quad \textit{Equation 2-17}$$

This, therefore, allows for the determination of face and interface temperatures in a composite structure at steady temperatures. The conductive heat flow through the composite structure may be determined from:

$$Q_s = U.A.(t_i - t_e)\ W \quad \textit{Equation 2-18}$$

Considering the conductive heat flow path through a composite structure having two structural elements and an air cavity as shown in Figure 2-1: Heat transfer through walls above,

$$\frac{(t_i - t_1)}{(R_{si} - R_1)} = \frac{(t_i - t_e)}{R_t} \quad \textit{Equation 2-19}$$

From which t_i can be determined. Similarly

$$\frac{(t_i - t_2)}{(R_{si} - R_1)} = \frac{(t_i - t_e)}{R_t} \quad \textit{Equation 2-20}$$

From which t_2 can also be calculated and so on

For a more accurate heat loss, surface conductance provides a more accurate methodology, Heat surface conductance denoted as h_s in the surface film combines the coefficients of heat transfer for convection and radiation and thus

$$h_s = eh_r + h_c\ W/m^2K \quad \textit{Equation 2-21}$$

By separating the components of convection and radiation, heat flux equation becomes

$$q = eh_r(t_r - t_s) + h_c(t_{ai} - t_s)\, W/m^2 \qquad \textit{Equation 2-22}$$

From the building heating model given in Equation 2-8, heat loss from buildings are grouped into fabric heat loss; which is the transfer of heat through the external shell of the building and ventilation heat loss; which is the transfer of heat through intentional and unintentional changes of air in the building. Factors that affect the rate at which heat is lost from a building are: the insulation of the building shell, exposed area of the building shell, temperature difference between the inside and the outside environment, air change rate, exposure to external climate, the efficiency of the services in the building and pattern of use

Buildings do not only lose heat but also gain as well. Buildings heat gain provide energy savings and can be grouped into two namely, solar heat gains from the sun and casual heat gains from occupants and equipment. The total energy in a building can, therefore, be expressed as shown in Equation 2-23 below.

$$Heat\ energy\ losses = heat\ energy\ gains\ \pm energy\ used \qquad \textit{Equation 2-23}$$

Furthermore, Harish and Kumar (2016) revealed that the net energy required as input to maintain the air temperature at desired comfort levels in building space can be written mathematically as

$$Q_{building\ space\ load} = Q_{loss} - Q_{gain} \qquad \textit{Equation 2-24}$$

There are two main analysis types that can be used in the building heating models, these are steady-state and transient analysis. Steady-state analysis can be defined as an analysis in which temperature and heat flow rates are independent of time. Martin et al 2011 observed that the inertia of the building envelope is important in the building energy demand, therefore models using only steady-state calculations are deemed insufficient and obsolete. In this case, transient analysis is considered due to its approach of considering daily temperature changes, the ability to control the HVAC system, natural ventilation and also utilization of solar energy gains (Martin et al., 2011).

Heat is lost through a solid floor in contact with the ground through edge loss and ground loss. Edge loss is known to be more significant and therefore rooms having ground floors with four exposed edges have a higher heat loss than rooms with floors having fewer exposed edges. The thermal transmittance of a solid floor in contact with the ground is given by

$$U = \frac{(2k_e \,.\, B)}{(0.5b \,.\, \pi) artanh\left(\frac{0.5b}{(0.5b + 0.5w)}\right)} \; W/m^2K \qquad \textit{Equation 2-25}$$

Where b is breath of the floor, w thickness of the surrounding wall and k_e is the thermal conductivity of the earth

The thermal transmittance of the composite structure can be adjusted if another material is added and it is given by Equation 2-26

$$U_n = \frac{1}{\left((1/U) + R_i\right)} \; W/m^2K \qquad \textit{Equation 2-26}$$

Where R_i is the thermal transmittance of the added material

2.6 Thermal Insulation

Thermal insulation as defined by Al-Homoud (2005) is a material or a combination of materials, that when applied properly, reduce the rate of heat flow by radiation, conduction, and convection. This material or combination of material reduces the flow of heat in or out of a building due to its high thermal resistance. The thermal insulation is obtained in solids by trapping/capturing air or gas inside the material in small cavities or by loosely filling solid particles (Kothandaraman, 2006). Furthermore, for every thermal insulation, the insulating property depends on both the material and the transport property of the gases filling the empty spaces (Kothandaraman, 2006).

"Thermal insulation is a major contributor, and an evident first step towards achieving energy efficiency, especially in envelope load dominated buildings located in sites with severe climatic conditions" (Mayer et al 2014).

Thermal insulation is one of the critical issues affecting energy-efficient initiatives of the building envelope together with thermal mass, windows/glazing and reflective/green roofs (D. H. W. Li et al., 2013). Thermal conductivity is the main characteristic of thermal insulation with the goal of achieving a low conductivity which gives rise to high thermal resistance and low thermal transmittance (Jelle, 2011). Figure 2-2 shows a comparison of the thermal conductivity of some common building material and insulation materials.

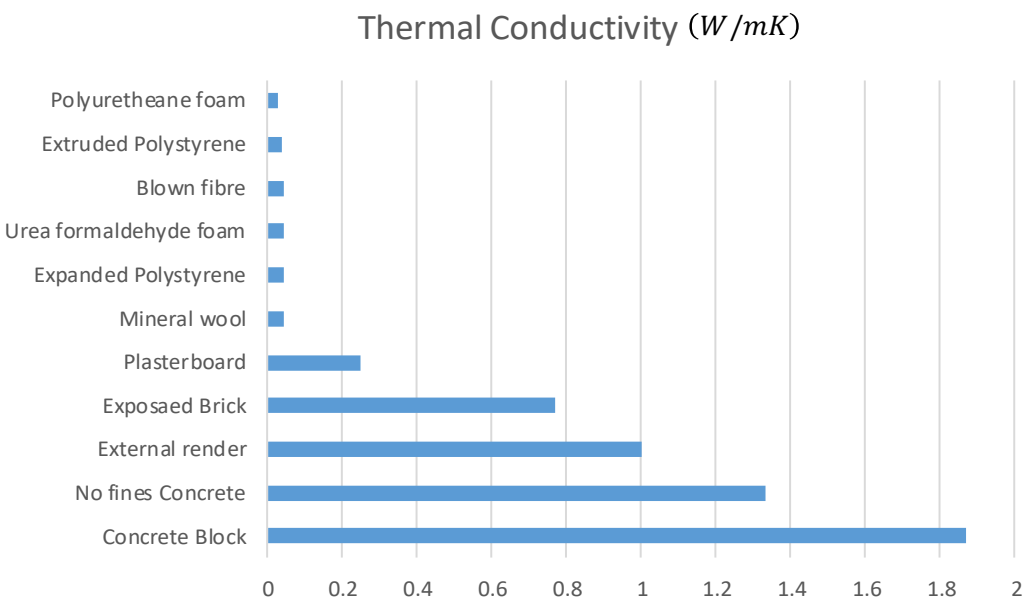

Figure 2-2: Thermal conductivity of common building insulation material

Nowadays, designers and building owners do not contemplate the question of using insulations, but what type of insulation, wall thickness, and how wall assemblies will be designed and built. Li, Yang, and Lam (2013) identified three features regarding insulation, which are outlined below

- Insulation in heating dominated buildings appear to be more cost effective and environmentally beneficial
- More insulation leads to less conduction which results in improved energy efficiency. This is not the case always, however. as over insulation leads to a decrease in heat loss during cooling mode which increases the cooling demand and hence could result in an increase in space conditioning energy usage.
- Simple economic cost analysis, life cycle energy, CO_2 emission analysis and cost optimal standards of minimum energy performance requirements for buildings and construction components can be used to assess the optimum thickness of insulation.

According to Berge et al 2012, the heat transfer can normally be divided through pores as shown in the equation below

$$\lambda_{tot} = \lambda_{gas} + \lambda_{solid} + \lambda_{rad}(W/(m.K)) \qquad \textit{Equation 2-27}$$

$$\lambda_{tot} = \lambda_{gas} + \lambda_{solid} + \lambda_{rad} + \lambda_{conv} + \lambda_{coupling} + \lambda_{leak}(W/(m.K)) \qquad \textit{Equation 2-28}$$

Where λ_{tot} is Total conductivity, λ_{gas} is Conductivity for gas conduction, λ_{solid} is Conductivity for solid conduction, λ_{rad} is Conductivity for radiation, λ_{conv} is convection thermal conductivity, $\lambda_{coupling}$ is thermal conductivity term accounting for second-order effects between various thermal conductivities and λ_{leak} is leakage thermal conductivity. However, according to Jelle (2011), the total overall thermal conductivity is given by Equation 2-28. Al-Homoud (2005) revealed that thermal insulating materials resist heat flow through microscopic dead air cells that contain convective heat transfer by preventing air movement. The thermal insulation is therefore provided by the air trapped within the insulation material.

2.6.1 Classification of insulating materials

Thermal insulating materials may be categorised by their chemical or physical structure. Papadopoulos (2005) identified that the most widely used insulating material are classified as organic materials, inorganic materials, combined materials, and new technology materials (see Figure 2-3). Al-Homoud (2005) identified that thermal insulations fall under the following inorganic materials, organic materials, and metallic or metalized reflective membranes. However, Kothandaraman (2006) stated that there are three types of insulating materials namely; Fibrous, Cellular, and Granular insulating materials

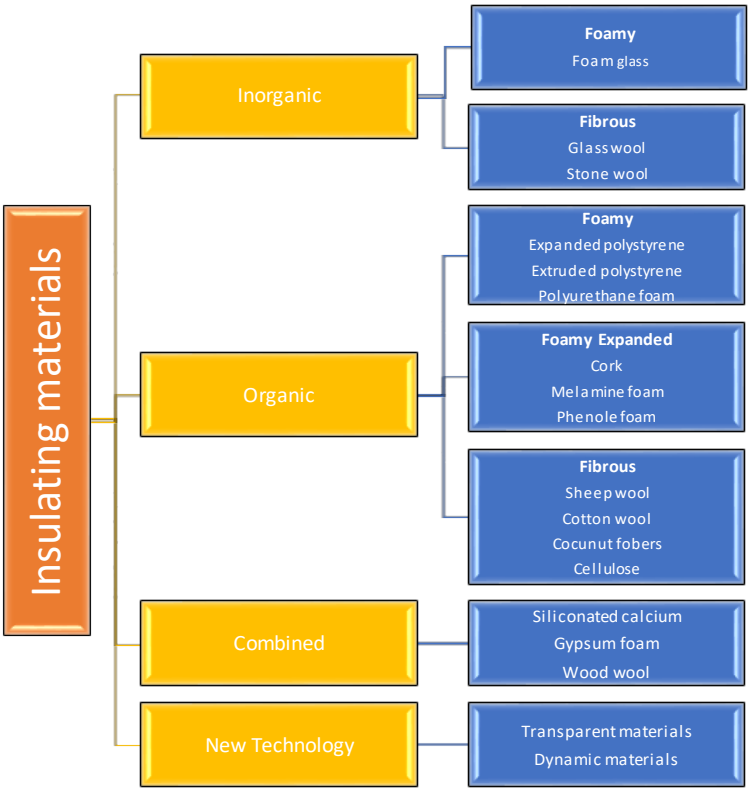

Figure 2-3: Classification and types of insulating materials Papadopoulos (2005)

Insulating materials are made in various forms as follows reflective materials, insulated concrete form, insulated concrete blocks, boards or blocks, sprayed or faomed in place, rigid boards, loose-fill that can be blown in and mineral fiber blankets.

Thermal insulations for example mineral wool, cellulose, cork, polyurethane, extruded and expanded polystyrene are termed traditional thermal insulation by researchers such as Jelle (2011). However, Jelle (2011) described another set of thermal insulations as state of the art building thermal insulations which have a very low thermal conductivity for example, vacuum insulated panels, gas-filled panels, aerogels, and phase change materials.

For the design and application of thermal insulation, certain factors have to be considered. The layer at which the thermal insulation is applied is one of the factors as thermal insulations are most efficient when applied as a continuous and on an even layer without penetration and breaks. This is because penetration creates thermal bridges while breaks permit airflow through and within the insulating layer. Thereby reduces the resistivity and effectiveness of the insulation (CIBSE, 2006).

Adding insulation to structures or bodies will always increase the resistance to conductions. Nonetheless, if the total resistance is a combination of convection and conduction resistance, in some cases the addition of insulation can reduce the resistance to convection due to the increase in surface area. Critical thickness is the term named when the thickness of insulation increases the heat flow and after which heat flow decreases (Kothandaraman, 2006).

2.7 Thermal comfort

Thermal comfort as defined in BS EN ISO 7730 is the *"condition of mind which expresses satisfaction with the thermal environment, i.e. the condition when a person is not feeling either too hot or too cold"*. According to ASHRAE standards, thermal comfort is measured by subjective evaluation. This means that a minority of individuals may feel uncomfortable even in thermal environments which are well regulated (Moss 2007).

Thermal comfort is important because it makes the thermal environment satisfying and influences productivity and health. Furthermore, Nicol et al (2002) identified that there are three reasons for understanding the significance of thermal comfort:

- Providing adequate conditions for people
- Regulation and control of energy consumption
- Setting and suggestion of standards

To retain the thermal comfort of a building, a certain amount of energy has to be added or removed (i.e. through cooling or heating). Furthermore, this energy depends on factors such as external air temperature, metabolic rate, mean radiant temperature, clothing insulation, operative temperature, relative humidity, heat, and moisture flow through walls, etc. (Harish & Kumar, 2016). Moss 2007 stated that it is widely accepted that there are four factors that directly affects human comfort, these are; dry bulb temperature, wet bulb temperature, mean radiant temperature and air velocity. However, HSE (2019) revealed that there are six factors affecting thermal comfort which are divided into two groups namely personal and environmental factors. These factors may be independent from one another but together they contribute to the human thermal comfort. Air temperature, radiant temperature, air velocity and humidity are environmental factors. While the personal factors are clothing insulation and metabolic heat.

Figure 2-4: ASHRAE seven-point scale

BS EN ISO 7730 and BS EN ISO 10551 provides guidelines on predicting thermal comfort. The standard suggests that Predicted Mean Vote (PMV) and Percentage People Dissatisfaction (PPD) can be used to define thermal comfort. The predicted mean vote index developed by Fanger predicts the mean response of a large group of people according to the ASHRAE thermal sensation scale (Djongyang et al., 2010). The ASHRAE thermal sensation scale is a seven-point scale that ranges from -3 to $+3$ as shown in Figure 2-4.

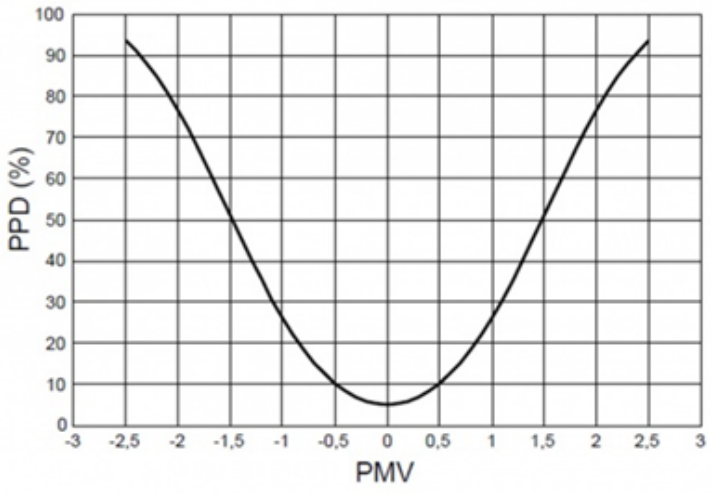

Figure 2-5: Predicted percentage of dissatisfied (PPD) as a function of the predicted mean vote (PMV)

As the occupants are not alike, there will always be a certain variation in the thermal sensation of a large group of people. Due to this issue, PPD was developed to know the percentage of people who would be dissatisfied with the environment. An empirical (Equation 2-29) and graphical (see Figure 2-5) relationship exists between PPD and PMV.

$$PPD = 100 - 95 * \exp(-0.03353 * PMV^4 - 0.219 * PMV^2)$$

Equation 2-29

From the equation above, at $PMV = 0$ (i.e. Neutral), about 5% of the occupants in a building may still be dissatisfied (Yang et al., 2014). Occupants are declared uncomfortable when they respond between ± 2 and ± 3, while those that respond ± 1 and 0 are declared comfortable (Djongyang et al., 2010).

2.7.1 Ventilation

Ventilation, as defined by CIBSE (2006), is the process by which fresh air is supplied to occupants and potentially harmful pollutants concentrations are diluted and removed from a space. Allard et al 2002 stated that "*Ventilation plays an important role in providing good indoor air quality and thermal comfort of the occupants"*. Furthermore, ventilation accounts for 30-60% of the energy use in buildings (Dodoo et al., 2011). According to Allard et al 2002, a proper design of a building that is energy-conscious building needs a balance between two factors which are

- Building envelope thermal efficiency and suitable selection of heating, cooling and daylighting techniques.
- Acceptable indoor climate in terms of comfort, effective ventilation and indoor air quality

Ventilation can also be used as a means of passive cooling and as a mechanism for distributing thermally conditioned air from heating and cooling plants to a building space. Ventilation in building is supplied by natural means, mechanical or mixed-mode methods also known as assisted or hybrid natural systems.

Natural ventilation as the name implies come from nature and is powered by wind and temperature climatic forces (wind effect and slack effect respectively). The benefit of natural ventilation is its contribution to a sustainable building environment as it does not require electrical energy for fans, which make up about 25% of the electrical energy consumption for mechanically ventilated buildings (Etheridge, 2011). Natural ventilation is limited to the

extent to which it can provide cooling due to its reliance on the climatic conditions, for instance in hot climates that are humid. The rate of natural ventilation in a building is influenced by different factors such as

- Shape and location of the building with respect to the buildings within the vicinity
- The wind direction and speed, which is influenced by geographical location, with respect to the orientation of the building
- The building height
- The level at which the building is sealed
- Windbreaks, natural and artificial

Mechanical ventilation as defined by CIBSE (2006) is a technique of ventilation that is enforced by means of driving fans and a network of ducts. Mechanical ventilation are divided into three namely supply only, extract only and balanced ventilation systems. Supply only ventilation provides fresh air with the use of mechanical supply fans and a network of passive vents for the exhaust of air. Extract only ventilation is the opposite of supply only ventilation and uses mechanical fans for extraction of air out of space and passive measures for fresh air supply. Balanced mechanical ventilation is a combination of both supply and extract ventilation system. In general, balanced mechanical ventilation provides air filtration, cleaning of extract air combined with the opportunity to recover thermal losses from the exhaust air for pre-conditioning air supply (CIBSE, 2006).

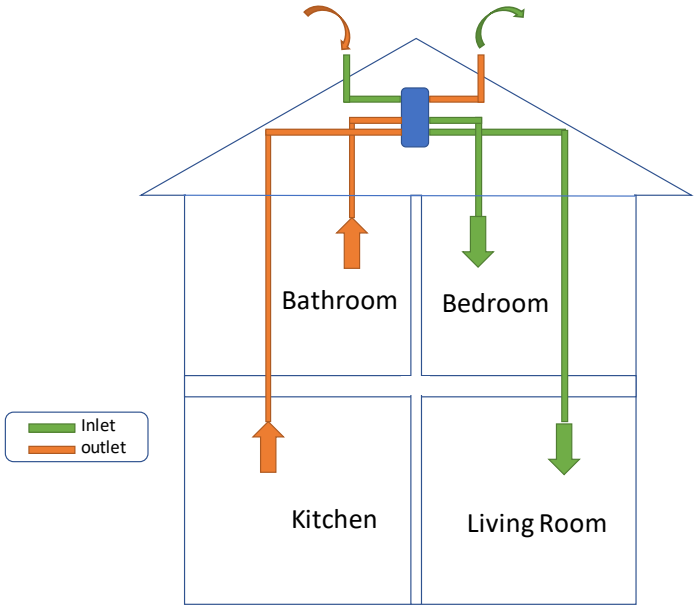

Figure 2-6: Concept of heat recovery

Mechanical ventilation is often used to achieve required air-flow especially in buildings with low infiltration. An example of mechanical ventilation used in buildings with low infiltration is the heat recovery system. Heat recovery as defined by Shurcliff (1988) is a device that extracts (remove), recovers heat or mass from an air stream and transfers it to another air stream. The concept (see Figure 2-6) behind heat recovery is energy that is usually lost would be used to heat the incoming air which helps in maintaining a comfortable temperature (Mardiana-Idayu & Riffat, 2012).

2.8 Sustainable buildings

"Sustainable development is a development that meets the needs of the present without compromising the ability of future generation to meet their own needs" (Brundtland, 1987)

Sustainability is an extensive term that deals with economic, social and environmental issues (Khatib, 2009), and therefore complex to define in definite terms (Bingel & Bown, 2009). Sustainability is a notion that has risen amid concerns about anthropogenic (man-made) changes to climate and overuse of the limited resources of Earth. In general, sustainability aims at encouraging the most efficient use of resources, environmental protection, ecosystem protection and creating a fairer world society (Bingel & Bown, 2009). Savastano, Santos, and Agopyan (2009) described sustainability as a concept of increasing concern in view of the world's shortage of natural resources and energy, generation of solid waste and gas emissions from various sources. The construction industry is a high consumer of natural resources in forms of energy, water, material, and land, hence construction has an impact on the environment (Khatib, 2009). Due to these sustainable buildings are being developed.

A sustainable building as defined by McMullan (2018) is a building that is deliberately designed to minimize the impact on the environment, to maximize efficiency when using resources such as materials, energy, and water, and to maintain this efficiency over the life cycle of the building. To achieve sustainability in buildings, it is not primarily about the absolute performance of the building. Green et al (2015) mentioned that a sustainable design/building is more about the adaptability, resilience and user understanding, rather than about predicted design performance-based on assumed patterns and user behavior. In other for building to be considered sustainable, energy and water usage, internal environmental quality, material selection and the building effect on-site have to be taken into account (Wells et al., 2018). There are different forms or targets of sustainable buildings and they include low energy buildings, zero energy buildings, and zero-carbon buildings. Others include the nearly zero energy buildings and zero net energy commercial building.

Low energy buildings:

There have been different definitions of low energy buildings from different researchers and organizations. A common definition of low energy building is a building which has a better energy consumption than a building corresponding to present building regulations and building traditions (Karlsson & Moshfegh, 2013; Pi & Yu, 2015). A low energy building as defined by Hui (2001) is a building in which the major goal is reducing the amount of energy purchased from an external source such as electricity and fuel gas. Abel (1994) defined low energy buildings as a building used for development and testing of new technologies focusing not only on decreasing space energy demand, but also to reducing the need for electricity.

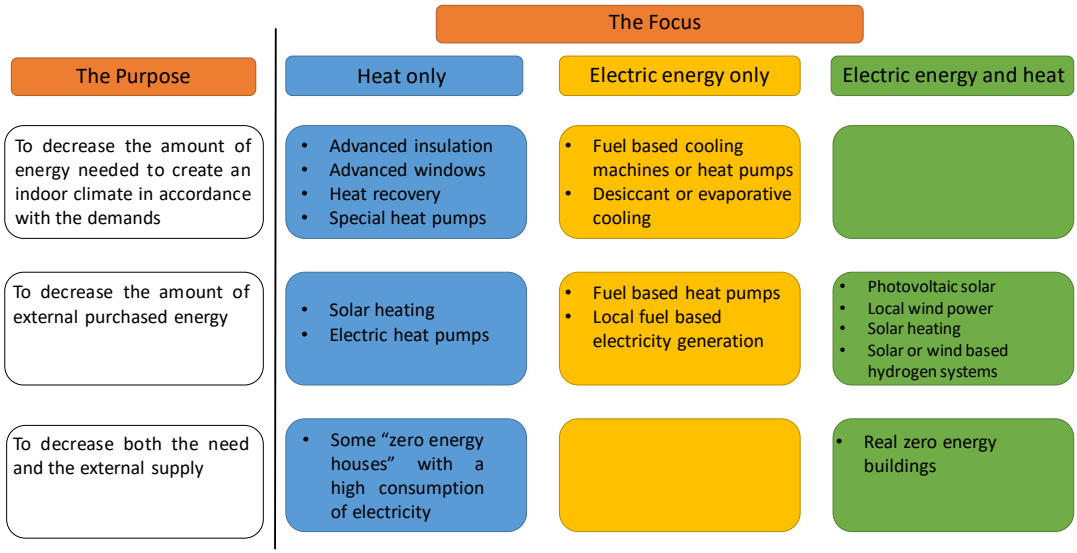

Figure 2-7: Low energy matrices indicating applicability in practice by Abel (1994)

A low energy building is not easy to define as buildings are influenced by factors/restrictions such as architectural features, indoor climatic conditions, and economic effectiveness. Therefore, the target for low energy buildings may defer from building to building. Due to this, Hui (2001) stated that the realistic aim of low energy buildings is to achieve the highest possible energy efficiency that needs the lowest possible energy requirement within the economic limits of reason. In early research by Abel (1994), the author produced a low energy matrix (see Figure 2-7) and identified that the ultimate goal of low energy buildings is a building that requires no energy or external energy supply or, at least, no supply of purchased energy.

Sarbu and Sebarchievici (2017) revealed that the notion of low-energy buildings is centered on primary energy reduction with the use of high insulation, high-efficiency heating or cooling systems and integrating renewable energy sources into the building plant. However, Karlsson and Moshfegh (2013) stated that low energy buildings are characterized by being a building that uses almost zero purchased energy.

Zero energy buildings and carbon buildings

Researchers still debate on the definition of net-zero energy buildings which can satisfy all participators in the field (Deng et al., 2014). A zero-energy building is a building that meets all of its energy demand through local renewable sources (McMullan, 2018). Deng, Wang, and Dai (2014) described a zero energy building as an integral solution to address problems of energy savings, protection of the environment, and reduction in CO_2 emission in the building sector. This building can also import off-site energy (from the grid electricity or gas) if necessary and can export the on-site energy (to the grid electricity) if in excess (see Figure 2-8). Deng, Wang, and Dai (2014) further defined a net-zero energy building in the form of a mathematical equation as shown in Equation 2-30. Different forms of zero energy buildings include net-zero site energy, net zero energy cost, net zero emission and net zero source energy (McMullan, 2018; Wells et al., 2018)

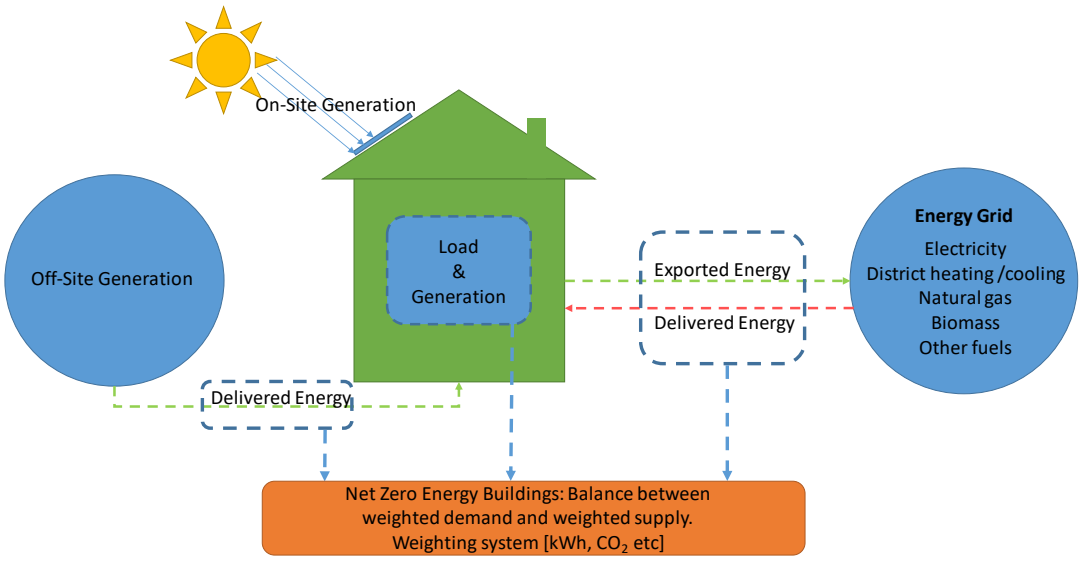

Figure 2-8: visual description of net-zero energy building

$$Net\ Energy = \ Output - Input \qquad \textit{Equation 2-30}$$

$$= \sum_i output\ energy\ (i) x\ weight\ (i) - \sum_i input\ energy\ (i) x\ weight\ (i)$$

Net-Zero site energy is a building which balances its annual energy consumption with on-site energy generated from renewable sources (McMullan, 2018). However, Wells, Rismanchi, and Aye (2018) described a net-zero site energy building as a building that generates a unit of energy for every unit of energy consumed. Furthermore, Wells, Rismanchi, and Aye (2018) revealed that the model definition of net-zero site energy does not govern the end-user's conservative use of energy or consider the efficiency of appliances directly.

Net-Zero source energy balances its annual energy use against externally generated energy from renewable sources (McMullan, 2018). Wells, Rismanchi, and Aye (2018) defined the net-zero source energy as a building that is responsible for creating a unit of energy for each energy unit used, except that it is measured at the source of energy for a net-zero source energy building. This definition accounts for energy that may be lost or wasted in the process of generation, transmission, and distribution (Wells et al., 2018)

A zero-carbon building is a zero energy building which has a zero net carbon dioxide emissions. This may also be regarded as a net zero-emission building in which the building generates emission free energy as it uses emissions producing energy (Wells et al., 2018).

A net-zero energy cost building as defined by Wells, Rismanchi, and Aye (2018) is a building whereby the owner has the utility bills of zero charges. This may be regarded as unachievable in some cases as utility providers charge maintenance and connection fees regardless of usage.

A nearly zero energy building is defined as a high performance building based on the annual energy consumption consistent with typical use, internal temperature control to maintain a preset temperature (European Commission, 2010).

2.9 Building Energy Simulations

A building provides shelter and protects the inhabitants against harsh weather condition. With the complexities and increase in the use of mechanical devices such as office equipment, and the computer-intensive operations with a lot of internal heat generation. With all this, energy analysis of buildings is required in other to achieve the desired output in the building itself and the system. Al-Homoud (2001) summarised the need for building energy analysis as a decision making tool, predictive tool, and a facilitating tool.

"Only Computer-aided Simulation holds the key to improving building energy efficiency (Hong et al 2000)"

Building simulation facilitates by means of a computer model the evaluation of a building or building component's response to specific external conditions. It is therefore an instrument intended to contribute to the understanding and overview of the decision problem by decision makers (De Wit, 2004). Energy analysis is a robust process that involves difficulties such as unsteady changes of variables, heat flux coupled with non-linear temperature expressions and various heat transfer mechanisms that work in complex ways (Martin et al., 2012). Therefore, with the advances in computer technologies, building energy simulation programs were created. Simulation of building performance is dependent on iterative process of understanding and representing the real-world problems (Hong et al 2000). Computer-based application tools in building design can be divided into two groups, which are

- Computer-aided documentation, design, and drafting: these applications are known to help building designers improve the productivity and have little effect on the efficiency of building performance.
- Computer-based simulations: this application uses engineering tools for heat gains and space heat loads calculations within the building envelope, predict the building energy performance, and provide diagnostics to enable automatic system and plant operation control. (Hong et al 2000)

The built environment is increasingly being complex with large buildings, multiple users and high demands for thermal comforts and data processing, hence analysing and evaluating the performance of building becomes a significant problem that can only be solved with computational software (Borgstein et al., 2016). According to Martinaitis et al (2015), the application of computational methods in architecture and civil engineering makes it possible

to evaluate building performance at early stages of design and also helps to efficiently minimize the overall energy consumption of buildings. According to Viot et al 2015, one dimensional heat transfer computation can be handled by most simulation tools.

For the assessment of building energy performance, Analytical or numerical integrated techniques are the basics of simulation tools. Martinaitis et al (2015) further stated that despite both methods having their strengths and weakness, both methods are suitable for assessing building energy performance. Building energy simulation programs are constantly being updated as the research community are working to reduce the gap in energy demand between real-life energy use of the dwellings and simulated values using computer tools (Martin et al., 2012)

For every building energy simulation, model development is essential. Models are created to simulate building energy systems and can be classified into physical, symbolic and mental models. The models can further be classified into mathematical or non-mathematical models. Models classified as mathematical can be divided into theoretical or experimental models. Theoretical models requires breaking down of larger systems into a number of smaller and simpler subsystems while experimental models are developed through empirical relations (Harish & Kumar, 2016). However, Coakley, Raftery, and Keane (2014) classified models as data-driven or law-driven and diagnostic or prognostic models. The author further revealed that building energy simulation models can be categorised as prognostic law-driven models since, given a set of well-defined laws, they are used to predict the behaviour of complex systems.

In building energy simulation, there are three broad and distinct modelling approaches namely forward, data-driven and grey box approach (see Figure 2-9a) (Coakley et al., 2014; Harish & Kumar, 2016). The forward approach or detailed model calibration uses a completely descriptive law-driven model of a building system and calibrates different inputs to match the measured or experimental data (see Figure 2-9b). The grey box approach formulates a physical model of the building system and identifies important parameters that are representative of certain key and aggregated physical parameters. Lastly, the black box or data-driven approach uses mathematical or statistical models, which relate to a set of influential input parameters to measured outputs.

Building energy analysis starts with the theory that six factors influence energy consumption which are climatic conditions, the building fabric, the building systems, operation and

maintenance, behaviour of occupants and internal environmental conditions (Borgstein et al., 2016). These are further discussed in Chapter 4; Section 4.4.1.

To simulate the energy performance of buildings, multizone or nodal Approach, zonal method and computational fluid dynamics are the three main thermal building models currently used. The multi-zone or nodal approach is considered as the simplest method between the three models (Foucquier et al 2013). The multizone method assumes that each building zone is a homogeneous volume characterized by uniform state variables and one zone is approximated to a node that is described by a unique temperature, pressure, concentration, etc (Foucquier et al 2013).

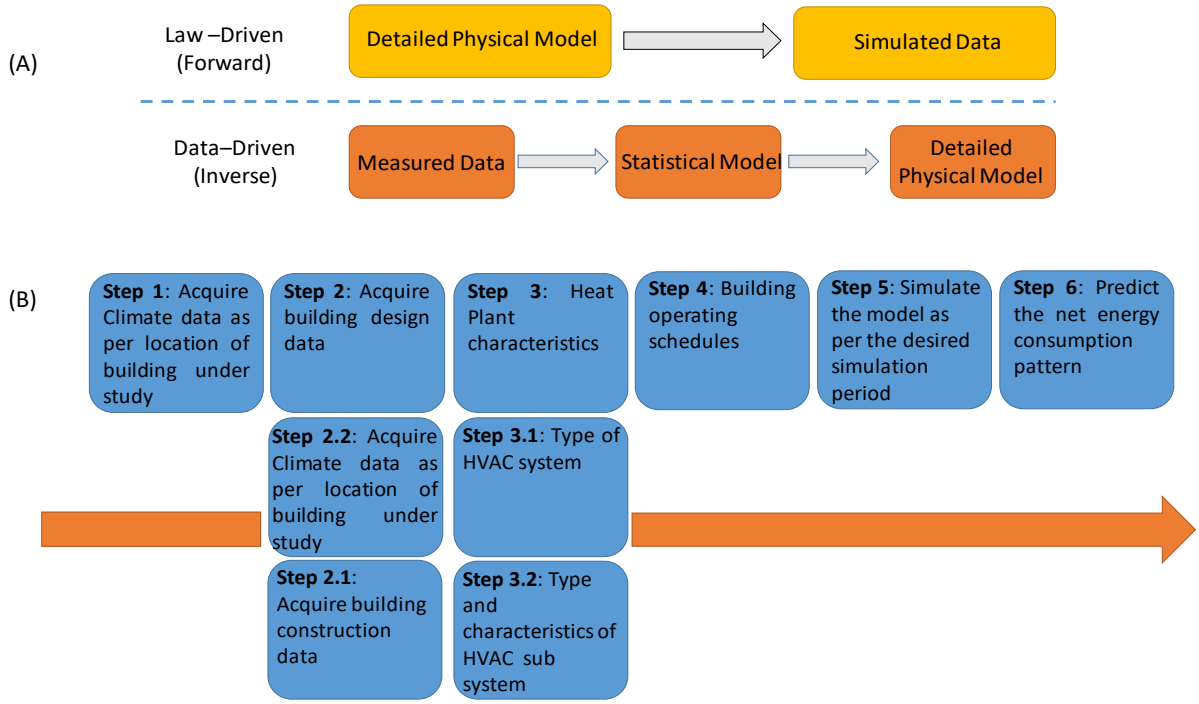

Figure 2-9: (a) modeling approach as classified by Coakley, Raftery, and Keane (2014) and (b) steps for forwarding approach by Harish and Kumar (2016)

For each node in the system, the thermal transfer equation is solved. It should be noted that a node represents a room, wall or the exterior of a building. It can also be more specific like heating and cooling systems, internal occupancy or equipment gains (Foucquier et al 2013). There are much different software that uses the multizone approach and they include; TRNSYS, EnergyPlus, IDA-ICE, ESP-r, Clim2000, BSim, and BUILDOPT-VIE, etc.

2.9.1 EnergyPlus

EnergyPlus is a simulation engine with input and output text files. It is a modular, structured code based on the most popular features and capabilities of BLAST and DOE-2.1E. According to Crawley et al 2008, the EnergyPlus building systems simulation module, with variable time step, calculates heating and cooling system and plant and electrical system response. This integrated solution provides more accurate space temperature prediction crucial for system and plant sizing, occupant comfort and occupant health calculations

Yu et al (2015) stated that users in EnergyPlus have to input certain parameters before the building energy simulation analysis can be carried out throughout the year, month or day for the entire building. These parameters include Location, weather, building envelope information, internal usage such as personnel, lighting, and equipment, the basic form of the heating, ventilation and air conditioning operating conditions and old or heat source parameters

Integrated simulation in EnergyPlus also allows users to evaluate the following; realistic system control, moisture adsorption, desorption in building elements, radiant heating, and cooling systems, and inter-zone airflow. Fabbri et al 2008 stated that EnergyPlus includes many innovative simulation capabilities such as

- Time steps of less than an hour,
- Modular systems
- Plant integrated with heat balanced based zone simulation,
- Multizone airflow,
- Thermal comfort,
- Water use,
- Natural ventilation and
- Photovoltaic systems.

According to Yu et al (2015) there are six modeling processes when using EnergyPlus as shown in the figure below.

Figure 2-10: Modelling process in EnergyPlus

Setting Information: in this process, Building location and weather information are provided and an overall description of the building needs to be described. This includes the building size, exterior, and interior walls, roofs, windows, doors, floors, and ceiling. Furthermore, lightning equipment, people and work schedule is set including air conditioning system operating parameters.

Building Zoning: In this process, the overall architectural model is divided into heat transfer surfaces and thermal storage surfaces. This is a thermodynamic concept of energy modeling rather than a geometric concept. The principle of zoning is using function, setting temperature and solar radiation heat gain. Therefore, two identical regions can be zoned as one.

Modeling the building construction: After the zoning process, the user classifies the building surfaces according to the temperature control. The number and complexity of the surfaces can be reduced by defining equivalent surfaces. Therefore, all the same, constructed surfaces, windows and shading can be defined as an equivalent surface. Another way of simplifying the model is through stitching complex surfaces into basic geometry. Furthermore, a more detailed description of the building can be made by setting envelope styles and materials.

Editing interior space data: People, lighting, equipment, air infiltration, and ventilation form can affect the indoor load. The peak load, design load and the corresponding timetable in EnergyPlus can describe the cooling or heating load.

Inputting HVAC system: Inputting the HVAC system is difficult and hence one needs to understand the HVAC system before inputting the data. Third-party interface software such as DesignBuilder has a more user-friendly and easy to operate interface.

Setting Economic Factor: EnergyPlus does not only calculate the building energy consumption but also performs cost analysis after inputting the energy rates. The energy rates need to be set according to the actual situation including energy costs, monthly service fees, basic costs, power factor costs, block fees, and other charges. (Yu et al., 2015).

2.9.2 DesignBuilder

DesignBuilder Software Ltd. Is a commercial software development and research company that started in 1999. The first DesignBuilder was released in December 2005 as the first Graphical user interface to the EnergyPlus simulation engine.

"We aim to bring advanced building design tools into the mainstream by providing software that is easy to use and highly accessible both in terms of initial cost and time taken to learn it. We are particularly keen to encourage the uptake of environmentally responsible design techniques and to play our part in reducing building-related pollution to sustainable levels." (DESIGNBUILDER 2017)

DesignBuilder coupled with the software tool EnergyPlus is a powerful tool for modeling three-dimensionally building geometries as well as assessing the energy performance. DesignBuilder combines rapid building modeling with state of the art dynamic energy simulation (Andarini, 2014).

Tronchin and Fabbri (2008) and Yu et al (2015) stated that DesignBuilder has a user-friendly interface together with the metrological database and sophisticated model to evaluate the energy supply for internal and solar energy supply. This software further allows for the dynamic evaluation of heating and cooling consumption during all seasons, including DHW and other energy consumption. The average temperature indoor and surface temperature during the year can also be obtained in DesignBuilder. The software provides a 3-dimensional architectural modeling tool and has an ability to easily input various parameters. Furthermore, DesignBuilder adopts an OpenGL solid modeler, which is easy to operate, and users can establish a block by stretching, shearing and other production in 3-dimensional space. This software produces output files, which provide rendering and animation relevant to architecture including the effect of the building envelope materials, sunshine shadows, and shading effects. (Yu et al., 2015).

DesignBuilder has been identified as a very useful energy simulation tool due to its extensive data templates for a variety of building simulation inputs such as typical envelope construction assemblies, lighting systems and occupancy schedules (Wasilowski & Reinhart, 2009). The software provides results that are compatible with a number of energy and carbon labeling schemes such as UK Energy Performance certificates, UK Building Regulation Compliance, UK BREEAM, and US Green Building Council LEED assessments. Rahman, Rasul, and Khan (2010) stated that DesignBuilder is one of the most comprehensive user interfaces

for EnergyPlus dynamic thermal simulation engine. Furthermore, DesignBuilder maintains the European Parliament Board of Directive (EPBD) standards.

In DesignBuilder, the time intervals of running period can be divided into annually, monthly, daily, hourly and sub-hourly. The output results from DesignBuilder shows the building energy consumption across the consumption of fuel and electricity. Heating and cooling design loads can also be obtained including CO2 output of the building. (Yu et al., 2015).. DesignBuilder also includes computational fluid dynamics modeling specifically adapted for analysing air movements and ventilation problems within building spaces (Wasilowski & Reinhart, 2009). The computational fluid dynamics model in DesignBuilder uses the Standard k-e turbulence model with wall functions and first-order upwind for the discretisation scheme.

The software EnergyPlus that is the solver for DesignBuilder uses a modular program structure, this makes the calculation method easy to understand. Furthermore, the EnergyPlus solution is based on the heat balance technique referred to as the prediction correction method and assumes that the room air is well stirred (M. M. Rahman et al., 2010). The Predictor corrector method is the principle behind this method is to predict the mechanical system load needed to maintain the zone air setpoint and simulate the mechanical systems to determine their actual capacity, and then recalculate the zone air heat balance to determine the actual zone temperature (M. M. Rahman et al., 2010)

EnergyPlus is tightly integrated into the DesignBuilder environment to generate detailed building energy performance data by simulation using real weather data (either measured or from the bureau of meteorology (BOM) data) (M. M. Rahman et al., 2010). In DesignBuilder, the simulation principle used is the most detailed simulation according to (M. M. Rahman et al., 2010) with dynamic parameters and they include all energy supply and energy dispersion.

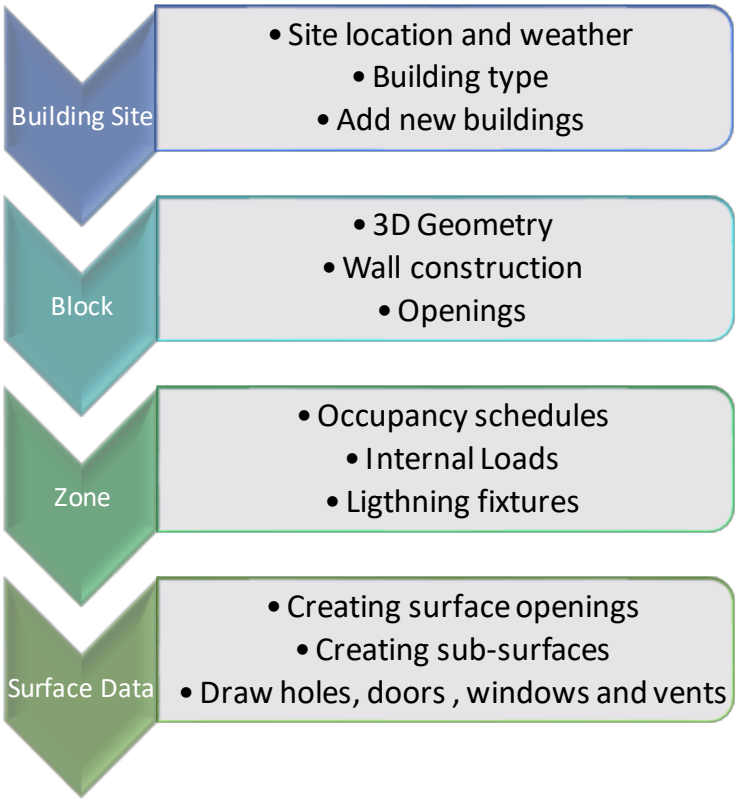

Figure 2-11: DesignBuilder Hierarchy Structure

DesignBuilder models are structured in order of building site, block, zone and surface data as shown in Figure 2-11. According to (Maile et al., 2007) the workflow of DesignBuilder starts with the selection of a location and the corresponding weather through a weather file. This is then followed by building the thermal model geometry with the integrated CAD software. This is done using the building blocks. Building blocks are basic geometric shapes that are used to assemble a 3D model similar to the actual building model (M. M. Rahman et al., 2010). In DesignBuilder, the building blocks are considered as composed of building elements such as walls, roofs, and floor slabs.

Partitioning of the then formed blocks internally forms a thermal zone. A thermal zone is a space or collection of spaces within a building having sufficiently similar space conditioning requirements so that conditions like temperature could be maintained with a single thermal controlling unit. For a thermal zone, certain parameters have to be specified and they include

- Total number of occupants and their schedule
- Total number of equipment within the zone
- Lighting fixtures

DesignBuilder has been used by different researchers across different energy disciplines. Martinaitis et al (2015) performed an analysis of the effects of typical domestic occupancy profiles on the energy performance of efficient houses and asses the applicability of default DesignBuilder occupancy profiles at local conditions. A 3D model of a one-storey quadrate shape house with a total area of 81m^2 was used as a case study. Four occupancy schedules ranging from 2 people per house to 4 people with four different thermal comfort strategies were created and compare to each other. Results showed that different profiles have an influence on indoor comfort, especially in the summer. Furthermore, simulation with default DesignBuilder profiles showed more overheating hours if no shading is used.

A rural residential pilot experiment energy-saving building with a total area of 198.27m^2 in Shenyang was modelled in DesignBuilder. The model was divided into eight areas due to different functions and parameters such as indoor temperature, humidity control, people density light, and electrical equipment were set. The building envelop was also set to different conditions and was simulated for a period of one year. Results showed the importance of civil envelope on energy consumption through the effects of wall thermal performance, roof thermal performance and window thermal performance on the total site energy (Yu et al., 2015).

Li & Rezgui (2017) introduced a method to calibrate u-values and air infiltration rates through simulation and experimental measurements. DesignBuilder was used to construct the simulation model and set up the input variables, schedules, detail HVACs and running the simulation. A number of datasets was obtained to investigate the energy consumption of different zones for a single day under different circumstances. A regression model was established to replace the EnergyPlus model for simulation purposes. A fitness function to evaluate the gap between the measured and predicted heat consumption was presented to search for the most appropriate U-values and air infiltration rate. Finally, a simulation with human activity involved was carried out and the results benchmarked with measured data

Rahman et al. (2010) investigated the opportunities for energy conservation measures in institutional buildings in hot and humid climates in Australia. A case study was conducted using a four-story building at central Queensland university in a subtropical climate Rockhampton, Australia. Different types of feasible and practical operational energy conservation measures such as major and minor investment measures (glazing) and zero investment measure (heating and cooling setpoints) were evaluated using DesignBuilder.

Results showed that energy saving of about 3% can be saved by implementing zero investment measures and 12.02% by implementing minor investment measures, which include diming daylighting control, and double-glazing. Furthermore, 26.68% can be saved by replacing constant air volume systems to variable air volume systems of HVAC systems and low coefficient of performance chillers to high coefficient of performance chillers.

Elshafei et al. (2017) evaluated the impacts of natural ventilation inside residential buildings on the human thermal comfort using numerical analysis validated with field measurements. The numerical analysis was carried out using the computational fluid dynamics module in DesignBuilder. Different parameters were considered in the study and they include air velocity, relative humidity, and air temperature. However. These factors are dependent on window sizes, placements, and shades. Result shows that there was an agreement between CFD simulations and experimental measurements in terms of air temperature, air velocity, and humidity profile. Due to the modifications in the window specification, results show a 600% increase in air velocity inside the building domain with a 2.5% decrease in air temperature. These results illustrate the improvement of thermal comfort.

Lapinskiene and Martinaitis (2013) combined simulation tools for the optimization of a building envelope. The simulation tools combined were DesignBuilder, SimaPro and a method of criteria complex proportional assessment COPRAS for decision-making. The building envelope was optimized based on energy demand, comfort, CO_2 emission, investment and exploitation costs. Three external wall alternatives were simulated in other to obtain the best alternative. Result showed that alternatives one and 2 were quite similar with a percentage difference of 1% while alternative 3 had a percentage difference of 6% to alternative 1 although the difference of U-value was 50%.

With the use of DesignBuilder, Feng & Hewage (2014) assessed the energy performance of a LEED Gold standard high occupancy building with exterior vegetation. The energy consumption of the facility was calculated using DesignBuilder and validated with the actual operational energy consumption in the building showing minimal discrepancies. To estimate the impact of green vegetation on energy savings, 3 scenarios were simulated which are, Green building without a green roof or wall, green building with a full green roof and green building with full green wall. Results showed that green buildings with a full green wall had a saving of 8.4% cooling demand energy consumption while losing about 1.8time heat during a typical summer week. Conclusions made in the research are

- Green vegetation has no significant impact on the energy savings in LEED standard buildings
- Green vegetation has a prominent influence on heat transfer in the summer and winter typical weeks
- Green vegetation has a significant impact on the start time and the period of heat gain through the roof and walls

Liang et al. (2017) studied a 145m^2 bungalow with a detached toilet and shower room located in south-western Beijing, China. The case study's space heating is supplied by coal-burning which consumes 3.47 tons in 2015. DesignBuilder was used to model and simulate the building. Result showed that before retrofitting, the building consumed 4.5tons of coal per year during winter with an average temperature as low as 10°C. After retrofitting, the annual coal consumption reduced to 3.47tone with an average indoor temperature of 15°C. The energy savings for the building by using the passive method resulted in a 23% saving.

Rahman et al. (2008) simulated an institutional 4-storey building in Australia using DesignBuilder. The results of the simulation were verified with measured data and then compared with different energy conservation strategies. The thermal performance of the energy conservation measures strategies was also evaluated and verified by thermal comfort index.

Taleb (2014) studied the usefulness of applying passive cooling strategies to improve the thermal performance and to reduce energy consumption of residential buildings in hot arid climate settings of Dubai, United Arab Emirates. The passive cooling strategies used in this study are

- Louver shading devices
- Double glazing
- Natural ventilation: windcatcher and cross ventilation
- Green roofing
- Insulation
- Evaporative cooling via fountain
- Indirect radiant cooling
- Light colour coatings with high reflection

The analysis was done using IES simulation software in which the passive strategies were implemented in the case study. Results obtained show that energy reduction of around 23.6% can be achieved with the application of the passive strategies.

Taleb & Sharples (2011) assessed the energy and water consumption of existing buildings in Saudi Arabia using DesignBuilder and BRE code water calculator respectively. The aim of the study was to establish guidelines for developing sustainable residential buildings. Results from DesignBuilder were validated with the actual utility bills. Taleb & Sharples (2011) applied energy measures to the simulations such as improved glazing, improving the thermal insulation of the external walls and roofs and fitting energy-efficient fluorescent lighting. Results showed that a total energy consumption reduction of around 32.4% can be achieved when the energy measures were implemented together with improved water conservation measures. The water conservation measures included the use of low flow taps and showerheads in which could potentially result in 55.4% reduction in water consumption rates.

Ascione et al. (2016) studied an integrated design procedure, which focuses on the problem of a large number of variables concerning the building envelope. The authors use a dynamic energy simulation tool and a constrained multi-objective optimization algorithm to study residential buildings in four cities (Madrid, Nice, Naples, and Athens). Different strategies were studied and compared which include, thermal properties of the building envelope, different window-wall ratio values, external and internal shading elements, etc. Results showed that it is difficult to understand the best trade-off between summer and winter performance by assuring a high standard of thermal comfort.

Lo et al. (2017)studied the energy conservation measures prioritization process for a residential Australian building. The case study was a 7000m^2 student accommodation at the University of Wollongong Australia. The building was simulated using DesignBuilder and validated with results from an energy audit conducted during the research. Different energy conservation measures were studied and observed. They include replacing the current lighting with LED lights due to the current lighting system contributing to 13% of the total amount of energy used. Furthermore, the heating setpoint was also changed and the building envelop was also examined because of air-leakages. The results showed energy savings due to the energy conservation, for instance, the LED lights contributed to 6%., Air leakage reduction, roof insulation, and glazing upgrade resulted in 8%, 2%, and 2% respectively.

2.9.3 Computational Fluid Dynamics (CFD)

Computational Fluid Dynamics (CFD) was first introduced to the buildings industry in the 1970s and has been extensively used in the industry with increasing computer speed and reduction in the cost of computing hardware (H. Wang & Zhai, 2016). Computational Fluid Dynamics (CFD) is considered as the most complete three-dimensional approach method in thermal building simulation. This method allows for details in the flow field through the microscopic approach of thermal transfer modeling. This method is based on the decomposition of each building zone in a large number of control volumes with homogeneous or heterogeneous global mesh (Foucquier et al 2013). CFD simulation can be expressed as a numerical solution of the governing equations of fluid flow. The conservation equations for mass, momentum, and energy (thermal) are solved for all nodes of a 2 or 3-dimensional grid inside or around the building. A generalized form of the conservation equation used in the CFD approach is given by

$$\rho \frac{\delta \Phi}{\delta t} + \rho \mu_i \frac{\delta \Phi}{\delta k_i} = \frac{\delta}{\delta k_i}\left(\Gamma \frac{\delta \Phi}{\delta k_i}\right) + S$$

Equation 2-31

Unsteady term + convection term = diffusion term + source term

The equations given above are identical but each term represents a different physical state variable. There are several CFD solutions for the building airflow simulations which include; Lattice Boltzmann methods, Reynolds averaged Navier-Stokes modeling, large-eddy simulations and direct numerical simulations (Hensen, 2004). According to Zhai et al 2002, CFD applies numerical techniques to solve Navier Stokes equations for fluid dynamics. Furthermore, CFD solves the conservation equation of mass for the contaminant species and the conservative equation of energy for building thermal comfort and indoor air quality analysis. There are a huge number of CFD software such as ANSYS FLUENT, COMSOL Multiphysics, MIT-CFD, PHOENICS-CFD, etc.

Hong et al 2000 observed that building simulation using CFD software is gaining popularity due mainly to new standards on health and comfort in the built environment and the need to design internal spaces and HVAC systems that meet the required standards. Furthermore, CFD tools are used to study the following; global warming, urban climate, micro climate, building ventilation, indoor and outdoor thermal comfort, fire safety and smoke extraction

According to Foucquier et al 2013, CFD is mainly employed for its ability to produce a detailed description of different flows inside buildings. With CFD dividing the volume into several

discrete control volumes, it allows for the study of very complex geometries of the building by minimizing locally the mesh of some specific parts. The accuracy and speed of CFD are influenced by many factors as identified by Wang and Zhai (2016) which include the numerical method, turbulent model, mesh quality, differencing scheme of discretization, and pressure-velocity decoupling algorithm.

An advantage of computational fluid dynamics is its ability to be coupled with other software such as building energy simulation software to solve complex problems. Zhai et al (2005) coupled EnergyPlus (a building simulation software) and MIT-CFD (a CFD software) to predict the cooling and heating demand for both an office and in an auto-racing complex. Wong and Wang (2008) coupled ESP-r (a building simulation software) and FLUENT (a finite volume analysis software for flow) to simulate the natural ventilation in residential buildings. Dols, Emmerich, and Polidoro (2016) coupled a CONTAM (a ventilation simulating software) with EnergyPlus (a CFD tool) to evaluate the indoor air quality in a building.

Turbulent modelling: This is a significant factor, which affects ventilation performance prediction. Due to the fact that almost all flows in the indoor environment are turbulent, the CFD problem can be solved using direct numerical solution, large-eddy simulations, and the Reynolds-Averaged Navier-Stokes equations. One of the most used turbulent models in building simulation is the Reynolds-Averaged Navier-Stokes model together with the k-Ɛ models.

Reynolds-Averaged Navier-Stokes (RANS): Reynolds first introduced Reynolds average in 1895. This method decomposes instantaneous velocity and pressure and other variables into a statistically averaged value and a turbulent fluctuation superimposed theorem. The RANS equations with the turbulent models solve the statistically averaged Navier-Stokes equations by using turbulence transport models to simplify the calculation of the turbulence effect.

2.10 Calculation Methods

2.10.1 Lumped Parameter Models.

Lumped parameter models are also known as lumped heat capacity systems is used to analyse a body with a known or specified temperature level exposed suddenly to surroundings at different temperature levels. Furthermore, the system is applicable when the temperature level in the body as a whole increases or decreases without any difference in temperature within the body (Kothandaraman, 2006).

Building structure elements have been known to have the characteristics of both thermal capacitance and resistance, therefore, a reduced-order lumped parameter model can be used to model the thermal performance of a building (H. Wang & Zhai, 2016). Lumped parameter modelling also known as “analogue circuit” models due to their connotation with electric circuits has the capability of hourly simulation of a whole building energy consumption but the computational intensity is much less (H. Wang & Zhai, 2016).

Building structural elements consists of several layers of different material and each layer has different characteristics such as thickness, specific heat capacity, density, and thermal conductivity. With lumped parameter models, elements consisting of n layers of materials can be combined to form two lumped thermal resistances and one thermal capacity as shown in Figure 2-12 (H. Wang & Zhai, 2016). Underwood (2014) observed that the Lumped parameter modelling method to building dynamic thermal response is motivated to find simpler and hence computationally less expensive methods for the analysis of building thermal energy response.

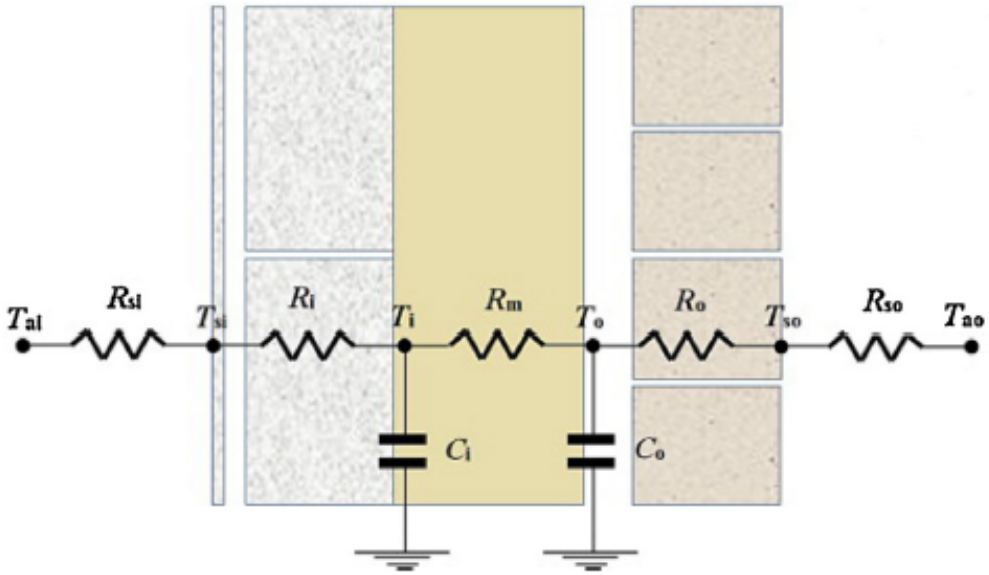

Figure 2-12:Simplified 2nd order construction element model (H. Wang & Zhai, 2016)

As shown in Figure 2-12, the lumped parameter model can be used to visualise the process of heating and cooling as charging and discharging the capacitor through the electrical analogy. From the equation of heat conduction in solids, (see Equation 2-5), and the heat flow due to convection (see Equation 2-2), a relationship is established which creates a dimensionless quantity named Biot number (Equation 2-32)

$$\frac{(\Delta T)_s}{(\Delta T)_c} = \frac{hL}{k}$$ *Equation 2-32*

Where $(\Delta T)_s$ is the temperature drop In the solid body, $(\Delta T)_c$ is the convection drop, h is the convective heat transfer coefficient, L is the thickness and k is the thermal conductivity.

The Applicability of the lumped parameter model is checked using the biot number. If the Biot number is less than 0.1, it is therefore acceptable that the lumped parameter model can be used without appreciable error. Therefore it is recommended that the Biot number be checked before attempting to solve a lumped parameter model.

2.10.2 Response Factor Method

The response factor method is another most adopted approach to solving transient heat transfer. The response factor method is based on Z-transform which was first proposed by Stephenson and Mitalas in 1967. This method assumes that coefficients are constant values, while the coefficient change with temperature variation (H. Wang & Zhai, 2016).

Wang and Zhai (2016) stated that the response factor method does not work properly with systems of radiant heat transfer. Furthermore, DOE-2 (simulation Program) adopts response factor to solve opaque retaining structure heat transfer and use the cooling load coefficient method to calculate the room load and temperature (Winkelmann et al 1993). This program does not calculate inner surface longwave radiation heat transfer directly but takes into account in convective heat transfer coefficient between inner surface and air (H. Wang & Zhai, 2016).

2.10.3 Conduction Transfer Function Method

This method is considered one of the most conventional approaches used to solve transient heat transfer calculations and also based on Z-transform. Transfer function method is used in several simulation software such as EnergyPlus, TRNSYS, and blast to evaluate the thermal loads through building construction (H. Wang & Zhai, 2016). Al-Raghbi et al (1997) stated that Conduction transfer method has been successfully programmed to predict the hourly cooling load of different types of walls, roof, and fenestration. There are three methods used to calculate the conduction transfer function coefficients namely Direct root finding method, State-space method and Frequency domain regression method (X. Q. Li et al., 2009).

2.10.4 Finite Element Method

The finite element method is a numerical technique for solving problems that are described by partial differential equations or can be formulated as functional minimization. The domain of interest in this method is represented as an assembly of finite elements.

This method together with the finite difference method are numerical methods used to solve partial differential equations that govern the conduction heat transfer through construction elements of buildings such as internal partitions, external walls, floors, and roofs. Different building simulation software use different methods in solving the thermal response of building elements such as

- ESP-r use Finite difference method
- EnergyPlus use Response factor method or Transfer Function method
- TRNSYS use Response factor method or Transfer Function method

2.11 Performance Gap and Uncertainty in Building Simulations

Borgstein, Lamberts & Hensen (2016) mentioned that building energy simulations use highly detailed building physics models and extensive parameter inputs by skilled professional and therefore should provide highly accurate predictions. However, this is not the case as there is a performance gap between predicted and actual performance as first introduced by CIBSE. De Wilde (2014) studied the performance gap between predicted and actual performance and divided the performance gap into three, which are: gap between machine learning and measurements, the gap between predictions and display certificates in legislation and gap between first principle predictions and measurements.

The discrepancy between prediction and measurement is inevitable due to numerical errors in simulation as mentioned by De Wilde (2014). The author further stated that the key is getting a reasonable agreement between the predicted and measured performance. De wit (2004) revealed that the first source of uncertainty is the lack of knowledge about the properties of the building or building component. Simplification due to the complexity of buildings leads to also further uncertainties. According to De wit (2004), uncertainties related to building simulation are classified into four namely

- **Specification uncertainty:** this arises from the incomplete specification of the system to be modelled. This may be caused by deviations from the design specification, which can occur during construction.

- **Modelling uncertainty:** this type of uncertainty arises from the physical model development. This may be caused by the introduction of assumptions or simplification of the model due to the complexity of the building.
- **Numerical uncertainty:** numerical uncertainty occurs due to numerical errors introduced in the discretization and simulation of the model.
- **Scenario uncertainty:** this occurs due to specification of the external conditions imposed on the building, for example, the outdoor climatic conditions and occupation behaviour.

2.12 Building Thermography

Objects radiate energy which is transported in the form of electromagnetic waves. These electromagnetic waves are not visible with the human eye. The human eye can only detect visible light waves or radiation of the electromagnetic spectrum between (0.39-0.77μm). thermal imaging expands the portion of the spectrum so that thermal energy emitted from an object can be seen and measured. Thermography is becoming more widely used amongst construction professionals for energy-related defect detection in buildings. There are many non-destructive methods and tools used for investigating the energy use in buildings. These methods include; computational simulation, heat flux measurement, co-heating tests, automated metre reading and air tightness testing (Fox et al., 2014)

These methods are all addressing specific aspects of building performance. Thermography is an optical measuring method (Grinzato, 2012) and can be seen as an emerging tool, which can be used to help identify common sources of heat losses (such as losses from conduction and ventilation) in existing and new buildings (Fox et al., 2014). Bianchi et al (2014) observed that assessing the thermal performance of building systems such as insulation, infiltration, HVAC performances can be employed by analysing thermograms which corresponds to an objects surface temperature

Infrared radiation is emitted from the surface of an object and thermal cameras are used to detect the infrared radiation, which is being converted into a thermal image. Thermography can be used as a tool to quickly identify building defects without the need to undertake costly and possibly damaging physical exploratory investigations, provided there is sufficient difference in heat or mass transfer across a material or building fabric (Fox et al., 2014).

Thermal cameras measure surface radiations rather than the actual temperature and include features such as image collection, in-camera evaluation, non-contact, real-time and

permitting multi-point detection. The surface radiation reading of temperature is important in thermography as changes in temperature reading help to indicate potential abnormalities (Fox et al., 2014). Furthermore, Bianchi et al (2014) conveyed the advantage of infrared thermography being a useful tool to conduct in situ analysis as it allows a quantitative survey to evaluate the surface temperatures of the envelope. The qualitative analysis leads to the assessment of easily recognizable imperfections such as air infiltration, bad insulation, and mould (Bianchi et al., 2014).

The temperature viewed by the camera known as the apparent temperature is the temperature that is apparent to the camera under the conditions at the time and is only that of the target surface. There are factors that affect the apparent temperature and they include surface emissivity, internal climate, external climate and reflected temperature (Fox et al., 2014). These factors create a misunderstanding of thermal patterns, to avoid any reflection of the thermographer or people passing by resulting in the image, measurement is advised to be performed at an angle preferably a minimum of 5% to a maximum of 50%.

According to Kylili et al (2014), successful infrared thermography requires data input and they include Emissivity factor, the reflective temperature, atmospheric temperature, and relative humidity. Furthermore, specific environmental conditions are required for the inspection such as the temperature difference between the interior and the exterior of the building should be at least 10°C. To achieve this temperature difference, researchers such as (Fox et al., 2014; Kylili et al., 2014) suggested that during the winter period, investigations are better at night time and during the summer period, the investigation is better during the day

In the United Kingdom, thermography inspections are usually done during the cooler winter months of October to March and during the coolest part of the day after the sun has set. Furthermore, other requirements include;

- Wind speeds lower than 5m/s
- Ensure that the building surfaces are free from direct solar exposure both during and hours before the survey
- Thermography should be undertaken during cloudy conditions to avoid reflecting a clear sky.

There are two approaches to thermographic inspections and they are passive and active. A passive approach measures the temperature differences of a structure under normal conditions while an active approach measures the temperature difference of a structure using an external stimulus, which may be an external heat source. Active thermography as stated by Kylili et al (2014) may be further broken down into two: Pulsed thermography and Lock-in thermography. Passive building thermography can be broken down into traditional walkthrough, street pass by, perimeter walk around, aerial, automated fly pass, repeat, mock target and time-lapse (Fox et al., 2014).

Infrared thermography has been used by many researchers in the building industry to solve problems. This problem ranges from thermal bridging, moisture detection, and electrical or mechanical fault detection. Kylili et al (2014) further stated that thermography is used in the building industry to evaluate the thermal characteristics of buildings, detect air leakages, missing or damaged thermal insulation of buildings and also monitoring for the preservation of historical buildings and monuments.

2.12.1 Mechanism of infrared thermography

The infrared camera is a non-contact device that detects infrared energy (heat) and converts it into an electronic signal which is processed to produce a thermal image or video. An infrared camera is equipped with a radiometrically calibrated matrix of detectors that senses the infrared radiation coming from the set target (Grinzato, 2012). The infrared camera receives radiation not only from the object but also from the surroundings reflected through the surface and radiation of the object from the atmosphere (see Figure 2-13).

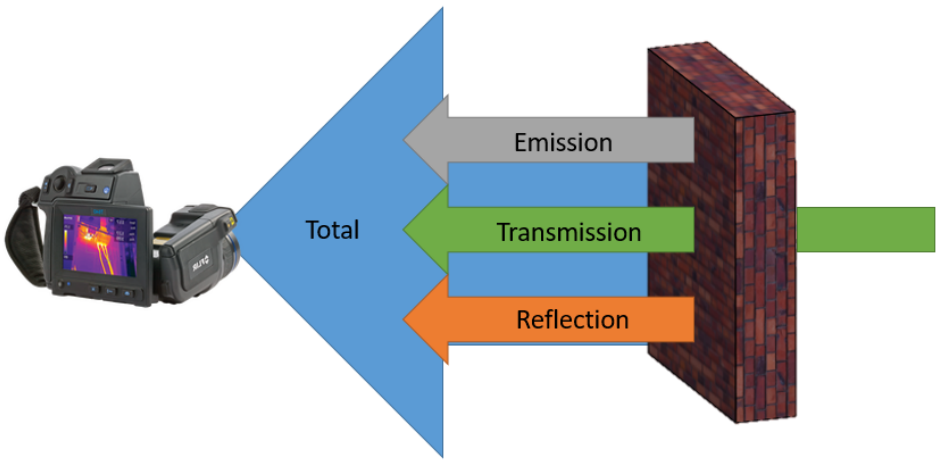

Figure 2-13:How infrared camera operates

Flir (2017) provided a description on the mechanism of infrared thermography using Figure 2-14. From the figure, (1) represents the surrounding, (2) the object, (3) the atmosphere and (4) the camera. An equation (Equation 2-33) was derived that gives the relationship between temperature (T_{source}), radiation power (W) and the camera output (U_{source}).

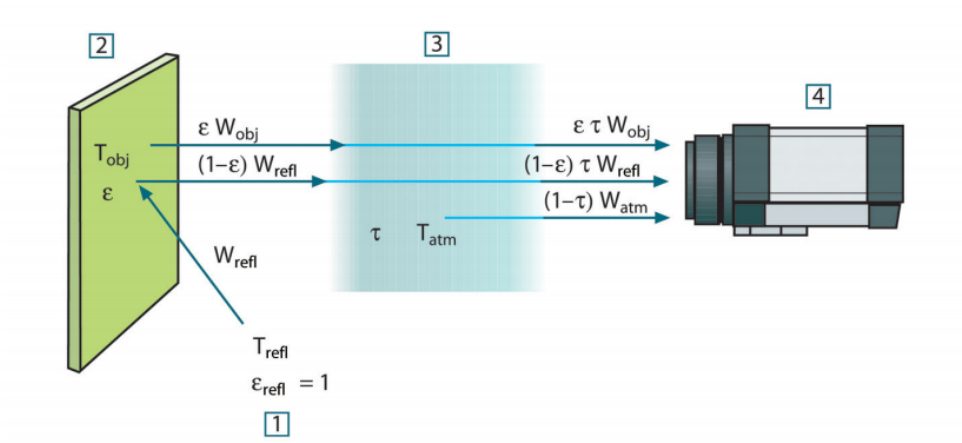

Figure 2-14: Schematic representation of the general thermographic measurement situation (Flir,2017)

$$U_{source} = CW\ (T_{source})$$ *Equation 2-33*

Where C is a constant. If the source is a graybody with emittance as Ɛ, the received radiation would be expressed as $ƐW_{source}$.

According to the temperature of the surface, the infrared radiation is partially emitted and partially reflected due to the optical characteristics of the surface, which is described by emissivity and absorptivity parameters (Grinzato, 2012). Emissivity is considered as the most important object parameter that affects thermography. It indicates the radiation of heat from a grey box according to Stefan Boltzmann Law, compared with the radiation of heat from an ideal black body. Objects materials and surface treatments (such as paints) normally exhibit emissivity in the range of 0.1 to 0.95. A value of 0.1 represents a reflective body, for instance, a highly polished mirror surface falls below 0.1 while a value of 0.95 represents a non-reflective surface.

As mentioned above, three radiation powers are received by the thermal camera which is from the object, surroundings, and atmosphere. Each of these parameters is expressed mathematically as follows;

Emission from the object: $\varepsilon\tau W_{obj}$ *Equation 2-34*

Where ε is the emittance of the object and τ is the transmittance of the atmosphere

Reflected emission from ambient sources $(1-\varepsilon)\tau W_{ref}$ *Equation 2-35*

Where $(1-\varepsilon)$ is the reflectance of the object

Emission from atmosphere $(1-\tau)\tau W_{atm}$ *Equation 2-36*

Where $(1-\tau)$ is the emittance of the atmosphere.

The temperature of the objects, ambient sources and atmosphere are T_{obj}, T_{ref} and T_{atm} respectively. From the above, the total received radiation power can be expressed as

$$W_{tot} = \varepsilon\tau W_{obj} + (1-\varepsilon)\tau W_{ref} + (1-\tau)\tau W_{atm} \quad \textit{Equation 2-37}$$

2.13 Summary

This chapter reviewed the various heat transfer mechanism in buildings and how they affect the energy consumptions in buildings. Sustainable buildings have been defined in different ways due to forms of target. The literature review highlights the different targets set by Government and individuals to achieve sustainable buildings. In other to achieve these targets, tools such as building energy simulation software are used. There are many software's available, such as EnergyPlus which was developed by the United States Department of Energy. The concepts behind energy simulation software are discussed. Several studies have been carried out using energy simulation software and infrared thermography to access the energy consumptions of buildings. However from the literature survey, there is no defined way (framework), on how these tools can be used effectively.

Chapter 3: Thermal bridges

3.1 Introduction

A thermal bridge poses a great influence on the total energy demand. To reduce or improve building energy consumption, certain interventions are required. They include improving the building thermal mass, increasing level of insulation and also the continuity of the insulation to avoid thermal bridge creation (Baba & Ge, 2016). With regards to the level of insulation In a building, Aguilar et al. (2014) mentioned that not only poorly insulated buildings are subject to substantial heat loss, but also well-insulated buildings. The losses may be due to thermal bridges characterised by complex configurations, joints, and assemblies. In another study, (Déqué et al., 2001) stated that the increase in the level of insulation of buildings increases the weight of thermal bridges in the overall energy consumption. Furthermore, Aguilar et al. (2014) conveyed the importance of appropriate analysis of thermal bridges to accurately evaluate the energy demand in buildings. Different researchers such as (Ge & Baba, 2015; T. G. Theodosiou & Papadopoulos, 2008) have identified that the problem of thermal bridges is not always dealt with properly. In this chapter, a review of thermal bridges, their effects and methods of analysing them are presented. The chapter aims to provide a summary of the current state of thermal bridges and identify the current limitations and challenges in the field.

3.2 Thermal bridge

One of the functions of a properly designed building envelope is to protect the inner space from harsh outdoor climatic conditions, hot and cold and also provide necessary thermal comfort to occupants. This is not necessarily the case in most buildings as some buildings lose heat or gain unwanted energy from the envelope. Sanea et al. (2012) stated that there are different ways that designers can reduce energy consumption. However, thermal bridges pose the highest threat to almost all measures taken to reduce the energy load.

According to EN ISO 10211, a thermal bridge is a discontinuity regarding the thermal physical properties of the building envelops, concerning the thermal resistance, due to material, thickness or shape variation. Thermal bridges as defined by Ascione et al. (2012) are critical parts of buildings, being envelope areas characterised by heat losses usually higher than those interesting the common walls. In general, one-dimensional heat transmission is lost. In another research, Ascione et al. (2012) described thermal bridges as criticisms of the building shell inducing heat flows, which are quite different compared to those interesting the current

walls. Furthermore, thermal bridges create areas of least resistance to the heat flowing through the building envelope (F. Sierra et al., 2015).

Dumitrescu et al. (2017) defined thermal bridge as areas in buildings that have a much higher heat transfer than the surrounding materials, thereby affecting the thermal insulation by causing a reduction in the overall U-value. Quinten et al. (2016) defined thermal bridges as part of the building envelope that has its U-value or R-value changed significantly by a full or partial penetration of the building envelope. This can be caused the presence of materials with higher or lower thermal conductivity, a reduction or increase in the thickness of the fabric and also differences between internal and external areas such as wall/floor/ceiling junction.

Bras et al. (2014) defined thermal bridges as high thermal conductivity elements or areas concerning a homogeneous multi-layer structure in which the heat flux should be perpendicular to the surface. However, according to Baba et al (2016), thermal bridges are created by repeated structural components in building envelopes and junctions between different components of the building envelope.

Nowadays, Buildings are designed and built using highly insulated material, Bianchi et al. (2014) observed that thermal bridges which are responsible for significant thermal losses affect the overall quality of a building. In thermal bridges, the most critical mechanisms for heat transfer are conduction between components. It is understood that heat from a higher temperature to a lower temperature is always transferred. Therefore, materials with higher conductivity, such as steel, transfer heat considerably higher than materials of lower conductivity. Moss (2007) further claimed that thermal bridges with high U-values might cause internal surface colouration and condensation in extreme cases.

Kosney et al. (2002) demonstrated that building energy simulation programs need to be improved to asses multi-dimensional heat transfer in buildings, especially concerning thermal bridges. This is because inaccuracy can affect the estimation of heat loads and seasonal energy requests (Ascione et al., 2013). Viot et al. (2015) stated that it is important to be able to correctly estimate heat losses and the inertia (which strongly affect comfort) due to thermal bridges

3.2.1 Thermal bridges classification

Authors have classified thermal bridges according to different criteria, which include the cause of the thermal bridge, location of the thermal bridge, the heat flow or the classification according to BS EN ISO 10211. Ascione et al. (2012) classified thermal bridges as bridges caused by material discontinuity and shape resulting in unregulated heat losses and hygiene problems. This could further result in the formation of vapour condensations and moulds. Furthermore, the author observed that on an estimate, thermal bridges would increase the energy needs of buildings and heat loads by 21%. Moreover Ge and Baba (2015) stated that up to 30% heating energy could be lost via thermal bridges for well-insulated residential buildings with high-performance windows and heavily insulated walls and roofs.

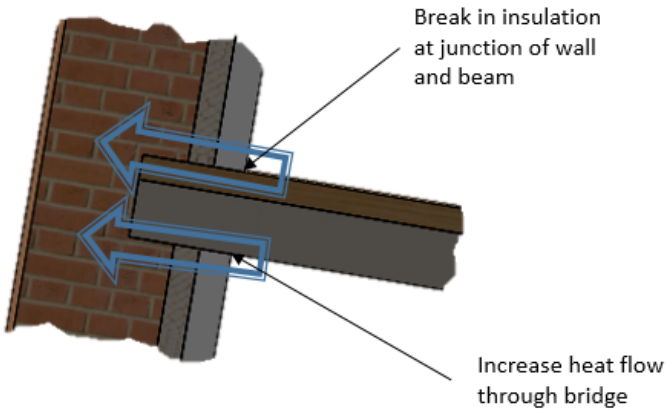

Figure 3-1: Heat flow through the thermal bridge

However, the heat loss and gain generated through thermal bridge depend on the method used to determine the effect of building energy demand estimation. Mao and Johannsson (1997) grouped thermal bridges in two, namely: thermal bridges within the building unit and thermal bridging between the joints of the structure.

According to Rosa et al. (2014), the use of advanced high-performance building material implicitly raises the effect of weak spots such as physical and geometrical thermal bridges in which the continuity of the system's integrity is undermined. Discontinuities of thermal insulations usually create thermal bridges as parts of building envelops and therefore have major effects on the thermal performances of these buildings. For example,

- Increased winter heat losses and summer heat gains
- The reduced temperature of the internal surface, thus increasing the risk of condensation and the production of mould in the wintertime.

(Ge & Baba, 2015)

Thermal bridges are known to cause a reduction in the overall thermal resistance and also affects the dynamic characteristics of the wall. The phenomenon of the thermal bridge as a result of mechanical and structural reasons according to Viot et al. (2015), these are

- The difference in thermal resistance
- Changes in material thickness loads
- Indoor and outdoor differences

Thermal bridges can be classified into two according to their effects on the building envelope, which are called linear and point thermal bridges ('BS EN ISO 10211 :2017). Larbi (2005) defined linear thermal bridges sometimes referred to as 2D bridges are those situated at the junction of two or more building elements and are characterised by a linear thermal transmittance value. Point thermal bridges which are sometimes referred to as 3D bridges are those that are situated in a wall pierced by a high thermal conductivity material or where three-dimensional corners occur and are defined by a point thermal transmittance

Anderson 2006 also categorised thermal bridges into repeating and non-repeating thermal bridges. Repeating and non-repeating thermal bridge differ according to how the additional heat flow caused by the thermal bridge is defined. For repeating thermal bridges, the additional heat flow is defined in the overall U-value while in the non-repeating thermal bridge, the additional heat flow is determined separately. Furthermore, CIBSE guide A defined repeating thermal bridges are those that occur at fixed intervals According to Ge and Baba (2015), thermal bridges can be categorised into two

- Thermal bridges created within the building envelope by the repetitive structural members.
- Thermal bridges created through the building junctions such as external walls and roof connections and also connections between balconies and external walls.

Ascione et al. (2013) further observed that the common thermal bridges are thermal bridges due to materials change, due to geometrical discontinuity or due to both geometrical discontinuity and material change as shown in Figure 3-2 below. However, Dumitrescu et al. (2017) stated that there are three ways in which thermal bridge develop, which are

- Via materials with a higher thermal conductivity than the materials surrounding them
- As a result of penetrations in the building envelope, and

- As a result of insulation gaps and discontinuities

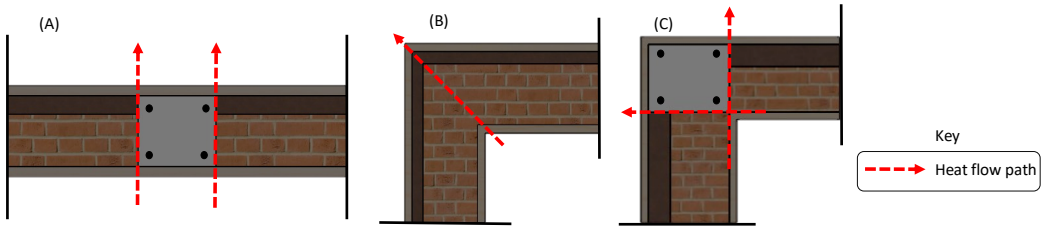

Figure 3-2: Diagrammatic illustration of common thermal bridges based on their causes (a) due to material change (b) due to geometric change and (c) due to both material and geometric

Moss (2007) observed that external walls might not have a thermal transmittance that is consistent over the wall area. Moreover, structural columns may form thermal bridges in a cavity wall. At these points, the rate of conductive heat flow is high compared with that of the wall. There are three types of thermal bridges

- Discrete bridges: these include lintels and structural columns which are flush with the wall or take up part of the wall thickness
- Multi webbed bridges: these include hollow building blocks
- Finned element bridges: where the structural column protrudes beyond the width of the wall

3.2.2 Combined Classification

Researchers have classified thermal bridges differently either according to their effects or their causes. This had led to differences relating to the identification of thermal bridges. This study aims to combine the classification of thermal bridges. The combined classification of thermal bridges due to how heat is lost from the envelope. Using the classification of EN ISO 10211 which are of two types namely linear thermal bridges and point thermal bridges. From the section above, Several researchers (Ascione et al., 2013; Dumitrescu et al., 2017) classified thermal bridges according to their causes which are due to material or geometry. The effect of linear thermal bridges depends on factors such as geometry, properties of materials, temperature variation in the environment and effect of heat transfer near the surface due to radiation and convection (Prata et al., 2018). This lead to further classifying point and linear thermal bridges according to the causes (see Figure 3-3 and Figure 3-4)

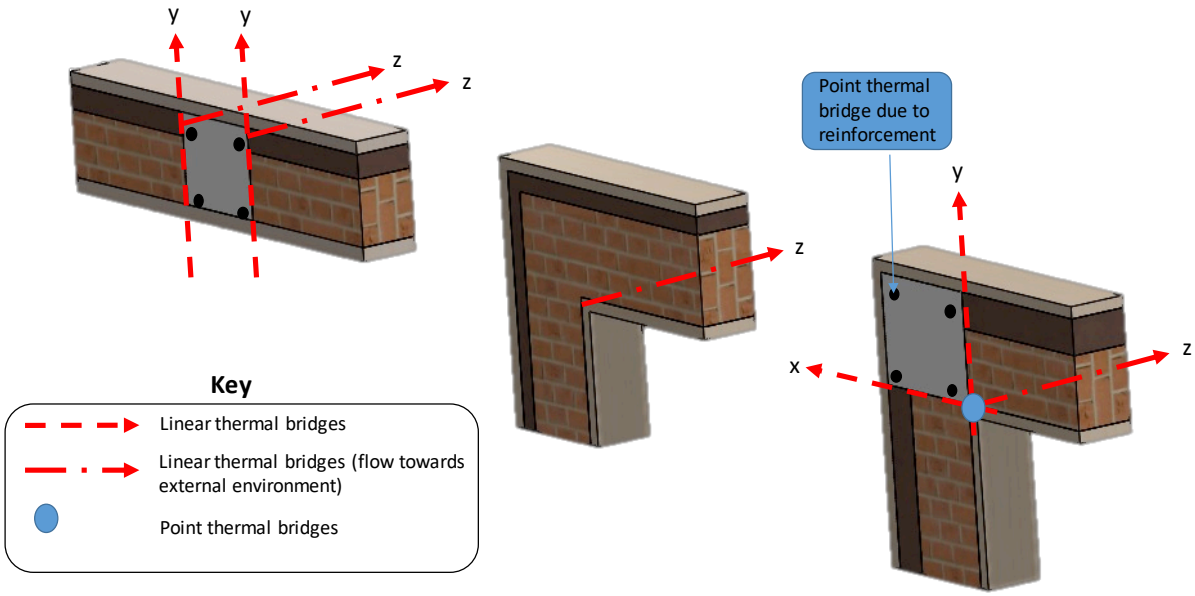

Figure 3-3: Thermal bridges flow pattern showing linear and point thermal bridging:

Ascione et al. (2012) stated that heat flux within the building envelope changes from one-dimensional to two or three dimensions as a result of discontinuities in material and building structure. Therefore, linear and point thermal bridges were further categorised according to their heat flow namely one dimensional, two-dimensional or three-dimensional heat flow.

When identifying a thermal bridge, it would be convenient to address the bridges as the heat flow pattern; cause and type to avoid confusion on the type of bridge. For example, a corner thermal bridge may be caused by geometry or material or a combination of both. Hence, the thermal bridge can be identified as a two-dimensional geometric linear thermal bridge, two-dimensional material linear thermal bridge or two-dimensional linear thermal bridge (caused by both material and geometry).

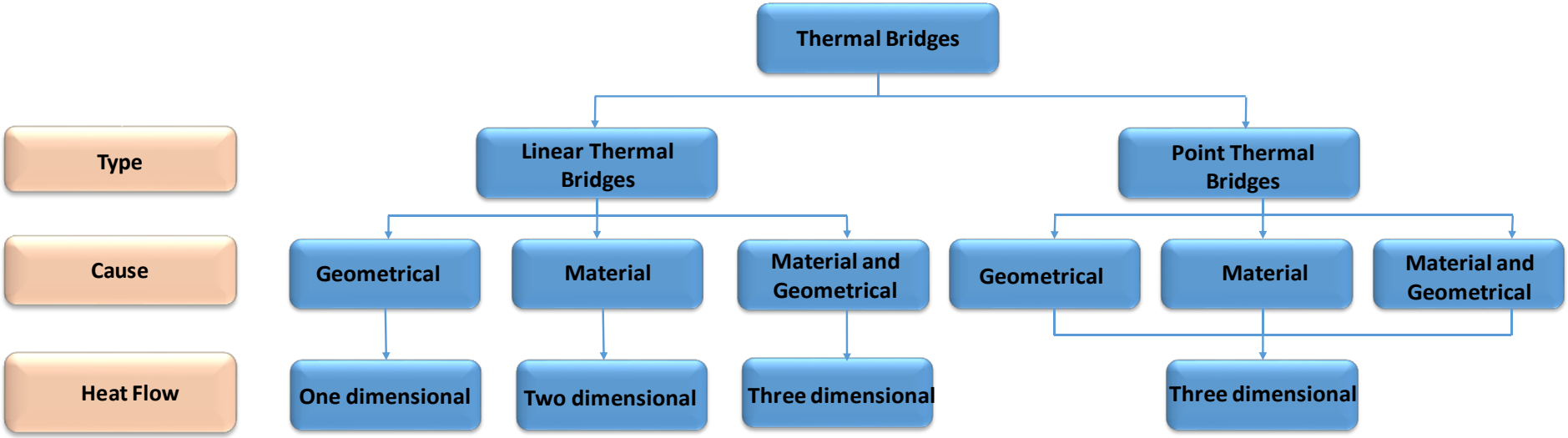

Figure 3-4: Classification of thermal bridges

3.2.3 Effects of thermal bridges so far

The effect of thermal bridges on energy performance has been described in several pieces of literature. Such effects include heat loss increase and the consequent risk of maintaining the structure, as stated by Ascione et al. (2013). According to Dumitrescu et al. (2017), many European countries do not consider the effect of thermal bridges on new buildings and even less on refurbished buildings in their regulations. Furthermore, Theodosiou and Papadopoulos (2008) revealed that most counties in Europe base their insulation standards and regulations on simplistic methods that reduce or ignore the effect of thermal bridges. This is because it can be difficult and time-consuming to calculate the heat loss from thermal bridges. However, with the need to reduce the CO2 emissions and increase energy efficiency, certain restrictions have been set for the building envelope by regulations within the European Union. This, in turn, leads to a significant influence of thermal bridges in the total energy demand of buildings as a result of the increasing level of insulation (Martin et al., 2011).

Table 3-1: EU countries and corresponding thermal bridge calculation approach

Country	**Approach**
Germany	Temperature factor f_{Rsi}
Denmark and the Czech Republic	Ψ_{max} values depending on joint type
France	Ψ_{max} values depending on building type
Romania	C107 Normative which includes an approximate, simplified, and detailed method
United Kingdom	EN 10211

There are different approaches for including thermal bridging in regulations of different countries regarding energy performances. These approaches range from simplified to detailed calculations with or without limiting values. Table 3-1 shows the approach used for thermal bridges in different countries across Europe. Bergero, Cavalletti and Chiari, (2017) noted that the European Commission had taken steps to reduce energy consumption by revising the Energy Performance Building Directives (EPBD) which are Directive 2002/91/EC, Directive 2010/31/EU and Directive 2012/27/EU. The standard EN 10211 proposes a methodology for a detailed calculation of thermal bridges. However, EN 14683 purposes a more simplified approach to thermal bridges which is the common method used in evaluating

thermal bridges. Ascione et al. (2012) observed that currently, EN ISO 10211 standard provides an adequate thermal bridge evaluation model. This is achieved using numerical methods which are centred on the finite-difference algorithms. The finite-difference algorithm is ideal for numerical evaluation of the thermal flow by properly assessing the effects of 2D and 3D discontinuity of the thermal resistance

Table 3-2: Simplified models of calculating thermal bridges according to different EU countries

Simplified Models of calculating thermal bridges in the EU	
Countries	**Approach**
Netherlands, Germany and Ireland	Adding to homogenous part of the envelope, an increase of thermal transmittance depending on the type of thermal bridge, thus considering an additional heat flow to the homogeneous part of the wall
Denmark, Norway and France	Limiting the value of the linear thermal transmittance depending on the type of thermal bridges. This will limit the added heat flow in a constructive solution due to the thermal bridge
Spain	Making a one-dimensional calculation of thermal transmittance of the thermal bridge and then pondering it with the remaining area of the homogeneous element
Sweden	Impact of thermal bridges are accounted for by increasing the calculated transmission heat transfer through building element by 20% regardless of the building system
Finland	Thermal bridges are accounted for by in the weighting thermal conductivity of different materials in calculating the transmission heat transfer through building elements

Martin et al. (2011) noticed that thermal bridges in most European countries are taken into account using simplifies procedures. In research by Kuusk et al. (2017), countries adopt simplified approaches (without considering thermal bridges) or use default thermal bridge (psi) values to calculate the energy losses as a result of thermal bridges thereby underestimating heat losses within the building envelope. Berggren and Wall (2013) surveyed the different methods of measurements and the influence of thermal bridges on the building heat transmission. Results revealed that the level of knowledge is not satisfactory, and no definite practice can be recognised as to which method is best suited and a need for simple and clear building regulations and guidelines developments. Furthermore, Martin et al. (2011) and Berggren and Wall (2013) outlined the simplified procedures used in some European countries as summarised in Table 3-2.

The effect of thermal bridges as identified by Martin et al. (2011) is still a problem that is ignored or not properly implemented in building energy calculations. Furthermore, Martin et al. (2011) identified that this is mainly due to the assumption that heat transfer via the building envelope is one-dimensional. It was also stressed by Gao et al., (2008) that assumptions on heat flow being one-dimensional causes an underestimation of the final heat loss coefficient by about 10-40% in various envelopes. The problem of not dealing with the effect of thermal bridges results in underestimating heat losses during the building design process, the insulation study and also leads to a higher estimation of energy requirements in practice (T. G. Theodosiou & Papadopoulos, 2008).

Studies have revealed that thermal bridges can cause up to 30% of extra thermal losses through the envelope during the winter period which in turn increases the energy heat demand (Bianchi et al. 2014; Theodosiou et al. 2008). Furthermore, according to the French CSTB (Scientific and Technical Centre for Buildings), thermal bridges are estimated to increase total heat demand by around 20% (Ascione et al., 2012). However, Martin et al. (2011) consulted diverse bibliography on thermal bridges and observed that the effect of thermal bridge varies from 5% to 39% in highly insulated residential houses with poor treatment of thermal bridge. In general, thermal bridges increases winter heat loss and summer heat gains (Larbi, 2005). Thermal bridges also affect that strength and durability of building envelope, which may arise as a result of sudden expansion or contraction, formation of ice dams and frost damage (Baba & Ge, 2016). Outcomes of researches show that U-values of walls and roofs assemblies are significantly reduced as a result of thermal. Thereby creating distortion on local temperature distribution and heat flow rate (Gao et al., 2008).

Thermal bridging does not only affect cold climate zone, Ge and Baba (2017) revealed that the presence of thermal bridges under cooler temperatures help dissipate the heat gained. Hence thermal bringing brings about a reduction in cooling loads.

Thermal bridges are known to cause condensation, mould growth, as mentioned by O'Grady et al. (2017a) and health problems due to the difference in the temperature gradient caused by the thermal bridge. This is because the temperature of the inner surface above a thermal bridge during summer is lower than that of the adjacent structure and vice versa winter. This was further stated by Sierra et al (2017), in which higher heat losses and a subsequent decrease in the internal surface temperatures are side effects of a thermal bridge. Ge and Baba (2016) also mentioned that thermal bridges increase buildings energy consumption, condensation risks and problems with thermal comfort. Furthermore, Bianchi et al. 2014 stated that the effect of weak spots within the building envelope is the presence of differentially cooled areas around thermal bridges, and therefore moulds and fungi develop, which result in poor indoor air quality conditions. Fantucci et al. (2017) investigated the influence of the insulating coat on mould growth as a result of thermal bridges using numerical analysis. Results reveal that the insulating coat prevents surface condensation and hence eliminates mould growth.

To assess the impact of thermal bridges on the building's energy performance, Hua et al. (2015) identified that the equivalent U-value method is the most used. The equivalent U-value method is used to modify the levels of insulation of a multi-layered one-dimensional envelope component so that its U-value is the same as the overall effective U-value of the thermal bridge envelope detail. Besides, the multi-layered component's material property is kept constant. Therefore, consideration is given to the effect of thermal bridges on the overall U-value, while ignoring the thermal inertia effect of the thermal bridge.

According to the CIBSE guide A, the relative effect of thermal bridging is becoming increasingly important with an increase in the thickness of insulation that is interrupted by the thermal bridge. Furthermore, Ge and Baba (2016) suggested that more effort should be made to design building envelopes with enhanced connection details to avoid thermal bridges, especially the envelope design has high levels of insulation and advanced windows.

Ascione et al. (2012) investigated and proposed a methodology on how an hourly energy simulated software such as EnergyPlus could be integrated with other software such as ANSYS FLUENT to solve thermal bridges. Ascione et al. (2012) proposed two different ways to achieve this, which are

- Modification of the EnergyPlus source code. The software will subtract its area by the common surface when the user indicates a thermal bridge and create a new sub-surface.
- For each time step, by using an autonomous sub software. A simulation will be conducted using hourly climatic data and a defined set point for the indoor air concerning the entire season. In parallel, the conventional simulation will be carried out by EnergyPlus. An additional load is considered as a result of the thermal bridge effect through modification of the term Q *(internal convective loads)* by defining a new *"energy gain or loss"* device. The new device will provide a thermal flux equivalent to the number of thermal bridges in the area, minus the heat flow already considered as EnergyPlus has not altered the wall surfaces after which a final simulation is performed.

The construction of a building defines if and how a thermal bridge may affect the envelope. Branco et al. (2004) used Boundary element method (BEM) to evaluate the transfer of heat and vapour through a brick wall. By using two different BEM discretisation models, a brick wall supposed to consist of a series of homogeneous layers bonded together revealed that the horizontal mortar strip between bricks serves as a thermal bridge. The result was observed only when the brick modelling took into account the brick's various material properties. In another study, Kosny and Christian (1995) observed that the U-value of a concrete wall reinforced with steel profiles decreases the resistance by around 48% due to the iron thermal bridge effect. Al Sanea and Zedan (2012) used finite volume methods to investigate the effect of thermal bridges caused by mortar joints cutting across insulation layers. The implications of mortar joint heights in the region of 0 to 20mm for a wall with an insulation thickness of 75mm was explored using Riyadh climatic data. Results revealed that the percentage increase in heating and cooling transmission loads was approximately equal to an increase in mortar joint height and an increase in transmission loads of 62% and 103% for 10 mm and 20 mm (respectively) mortar height relative to a wall without mortar joints.

Thermal bridges have to be implemented in transient simulations in other to understand the effects of thermal bridges fully. Martin et al. (2011) observed that the implementation of thermal bridges in the construction of energy simulations concerning transient aspect is difficult. This as a result of multi-dimensional flow characterisation. In general, Martin et al (2011)concluded that the problem of including the dynamic impact of thermal bridges in building energy simulation programs is categorised into two, which are:

- Simulation Programs solve one -dimensional heat transfer equations, while
- Thermal bridges produce multi-dimensional heat flow

Martin et al. (2012) developed and compared five numerical models for two thermal bridges of different types. The two thermal bridges differed with one having identical inertia with the homogeneous wall while the other thermal bridge has much lower inertia. The finite element software FLUENT was used to perform dynamic simulations for the two thermal bridges. Results showed that there is no hybrid model that can accurately describe the dynamic state of all types of thermal bridges.

Ge and Baba (2016) used a WUFI Plus software to examine the effect of thermal bridges on the energy efficiency of a high rise building. The balcony slabs comprising 60 percent of the perimeter of a typical floor were analysed using the direct 3D modelling and equivalent U-value method. It was inferred from the results that the dynamic effect of thermal bridges affects the cooling load much more than the heating load. Also, the dynamic effect of the balcony slab on energy efficiency was observed to increase with the increase in the number of thermal bridges and better-insulated envelopes. Nevertheless, the gap in energy performance as a result of the modelling approach has been minimised with the enhancement of the balcony design by introducing thermal breaks. Thermal bridges do not only affect cold climates as Baba and Ge (2016) stated the importance of minimising thermal bridges for all climates.

Ascione et al. (2012) compared results obtained using simplified 1 D models with sophisticated 2 D and 3 D models in order to point out differences in terms of equivalent conductivity and thermal transmittance. Furthermore, three different approaches were used to analyse a thermal bridge represented by a roof structure for a typical office building. It was observed that an overestimation of the heat losses, determined by an approximate evaluation, induces higher cost of refurbishing, higher cooling energy requests in summer

and minor thermal comfort in naturally ventilated buildings. Therefore, in conclusion, the outcomes of the research showed that proper modelling is necessary.

Deque, Oliver and Roux (2001) studied a modelling approach to adequately assess the impact of thermal bridges on the building's energy performance. This was achieved by modelling 2D heat transfers in walls to observe and analyse the thermal bridges and integrating the model into Clim 2000 (a building energy simulation software). This approach was applied to a case-study and results revealed that by considering 2D thermal bridge models, the accuracy of the heat losses increased by about 5-7%.

In dynamic energy simulation, Ascione et al. (2012) proposed a new method for implementing bi and three-dimensional heat transfer. The proposed methodology includes a theory of state representation of transfer functions and further simplifications to reduce computational time. The simplification assumes that nodal temperature is not affected during the time interval between consecutive simulation steps by variations of environmental inputs. Two thermal bridges were analysed, comparing numerical solutions using FLUENT (Finite Volume Method) with the proposed methodology. Due to discontinuities in both material and geometry, the thermal bridges show bi-dimensional heat flows.

Ascione et al. (2012) analysed the effect of various modelling techniques on the energy efficiency of an office building for a typical roof thermal bridge. The roof structure made up of a mixed layer of iron plate, reinforced concrete and extruded polystyrene was modelled in three different:

- Using an equivalent homogeneous structure
- Detailed subdivision in "in series" and "in parallel" layers
- Numerical modelling of actual structure using FLUENT

The results of the thermal bridge analysis were implemented in a building energy dynamic simulation, that yielded varying results. The results showed that depending on the modelling approach; the energy demand is somewhat variable.

Dumitrescu et al. 2017 assessed the effects of the thermal bridge in the thermal rehabilitation process, using numerical modelling of the thermal field and thermal bridge catalogues. This was achieved by studying two representative educational buildings in which different degrees of thermal insulation were proposed, and specific energy indicators were calculated. Seven retrofitting scenarios by adding supplementary external insulation layers

on the building envelope were proposed. It was observed that even when thermal rehabilitation measures were well implemented, the thermal bridges in the building envelop remains a weak part in the construction. Connections of structural elements were observed to often lead to high heat losses and low surface temperatures in the room.

Ramalho et al. (2018) evaluated the impact of thermal bridges of reinforced concrete structure on the thermal energy performance of a residential building in southern Brazil. This was achieved using three different possibilities to model the thermal bridge in energy plus software. The first approach was to model the building considering the shape of the structure where the thermal bridges occur. The second approach, defined as a simplified approach, was modelled using the equivalent wall method. This considers only the thermal transmittance of the building's masonry wall. The third approach was similar to the second, but the thermal transmittance of the wall was increased based on the standard EN ISO 10211. Results showed that the third approach has the highest energy consumption when compared to the others as this considers the thermal bridge effect. It was concluded that modelling in the traditional way (approach 2) leads to an underestimation of the thermal effect on the energy consumption of buildings. However, results showed that when the approaches were compared to a building with high and less insulation, approach one overestimates the consumption for a less insulated building and underestimates the consumption for a highly insulated building. Therefore the authors concluded that the first approach is not suitable for energy modelling as it can underestimate or overestimate the energy consumption.

Kotti, Teli and James (2017) analysed the impact of thermal bridging on the overall heating load of a single-family building using TRNSYS. Results showed that the thermal bridges increased by about 13% of the overall annual heating load. Retrofit solutions such as external insulation and introduction of south solar greenhouses produced a 4-10 percent reduction in the annual heating energy demand.

Walls are not the only building components to be affected by the presence of thermal bridges. Thermal bridges can occur from windows and door (mainly due to positioning and frames). Cappelletti et al. (2011) analysed the incidence of window installation due to the installation configuration on its thermal performance by quantifying the percentage increase in thermal transmittance of the window. The position of the window plays an important role; results show that the linear thermal transmittance reduced by up to 70-75% by switching the window from internal to external positions.

Angelis et al. (2014) revealed that the thickness of insulation layers is the most important parameter. Thermal transmittance growth of approximately 35% in various cases with an increase in insulation layers. Steel studs were observed to have contributed the highest in the thermal transmittance of the walls.

3.3 Thermal Bridge Analysis

Thermal bridges are analysed in different ways according to standards. The International Standard EN ISO 14683 states three different ways in which thermal bridges can be evaluated. These are:

- Numerical calculation of the coefficient values (Linear and Point thermal transmittance)
- Previously assessed and ready to use catalogues of thermal bridges in the standard
- Steady-state calculations using computer simulations

Martin et al. (2011) identified that quantifying the heat loss and gain generated by thermal bridges is heavily dependent on the method used in the calculation of building energy demand to implement the thermal bridge effect. Therefore, the accuracy of the analysis is dependent on the method adopted. According to EN ISO 14683, numerical calculations have an accuracy of about ±5 %, thermal bridge catalogues and manual calculations have an accuracy of ±20% while default values have an accuracy range of 0-±50%. The most common method used according to Ascione et al. (2012) is the thermal bridge catalogue.

The standard guides on the appropriate method to be used, this guidance are outlined below

- In scenarios where details are not yet designed, but the size and form of the building is defined, such that areas of roofs, walls and floors are known. Then a rough estimate of the thermal bridge contributions to the overall heat loss can be made
- In scenarios where there is sufficient information, more accurate values of the linear thermal transmittance for each linear thermal bridge can be obtained by comparing the detail with the best fitting example from the thermal bridge catalogue. Manual calculation method can also be used in this case.

The accuracy of the calculations is not only dependent on the type of method (numerical, simplified or manual) used but also due to the measuring method. Measuring method in the thermal bridging calculation may be due to internal or external measurements. In the standards for energy calculations, there is no defined correct measuring method as observed by Berggren and Wall, (2013). The authors noted that if internal measurements are used, the

proportion of thermal bridges is always the highest irrespective of exterior wall construction (Berggren & Wall, 2013)

Over the years, thermal bridges have been analysed in different ways that include but not limited to the following; numerical analysis, experimental analysis, analysis using building simulation etc. in some cases, two or three methods are combined to evaluate the effect of thermal bridges. Table 3-3 summarises the outcomes of the papers reviewed in this chapter. The review includes the type of analysis used and type of thermal bridge analysed. It can be observed that 56% of the papers were analysed using numerical analysis, 19% with infrared thermography, 13% with experimentation, 3% using building energy simulation software and 29% using other analytical methods. A combination of methods is also employed to analyse thermal bridges with 13% of the papers reviewed using two or more methods.

The effect of thermal bridges, according to the researchers, were also summarised according to the increase in energy or heat demand on a building. Out of a total of 51 reviewed papers, 23% provided details on the impact of thermal bridges on the energy or heat losses. The effect of thermal bridges on the energy demand or heat demand ranges from 5% to 42% as shown in Table 3-3.

3.3.1 Thermal bridging hand calculation

Thermal resistivity and transmittance are used when calculating thermal bridges. Thermal resistivity (R-Value) is identified as a key parameter used to characterise the effectiveness of the building envelope in terms of heat transfer and therefore, thermal bridge effects. The widely used R-value, however, is based on steady-state conditions and is therefore constant for a given structural configuration and surface conditions (Al-Sanea & Zedan, 2012).

Table 3-3: Review of thermal bridges

SUMMARY OF REVIEWED THERMAL BRIDGE PAPERS												
S/N	Author	Year	Thermal bridge type			Analysis Method					Increase in Energy Demand/Heat Losses
			Linear	Point	other	Numerical	Infrared thermography	B.E.S	Experiment	Other	
1	Mao et al	1997	×	×	×	×	×	×	×	Frequency response method	×
2	Deque et al	2000	×	×	×	✓	×	×	×	×	×
3	Deque et al	2001	×	×	×	✓	×	×	×	×	5-7% increase in heat losses
4	Branco and Tadeu et al	2004	×	×	×	×	×	×	×	Boundary Element method	×
5	Larbi	2005	×	×	2D	✓	×	×	×	Statistical Analysis	×
6	Theodosiou et al	2008	×	×	×	×	×	×	×	×	×
7	Gao et al	2008	×	×	×	✓	×	×	×	×	9-19% increase in heat losses
8	Totten et al	2008	×	×	×	✓	×	×	×	×	26.2% increase in heat losses
9	Zalewski et al	2010	✓	×	×	✓	✓	×	×	×	×
10	Tadeu et al	2011	✓	×	×	×	×	×	×	Boundary Element method	×
11	Cappelleti et al	2011	×	×	×	✓	×	×	×	×	Savings of 8.3% and 7.9% in annual primary energy demand in comparison with building with thermal bridge
12	Evola, Margani and Marletta	2011	×	×	×	×	×	✓	×	×	×
13	Marttin et al	2011	×	×	×	✓	×	×	×	×	×
14	Asdrubali et al	2012	✓	×	×	✓	✓	×	×	×	×

15	Ascione et al	2012	✓	×	×	✓	×	×	×	×	×
16	Martin et al	2012	×	×	×	×	×	×	×	Equivalent wall method	×
17	Martin et	2012	×	×	×	✓	×	×	×	Equivalent wall method	Increase in transmission loads by 63% and 103% for 10mm and 20mm mortar joint height
18	Al-Sanea and Zedan	2012	×	×	×	✓	×	×	×	×	Heat transfer losses of about 2-17% for concrete walls with external insulation, 7-27% for wooden frame walls with insulation and 14-39% for precast concrete sandwich walls
19	Berggren and Wall	2013	×	×	×	✓	×	×	×	Survey	×
20	Ascione et al	2013	×	×	L & T Shaped	×	×	×	×	×	×
21	Capozzoli et al	2013	×	×	×	×	×	×	×	Sensitivity Analysis	9% increase in heat losses
22	Bianchi et al	2014	✓	×	×	×	✓	×	×	×	×
23	Ascione et al	2014	×	×	L-Shaped	✓	✓	×	✓	×	×
24	Aquilar et al	2014	×	×	×	×	×	×	×	Equivalent wall method	×
25	Bras et al	2014	✓	×	Structural	×	×	×	✓	Boundary Element method	×
26	De Angelis et al	2014	×	×	×	✓	×	×	×	×	×
27	Garay et al	2014	×	×	×	✓	×	×	✓	×	×
28	Bruma et al	2015	×	×	×	✓	×	×	×	×	×
29	Boafo et al	2015	×	×	×	×	×	✓	×	×	Annaul heating load increases by 18% in cold climate and increase by 30% in hot climate. The annual cooling load increases by 20%
30	Baba and Ge	2015	×	×	×	✓	×	×	×	Equivalent U-value and wall	×

31	Marincioni et al	2015	×	×	×	✓	×	×	×	×	×
32	Theodosiou et al	2015	×	✓	×	✓	×	×	×	×	×
33	Sierra et al	2015	×	×	×	✓	×	×	×	×	×
34	Quinten et al	2016	×	×	×	×	×	×	×	Equivalent wall method	û
35	Dikarev et al	2016	×	×	×	✓	×	×	✓	×	13% increase in annual heating load
36	Baba and Ge	2016	×	×	×	✓	×	×	×	Equivalent U-value method	Increase in heat losses between 7-11% due to window frame positioning
37	Zedan et al	2016	×	×	×	×	✓	×	×	×	The inclusion of thermal bridges increased space heating by 38.9% - 42.4% and space cooling reduced by 8.4% - 25.6%.
38	Kotti et al	2017	×	×	×	✓	×	×	×	×	×
39	Sierra et al	2017	✓	×	×	✓	×	×	×	×	×
40	Ge and	2017	×	×	×	×	×	×	×	×	×
41	Kuusk et al	2017	×	×	×	×	×	×	×	×	×
42	O'Grady et al	2017	×	×	×	✓	✓	×	✓	×	×
43	O'Grady et al	2017	×	×	×	×	✓	×	✓	×	×
44	Dumitrescu et al	2017	✓	×	×	✓	×	×	×	×	×
45	Theodosiou et al	2017	×	✓	×	✓	×	×	×	×	×
46	Fantucci et al	2017	×	×	×	✓	×	×	×	×	×
47	Ramalho et al	2018	×	×	×	×	×	×	×	Equivalent method	×
48	Garrido et al	2018	×	×	×	×	✓	×	×	×	×
49	Baldinelli et al	2018	✓	×	×	×	✓	×	×	×	×
50	Prata et al	2018	✓	×	×	×	×	×	✓	Boundary Element method	×
51	Sfarra et al	2018	×	×	×	×	✓	×	×	×	×

For walls with a discrete bridge (see Figure 3-5 top), the average thermal transmittance

$$U = P_1.U_1 + P_2.U_2 \qquad \textit{Equation 3-1}$$

Where P_1 is Unbridged area/ total area and P_2 is Bridged area/ total

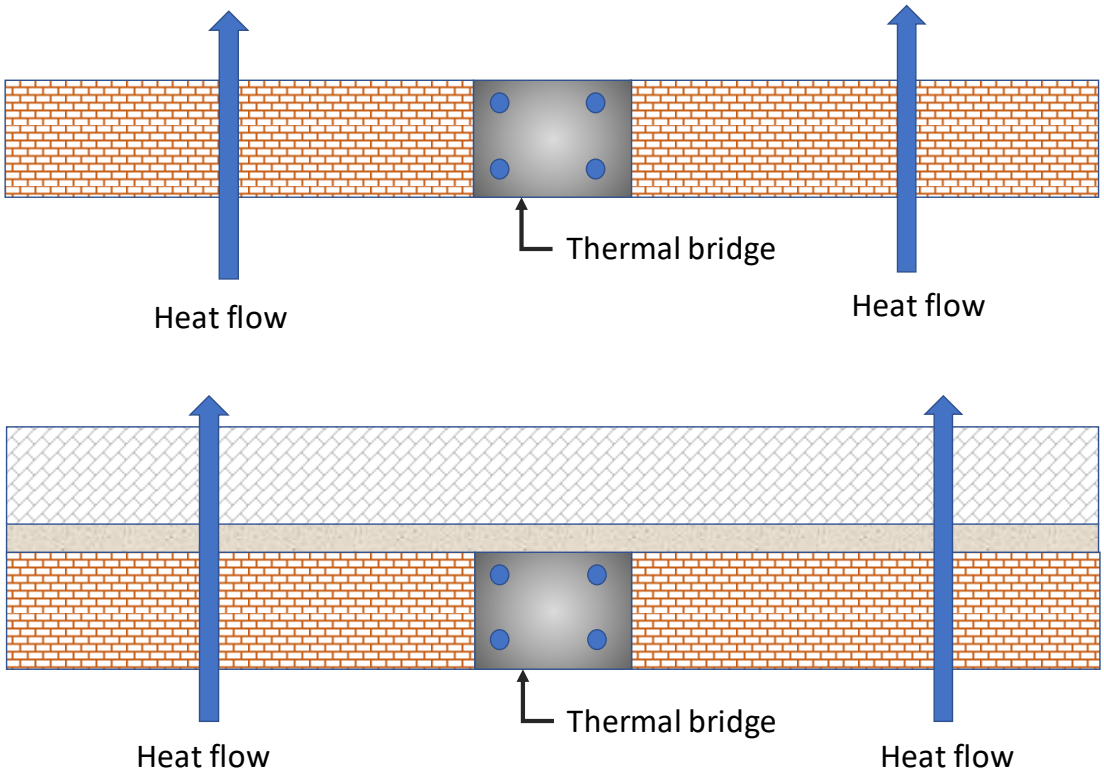

Figure 3-5: Brick wall with a concrete pillar as a thermal bridge (top) and twin wall with pillar thermal bridge (bottom)

The bridged area P_2 the calculation involves the surface area of the protruding part of the thermal bridge for a twin leaf wall with a discrete bridge in one of the leaves (Figure 3-5 bottoms)

$$U = \frac{1}{(R_b + R_h)} \qquad \textit{Equation 3-2}$$

Where

$$R_b = bridged\ resistance = \frac{1}{\left(\left(\frac{P_1}{R_1}\right) + \left(\frac{P_2}{R_2}\right)\right)} \qquad \textit{Equation 3-3}$$

$$R_1 = R_{si} + \frac{L}{k} + 0.5R_a \qquad \textit{Equation 3-4}$$

$$R_2 = R_{si} + \frac{L}{k} + 0.5R_a \text{ (Bridged)} \quad \textit{Equation 3-5}$$

$$R_h = homogeneous\ resistance = R_{so} + \frac{L}{k} + 0.5R_a \quad \textit{Equation 3-6}$$

The Building research establishment provides the basis for U-value calculation in their report BRE 443 by Anderson (2006). In the report, mortar joints were advised to be treated as a bridging material as it is regarded as a repeating thermal bridge. However, there are conditions about the treatment of mortar joint which are;

- Joints may be disregarded if the thermal resistance of the mortar joint (bridging material) and the brick or block wall (bridged material) is less than 0.1 m^2K/W
- Joints may be disregarded when the thermal conductivity of the masonry units is greater than $0.5W/mk$, and the thickness of the blocks or bricks is not more than $105mm$

The second condition was stated to apply to almost all brickwork and walls built with dense masonry units. For mortar joints that are to be included, the fraction of mortar is calculated as shown below

$$1 - \frac{b_L x b_H}{(bb_L + joint\ thickness)x\ (b_H + joint\ thickness)} + 0.001 \quad \textit{Equation 3-7}$$

Where b_L and b_H are block length and block height, respectively.

3.3.2 Thermal transmittance involving steel frame

For steel frame constructions, Doran and Gorgolewski (2012) provided the guidance in calculating the U-value in the Building Research Establishment digest (465). The method used for calculating the thermal transmittance is centred on the proportional area method described in BS EN ISO 6946.

Using the upper and lower limits of thermal resistance, the total thermal resistance for a warm frame construction where the steel frame does not bridge the insulation is given by

$$R_T = 0.5R_{max} + 0.5R_{min} \quad \textit{Equation 3-8}$$

The thermal transmittance thereby is

$$U = \left(\frac{1}{R_T}\right) + \Delta U \quad \textit{Equation 3-9}$$

Where ΔU is a U-value correction for metal fixing and air gaps, the equation used for calculating the corrections is given in Chapter 4.

However, for cold and hybrid frame construction, the total thermal resistance differs from the warm frame as the proportion method is used (see Equation 3-10)

$$R_T = pR_{max} + (1-p)R_{min} \qquad \textit{Equation 3-10}$$

Where the proportion (p) is calculated using

$$p = 0.8\left(\frac{R_{min}}{R_{max}}\right) + f_w - 0.2\left(\frac{600}{s}\right) - 0.04\left(\frac{d}{100}\right) \qquad \textit{Equation 3-11}$$

where f_w Is a coefficient that differs as in terms of the flange width. The term f_w Is 0.32 if the flange width does not exceed 50mm and 0.24 when the flange widths are above 50mm but are not known to exceed 80mm. The stud spacings are denoted by s, and the stud depth is denoted by d

3.3.3 Numerical calculation for thermal bridges

Thermal bridges are known to usually occur were, i) the presence of high conductivity materials, ii) due to geometry iii) heat flows are two or three dimensional. Simple calculations may not be satisfactory in these cases to assess the envelope's thermal performance, and numerical modelling is therefore essential for the envelope analysis.

Using numerical analysis, thermal bridges can be calculated, and it involves the use of numerical resolution methods such as finite element analysis or finite difference methods and also the boundary element method. Standards such as EN ISO 10211 and BRE 497 specify how numerical modelling to analyse thermal bridges can be used accurately. From BRE 497, the concept of 2D is essential, where there is a linear thermal bridge. This is because it is much easier and quicker to specify a detail in 2D rather than 3D. However, a 3D model may be necessary and suitable to analyse the influence of repeating thermal bridges. An accurate numerical method is introduced in the standard EN ISO 10211 which can be used to assess three-dimensional temperature over a thermal bridge. In other to assess the extent at which thermal bridges intervene, it is important to identify as accurately as possible the physical and geometrical configuration of the areas affected and determine the linear coefficient of heat transfer by numerical simulations of temperature fields (Dumitrescu et al. 2017).

The numerical solution provides a response to problems identifies by researchers such as (Déqué et al., 2001). The problem which is standard configurations and calculation modes are not often enough to classify, calculate and consider innovative building and insulation techniques relating to thermal bridges. Furthermore, the use of fixed tabulated values as that of EN ISO 10211 can result in underestimating heat losses caused by the thermal bridge.

Building energy simulations such as EnergyPlus, TRNSYS and CODYBA 6.0 solve heat transfer through walls by considering one-dimensional heat flows and neglecting thermal bridges in which the accuracy of the analysis using dynamic energy simulation is strongly limited. Therefore building energy simulation programs have limits about thermal bridges evaluation according to the hypothesis of one-dimensional heat transfer and so three-dimensional heat transfer models must be included in the simulation programs (Ascione et al., 2013; Gao et al., 2008).

There are different numerical methods capable of analysing thermal bridges, these are

- Finite element methods (FEM) and Finite Volume Methods (FVM): these are precise in solving multi-dimensional heat transfer.
- Computational Fluid Dynamics

According to the standard EN ISO 13786, it states that "The calculation of dynamic thermal characteristics of non-plane components and components containing significant thermal bridges will be made by resolution of the heat transfer equation with periodical boundary conditions. To this end, the rules in conjunction with numerical methods (such as finite element method or finite difference method) refer to the model set out in EN ISO 10211". Furthermore, it states that thermal bridges generally used in building components do not significantly affect the dynamic characteristics of the wall and hence can be ignored. The two statements seem to create a contradiction, as observed by Martin et al. (2011). The standard specifies that the transient thermal bridge study can be ignored while in the first statement, it states that numerical methods with periodic boundary conditions will calculate significant thermal bridges.

Using a low order model developed using state reduction techniques (Gao et al., 2008) implemented the effect of thermal bridges by coupling the model with a one dimensional model with TRNSYS software. Additional heat losses with the model due to thermal bridges were between 9% to 19%.

Ascione et al. (2013) produce a simplified method to the conduction transfer function methods which produced an accurate and rapid process for calculating bi-dimensional heat flows. The method's reliability was validated using finite volume methods on two thermal bridges. Furthermore, Ascione et al. (2014) studied an L-shaped thermal bridge using a numerical code validated by comparing with experimental measures. The thermal bridge was identified using infrared thermography. For the experimental study, heat flux sensors were

placed on the internal surface of the wall, heat flow meters placed to ensure the one-dimensional regime of the heat flux and temperature probe was used to monitor the internal and external temperatures. Results revealed that the numerical code was reliable and accurate as comparisons with the experimental results were satisfactory. The percentage of deviations obtained when comparing the methods ranges from -12% to +6%.

Kosney et al. (1995) investigated several thermal bridges of metal studs wall with the use of finite element models and proposed correct average values of thermal resistance. Sierra et al. (2017) confirmed the importance and investigated the impact of the location of the window as this represents a thermal bridge and an area with high surface condensation risks due to the distortion of the temperature of the surface in the area. The author used numerical software called HEAT2D, to analyse the impact of thermal bridges. Results showed that there was an increase of between 7-11% heat losses due to the position of the window frames. Furthermore, the simplified method underestimates heat losses by up to 33%.

Boundary element methods have been used in different studies to analyse thermal bridges such as (Branco et al., 2004; Prata et al., 2018; Tadeu et al., 2011). According to Tadeu (2011), boundary element method allows for a compact description of the region of interest and discretising only heterogeneities of the material. Boundary element method reduces the size of the system of equations to be solved in comparison with the finite element methods. A disadvantage of the boundary element method is that when the fundamental solution is known, it can only be applied to more general geometries.

Using the boundary element method Tadeu et al (2011) investigated the transfer of heat across a concrete wall involving a thermal bridge. Three case studies were studied, a wall without thermal insulation, the wall with thermal insulation on the outer surface and wall with thermal insulation on the inner surface. Results revealed that computations under steady-state underestimates the linear thermal transmittances and overestimates the surface of the wall near the thermal bridge.

Branco et al. (2004) used the boundary element method to analyse the steady-state heat and moisture diffusion across a double brick wall. Results revealed that the horizontal mortar strip between bricks acts as a thermal bridge. This can only be seen if the brick modelling takes into account various properties of the brick material. Prata et al. (2018) experimented on the dynamic thermal behaviour of a linear thermal bridge in a wooden building corner using a calibrated hot box. The result of the experiment was compared with a boundary

element model. Results revealed that near the corner linear thermal bridges, the influence of thermal insulation is greater than in the centre of the panels. In a thermal bridge, the amplitudes of the surface temperature and heat fluxes in the inner wall are greater when thermal insulation is applied

Deque et al. (2000) performed a two-stage approach to modelling thermal bridges, which involved using Sisley and CLIm2000. The accuracy of heat losses improved by 5-7%, taking into account the 2D models of thermal bridges. Dikarev et al. (2016) performed a numerical and experimental analysis on a joint connection between floor slabs with thermal breaks. The thermal breaks provided a buffer of about 8C which protects the hot zone from heat losses. Larbi (2005) used statistical models and computer models (using BISCO) to calculate the linear thermal transmittance of three thermal bridges. The regression models produced results with relative errors of less than 3%.

Equivalent U-Value Method and wall method

Researchers have used equivalent wall method developed by Kossecka and Kosney (1997) (Aguilar et al., 2014; Ge & Baba, 2017; Martin et al., 2012; Quinten & Feldheim, 2016) to analyse thermal bridges. This method is centred on the definition of a multi-layered wall with the same dynamic and steady behaviour as the original solution, which can be substituted for the complex structure in building energy simulation. This is achieved by calculating the equivalent thermal properties of different homogeneous layers of the wall (Martin et al., 2012).

A technique was developed by Martin et al. (2012) to quantify an equivalent wall with the same dynamic behaviour of a thermal bridge. The thermal properties of the equivalent wall are calculated using thermoelectric analogy and solving state equations using system identification. Aguilar et al. (2014) showed that the equivalent wall method applies to thermal bridges high inertia models provided that the thermal properties of the equivalent walls are correctly calculated by modifying the method. The modified method was further by Aguilar et al. (2014) used by Ge and Baba (2017). Quinten et al. (2016) compared different ways to determine an equivalent wall by testing them on simple 1-dimensional structures. A mixed-method was proposed which is inspired by structural factor and harmonic methods. The equivalent wall methods have been tested by the researchers above and have concluded that it provides the same thermal behaviour as the thermal bridge though the methods have been used on simplified models and not whole building energy simulation models.

The equivalent U-value method is another method for solving thermal bridges. The equivalent U-value method involves adjusting the thermal transmittance of a multi-layered one-dimensional envelope component to match the effective overall thermal transmittance of the envelope. In this case, the effect of thermal bridges on the overall thermal transmittance is considered with the thermal inertia effect is ignored (Ge & Baba, 2017). Purdy and Beausoleil-Morrison (2001) developed a further improvement to the equivalent U-value method called the Combined thermal properties method (CTP). Ge and Baba (2017) used a two-dimensional conduction transfer analysis program called THERM to represent thermal bridge junctions.

Equivalent U-value and wall method were compared by Ge and Baba (2017), which revealed that the equivalent wall method performs better than the U-value method. Using the equivalent U-value method, it was further observed to underestimate the annual space heating energy demand and overestimate the annual space cooling demand.

3.3.4 Linear thermal transmittance and Point thermal transmittance

To fully understand and assess the effect of thermal bridges, A parameter called linear thermal transmittance and point thermal transmittance have to be considered. According to the methodology defined in EN ISO 14683, the overall coefficient of heat transfer is given by

$$H_D = \sum_i U_i . A_i + \sum_k \Psi_k . l_k + \sum_j \chi_j \qquad \textit{Equation 3-12}$$

Where χ_j is the point thermal transmittance and Ψ_k. is the linear thermal transmittance

Linear thermal transmittance: This is defined as the heat flow rate of a thermal bridge per degree per metre that is not taken into consideration when calculating the U-value of the building element around the thermal bridge.

Generally, heat transfer from the building envelope is usually approached as one-dimensional heat flow across the entire surface of the envelope. Considering the additional linear heat transfer associated with the edge length in which two-and three-dimensional heat flow occurs, the heat loss from the thermal bridge is calculated using the formula below

$$\Psi = L^{2D} - \sum U_j \, l_j \qquad \textit{Equation 3-13}$$

Where Ψ is the linear thermal transmittance, L^{2D} is the thermal coupling coefficient, U_j is the thermal transmittance and l_j is the length at which the thermal transmittance applies.

$$L^{2D} = \frac{Q}{T_i - T_e}$$ *Equation 3-14*

Where Q is the total heat flow (in W/m), T_i is the internal temperature and T_e is the external temperature.

From the equations above, the linear thermal transmittance value expressed as $W/m.K$ represents the additional flow over and above the linear thermal bridge through adjacent plane elements. Also, for a two-dimensional junction, the linear thermal transmittance is the residual heat flow from the inner to the outer environment after the one-dimensional heat flow has been subtracted through all flank elements.

When determining the value of the linear thermal transmittance, it is mandatory to define the dimensions used, i.e. internal or external dimensions. This is because the dimensions ascertain the value of the linear thermal bridges for different types of thermal bridges (Garrido et al., 2018).

Linear thermal transmittance (used to depict the heat flow added by thermal bridges to nearby elements) are features used to incorporate the effect of thermal bridges in transient building simulation programs such as TRNSYS. Other models adopt different assumptions and therefore produces different results. *Hence the need to know the real dynamic behaviour of thermal bridges* (Martin et al., 2011).

In BRE 497, an alternative method is specified for linear thermal transmittance calculation when the change in temperature across one or more flanking elements in a particular modelled junction is not the full temperature difference between the interior and exterior environment. This arises for models of junctions that have a third temperature boundary in the model that is different from the internal or external temperature. Therefore, the alternative expression is as follows

$$\Psi = \frac{Q^{(2D/3D)} - \sum(U\ x\ \Delta T\ x\ l)}{(T_i - T_e)}$$ *Equation 3-15*

Where $Q^{(2D/3D)}$ is the heat flow in two or three dimensions, U is the thermal transmittance, ΔT is the temperature difference across the envelope, l is the length of the thermal bridge, $T_i$is the internal temperature and T_e is the external temperature.

The CIBSE Guide A mentions that heat losses govern the transmission heat loss in buildings with relatively poor standards of insulation via the plain area of the building fabric. Therefore,

at junctions, the thermal bridge is usually a relatively small proportion of the total heat loss. This was not generally considered in calculations in the past. However, for buildings with better insulation, the reasonable effect of the thermal bridge can be substantial but can also be reduced using good design details.

Another type of a thermal bridge defined by a point transmittance is called a point thermal bridge. The point thermal bridge is found at locations where thermal insulation is locally interrupted at one point, such as in three-dimensional corners. Point thermal transmittance also known as punctual thermal transmittance is given by

$$\chi = L^{3D} - \sum U_j \, l_j \qquad \textit{Equation 3-16}$$

Where χ is point thermal transmittance, L^{3D} is the coefficient of thermal coupling, U_j is the thermal transmittance and l_j is the length over which the thermal transmittance applies.

From the equation, the value of Ψ (Linear thermal transmittance) and χ (point thermal transmittance) provides a quantitative classification of thermal bridges by providing the heat flow transferred across the surface per length and unit temperature in steady-state conditions.

Theodosiou, Tsikaloudaki and Bikas (2017) reported that consideration is given to the impact of thermal bridges, but only linear thermal bridges. Therefore, point thermal bridges or three-dimensional thermal bridges are typically ignored. This is due to the fact that their impact on the heat flowing through the building envelope is regarded as very small and difficult to evaluate as the calculations are based on using finite element analysis tools which may not be tedious for the construction industry. Furthermore, due to the lack of special legislation and requirements concerning point thermal bridges, Theodosiou, Tsikaloudaki and Bikas (2017) further observed that it is relatively common to ignore the presence of the effects.

Point thermal bridges are usually common in double skin facades as these buildings require considerable points to secure the external envelope. In order to secure the envelope, aluminium or steel brackets are used which will, in turn, penetrate the insulation layer. It can be argued that while the volume of the brackets is incredibly small in comparison to the insulation layer, the thermal transmittance can be more than 2000 times higher which can lead to excessive thermal bridge heat flow (T. Theodosiou et al., 2017).

Theodosiou et al. (2017) used the numerical simulation tool ANSYS Workbench to analyse the thermal bridge effect of cladding system (E2 VENT). Using thermal break pad between the wall and bracket, it was observed to exceedingly decrease the development of a thermal bridge. However, it was observed that other factors also affect the flow of heat in through the point thermal bridge, these include

- The material of the substrate wall
- Anchor type
- Insulation thickness

In previous research, Theodosiou et al. (2015) examined a lightweight cladding system using finite element analysis software Abaqus to evaluate the impact of point thermal bridges on the undesirable heat flow. Thermal breaks were revealed to have decreased the direct heat flow due between the bracket and substrate. However, the thermal break was not able to provide a completely effective measure against increased heat flow localised around the fasteners. The authors recommended that special consideration has to be paid during design of cladding systems as the magnitude of the underestimated heat flow can vary from 5 to 20% and current national methodologies do not take them into account.

Bergero et al. (2017) investigated the energy improvement of a cavity of 45-80years building cavity walls using insufflation and thermal bridge correction using thermal transmittance limit values given by DM 26.06.2015. It was noted that the surplus ratio of 50% or more results in no significant increase in mean thermal transmittance. Furthermore, the limit values given by the Decree of 26.06.2015 can not be upheld in the presence of windows, even in the case of exemptions and regardless of the climate zone

A sensitivity analysis of thermal bridges was performed by Capozzoli et al. (2013) to provide designers and policy-makers with a practical way to identify key design variables that affect heat losses through thermal bridges. Results revealed that insulation layer thickness is an important factor influencing linear thermal transmittance deviation. The thermal conductivity of masonry also has a significant effect on the linear thermal transmittance variation than the thickness of the masonry.

3.3.5 Thermography evaluation of thermal bridges

The role of infrared thermography is very important in conducting in situ analyses of building as the techniques enable a qualitative survey to measure the temperatures of the building

envelope surfaces (Asdrubali et al., 2012). It is a non-invasive method of measuring the thermal performance of buildings (O'Grady et al., 2017b).

Baldinelli et al. (2018) described the thermographic survey as a useful method for detecting defects and anomalies which are responsible for the reduction of the entire energy performance. Furthermore, the analysis of thermographic images may result in different evaluations depending on the depth and scope of the survey. The evaluations may provide

- Qualitative information on the correct positioning of the building element
- The quantitative analysis which provides data building envelope heat transfer.

Several factors can affect the thermal image such as climatic conditions, material emissivity and reflected temperature. Thereby during the energy investigation of the building envelope,a proper interpretation of the images is required to determine the real defects.

The infrared image reveals the surface temperature of each pixel by considering the emitted radiation from the surface. Hence, from the definition of a thermal bridge in which it portrays a region whose thermal properties (Thermal conductivity or Thermal resistivity) are slightly different from the others. In that case, the internal temperature of the building envelope would be characterised by significant thermal discontinuities while the same surface temperature is supposed to be homogeneous in the part of a building in which the heat flux can be regarded as one-dimensional (Bianchi et al., 2014).

Thermography enables the detection of thermal bridges in building envelope, along with doors and windows (Bianchi et al., 2014). Balaras et al. (2002) stated that infrared thermography is an effective method of diagnosing the impact of non-homogeneous elements within the building envelope. Furthermore, Zalewski, Lassue, Rousse and Boukhalifa (2010) stated that thermography allows for heat losses visualisation on-site, from a distance, at the building scale and also without infringing the building walls (non-destructive technique)

As for building retrofits, the thermographic survey provides a platform to perform a comprehensive energy evaluation on the actual conditions the building elements as a whole. This would further lead to aid manufacturers, and designers improve the energy behaviour of the building envelope (such as thermal bridges) (Baldinelli et al., 2018).

With the use of thermography, thermal bridges can be quantified by a method proposed by Asdrubali et al. (2012), which is called thermal bridge incident factor denoted by I_{tb}. The

thermal bridge incident factor is characterised as the ratio of the actual heat flow to the heat flow without the thermal bridge. Mathematically it is defined as:

$$I_{tb} = \frac{Q\ with\ thermal\ bridge}{Q\ without\ thermal\ bridge} = \frac{Q_{tb}}{Q_{1D}} \qquad \textit{Equation 3-17}$$

Furthermore, the incidence factor of the thermal bridge can be expressed in terms of increase of the thermal transmittance U_{1D} of the undisturbed zone using the steady equation below

$$U_{tb} = U_{1D}\ x\ I_{tb} \qquad \textit{Equation 3-18}$$

Where U_{tb} is the U-value for the thermal bridge, I_{tb}thermal bridge incident factor and U_{1D} is the thermal transmittance of the undisturbed zone.

Bianchi, Pisello, Baldinelli and Asdrubali (2014)used a four-step methodology to assess thermal bridges in buildings using a testing rig. The steps are

- In-field thermography
- Monitoring of internal and external conditions
- Data processing
- Quantitative analysis

Using the quantitative index called the incidence factor of the thermal bridge proposed by the author in 2012 (Asdrubali et al., 2012), was used to quantify the thermal losses through the building envelope. It was observed that the thermal bridges resulted in the increase of thermal losses through the building envelop to about 9%.

Baldinelli et al. (2018) analysed three thermal bridges (pillar, beam to pillar joint and wall to wall joint) in a calibrated hot box apparatus. Using the thermal bridge incidence factor proposed by Asdrubali et al. (2012), Baldinelli et al. (2018) applied a mathematical algorithm to improve the infrared image resolution and implement the calculation of the incidence factor with higher accuracy. Thereby evaluation of the building heat losses was improved. Results revealed that the new enhanced approach yielded results nearer to the experimental results with an improvement of approximately 2% compared to the first method by Asdrubali et al. (2012)

Garrido et al. (2018) proposed a new technique for automated thermal bridge detection using building thermographic images. The study was an update to the research conducted by Cereijo et al. (2014). With regards to the study of Cereijo et al. (2014), Garrido et al. (2018)

achieve a 15% increase in precision for detecting thermal bridges. When compared to the methodology of Cereijo et al. (2014). To improve the geometric analysis in the images to be studied, Garrido et al. (2018) introduced an image rectification procedure as a first step. Furthermore, a new criterion was introduced to acquire the value of each thermal bridges linear thermal transmittance. The authors achieved a success rate of 55% in detecting thermal bridges (50 thermal bridges out of 74%); this was an improvement to the method defined in Cereijo et al. 2014.

Zalewski, Lassue, Rousse and Boukhalifa (2010) analysed a wall of prefabricated steel framework thermal insulated. The wall was built in the laboratory between two controlled temperature climatic cells. In other to detect the thermal bridge, the wall was first observed using infrared thermography. Results obtained from the experiment were compared with results from the numerical analysis of the wall using TRISCO. Furthermore, to evaluate the relative influence of thermal bridges, the vertical steel framework was eliminated from the model. This showed that without the steel framework for the same wall, the heat losses would be reduced by 26.2% when compared to the wall with the thermal bridge. However, by replacing the unventilated air space with 4cm of insulation and 8cm of insulation plus 1cm of plasterboard. The heat losses reduced to about 17.3% and 41.8% respectively when compared with the wall with the thermal bridge

Theodosiou and Papadopoulos (2008) investigated the impact of thermal bridges on the energy demand of buildings by studying a representative wall thermal insulation used in Greek buildings. This wall was observed to be susceptible to the occurrence of thermal bridges, in contrast to a typical thermal insulating façade. Theodosiou and Papadopolous (2008) Concluded that the existing legislative frame is inadequate, leading to a significant underestimation of actual energy consumption. Furthermore, it was observed that underestimation of thermal losses is more misleading in cases of fully insulated buildings than in the cases of partially insulated ones.

O'Grady et al. (2017b) analysed the effect of wind velocity on thermal bridges heat loss using infrared thermography, numerical analysis and experimental study. Results revealed that the heat loss from a building surface is influenced significantly by wind velocity with the linear thermal transmittance values increasing with an increase in velocity. In another research, O'Grady et al. (2017a) presented a methodology of analysing thermal bridges solely using infrared thermography. The methodology was validated using a hot box with good agreements.

3.4 Factors affecting thermal bridging

To evaluate the heat losses or gains provided through thermal bridges, there are several factors to consider such as climatic conditions, insulation levels, thermal bridge constructive solution and building type (Martin et al., 2011). Other factors that affect thermal bridges are the conductivity of the bridging material, thermal bridge cross-sectional area, and surface resistances of the thermal bridge facing the heat source and the heat sink (Schöck, 2015)

Insulation thickness is seen as one of the most significant factors affecting thermal bridging. Studies (Baba & Ge, 2016; BrumĂ et al., 2016; Capozzoli et al., 2013; De Angelis & Serra, 2014; Déqué et al., 2000, 2001; Larbi, 2005; Martin et al., 2011; Prata et al., 2018) reveal that the effect of thermal bridging increases with increase in insulation thickness. Some reveal that thermal bridging can bring about up to 35% increase in the thermal transmittance with an increase in the insulation layers.

Masonry thermal conductivity also affects the thermal resistance of a wall. This was observed by Capozzoli et al. (2013) in which they concluded that the thermal conductivity of masonry has a greater impact than its thickness on the linear thermal transmittance.

3.5 Possible solutions to thermal bridging

Solutions to thermal bridging are subjective to the type of building, materials and the type of thermal bridge; therefore, the solutions highlighted in this section may not apply to all thermal bridges or buildings. The possible solutions to thermal bridging as stated in studies are

Thermal breaks: Thermal breaks are used in connections usually between floor slabs, balcony and floors etc. Studies such as (Dikarev et al., 2016; Evola et al., 2011; Ge & Baba, 2017) have used thermal breaks as solutions, and all were satisfied with the effect of the solutions. Dikarev et al. (2016) observed that thermal breaks provided a buffer of about 8°C between the indoor and outdoor environment. This outcome protected the hot zone from heat losses. In the study of Evola, Margani and Marletta (2011), a specially thermal efficient load-bearing connector manufactured by Schock was used. The connectors consist of a high-performance micro-fibre pressure bearing module connected to stainless steel bars that are polystyrene insulated.

Increase level on insulation: Although the levels of insulation are seen as a factor that increases the effect of thermal bridging with an increase in thickness. This can also help in mitigating the thermal bridge effect. Strategies used to minimise thermal bridging at

connections, as mentioned in the study of Ge and Baba (2017) is by moving the internal insulation to the external part of the structural element. Furthermore, the authors observed that the dynamic impact of thermal bridges reduces with increase in insulation levels.

3.6 Summary

This chapter reviewed the definition, classification, effect, factors affecting and possible solutions to thermal bridges. In summary, thermal bridges are defects that impose several problems on buildings such as increased winter heat loss, increased summer heat gain, and reduces the interior surface temperature, which brings about mould growth and condensation. Thermal bridges affect the building envelope reduction of thermal resistance, which increases thermal transmittance. Due to the vagueness of thermal bridging classification, a combined classification of thermal bridging was proposed which classifies thermal bridging based on the type of heat flow, causes and type of thermal bridge as classified by BS EN ISO 10211.

Chapter Contribution: Review and Classification of thermal bridges

The effect of thermal bridging has been underestimated over the years. Therefore this chapter provides an extensive literature review of thermal bridges that includes classification, effects and thermal bridging calculation methods. Furthermore, a combined classification of thermal bridging that considers the causes, effects and type of heat flow through the thermal bridge was achieved

Chapter 4: Energy Investigation Framework

4.1 Introduction

There is a global initiative to reduce the anthropological effect on the environment (as a result of climate change), fuel consumption and understanding how buildings behave is imperative in energy analysis (Marshall et al., 2017). Over the years, building energy frameworks have been created to optimise, analyse, predict and manage to build energy performance (Danish et al., 2019; Fosas et al., 2018; Konis et al., 2016; Lapinskiene & Martinaitis, 2013; Weerasuriya et al., 2019). Danish et al. (2019) proposed a framework which systematically integrates the energy sustainability requirements, together with the corresponding cost assessment for an energy-efficient building over its life-span. The study explored innovations in a systematic manner of energy-efficient building Implementations, as well as sustainable decision making, is preferred to facilitate the conflicting nature of both energy efficiency and management performance indices.

In studying whether insulating dwellings increase the risk of overheating, Fosas et al. (2018) developed a framework involving EnergyPlus and Python. Models were validated against data recorded in an apartment, and the results revealed that insulation plays a minor role in overheating even when comparing un-insulated buildings to super-insulated buildings. Furthermore, the authors elaborated that in cases with acceptable overheating levels, the use of improved insulation levels may help in delivering better indoor thermal environments.

Heat loss has a huge impact on the total energy consumed by buildings during operation (Najjar et al., 2019). Therefore, Najjar et al. (2019) developed a framework to estimate the heat energy loss in building while it was occupied. The framework consists of four stages, namely performance parameters, Design factors, conceptual framework and visualisation aid. Applying the framework to a single-family house case study, revealed that the total heat energy loss of buildings in tropical and dry climates could reach values of 16% to 8% respectively when compared to moist subtropical mid-latitude climates — however, the effects of thermal bridges were not quantified in this study.

This chapter covers in detail the methodology used for energy investigation. Different methods (which include; building audit and monitoring, energy simulation, infrared thermography and numerical analysis) are being utilised in various ways to examine the energy performance of buildings. A framework for energy investigation, which involves the

combination of the methods mentioned used in a specific manner, is developed. The proposed framework in this study differs from the existing frameworks (Danish et al., 2019; Fosas et al., 2018; Konis et al., 2016; Lapinskiene & Martinaitis, 2013; Weerasuriya et al., 2019). This is because the framework examines the effects of thermal bridging, predicting the energy performance of the building in the future, and assessing overheating risks within one framework. Furthermore, the framework aims to address the problem of over and underestimation of heat losses and their effects on the energy consumption of buildings.

4.2 Overview of Energy investigation

Understanding and improving the building energy performance is crucial in other to accomplish targets such as the EU's 2020 and the United Kingdom's reduction of 80% CO_2 by 2050 (Gupta & Gregg, 2018). Energy investigation is proposed as a means of achieving the set targets for the current and future building stock. Energy investigation consists of the following phases

- Infrared thermography (Steady state analysis)
- Computer simulation (Transient analysis)
- Effect of thermal bridging
- Overheating assessment

A framework (see Figure 4-1) called the energy investigation framework is developed. It relies on a systematic transfer of information between the phases (see Figure 4-2). The energy performance of buildings is initially investigated using both infrared thermography and computer simulations. The building audit and monitoring section is used to ensure that the model behaves in the same manner as the actual buildings. The infrared thermography phase provides the platform for detecting anomalies and defects in the building envelope. In the numerical analysis section, numerical models of the defects identified from the infrared thermography are developed. These models are used to examine the extent of the defects. New buildings and the current building stock are required to last at least 20-30years, the effect of climate change and global warming on these buildings can be assessed using predicted future weather data. Validated models can be used to evaluate overheating risks during the summer period for current and future data.

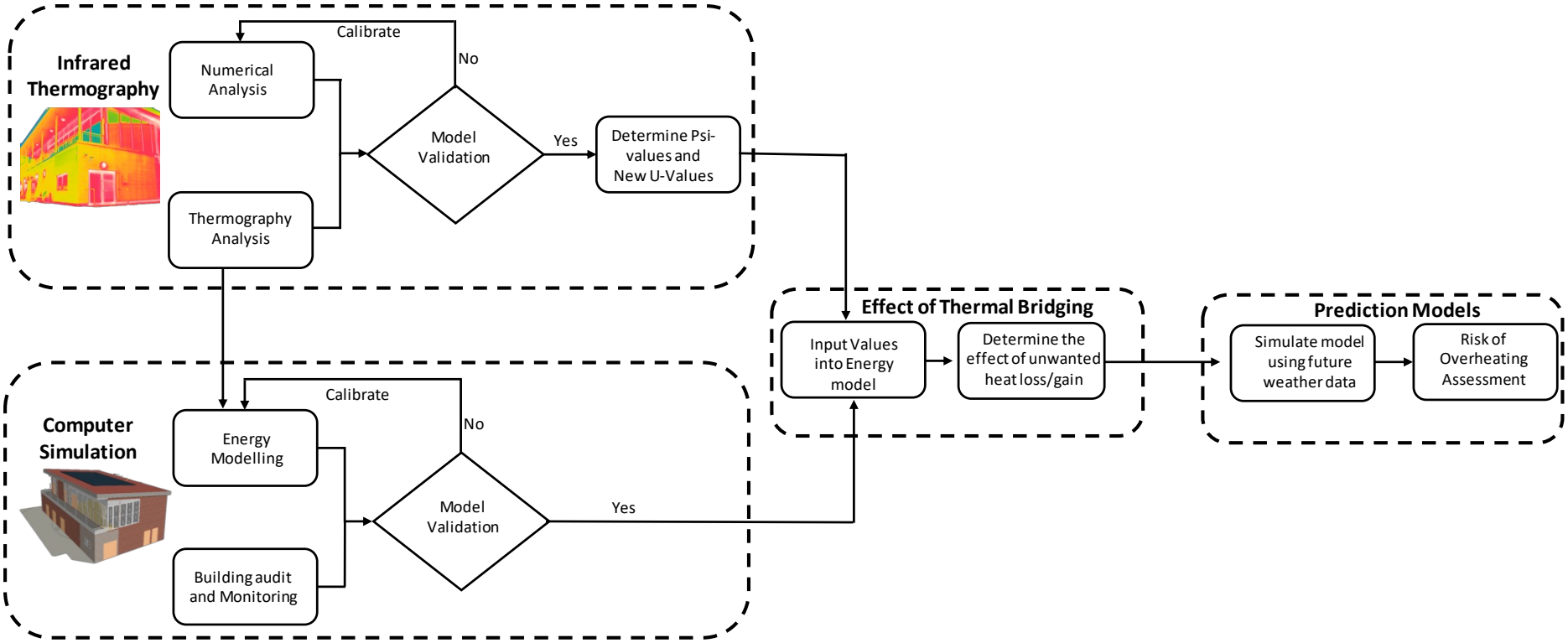

Figure 4-1: Energy Investigation Framework (EIF)

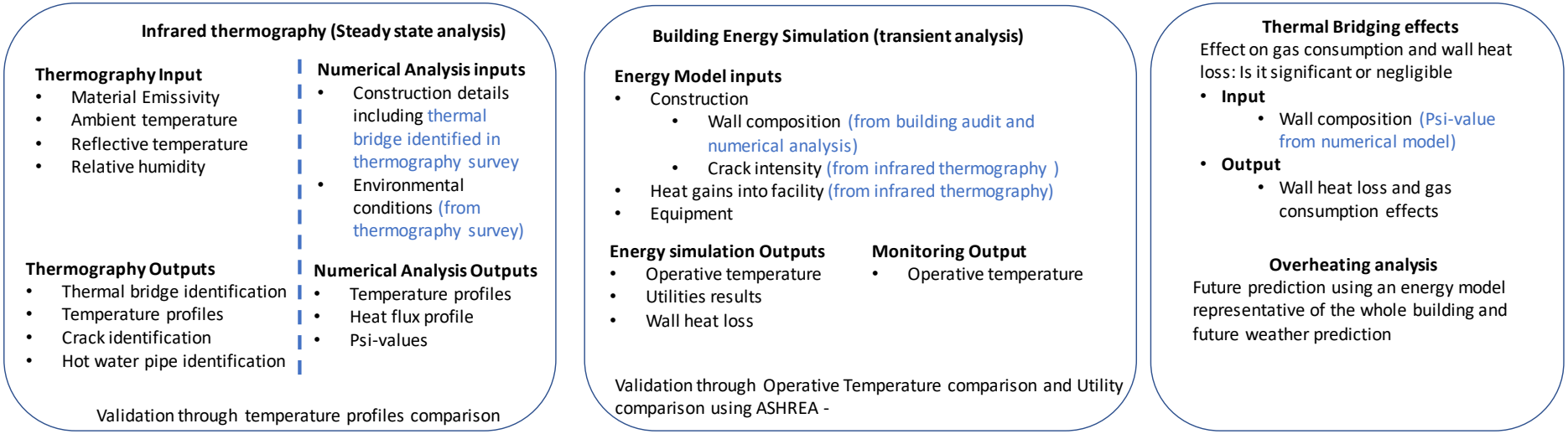

Figure 4-2: information/data transferred from one phase to another

4.3 Infrared Thermography Phase

This is the first step in the energy investigation framework, and the primary objective of the infrared thermography is to identify defects within the building envelope The infrared thermography phase is an independent phase which is divided into four sections namely thermography analysis, numerical analysis, model validation and Psi-value and U-value determination. The standard EN ISO 13187 and BSRIA Guide should be used as guidelines when performing the thermographic survey of the case study.

4.3.1 Thermography Analysis

Irregularities in buildings thermal performance can be identified using infrared thermography. The surface temperature distribution obtained from the thermography is affected by airflow within and through the building envelop, thus can be used to detect thermal irregularities due to

- Insulation defects
- Moisture related defects
- Air leakages etc

4.3.1.1 The Infrared Camera

The infrared camera (see figure 4-3) is a device that produces a sequence of thermal distribution images and is calibrated at different temperatures to measure the emissive power of surfaces in an area. The optics focus the radiation emitted from the target onto the infrared sensor, and the electrical response signal is converted into a digital image (Kylili et al., 2014).

Figure 4-3: Flir T series

Flir T600 (Figure 4-3) is a thermal camera for predictive maintenance that allows detecting hidden signs of electrical resistance, mechanical wear and tear, and other heat-related problems with an accuracy of ±2° C. It has a temperature calibration to 2000°C with a 640 x 480 pixels which provides a high-quality image (provides 307,200 measurement points in one image) and clarity needed to diagnose problems. The T-series is also equipped with a 5 Mpixels built-in digital camera with LED lights capable of detecting temperatures within the range of -40°C to 650°C.

Table 4-1: Flir T600 thermal camera technical specifications

FLIR THERMAL CAMERA T600	
IR Resolution	640 x 480 pixels
Field of view (FOV)	15° x 11°
Spatial resolution (IFOV)	0.41mrad
Thermal sensitivity (NETD)	<30 mk @ ± 30°C (+86°F)
Image frequency	30 Hz
Temperature range	-40°C to 650°C
Accuracy	± 2°C (±3.6°F) or 2%

4.3.1.2 Thermal Image Calibration

A thermal camera does not directly measure temperature but receives radiation (within a defined range of infrared wavelengths) from the object and the surroundings reflected through the object surface. (Taylor et al., 2014) The received radiation collected in a thermal camera is divided into; emission from the object and atmosphere and the reflected emissions from ambient sources. These signals are processed so that the measured radiative flux is converted into temperature readings. In other to calibrate the thermal camera, several parameters have to be specified. These are

- The emissivity of the objects
- Relative humidity
- Object distance
- The ambient reflected the temperature
- The temperature of the atmosphere.

Emissivity

According to Stefan-Boltzmann theory, the overall radiant energy released by an object is associated with the emissivity

$$R = \varepsilon\sigma T^4 \qquad \textit{Equation 4-1}$$

Where R is irradiance(Wm^{-2}); ε is emissivity; σ is Stefan-Boltzmann constant $(5.67\ x\ 10^{-8} W\ m^{-2}K^{-4})$ and T is temperature

An object's emissivity varies with its temperature, radiation wavelength, and angle of view of the object. The value of emissivity ranges between 0 – 1, in which an emissivity of 1 represents a theoretical black body. Therefore, objects with high emissivity (closer to 1) release a comparatively high proportion of infrared radiation and reflect a significantly lower proportion of radiation from the environment. Surfaces or objects with low emissivity reflect more radiation from objects with high-temperature. Therefore this needs to be considered for when analysing a thermal image (Taylor et al., 2014).

The change of emissivity with temperature and wavelength can be overlooked within the temperature range present in buildings. For this study, Table 4-2 below shows the materials with their corresponding emissivity

Table 4-2: Materials with the corresponding emissivity

Materials	Emissivity
Brick	0.93-0.96
Block	0.88-0.94
Glass	0.90-0.95
Wood	0.90-0.94
Mortar	0.80

For unknown emissivity of a material, the emissivity can be obtained using the reference emissivity material method or the contact method. The reference emissivity material method involves the use of a known emissivity piece of electrical tape. The tape is placed on the material and temperature of the tape is obtained from the thermal camera. The same process is repeated, but the temperature of the material is obtained. Using Stefan-Boltzmann

law, the configuration of the emissivity is adjusted until the same temperature is obtained. The final configured emissivity is the emissivity of the material/object.

Environmental data and Climatic conditions

BS EN 13187:1998 recommends environmental conditions for thermography, which are summarized below

- The temperature difference across the building envelope should be large enough to allow thermal abnormalities to be detected
- During the survey, there should be no direct solar radiation on the inspected building
- Preferably, the thermography should be done with constant temperature and the pressure differentials across the envelope
- Thermography shall not be conducted when the wind, external air and internal air temperature varies significantly

In other to satisfy the conditions, steps were taken, these are

- Observing the local weather climate for at least two days before the start of the survey
- The survey was conducted during the night the winter period due to buildings being subjected to less solar radiation and achieve the desired temperature difference
- The heating system in the building was switch on at least two hours before the survey was carried out.

As mentioned in section (4.3.1.2) above, certain parameters must be specified to ensure that the thermal camera is calibrated. The environmental data associated with the calibration process are

- **Reflective apparent temperature:** Infrared is emitted in the same manner as light. Therefore the apparent temperature of an image or part of an image may not be the true temperature. Therefore, the apparent reflected temperature is used to account for the reflected radiation in the object. To obtain the reflected temperature, two methods are used which are the direct method and the reflector method. The reflector method involves the use of a crumpled and re-flattened piece of aluminium foil (considered a perfect reflector). The foil is positioned in the infrared camera field of view, and the aluminium foil temperature is measured assuming an emissivity of one and a zero distance. The reflected temperature is then inputted into the thermal camera. For the external reflected temperature, the aluminium foil is placed at an

angle to the sky so that the reflected temperature of the sky can be obtained. The direct method, on the other hand, involves identifying reflection sources by considering the incident angle (reflected angle). The reflection source is modified by obstructing the source using a piece of cardboard while the intensity of the radiation (apparent temperature) is measured from the source using emissivity as one and object distance as zero. The BSRIA observed that most materials radiate infrared reasonably uniformly at angles up to 45° from the perpendicular. To avoid reflection, the measurement is performed at an angle between 5° to 45° of the thermographers to the target object.

- **Atmospheric temperature:** the atmospheric temperature can be obtained with the use of a plain white paper. The plain white paper is placed at strategic points to avoid the influence of any heat source and left for about 30mins to an hour. The temperature of the plain white paper is obtained from the infrared camera, and this temperature is the atmospheric temperature of the room.
- **Relative humidity:** A characteristic of a thermal camera is to make up for the fact that the transmittance depends on the atmosphere's relative humidity. Therefore, it is important to set the correct value of relative humidity. To obtain the humidity, a hygrometer is used.
- **Wind:** a wind vane anemometer was used to measure the wind speed. Together with a compass, the wind direction was obtained,

4.3.2 Numerical Analysis using ANSYS

Finite element method is a mathematical technique for setting up and solving systems of partial differential (or integral) equations. This process involves dividing a system where behaviour cannot be predicted using closed-form equations into small pieces (elements) whose solution is known (Thompson & Thompson, 2017).

Link to previous steps: *Defects identified within the thermographic phase are numerically analysed to identify the extent of the defects. Boundary conditions such as surface heat transfer coefficient are obtained from the energy model and used in the numerical analysis*

ANSYS 18.1 mechanical APDL is used to create the models of the defects detected from the thermography survey. The standards EN ISO 10211 and BRE 497 were used as guidelines for the numerical modelling of the affected building envelope. BRE 497 provides guidelines on the extent at which a model is created as this affects the temperature factor and heat flows. The model's flanking element (i.e. the plane areas nearest to the thermal bridge) should be

taken to at least 1 metre or three times the thickness of the flanking element, whichever is higher, away from the thermal bridge or up to a plane of symmetry in the case of repeating features. In cases where there is uncertainty as to whether the model extends far enough, the internal or external surface temperature at the adiabatic edge of the particular flanking element should be noted. The model should be extended by at least the thickness of the flanking element and the surface temperature at the new adiabatic edge of the flanking element recalculated.

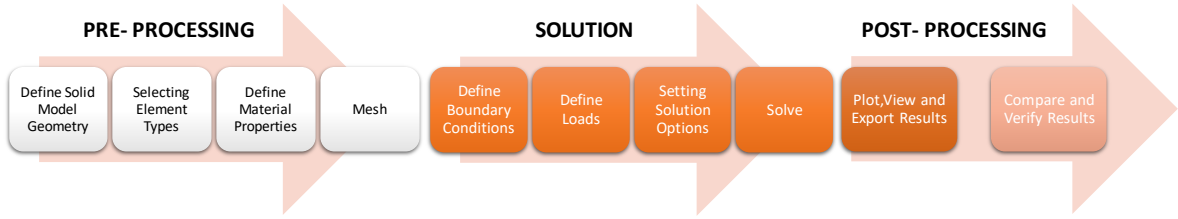

Figure 4-4: Numerical analysis steps

Any finite element analysis process is divided into three steps: pre-processing, solution and post-processing as outlined in Figure 4-4. The pre-processing phase involves creating the geometry and discretising to create finite elements. The solution phase provides the platform to set boundary conditions and set the appropriate solution options such as steady-state or transient solution.

4.3.2.1 Material Modelling

Thermal mass Brick and node 8 - SOLID 278 (Figure 4-5)., which has a 3D thermal conduction capability is used. This element has eight nodes with a single degree of freedom and temperature at each node. Therefore the element is applicable for 3D steady-state or transient analysis. When used in irregular regions, the element permits for a prism and tetrahedral degenerations. Solid 278 is available in two forms, namely homogeneous thermal solid and layered thermal solid.

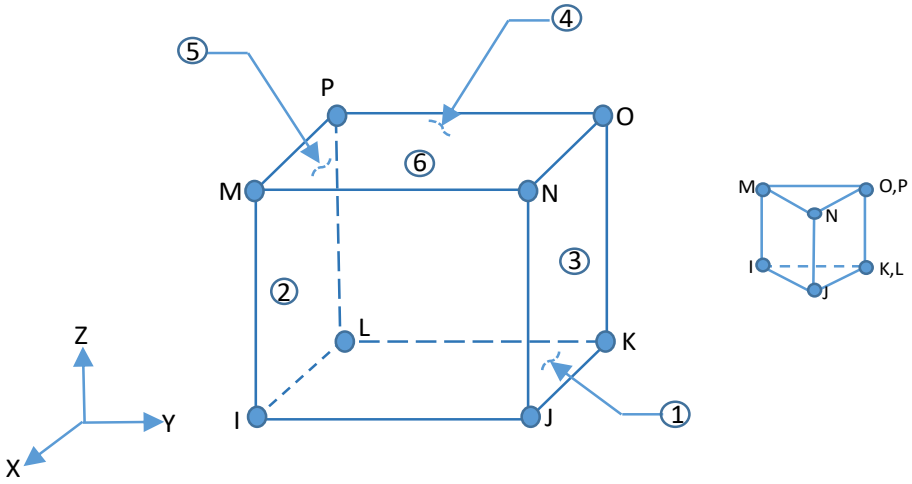

Figure 4-5: Geometry and node locations for Solid 278 with prism option (right)

Layered thermal solid 278 is suitable for modelling heat conduction in layered thick shells or solids which also allows for prism degenerations. The input data for layered thermal solid 278 includes anisotropic material properties. The direction of anisotropic material refers to the coordinate directions of the surface, that are centred on the coordinate system of the element. The coordinate element system maintains the shell convention where the z-axis is normal to the shell surface.

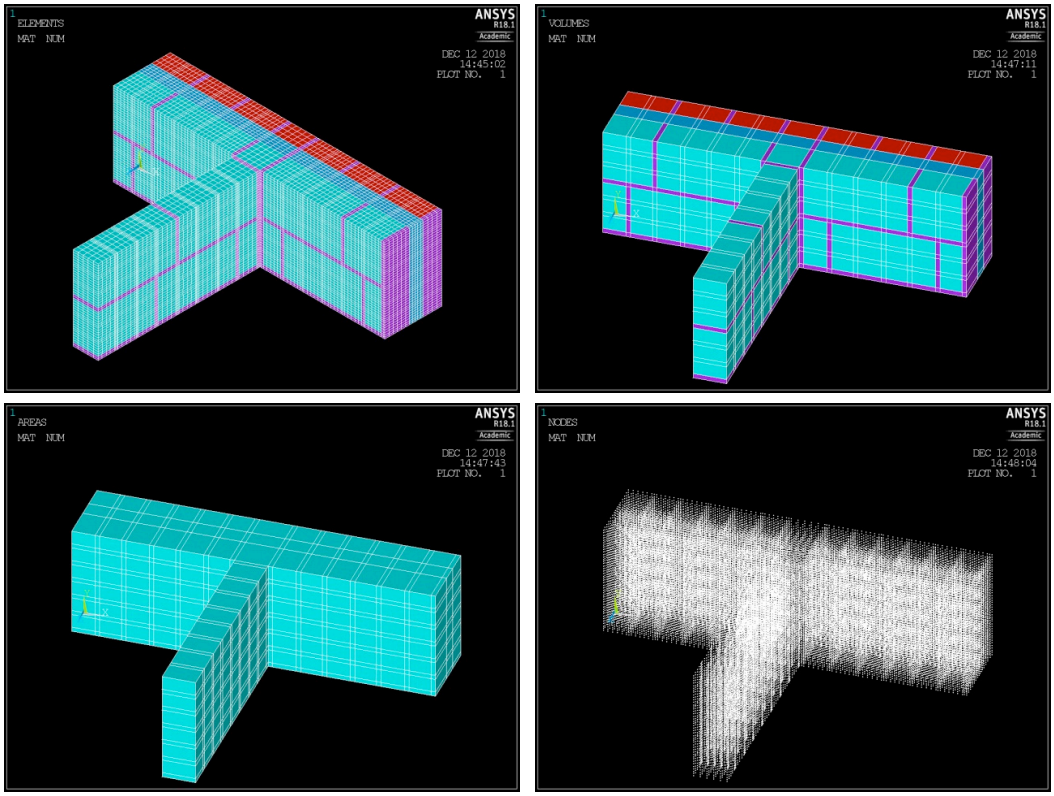

Figure 4-6: Elements (top left), volume (top right), area (bottom left) and nodes (bottom right) of corner wall in ANSYS

4.3.2.2 Material Models

A material model is a numerical representation of a material's expected behaviour in response to an applied load. These models define how a material behaves which may include material linearity, the spatial and time-temperature dependencies of the material model and the permissible material model combinations. For thermal analysis, certain material properties have to be defined; these are highlighted in Table 4-3

The properties of materials used in the numerical model were obtained from the building plans and are outlined in the table below. Material properties that were not specified in the building plans were obtained using standard properties from CIBSE Guide (2006)

Table 4-3: Material properties and corresponding analysis types

Material properties	Analysis type
Thermal conductivity	For all analysis
Density	Transient thermal analysis
Specific heat	
Enthalpy	Analysis involving a phase change
Viscosity	Analysis involving mass transfer
Fiction coefficient	

Table 4-4: Numerical model material properties

	Material Models				
	Brick	**Mortar**	**Block**	**Steel**	**Insulation**
Density ($\boldsymbol{kg.m^{-3}}$)	1700	1900	720	7800	25
Specific Heat ($\boldsymbol{J.kg^{-1}K^{-1}}$)	800	840	840	480	1000
Thermal Conductivity ($\boldsymbol{W.m^{-1}K^{-1}}$)	0.77	0.93	0.18	45	0.037

4.3.2.3 Boundary Conditions

The heat transfer between the internal or external environment and the building's surface are a complex process, based on a mixture of radiation from the surrounding materials and movement of air through convection over the surface. Boundary conditions are critical for obtaining the correct solution to a given problem. Boundary conditions can be divided into two; geometric and natural or forced boundary conditions.

Boundary conditions applied to the system from an external source are classified under loads. These include forces, pressure, voltages and temperature etc. The aim of this is to determine the behaviour of the model in response to the loads. For steady-state analysis, the boundary conditions applied are temperature and heat transfer coefficient due to convection.

The heat transfer coefficient due to convection is divided into internal and external convective heat transfer coefficients. The atmospheric temperature and convective heat transfer coefficient govern the external and internal boundary condition and are essential to assess the building facades convective heat gains and losses.

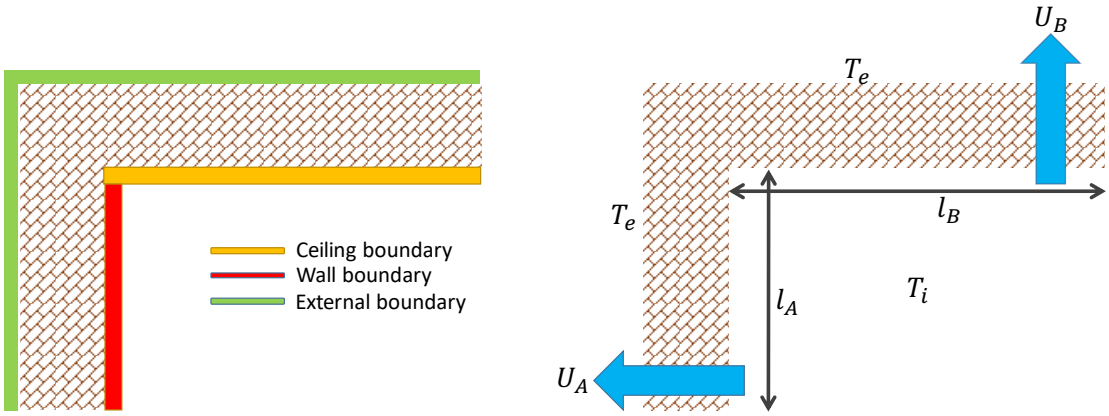

Figure 4-7: Boundary conditions (left) and heat flow path with corresponding length (right)

$$\Psi = L^{2D} - (U_A \, x \, l_A) - (U_B \, x \, l_B) \, \frac{W}{mK} \qquad \textit{Equation 4-2}$$

The convective heat transfer coefficient is influenced by factors such as the geometry of the building, the building surroundings, location of the building envelope, the surface roughness of the building and environment conditions. The environmental conditions include wind speed and direction, local airflow patterns and surface temperature variations. To calculate the linear thermal transmittance, equation 4-2 Is used.

Table 4-5: Values of surface resistances for External and internal surfaces

	The direction of heat flow		
	Upwards	Horizontal	Downwards
Inside Surface			
R_{si}	0.10	0.13	0.17
h_{si}	10.0	7.69	5.88
Outside Surface			
R_{se}	0.04	0.04	0.04
h_{se}	25.0	25.0	25

Table 4-6:Values of surface resistance at various wind speeds (BSRIA 2011)

Wind Speed (m/s)	**R_s (m^2K/W)**	**Wind Conditions**
0.13	0.13	Calm: the assumed indoor condition in calculation of U-values
1	0.08	Light air
2	0.06	Light breeze: assumed sheltered outdoor condition in U-values
5	0.04	Gentle breeze: assumed normal outdoor condition in U-values
7	0.03	Moderate breeze
10	0.02	Fresh breeze: assumed exposed outdoor condition in U-values

Table 4-7: Boundary conditions

	Boundary Condition	
	Temperature ($°C$)	Surface Coefficient (m^2K/W)
Internal	23	0.13
External	4	0.04

4.3.2.4 Meshing

Meshing is an essential part of the computer-aided engineering simulation process (ANSYS, 2018). Mesh is defined as any of the open spaces or interstices between the strands of a net created by the predefined connection of nodes (Liu 2003). Meshing influences the speed, convergence and most importantly the accuracy of the solution. Depending on the methods used, meshing may be called grids (FDM), volumes or cells (FVM) and elements (FEM) (Liu 2003). Meshes are pre-defined to provide a relationship between the nodes. There are six steps to meshing using ANSYS as shown in Figure 4-8 below.

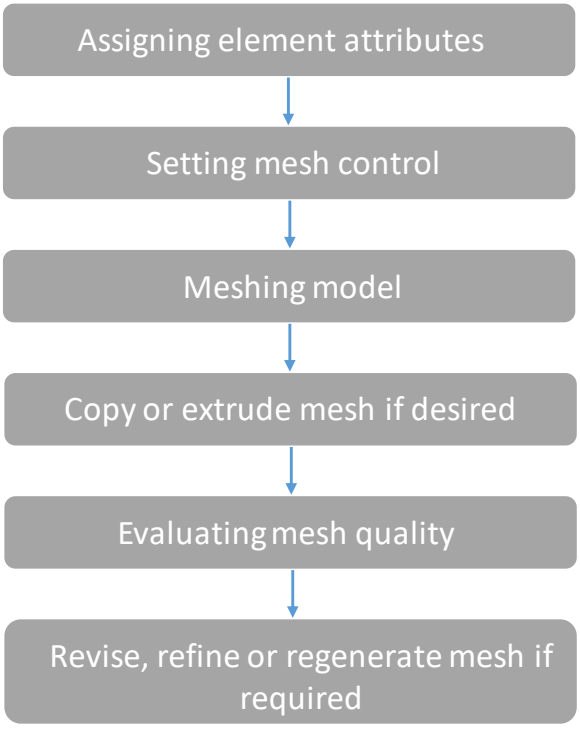

Figure 4-8: steps for meshing

The finite element program ANSYS creates meshes of two types, namely free meshes and mapped meshes. Free meshes do not have constraints on the organisation of its element or on the geometry type, which will be meshed. For a free mesh, the triangular and quadrilateral element can be used for areas while for volumes, only tetrahedral elements can be used. Mapped meshes contain elements organised in a regular pattern. Therefore, mapped meshing can only be used for areas confined by three or four lines and volumes confined by four, five and six areas. For mapped meshing, triangular and quadrilateral elements are used for areas, while only brick elements are used to map mesh a volume (Thompson & Thompson, 2017).

4.4 Computer Simulation Phase

Computer simulation is the second phase of the energy investigation, and it consists of three sections namely building audit and monitoring, energy modelling and model validation. The computer simulation phase is dependent on the infrared thermography phase. This is due to results and observations from thermography analysis is used as inputs to the energy modelling section.

Link to previous steps: *Observations from the infrared thermography are used as boundary conditions to the energy model. These observations include the crack intensity and areas of heat gains and losses*

4.4.1 Building Audit and Monitoring

4.4.1.1 Auditing

This provides a comprehensive energy analysis that can be used for the development of a baseline. Building drawings (structural, architectural, mechanical and electrical drawings) and specification are studied. The main aim of the building audit process is to gather information regarding the building envelope and the use of the building. The information required for the audit are outlined below

- Utility data: The historical electrical and gas consumption data to identify patterns of energy usage
- Check current procedures for operation and maintenance
- Determination of recent ligtning, equipment (if any) and HVAC operating conditions
- Estimate the use of space, equipment, lightning and also occupancy (energy density and operation hours)
- Building plans: Floors plans, structural section, mechanical and electrical drawings
- Obtaining all equipment occupancy and operating schedules (including lightning and HVAC system)
- Obtaining data on building construction materials and their properties (such as thickness, thermal conductivity and specific heat capacity)

The information obtained from the building audit is used as input for the building energy model so that an accurate model can be achieved. Defects (such as cracks and condensation) within the building affects the energy performance of buildings and therefore have to be identified.

4.4.1.2 Monitoring

Building energy metering and monitoring of the environment provide stakeholders with vital information on how buildings operate and perform as well as being a driving force for reducing energy consumption and related green gas emission (Ahmad et al., 2016). For a simulation model to be valid, the building parameters inputted into the model must closely match the structure of the real-life. In this phase, a sensing system is considered in the building where temperature and humidity are monitored. These parameters, especially indoor temperature, are used to validate the model. If discrepancies between temperatures from the model and real-world building are significant, the building model will be calibrated until indoor temperatures have a close match. The accurate building model will then be used to analyse and evaluate the energy consumption of the building. The selection of a monitoring device can be challenging as it relies on many factors such as accuracy, robustness, data storage, miniaturisation and also the ability to connect to other software or devices (for example building energy management system).

Figure 4-9: Sensor locations: main lounge (left) and changing room (right)

Three Temperature and humidity sensors where installed, as shown in Figure 4-9. The sensors were installed in the main lounge and changing rooms at strategic places to avoid the direct influence of HVAC systems, Electric appliances and a direct heat source or light (Figure 4-9). The sensors known as Log Tag Haxo-8 is are temperature and humidity loggers that monitors and stores up to 8000 sets of high-resolution humidity and temperature readings within a measurement range of

- 0 to 100% Relative Humidity
- -40°C to +85°C Temperature

The sensors battery life is within two to three years of normal use which is dependent on 15-minute logging and monthly data download. Therefore this was used in other to have optimum performance. The temperature and humidity resolution of the Haxo-8 sensors are have an accuracy of more than 0.1°C or 0.1°F and 0.01%RH respectively. Furthermore, an

integrated real-time clock with a rated precision of ±25ppm @ 25°C which is equal to 2.5 seconds/day.

Note: The sensors were installed close to the ceiling to avoid students tempering with the sensors

4.4.2 Energy Simulation

There is numerous energy simulation software such as IDA ICE, TRNSYS and DesignBuilder. Computer models are used to mimic the actual buildings. The purpose of this methodology is to analyse and evaluate the current and future energy consumption of the building.

> ***Link to previous steps:*** *In other to achieve an energy model that behaves like the real building, observations from the infrared thermography are used as inputs to the energy model and the monitored data are compared to the simulated data. In the case of high discrepancies, the monitored data is used to calibrate the model.*

For software to be able to perform energy analysis, ASHRAE Guideline 14-2002 has provided the criteria that every simulation programs must possess. These are

- Ability to perform 8760 hourly calculations
- Model thermal mass effect
- Occupancy modelling and operating schedules which can be distinctly defined for each day of the week and holidays
- Provide individual set-points for thermal zones or HVAC components
- Model actual weather data
- Provide user-definable part-load performance curves for mechanical equipment and
- Provide user-definable capacity and efficiency correction curves for mechanical equipment operating at non-rated conditions.

Three steps (Figure 4-10) are required for any energy simulation, and these steps are model creation, solution and post-processing.

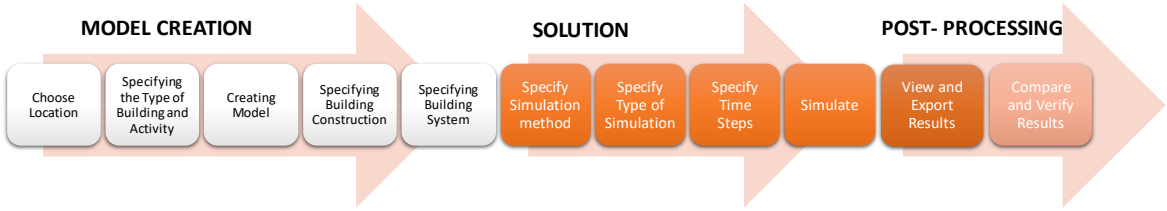

Figure 4-10: Energy simulation steps

For this study, DesignBuilder was chosen because of its ability to conduct energy analysis using EnergyPlus and also conduct numerical analysis using the CFD tool. DesignBuilder employs finite volume method for its CFD tool to solve a series of partial differential equations which represents the conservation of energy, mass and momentum equation. The equation set includes the three momentum equations of the velocity component which are: Navier Stokes equations, k-Ɛ turbulence model and turbulence kinetic energy and the dissipation rate of turbulence kinetic energy. Results from the thermographic survey are to be used as input (boundary conditions) for the CFD analysis.

4.4.2.1 Model Creation

Model creation is the first step in any energy simulation as this provides information on the building is analysed. Model creation involves certain steps (see Figure 4-10) which are explained below:

Choice of Location

"Climate data is the most unpredictable driver that affects the behaviour of a building (CIBSE AM11)"

The choice of location plays an crucial role in energy simulation as it provides the weather data. For thermal building simulation, weather data is a fundamental variable required which should be exclusive and relies on the building location (Andarini, 2014). Furthermore, Fumo (2014), stated that the weather parameters affects buildings' load and energy demand. There are different types of weather data which include Design Summer Year Weather Data (DSY), Typical Meteorological Year (TMY). Weather Year for Energy Calculations (WYEC) and Test Reference Years (TRY). The choice of weather data depends on the type of analysis.

- **Design summer years:** These are usually required for overheating analysis and sizing for cooling plants, as they include near extreme warm summers based on a period of 20 years measurements for different locations.
- **Test reference year:** This type of weather data is a composite of 12 typical months, which may not necessarily be of the same year. The test reference years are required for energy analysis as they average temperatures.
- **Typical meteorological years and weather year for energy calculations**: These are recommended because they replicate a year that can estimate energy consumption and energy costs closer to the long term average (Fumo 2014),.

Although there are different types of climatic data, they all include a pattern of data as shown in Table 4-8

Table 4-8: Climatic data

Climatic Data
Location latitude and longitude
Month number
Day number
Day hour
Precipitation (mm)
Atmospheric pressure (mbar)
Wind Speed (ms^{-1})
Wind direction (degree from the north)
Dry bulb temperature (°C)
Wet-bulb temperature (°C) or relative humidity (%)
Global horizontal solar radiation (Wm^{-2})

Type of building and activity

Building activities are vital to energy modelling because they define how energy is used in buildings. Building activities include the occupancy levels, the temperature set points, the equipment used with their respective heat gains. The input parameters relating to building activities are very sensitive in energy models. Therefore extreme care should be given to the parameter to accurately represent the building under study (Azar & Menassa, 2012).

The occupancy density defines occupancy in energy simulation, which is the number of people in the building/room per area in square meters. Occupants affect the energy consumption of building through different activities such as thermostat settings adjustments, operation of windows (opening/closing), operation of lights (dimming/switching), operation of blinds (pulling up/down) , turning the HVAC system on/off and movement within spaces. Activity relating to occupants must be defined as this provides the amount of heat emitted (internal gains) from the human body to the environment. From the CIBSE guide A, the sensible heat gain from a human body is assimilated and stored in the material by the surrounding surfaces.

Type of activity in the building also defines the energy use in a building; for example, a gym would have more internal heat gains into the building than a classroom or an office building.

When defining the activity of a building, the total, sensible and latent heat emission has to be defined. Values for these can be found in standards such as the CIBSE guide A and ASHRAE handbook.

Equipment and lighting are a major source of energy usage and internal heat gains into the building. The electrical energy used by a lamp is emitted as heat by means of conduction, radiation and convection. Upon absorption of the room surface, radiant energy released by a lamp (invisible and visible) will lead to heat gain into the building space (CIBSE, 2006). Defining the lightning and equipment are thereby vital in energy simulation. Lightning is defined in energy simulation in terms of the task illuminance (lux), and the average installed power density ($W.m^{-2}$). Internal heat gain due to equipment such as printers, personal computers are distributed as an allocation in watts per square metre ($W.m^{-2}$) of net accessible floor area (CIBSE, 2006).

4.4.2.2 Creating the model

A model, which is a representation of a building (being analysed/studied), has to be created. Different energy simulation software has different approaches to creating the model such as DesignBuilder uses a graphical user interface to create an EnergyPlus model. Other software includes the use of a graphical programming environment for modelling such as Simulink and Dymola.

Creating a model requires the modeller to have substantial information on the building plans and building façade. The volume and floor area affect the energy consumption results and therefore have to be as accurate as possible. For this research, DesignBuilder was used to create the model.

4.4.2.3 Building construction

The Building construction is a crucial element in all energy analysis as heat is being lost within the building envelope. The building envelope is defined by the U-value, which dependent on the thickness and the thermal conductivity of the material; therefore have to be specified in other to perform energy simulation. Glazing within the building envelope has to be defined as this also affects the energy performance as a result of the number of solar gains and heat losses within the building. Another important aspect of building envelop is the infiltration rate (airtightness). The rate of inflitration is the rate of entry of unintentional air from the external part of a building through cracks, holes and the fabric porosity (DesignBuilder, 2019).

4.4.2.4 Building system

The building system (HVAC system) maintains and controls the temperature and humidity levels to provide an adequate indoor environment. A representation of the building system must be specified for the energy simulation. This is done either through a simple or detailed model of the HVAC system.

A detailed HVAC option provides the platform to assemble various components of the HVAC system, which are combined with the building models for energy simulation. The HVAC system includes the following

- Radiators, Boilers with Natural ventilation
- Ground source heat pumps
- Underfloor heating
- The domestic hot water system
- Heat Recovery Units

Different components (such as air and water loops, setpoint managers and the HVAC components) are used to create a detailed HVAC system.

4.4.2.5 Model Solution

Model simulation is the final step for the pre-processing stage. Energy simulation are of different types, and they include the following

- Annual
- Monthly
- Seasonal (Winter simulation or Summer simulation)
- Weekly (Typical winter week, typical summer week, design summer week and design winter week)
- Daily

Depending on the type of simulation, the time steps per hour and output intervals for reporting have to be specified. Control radiant fraction is also specified as this controls how the setpoint temperature can be interpreted. The set-point temperature can be interpreted as follows

Air temperature: this controls the room mean air temperature to the heating and cooling setpoint temperatures. The use of air temperature control has a disadvantage of underestimating energy consumption in poorly insulated buildings, buildings with large unshaded glazing areas or buildings with high ventilation rates (DesignBuilder, 2019).

Operative temperature: this controls the room temperature using 0.5 radiant fractions. This temperature control is useful for calculating realistic heating and cooling energy loads, which are, based on published summer and winter temperature requirements for activities in each zone (DesignBuilder, 2019).

4.4.2.6 Modelling Free running buildings

Free running buildings/rooms are buildings without mechanical cooling or ventilation. These type of buildings use natural ventilation as a means of cooling, i.e. passive measures. Modelling free-running buildings is carried out to investigate the performance of buildings during summer.

Standards such as CIBSE guide A, BS EN 15251 and BS EN 13791 provide guiltiness modelling buildings without mechanical cooling. From the guidelines, it is becoming more common to base acceptable thermal comfort limits on the operative temperature calculated from the running mean temperatures (CIBSE, 2015). Not all simulation programs are capable of modelling the summer conditions of free-running buildings. Programs capable of simulating the summer conditions must possess the following criteria

- Capable of calculating operative temperatures
- Possess algorithm to reproduce user behaviour in opening windows
- Capable of main modelling strategies for reducing and removing heat gains by providing advanced glazing, blinds, shading systems, natural ventilation using thermal mass, variable occupancy and ventilation.

4.4.3 Model Validation and Calibration Methodology

4.4.3.1 Calibration

In general, models are classified as Diagnostic or prognostic and Law driven or data-driven model. Building energy simulation programs can be classified as prognostic law-driven models as they are used to predict the behaviour of a complex system given a set of well-defined laws. The use of monitored data from buildings can be used to produce models capable of accurately predicting system behaviour (Coakley et al., 2014). This approach is called a data-driven (inverse approach) and can be classified into three, namely black box, grey box and detailed model calibration

The detailed model calibration uses a descriptive law-driven model of a building system and tunes the inputs to match the measured data. Due to the model being linked to the physical building, system and environmental parameters, this method provides a detailed prediction

of building performance. Furthermore, detailed model calibration provides the platform for assessing the impact of changes.

Coakley (2014) stated that there are two current approaches to model calibration, which are manual and automated calibration. Manual calibration relies on iterative pragmatic intervention by the modeller while automated calibration is a non-user driven (automated) process to assist or complete the calibration. There are different procedures for manual calibration technique revealed by Coakley (2014) which is as follows:

- Characterisation technique: This involves developing an intimate knowledge of the physical and operation characteristic of the building
- Building and site audit: This involves evaluating where a building or plant uses energy and identifying opportunities to reduce consumption. Three levels of building audits were identified, which are walkthrough. Standard audit and investment grade.
- Short term end-use monitoring: This involves the use of specialised software and hardware tools to systematically gather and analyse data typically over a short period to evaluate the performance of the energy systems.
- High-resolution data: this involves the use of high quality, high-resolution data and empirical evidence for model calibration and validation.
- Intrusive testing: this involves determining the building parameters using controlled heating and cooling tests over a short time (usually 3-5days).

The calibration method used in this study involves the use of the monitored data to manually alter the model (such as modifying the HVAC operation and schedule) until there is a significant match between the model and monitored data.

4.4.3.2 Validation

Studies (Martinaitis et al., 2015; M. Rahman et al., 2008; M. M. Rahman et al., 2010) have revealed discrepancies between simulated models (Numerical and Building energy models) and the actual model. The model validation describes the extent at which a model produces results that are comparable with an alternative or standard methods (Underwood, 2014). Building models seldom perform as real-world buildings even when sophisticated energy simulation methods are used (Martinaitis et al., 2015). Therefore building models have to be validated. Model validation is understood to mean the extent at which a model produces results that represent the real-world behaviour, while model verification describes the extent at which a model produces results that are comparable with an alternative or standard method (Underwood, 2014). Rahman et al. (2010) conveyed the importance of model

validation as an essential task to ensure that the architectural, mechanical and electrical systems are properly modelled together to estimate the energy performance of the building accurately. Three methods are widely employed for testing the performance of building energy calculation methods and programs (Underwood (2014)):

- Empirical validation
- Analytical verification
- Inter-model comparison.

There have been different methods for assessing calibration performance. Rahman et al. (2010) made recommendations for the allowable difference between the predicted and measured data. The recommendations are outlined below;

- Monthly Comparison should be within 5%
- A daily comparison should be within 15%
- Between 15-25% monthly comparison for simulation of HVAC systems
- Between 25-35% daily comparison for simulation of HVAC systems

Statistical analysis specified in the ASHRAE guideline 14-2002 was followed, which entails determining two dimensionless indicators of error, mean bias error and coefficient of variance of root mean square error.

Mean Bias Error

This is a sum of errors between the simulated and measured data for each data point. This is a good indicator of the overall sum of errors as it takes the mean difference between the measured and simulated data points.

$$\frac{\sum_{n=1}^{n}\left(X_{1,t}-X_{2,t}\right)}{\sum_{n=1}^{n}\left(X_{1,t}\right)} \qquad \textit{Equation 4-3}$$

Where $X_{1,t}$ and $X_{2,t}$ are the respective measured and simulated data points, and n is the total number of data points (i.e. for energy analysis, n monthly = 12 and n hourly = 8760).

Root mean square error

This is a measure of the variability of the data. For energy simulation, the root mean square error is obtained by calculating and squaring the error (difference in the paired data points) for every 60 minutes. The sum of the squared errors (denoted as SSE) each month are added

and divided by their corresponding number of point which provides the mean squared error (denoted as MSE). The square root of the mean square error is obtained, which is then expressed as the root mean square error (denoted as RMSE). Mathematically, root mean square error is given by Equation 4-4

$$\sqrt{\frac{\sum_{n=1}^{n}\left(X_{1,t}-X_{2,t}\right)^{2}}{n}} \qquad \textit{Equation 4-4}$$

Where $X_{1,t}$ and $X_{2,t}$ are the respective measured and simulated data points and n is the total number of data points (i.e. for energy analysis, n monthly = 12 and n hourly = 8760)

Coefficient of Variance (root mean square error)

The coefficient of variation of the root mean square error allows the evaluation of how well a model matches the data by taking offsetting errors between simulated and measured data. This is obtained by dividing the root mean square error by the mean. Mathematically, root mean square error is given by Equation 4-5

$$\frac{RMSE}{\bar{m}} \qquad \textit{Equation 4-5}$$

Where $\bar{m}$ is the mean of the data and $RMSE$ is the root mean square error.

The ASHRAE guideline 14 specifies value acceptable for MBE and CVRMSE for both monthly and hourly simulations. Other standards include International Performance Measurements and Verification Protocol (IPMVP) and Federal Energy Projects (FEMP).

In comparison to MBE, the CVRMSE is seen as the method that closely reflects the accumulated degree of error due to it being a measure of cumulative error normalised to the mean of the measured values (Royapoor & Roskilly, 2015).

4.5 Thermal Bridges Calculation

The effect of thermal bridging phase analyses the influence thermal bridges have on the building energy performance. This phase is dependent on both the infrared thermography and computer simulation phase. For the thermal bridge effect on the building's energy performance to be evaluated, the heat loss from the thermal bridge has to be calculated. This was achieved using both thermography and numerical analysis of the affected areas within the envelope. With the heat loss obtained, the linear thermal transmittance of the thermal bridge can be evaluated using equation 4-6 provided in EN ISO 10211.

$$H_D = \sum_i U_i . A_i + \sum_k \Psi_k . l_k + \sum_j \chi_j \qquad \textit{Equation 4-6}$$

The building research establishment in a digest published in 2002 provided a means of calculating the thermal transmittance of a wall with steel frame structure using the methodology described in BS EN ISO 6949, 2007. Doran, S and Gorgolewski, M, 2012 in BRE Digest 465 introduced a parameter (p), which depends on the details of the construction. The value of p is given by equation 4-7 below. The parameter that affects the value of p is as follows; the flange width, the spacing between the studs and the stud's depth (i.e. the dimension of the stud in the direction of inside to outside).

$$p = 0.8\left(\frac{R_{min}}{R_{max}}\right) + 0.32 - 0.2\left(\frac{600}{s}\right) - 0.04\left(\frac{d}{100}\right) \qquad \textit{Equation 4-7}$$

Where R_{min} is lower resistance limits, R_{max} Is upper resistance limits, s is Stud spacing, d is the stud depth. Using the methodology described in BS EN ISO 6949 and BRE Digest 465, the corresponding U-value was obtained from the equations below

$$R_T = pR_{max} + (1-p)R_{min} \qquad \textit{Equation 4-8}$$

Where p is the proportion

$$U = \left(\frac{1}{R_T}\right) + \Delta U_g + \Delta U_f \qquad \textit{Equation 4-9}$$

Where R_T is total resistance value, ΔU_g is Corrections for the air gap,ΔU_f Is corrections for fixings. If there are any air gaps with the details, a further adjustment in U-Value due to the air gap must be added to the total U-value as shown in equation 4-9 above. The additional change in U-value as a result of the air gap is given by

$$\Delta U_g = \Delta U^{"} \left(\frac{R_i}{R_t}\right)^2 \qquad \textit{Equation 4-10}$$

Where R_i is air gaps thermal resistance,R_t is total thermal resistance, which the element would have, in the absence of air gaps and fixing, $\Delta U^{"}$ is the air gap correction factor as defined on BS EN ISO 6946.

An additional change to the U-Value is made through that of the steel fixing. This is given by the equation below.

$$\Delta U_f = \propto \lambda_f A_f n_f \left(\frac{R_i}{R_T}\right)^2 / d_i \qquad \textit{Equation 4-11}$$

Where, λ_f is the fixing thermal conductivity, A_f is the crossectional area of the fixing, n_f is the number of fixings per square metre of area

4.6 Overheating Risk

In recent years, there has been much debate regarding temperature rising in future. These have led to researcher pondering about climate leading to the risk of overheating or hothouse effect. CIBSE described overheating as a term used widely; which is not accurately defined or understood. Furthermore, they defined overheating as the time at which building occupants feel uncomfortably hot and that the indoor environment causes discomfort.

Link to previous steps: *Boundary conditions from the energy model are used in this phase as inputs. The influence of the unwanted heat gains and losses into the system on overheating and the risk of overheating in the future are analysed.*

Overheating is usually assumed to indicate that the temperature of the indoor environment is too hot for comfort. CIBSE evaluated that temperature is not the only factor to be considered, there are other important factors such as

- Environmental factors
    - Air movement and humidity
- Contextual factors such as
    - Building's purpose
    - Building management and design
    - Attitude of occupants

However, CIBSE stated that overheating happens in buildings either through the following or through a combination of the following, which are bad design, poor management,

inadequate services. Therefore, buildings without mechanical ventilation or cooling are more prone to overheating than buildings with mechanical ventilation or cooling.

To access the extent of risk of overheating in building energy simulation, it is suggested by CIBSE Guide A that the Design summer year weather files be used. This is because the Design summer years implement a more rigorous test of overheating risk than the rest of the weather files such as test reference years.

There are two ways of estimating/predicting overheating in buildings according to the CIBSE Guide, which is prediction by simulation and prediction by monitoring. For prediction by simulation, there is a recommendation that all simulation software should have. These are:

- Simulation software should be able to predict operative temperatures in occupied buildings
- Simulation software should include a reasonable allowance for the use of window opening in free-running buildings
- Various sources of heat gain to the building as well as effects of solar radiation through windows are fully and realistically accounted for.

4.6.1 Overheating Criteria

There has been two guides to accessing overheating which have been developed by CIBSE. These are

- CIBSE Guide A and
- CIBSE TM52

According to CIBSE guide A, the recommended acceptable internal temperature for non-air conditioned buildings during summer are given below

Table 4-9: Operative temperature for indoor comfort in summer recommended by CIBSE Guide A

BUILDING TYPE	OPERATIVE TEMPERATURE FOR INDOOR COMFORT IN SUMMER °C
OFFICES	25
SCHOOLS	25
RESIDENTIAL (LIVING AREAS)	25
RESIDENTIAL (BEDROOMS)	23
RETAIL	25

The recommended comfort criteria for sports halls according to the CIBSE guide are shown in the table below

Table 4-10: Recommended sports hall comfort criteria by CIBSE Guide A

SPORTS HALL RECOMMENDED COMFORT CRITERIA

CRITERIA / LOCATION		Changing rooms	Hall
WINTER OPERATIVE TEMPERATURE RANGE FOR ACTIVITIES AND CLOTHING LEVEL	Temperature(°C)	22-24	13-16
	Activity (met)	1.4	3.0
	Clothing (Clo)	0.55	0.4
SUMMER OPERATIVE TEMPERATURE RANGE FOR ACTIVITIES AND CLOTHING LEVEL (AIR CONDITIONED BUILDINGS)	Temperature (°C)	24-25	14-16
	Activity (met)	1.4	3.0
	Clothing (Clo)	0.35	0.35
SUGGESTED AIR SUPPLY RATE ($L.s^{-1}$ PER PERSON)		6-10 ACH	10
FILTRATION GRADE			
MAINTAINED ILLUMINANCE (LUX)		100	300
NOISE RATING (NR)		35-45	40-50

The comfort criteria for summertime period were specified for air-conditioned buildings. Therefore higher temperature is accepted for buildings that do not have air- conditioning. The thermal performance of a building during summer is usually measured against a benchmark temperature that should not be exceeded for a designated number of hours or a percentage of the annual occupied period (CIBSE Guide A).

According to CIBSE Guide A, a building is said to have overheated when the operative temperature exceeds the benchmark temperatures shown in Table 4-11 below. Furthermore, if the temperature is above the benchmark temperature for more than the designated amount of time, the building is said to be over-heating. The designated amount of time is calculated as one per cent of the annual occupied hours.

Table 4-11: Benchmark summer peak temperature and overheating criteria by CIBSE Guide A

BUILDING TYPE	BENCHMARK SUMMER PEAK TEMPERATURE °C	OVERHEATING CRITERIA
OFFICES	28	1% annual occupied hours over the operative temperature of 28
SCHOOLS	28	
RESIDENTIAL (LIVING AREAS)	28	
RESIDENTIAL (BEDROOMS)	26	1% annual occupied hours over the operative temperature of 26

Observations were made in regards to the overheating criteria set by CIBSE guide A, which gives a single temperature above which the building or room is said to overheat. The observations were that at some point in time, the threshold temperature might be considered to be acceptable depending on other conditions.

4.6.2 CIBSE TM52 Criteria

CIBSE TM52 overheating criteria considers both frequency and the length of time that high temperatures may occur. For defining overheating, CIBSE developed three criteria that provide a robust and balanced assessment of buildings. The recommendation is that a building is regarded as overheating if it fails any two of the three criteria.

Criteria 1: Hours of exceedance (H_e)

The number of hours (H_e) during which ΔT is greater than or equal to one degree (K) during the period of May to September inclusive shall not be more than 3 percent of occupied hours.

This sets a limit for the number of hours that the operative temperature can exceed the upper limit of the range of comfort temperature by 1 K or more during the occupied hours of a typical non-heating season. This is usually between the 1st of May to 30th of September.

$$\Delta T = T_{op} - T_{max} \qquad \textit{Equation 4-12}$$

Where ΔT is the difference between the temperatures, T_{op} is the operative temperature and T_{max} is the limiting maximum acceptable temperature and is given by

$$T_{max} = 0.33T_{rm} + 21.8 \qquad \textit{Equation 4-13}$$

$$T_{comf} = 0.33T_{rm} + 18.8$$ *Equation 4-14*

Where T_{rm} is the running mean of the outdoor temperature, The 3 percent occupied hours criteria was obtained from BS EN 15251.

Criteria 2: Daily Weighted Exceedance (W_e)

To allow for the severity of overheating the weighted exceedance (W_e) shall be less than or equal to 6 in any one day where:

$$W_e = \left(\sum h_e\right) x\, WF$$
$$= (h_{e0}\, x\, 0) + (h_{e1}\, x\, 1) + (h_{e2}\, x\, 2) + (h_{e3}\, x\, 3)$$ *Equation 4-15*

This sets an acceptable level for the severity of overheating according to BS EN 15251 Degree hours criteria Annex F method B. This is the time during which the operative temperature exceeds the specified range during the occupied hours, weighted by a factor that is a function depending on how many degrees the range has been exceeded. The criteria set a value of 6 as an initial assessment of what constitutes an acceptable limit of overheating on any single day.

Criteria 3: Upper Limit Temperature (T_{upp})

To set an absolute maximum value for the indoor operative temperature the value of ΔT shall not exceed 4K

This sets a limit after which normal adaptive actions would be insufficient to restore personal comfort and occupants would complain of being too hot. The 3rd criteria cover the extremely hot weather condition and future climate scenarios.

Category	**Explanation**	**Suggested acceptable range**
I	High level of expectation (only used for spaces occupied by very sensitive and fragile persons	± 2K
II	Normal expectation (for new buildings and renovations)	± 3K
III	A moderate expectation (used for existing buildings)	± 4K
IV	Values outside the criteria for above categories (only acceptable for a limited period)	> 4K

Operative temperature

CIBSE defined operative temperature as a combination of the air and mean radiant temperature into a single value to express their joint effect. Furthermore, it is the weighted average of the two, dependent on the heat transfer coefficient by convection and radiation at the clothed surface level the operative temperature can be expressed as

$$T_o = HT_{ai} + (1 - H)T_r \quad \textit{Equation 4-16}$$

Where T_o is the operative temperature in °C, H is the dimensionless ratio between the surface heat transfer coefficients by convection and by radiation expressed in $\frac{W}{m^2}.K$, T_{ai} is the indoor air dey bulb temperature in °C and T_r is the mean radiant temperature in °C.

The operative temperature can be expressed in terms of airspeed, this is due to the difference in the estimation of the heat transfer coefficients. Therefore H is expressed as $\sqrt{(10v)}$ Where v is the airspeed in m/s. However, at indoor speeds of less than $0.1m/s$, natural convection is assumed to be equivalent to $v = 0.1m/s$ and operative temperature T_o can be expressed as

$$T_o = 1/2T_{ai} + 1/2T_r \quad \textit{Equation 4-17}$$

Operative temperature influences the thermal comfort of a building by providing the upper and lower limit operative temperature. From BS EN 15251, the upper limit and lower limits operative functions are a function of the exponentially weighted running mean of outdoor temperature. According to the CIBSE guide, A, the upper limit and lower limit temperatures can be expressed as

Free running buildings

$$T^n_{c,max} = 0.33T^n_{rm} + 20.8 \quad \textit{Equation 4-18}$$

$$T^n_{c,min} = 0.33T^n_{rm} + 16.8 \quad \textit{Equation 4-19}$$

Heated and cooled buildings

$$T^n_{c,max} = 0.09T^n_{rm} + 24.6 \quad \textit{Equation 4-20}$$

$$T^n_{c,min} = 0.09T^n_{rm} + 20.6 \quad \textit{Equation 4-21}$$

4.7 Computational Fluid Dynamics

Computational fluid dynamics is a term used to describe a family of numerical methods used to calculate the temperature, velocity and various other fluids properties throughout a region of space (DesignBuilder 2019). Computational fluid dynamics can be applied for the following purposes;

- Detailed modelling of thermal environmental conditions
- Detailed modelling of physiological heat exchange of individual people with their surroundings.

Link to previous steps: *Defects and boundary conditions obtained from thermography and energy modelling are used in this step to analyse the fluid properties within the affected areas.*

According to (CIBSE, 2015), CFD is arguably the most complex ventilation modelling technique in use. CFD is governed by three fundamental principles which are; conservation of mass, energy and momentum given in equations below.

$$\frac{\partial p}{\partial t} + \frac{\partial}{\partial x_j}(pu_j) = 0 \qquad \textit{Equation 4-22}$$

$$\frac{\partial}{\partial t}(pu_j) + \frac{\partial}{\partial x_j}(pu_i u_j) = \mu \frac{\partial \tau_{ij}}{\partial x_j} - \delta_{ij} \frac{\partial p}{\partial x_j} + B_i \qquad \textit{Equation 4-23}$$

$$\frac{\partial c}{\partial t} + \frac{\partial}{\partial x_j}(pu_j c) - \frac{\partial}{\partial x_j}\left(\Gamma_c \frac{\partial c}{\partial x_j}\right) = 0 \qquad \textit{Equation 4-24}$$

From Equation 4-22, the conservation of mass states that the rate of change of mass within a volume is equal to the net flow of the mass across the boundaries of the fixed volume. This equation is derived by considering a fixed volume in space and assuming that the flow of air into the volume is equal to the flow of air leaving the volume. Equation 4-23 represents the conservation of momentum equation, also known as the Navier-Stokes equation, which is derived from Newton's second law. Equation 4-24 is the representation of the conservation of energy which states that the rate of change of internal energy of a volume is equal to the heat supplied to that air minus the work is done by the volume of air on its surroundings expressed using enthalpy.

The numerical analysis is conducted by dividing the geometric spaces into several non-overlapping adjoining cells, which are known as the finite volume grid. A non-uniform rectilinear Cartesian grid, which are parallel grid lines with the major axis and a grid line spacing that enables non-uniformity, is used in DesignBuilder.

In the DesignBuilder inbuilt CFD analysis module, there are two types of CFD analysis, namely

- External CFD: provides the distribution of air velocity and pressure around the building structure due to the effect of wind.
- Internal CFD: provides information on the distribution of air velocity, pressure and temperature throughout the internal building space.

Boundary conditions play an important role in the CFD analysis. For internal analysis, zone surface boundaries (such as extract grills, supply diffusers, temperature and heat flux patches) and model assemblies representing occupants, radiators and fan-coil units are required. Boundary condition can be imported from an EnergyPlus simulation (hourly data results) to be used for CFD simulation. The data that can be imported as

- surface inside temperatures of walls, floors, roofs, windows, partitions, ceilings, doors and sub-surfaces
- flow in and flow out of windows, vents and doors

An important requirement for CFD analysis is to balance the flow in and flow out in a system. This can be done manually or automatically when setting up the boundary conditions. For internal CFD analysis, the internal boundary conditions can be defined in three ways:

- Using surface temperatures
- Zone surface boundary conditions
- Using component blocks and component assemblies.

4.8 Summary

This study proposes a building energy investigation framework, which combines infrared thermography and computer simulation methodologies to analyse effects of thermal bridges on the performance of a building. The infrared thermography methodology is composed of an analysis of thermal images of the building and generation of numerical models simulating thermal conductivity of building parts with thermal bridges. The computer simulation methodology encompasses the design of building energy simulation model and measurement collection of the same building. Measured temperatures are used to calibrate and validate the building model. Effects of thermal bridges and building performance with anticipated climate changes are simulated inputting calculated U-values and psi-values from the infrared thermography analysis to the calibrated building model.

Chapter Contribution: Development of Energy Investigation Framework

The main objective of the research is to develop a framework capable of assessing the energy performance of the building (modern and old) considering the effect of defects such as thermal bridges and also an assessment of building in future weather scenarios. This was achieved using a systematic combination of relevant methodologies such as infrared thermography, numerical simulations, and building energy simulations.

Chapter 5: The case study: Clifton Clubhouse

5.1 Introduction

Nottingham Trent University is committed to creating a sustainable campus by investing in their buildings, environment and spaces and has been ranked as the fifth most sustainable university in the world by the UI Green Metric World University Ranking. Buildings have been renovated and built to achieve high standards such as The Pavilion (renovated), and this generates more energy than it consumes, and The Clifton Clubhouse (newly built) built as a low energy building

In other to bridge the performance gap between the predicted and the measured performance, De Wilde (2014) suggested three forms, one of the forms is by conducting a single case study using a relationship of 1:1 between prediction and measurement. Therefore, the energy investigation framework (EIF) is used to analyse the case study (Clifton clubhouse) which was built as a low energy building with both passive and active energy measures. Energy simulation software, DesignBuilder is used to create and analyse the Clifton clubhouse model. The software was used because of its EnergyPlus simulation engine, ability to perform CFD analysis and also follows ISO 13790:2009 and agrees with EN 15265:2007. Results from the model are compared with monitored data (July 2017-July 2018) for calibration and validation purposes. Infrared thermography of the building and numerical analysis of defects are developed and analysed

5.2 The Clifton Clubhouse

The Clifton clubhouse building, a two-storey building, located at Nottingham Trent University Clifton campus is used as a case study (Figure 5-1-Figure 5-2). The building built as a low energy building with both passive and active energy measures used in the building. Nottingham is a 74.61 km^2 city located in the eastern midlands of the United Kingdom with the latitude of 52.9548^o N, a longitude of 1.1571^{o}W and altitude of 117m. Nottingham city has 25% of its wind from the southwest direction, followed by 24% in the west direction. The average speed of the wind between January 2000 and December 2017 is 12.8 kph with the months January and February having the highest wind speed of 14.4 kph and 14.3 kph respectively.

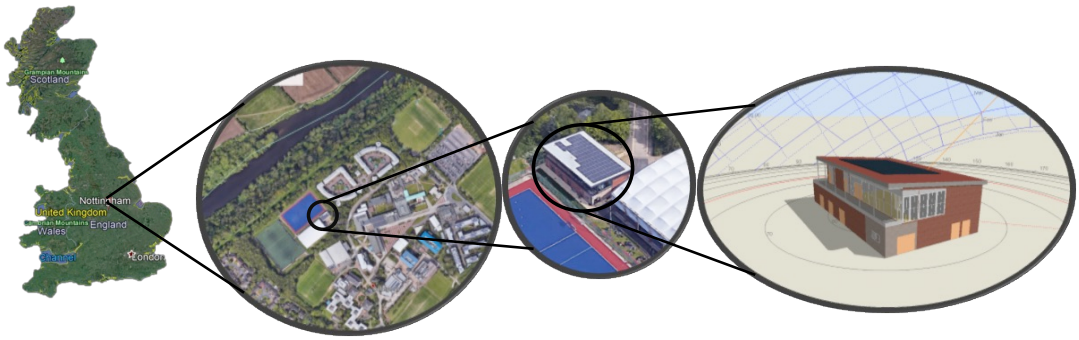

Figure 5-1: Clifton Clubhouse and its location. Left to right: location in the UK, location and orientation in the campus, bird's view and DesignBuilder model.

Nottingham has a warm and temperate climate with substantial rainfall averaging 648mm. The driest month of February in Nottingham also has lots of rain with an average of 46mm precipitation while August has the most precipitation averaging 60mm. The average annual temperature is 9.8°C in Nottingham with July being the warmest and January the coldest month with an average temperature of 2.9°C. The Koppen-Geiger classification (see Figure 5-3) of Nottingham is Cfb (Warm temperate-fully humid and warm summer)

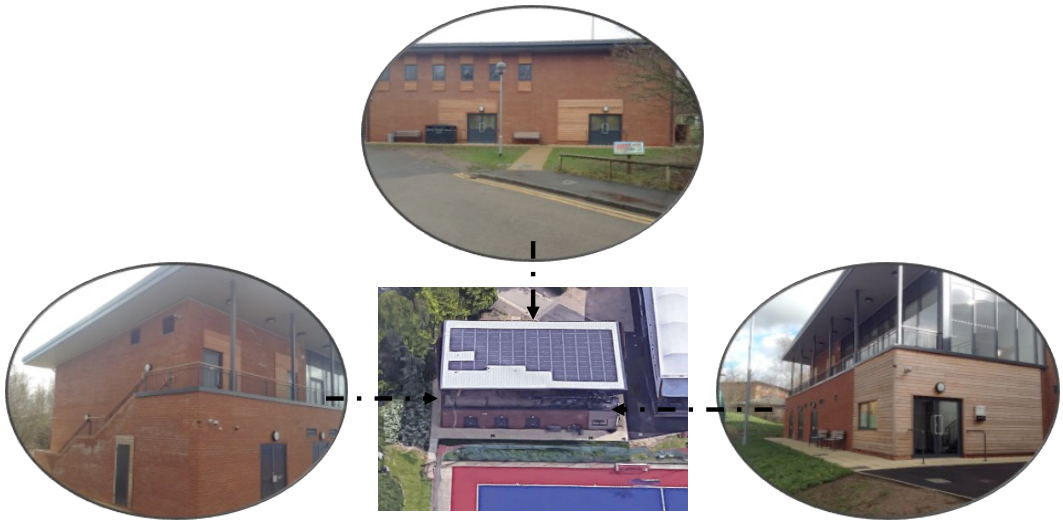

Figure 5-2: Clifton clubhouse satellite image (mid), left perspective, right perspective and back perspective (top)

Due to the location of Nottingham, the sun's location at different times of the year are;

- Highest position: 21st of June, 60.4°
- Lowest position: 21st of December, 13.5°
- Autumn Equinox: 23rd of September, 37.2°
- Spring Equinox: 23rd of March, 37.5°

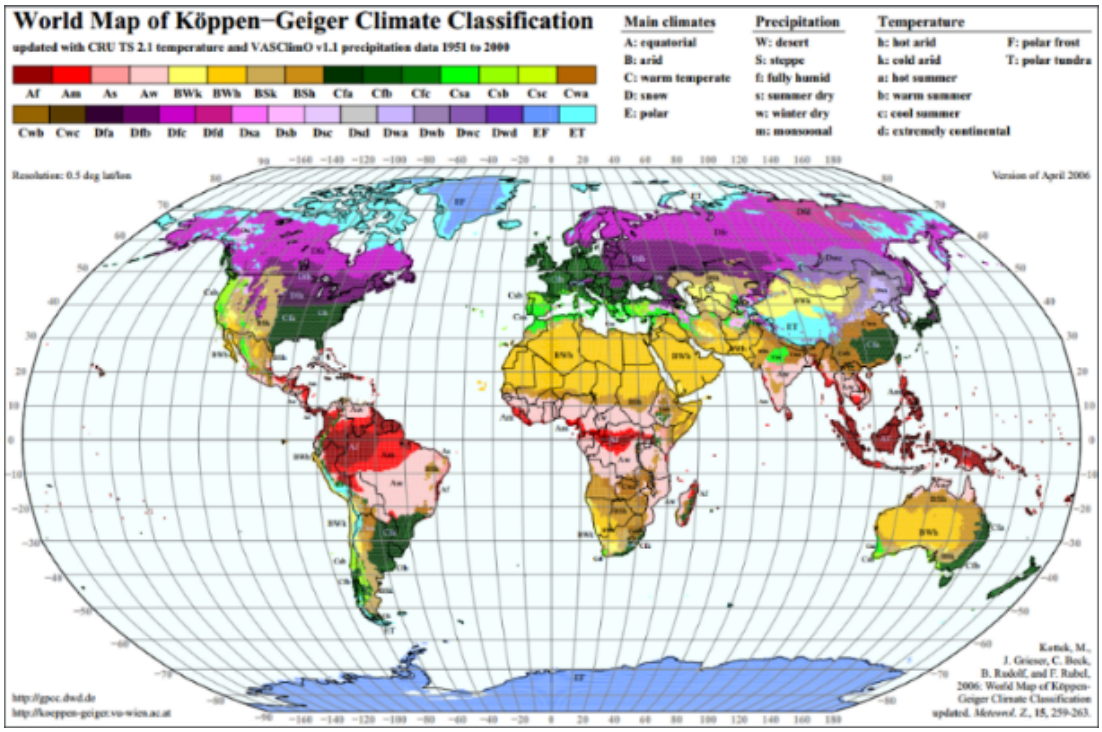

Figure 5-3: Koppen-Geiger classification

The clubhouse is composed of two floors (the ground floor and the first floor) with the orientation of the clubhouse in the North direction. The Ground floor of the building is composed of changing rooms, showers, storage rooms, plant rooms and the main entrance to the first floor. The first floor also has a main-lounge and two changing rooms with showers as shown in Figure 5-4. The main function of the building is for a changing facility with showers, and it is mainly used during term time. The occupancy scheduled was assumed to be constant during term time with a schedule of 8:00 to 17:00 from Monday to Friday except for Wednesday (sports day) which has a schedule of 8:00 to 20:00.

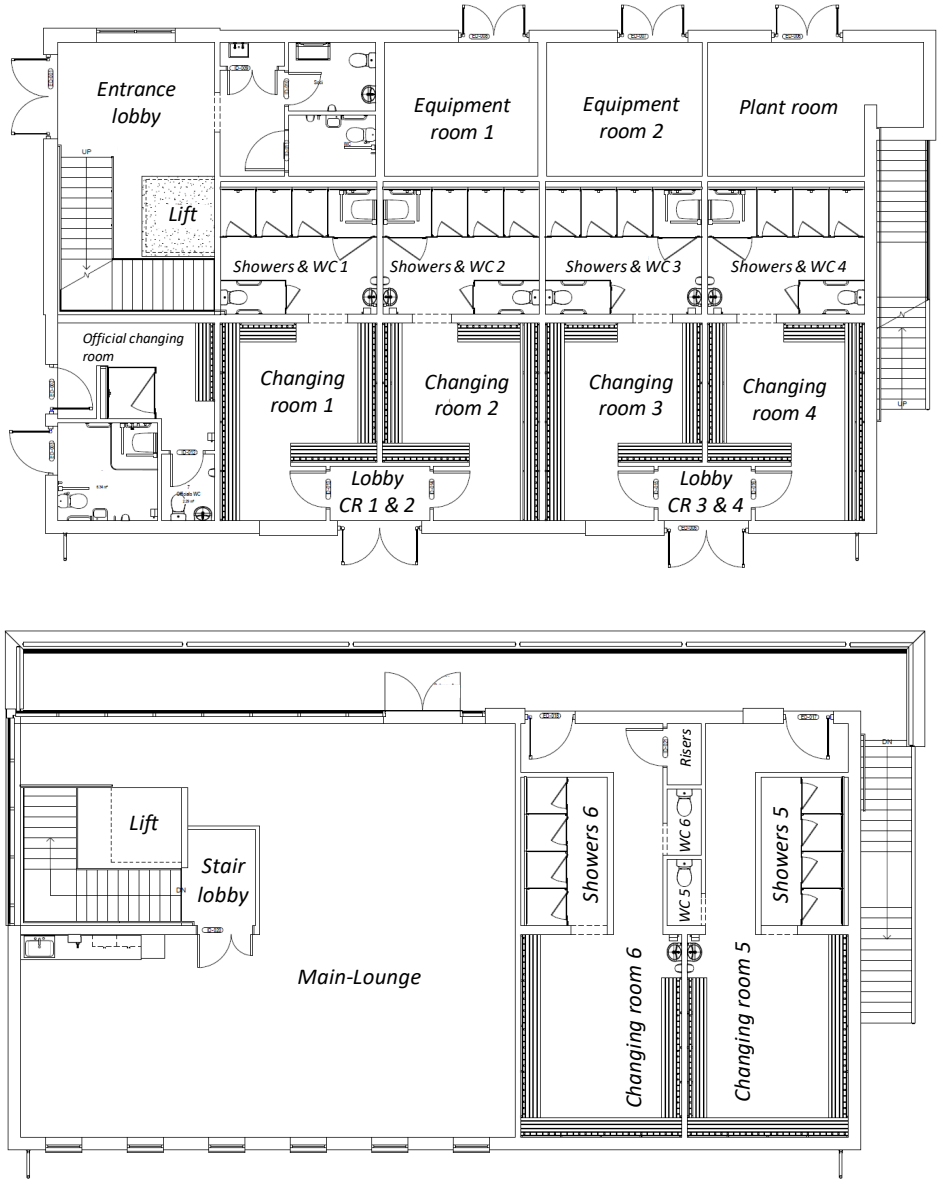

Figure 5-4: Ground (top) and First floor (bottom) plan

The external wall is composed of old red Trafford brickwork with a thermal conductivity of 0.77W/mK on the outer surface with Knauf-Dritherm cavity slab as an insulation material with a thermal conductivity of 0.037 W/mK, Thermalite Hi-strength concrete blocks with a conductivity of 0.18 W/mK and density of 730kg/m^3 on the inner surface. Part of the outer-wall has an additional horizontally laid timber on the surface. The thermal resistance of the external wall is 3.070m^2k/W, which gives a U-value of 0.326W/m^2k.

The Building has natural ventilation in the main lounge and is equipped with air exchangers in the showers and changing rooms. During occupancy hours, the air change rate of the building was kept constant. The clubhouse is also equipped with 34kw solar panels. Heating is available on both floors of the building using natural gas. The main lounge is being cooled

using natural ventilation from the glazing. Furthermore, the building is equipped with a Heat Recovery Unit (HRU) in all the changing rooms and shower rooms as shown in Figure 5-5 below

Most of the building lightning are LED lights that operate during occupancy hours. The lighting level of the building Is 300lux. For lighting control, LED lights are equipped with sensors to switch off the light during non-occupancy hours except for the main lounge, which has a manual control switch.

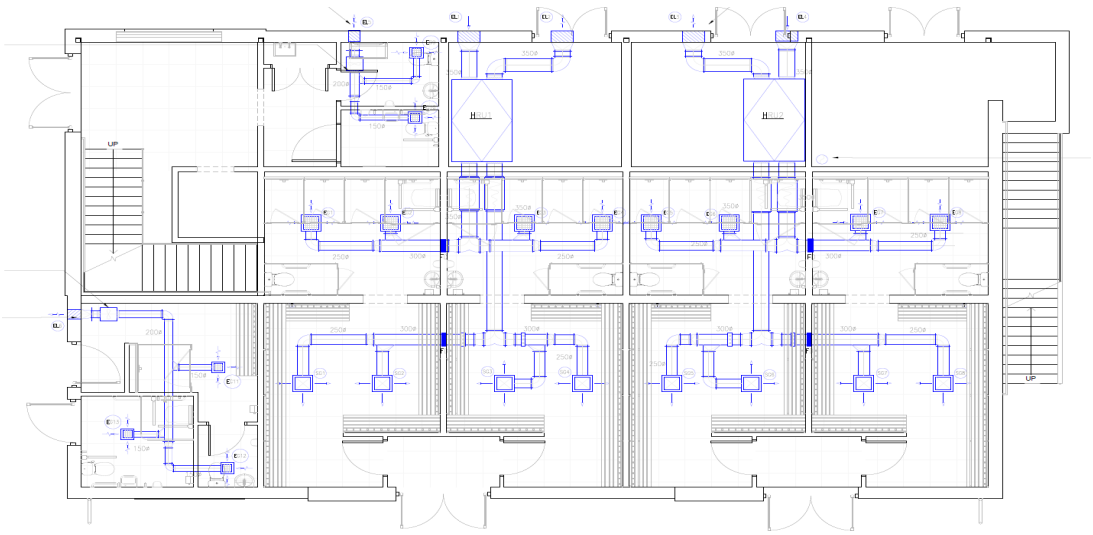

Figure 5-5: Heat Recovery Unit Plan

5.3 Infrared thermography

5.3.1 Thermography Analysis

To fully understand how energy is being distributed in a building, thermal image of the Clifton Clubhouse was studied. The thermal images were studied during the winter period in order to have a sufficient temperature difference between the indoor and outdoor temperature. This is because a minimum temperature difference of 10-15°C between the external and internal environment is required to evaluate the heat distribution in buildings, as stated by Asdrubali et al. 2012. Furthermore, in other to have the actual building energy pattern, the thermography was taken after the sun has set so that the solar radiation emitting from the building can be avoided. Traditional thermography was used in this study as this allows detailed thermographic analysis, as stated by Fox et al. 2016. This provides the advantage of viewing defects from different angles and distances. Furthermore, Fox et al. 2016 stated that the results from thermography could be used with other techniques such as computer simulation which enhances understanding and evaluation of defects through comparison with thermal models.

5.3.1.1 The Building Exterior

For every thermography, certain parameters such as air temperature, reflective temperature and emissivity have to be taken into account. To measure the air temperature and reflective temperature, plain white paper and a scrunch aluminium foiled paper were used respectively, as shown in Figure 5-6.

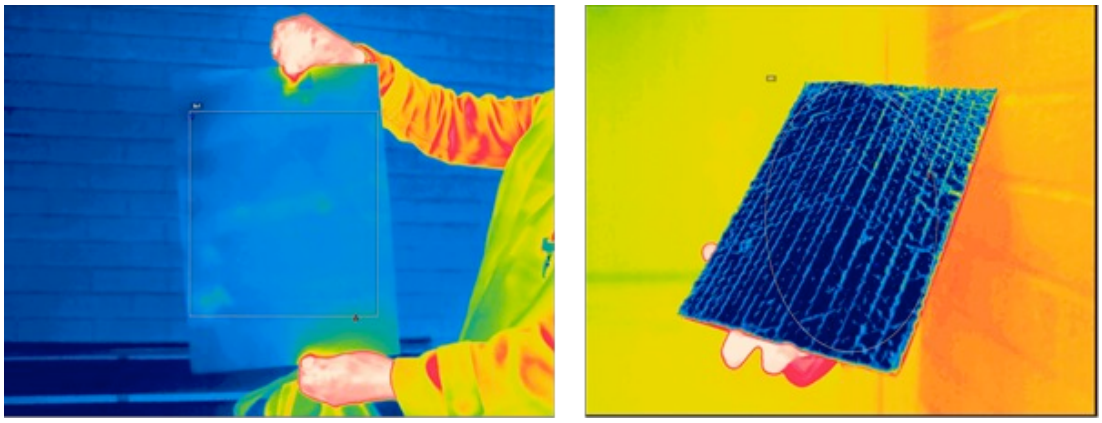

Figure 5-6: External calibration procedure for atmospheric temperature (left) and reflective temperature (right)

To obtain the reflected temperature, the scrunch aluminium foil paper was placed in other that it was facing the sky at an angle. The emissivity of the camera was set to the unitary value. Due to the highly reflective nature of the aluminium foil, the camera settings, the thermogram obtained gives the reflected temperature which is linked to the radiative heat sources and influence of the measured environment (in this case the sky).

The air temperature and reflective temperature at the time of the building survey was found out to be 6.6°C and -18.2°C, respectively. This was obtained by taking the average temperature of the papers avoiding the reflection of the thermographer. Furthermore, reflection from nearby buildings may have a large effect on the thermal image, as shown in Figure 5-7 and therefore have to be avoided.

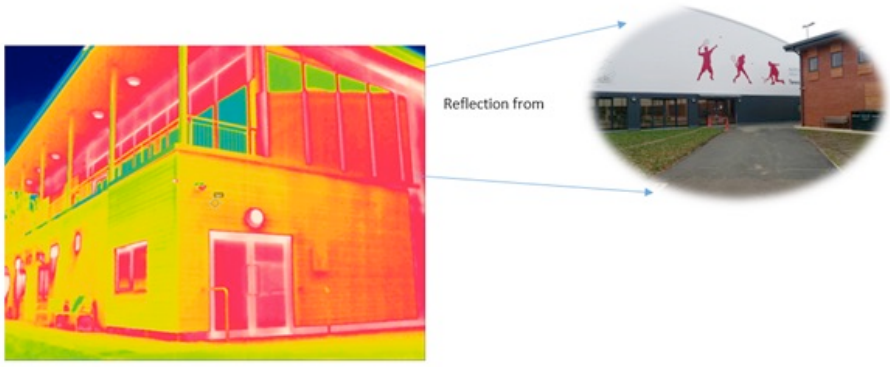

Figure 5-7: Thermal image showing the influence of reflection (from the adjacent building)

From the images acquired, it was observed that there were heat-losses within the building envelope on the west and east side of the building. This heat-loss was observed to be from the roof connection and on the beam between the two floors (see Figure 5-8 and Figure 5-9).

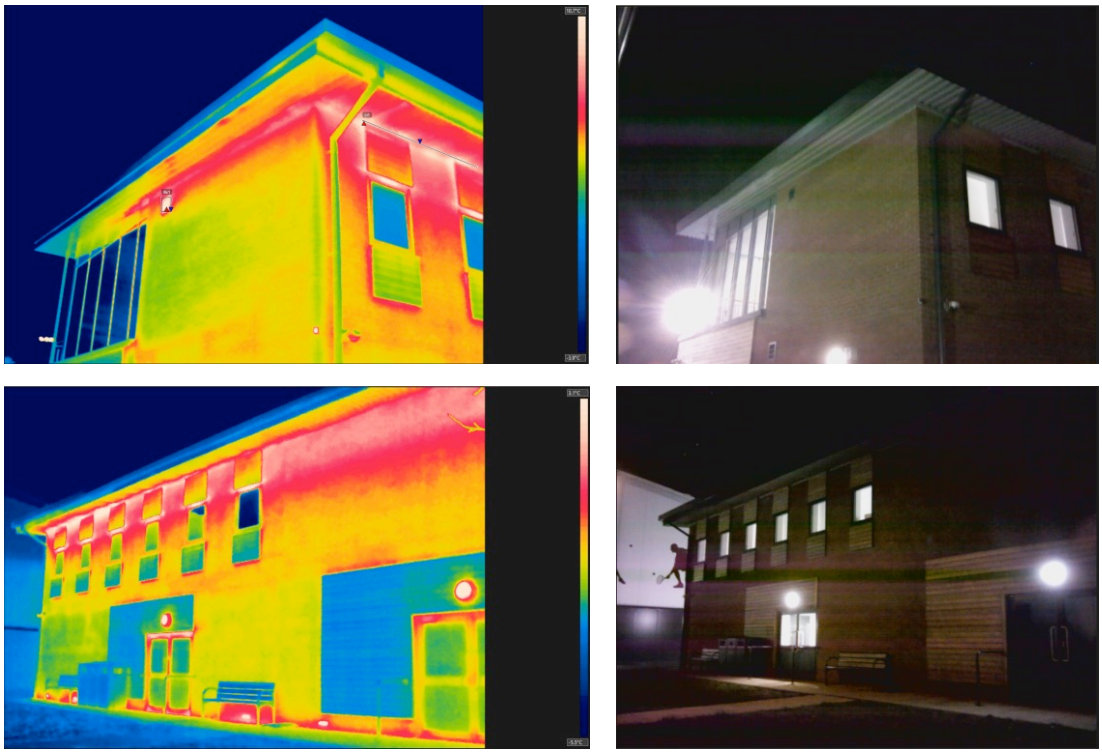

Figure 5-8: Heat losses from the external wall with corresponding digital images

Losses can also be seen in Figure 5-8 from underneath the wooden sub-surface. This was further analysed and was as a result of a different material used beneath the wooden sub-surface. The material used on the upper side of the wooden sub-surface is a catnic cx50 which is metal used to support the load on the windows while that of the bottom is a concrete block.

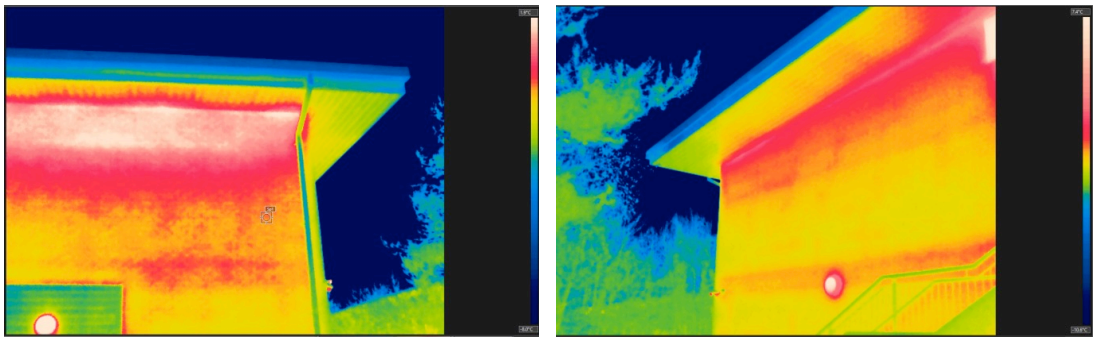

Figure 5-9: Heat loss from roof connection and floor beams

5.3.1.2 Changing Room

The air temperature of the changing room was obtained by hanging a plain white paper at about 1.5m above the floor to obtain an absolute air temperature of the room (Figure 5-10 top). The reflective temperature was obtained using the scrunch foil paper and was placed in the corner of the room so that an accurate reflective temperature can be obtained (Figure 5-10 bottom).

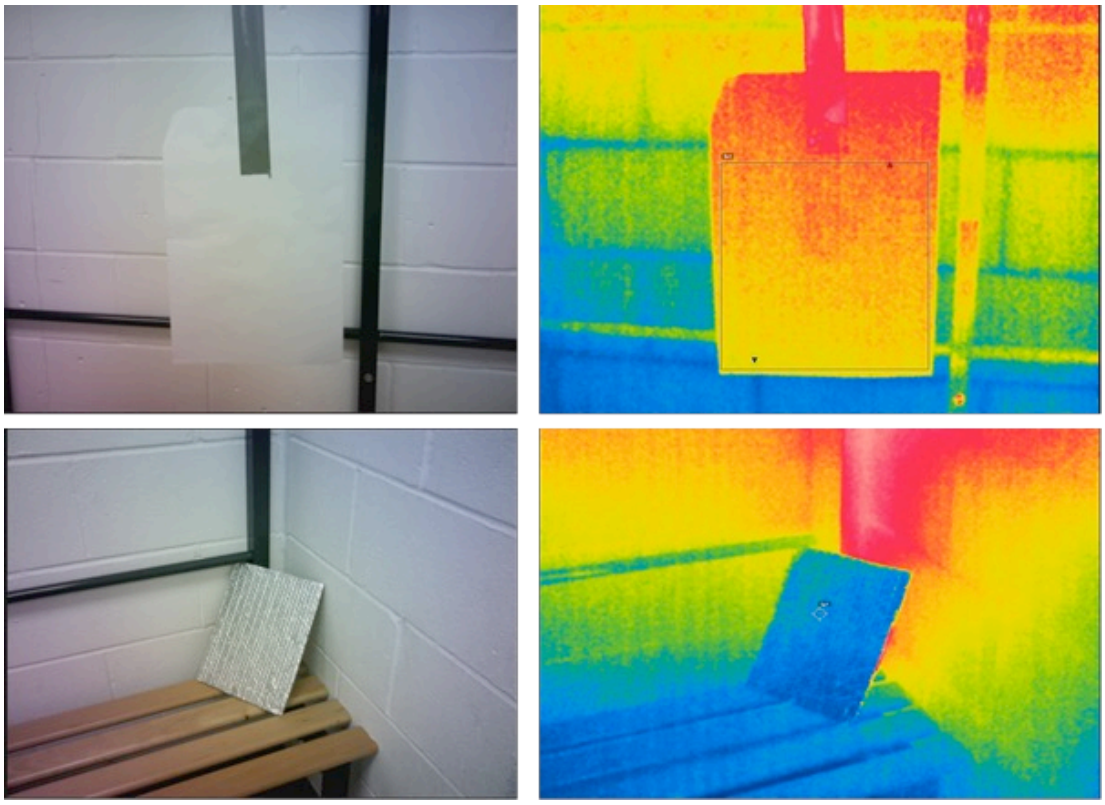

Figure 5-10: Internal Calibration procedure for atmospheric temperature (top) and reflective temperature (bottom)

From the thermal images acquired, it was observed that there were heat gains and heat losses in the changing rooms. The heat gains were mostly due to the presence of domestic hot water pipes in the rooms and from internal walls while the heat-loss were mainly from external walls.

In changing room 1, it was observed that there were cracks on the internal walls, which are causing cold spots on the wall (see Figure 5-11 bottom). The cracks were observed to be a pathway for heat loss within the room. Furthermore, the mortar joints on the walls were also observed to be adding to the heat loss within the room. Another observation was from the corners where there was heat gains into the room (Figure 5-11 top)

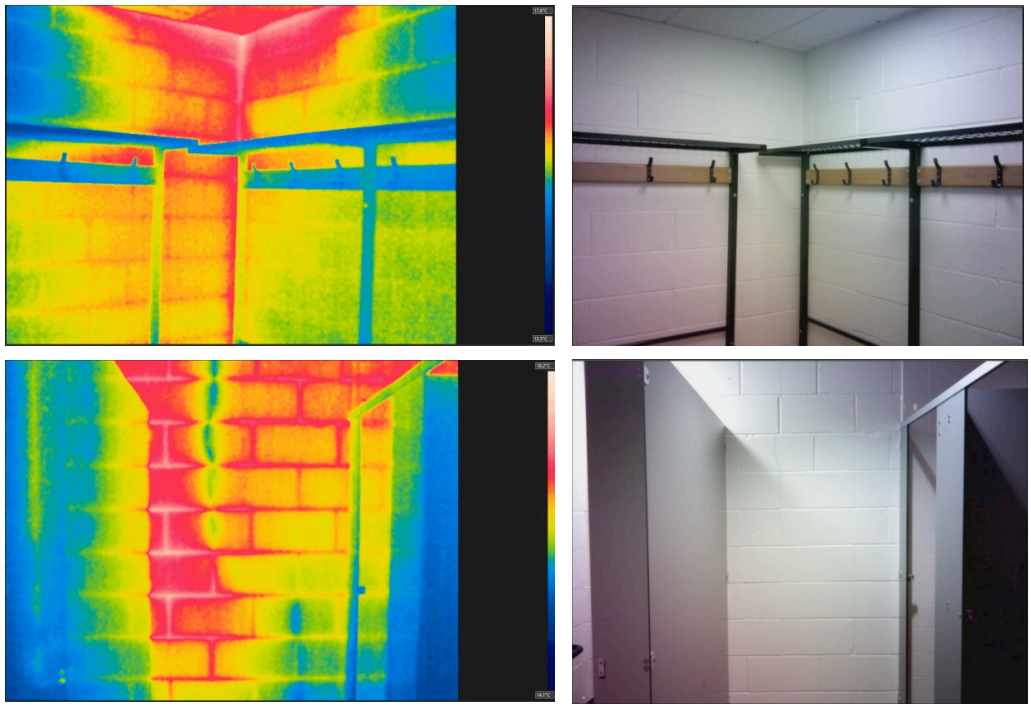

Figure 5-11: Heat-loss and Heat gain from cracks and mortar joint respectively

For changing room 2, Heat exchange from changing room one was causing heat gain through the internal wall as shown in Figure 5-12. The cracks on the wall were observed to have heat loss through them (Figure 5-12). Furthermore, it was observed that there was heat gain at the corner of the changing where the ceiling and two internal walls meet (Figure 5-12).

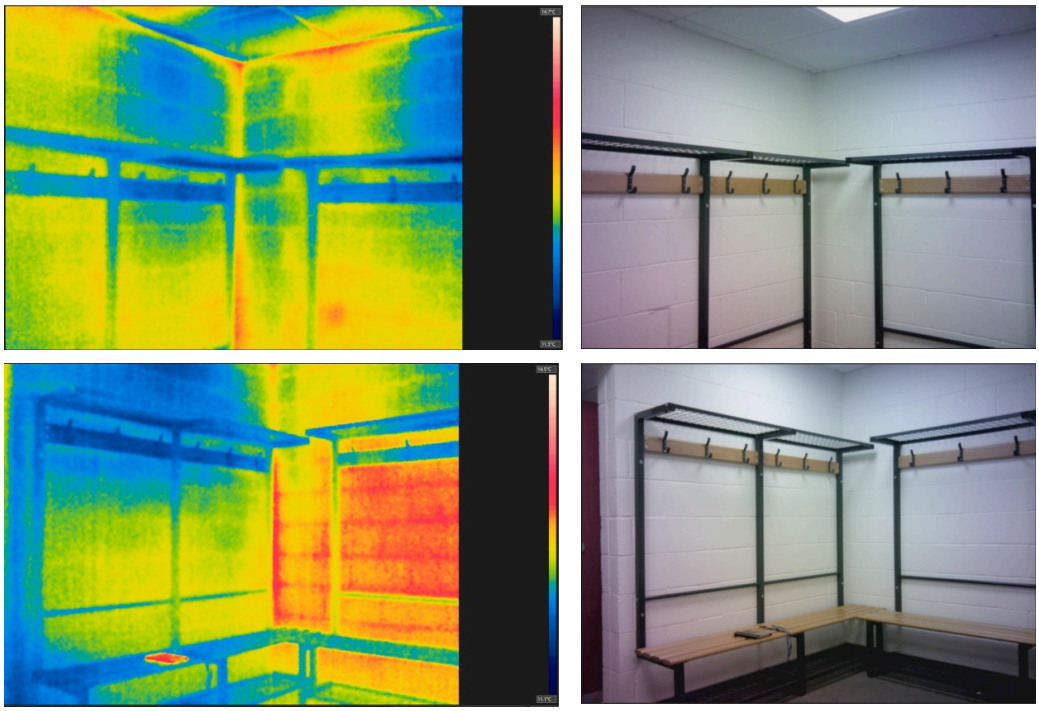

Figure 5-12: Heat losses and gains with corresponding digital images from changing room 2

Domestic hot water pipes at 55°C were creating heat gains into changing room 3 (Figure 5-13). The domestic hot water pipes situated in the shower rooms, but due to conduction, heat gains were observed in the changing room's wall (Figure 5-13 top).

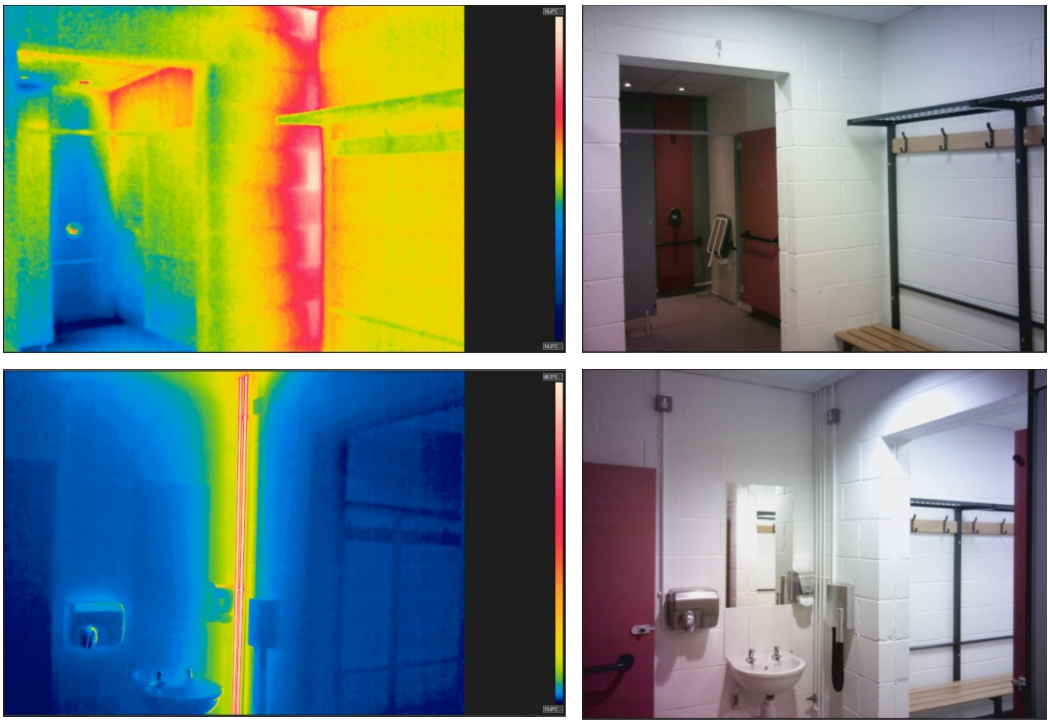

Figure 5-13: Domestic hot water pipes influencing heat gain into changing room 3

In changing room 5, it was observed that there was of influence of external environment which was causing heat loss through the mortar joints (Figure 5-14 top). Exchange of heat from the ceiling to the wall can also be seen (Figure 5-14 bottom) which is due to the service pipes running through the changing room. Furthermore, it was observed that the domestic hot water pipes were adding a significant heat gain into the room, as the pipes were as high as 60°C (Figure 5-14 mid). Another heat gain into the room was identified from a service room with heating pipes and domestic hot water pipes, as shown in Figure 5-14 (top).

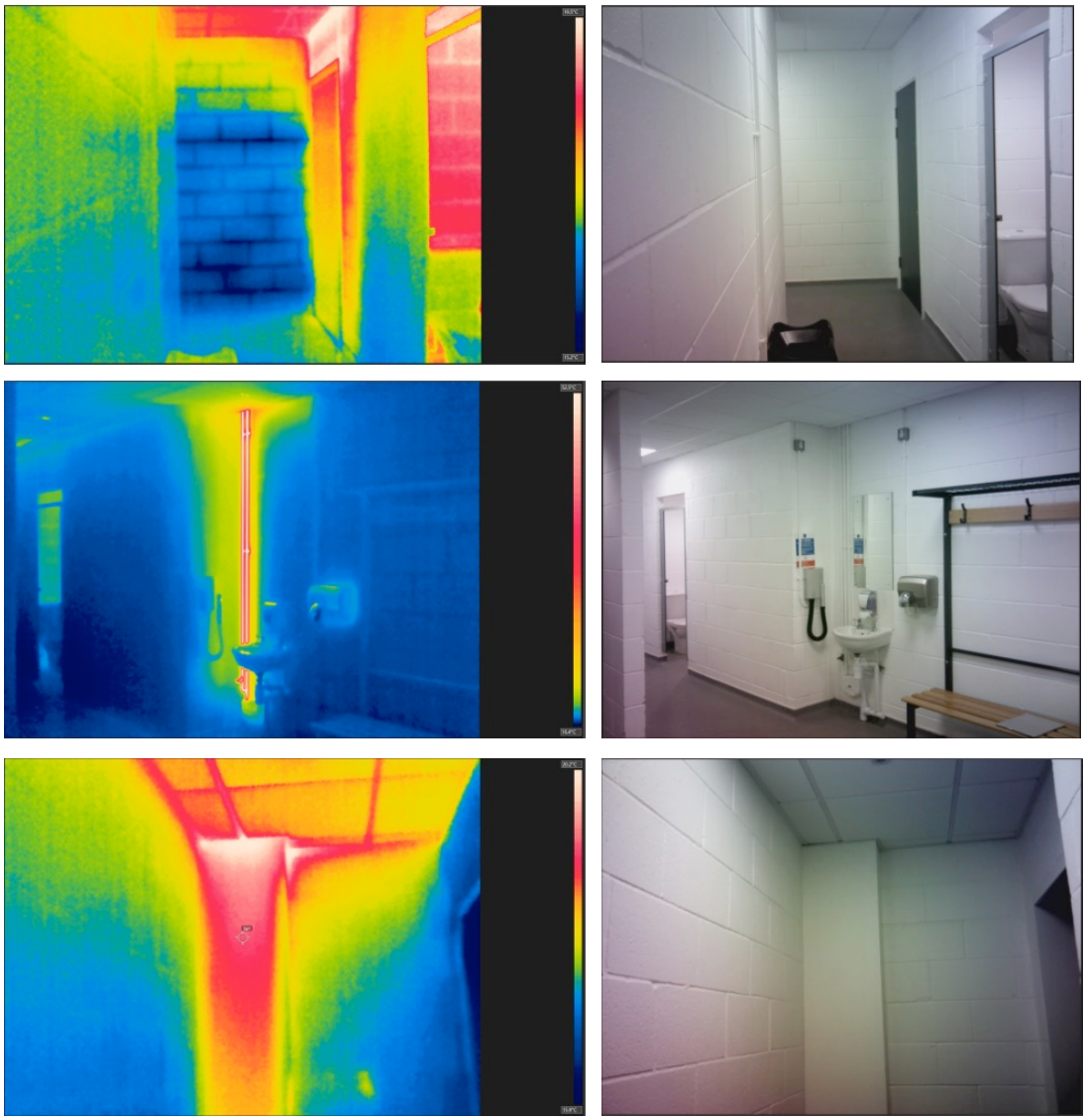

Figure 5-14: Heat losses and gains from changing room 5 with digital images (right)

For changing room 6, cold spots were identified in the corner of the building, and also mortar joints on the blockwork were observed to cause heat loss within the building envelope. Furthermore, it was observed that there was a huge influence of heat exchange from the exterior wall, as there was enough difference in temperature between the internal and external wall (Figure 5-15 top). Moreover, there was a heat gain from the internal wall between the service rooms and changing room 6 (Figure 5-15 top). Heat exchange within the changing room and main-lounge provided heat gain into changing room (Figure 5-15 mid), this is due to the main lounge being heated while the changing room only operated on heat recovery with the wall also being uninsulated (partition wall). The domestic hot water pipes were also adding to the heat gain in the room as the temperature of the pipes were as high as 57°C (Figure 5-15 bottom).

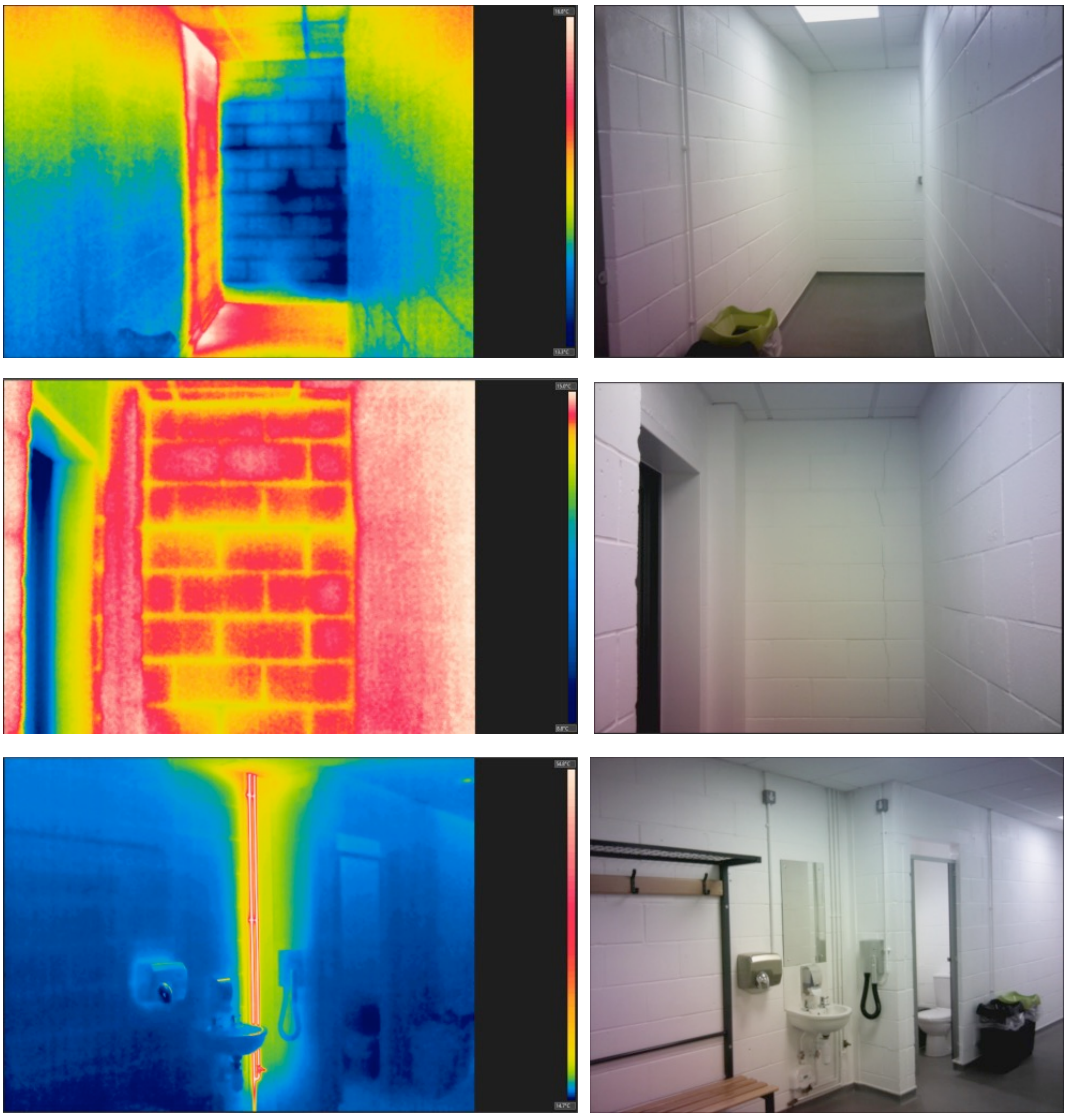

Figure 5-15: Heat losses and gains in changing room 6 with digital images (right)

5.3.1.3 Main-lounge

For the main-lounge, it was observed that there were heat losses, especially from the mortar joints, as shown in Figure 5-16. The walls affected were external walls, and therefore there was a difference of about 18°C between the interior and exterior environment. An expansion Joint was also observed to have an effect causing heat loss. The expansion joints are located on the south-exterior wall and are four in number (Figure 5-16 mid). These combined bring more heat losses in building envelope. Furthermore, it was observed that heat is lost in the corner edges of the room (Figure 5-16 mid).

Figure 5-16: Heat gains and losses in main-lounge with corresponding digital images (right)

5.3.1.4 Entrance

The entrance to the clubhouse is seen to have heat losses and heat gains, particularly in the mortar joints (see Figure 5-17 bottom). This was observed to be throughout the changing room. Another observation was from the entrance door where a certain block was seen to have a different contour, showing heat loss within the wall (see Figure 5-17 top). This was further investigated, and the result was due to the different material properties of the block. The block was a high-density block which is due to the beam (lintel) above the door and so has a different thermal conductivity.

Figure 5-17: Heat losses and gains from the entrance with digital images (right)

5.3.1.5 Official changing rooms

The official changing room situated on the ground floor of the clubhouse had similar defects with that of the entrance. A high-density block causing heat loss was also used in the official changing room, which is also due to the lintel above the door (Figure 5-18 top). Heat losses within the walls were also observed due to mortar joints. Another defect observed was the heat loss from below the door (Figure 5-18 bottom). This was considered as a defect because of the door being an external door thereby creating a link to the external environment.

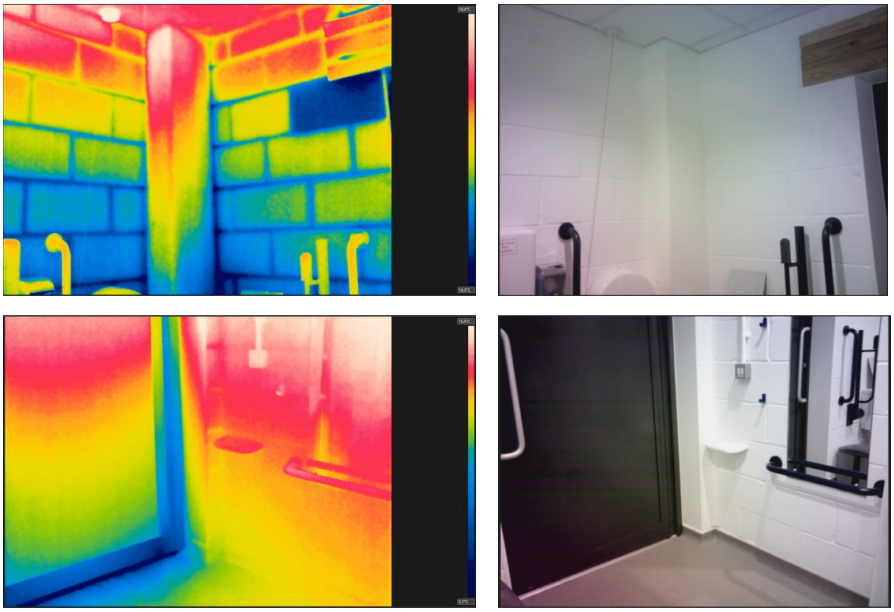

Figure 5-18: Heat loss and gains from official changing room with corresponding digital images

5.3.1.6 Other Building Defects

During the building audit survey, defects within the building envelope were examined; these defects include condensation on walls or water ingress and cracks on walls. In Figure 5-19, it can be seen that a crack runs throughout the external wall in the main-lounge. The cracks are observed to run through the blockwork, but it was further noticed that the cracks terminate at each of the steel sections in which there are five (see Figure 5-20). These cracks were thought to have been caused by settlement of the building or due to the strength of the low-density blocks. The blockwork is settling faster than the steel frames embedded within the external wall.

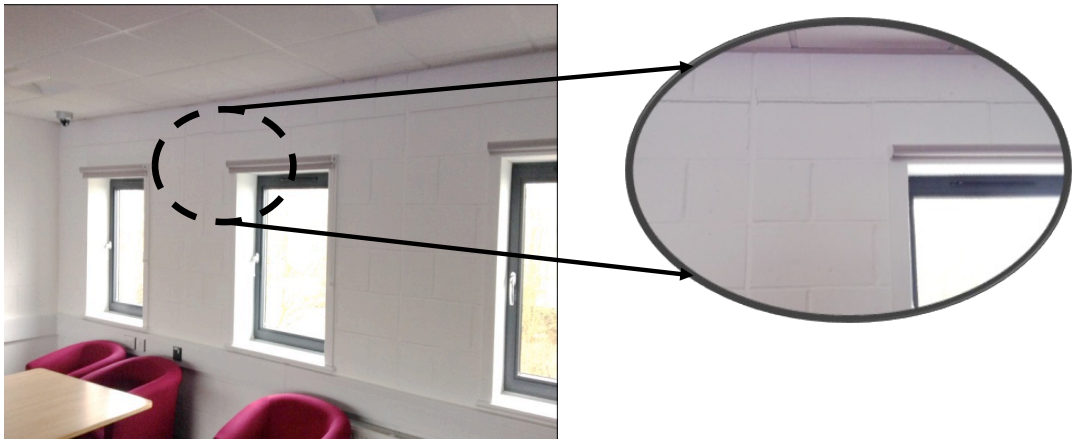

Figure 5-19: Crack on the external wall (main-lounge)

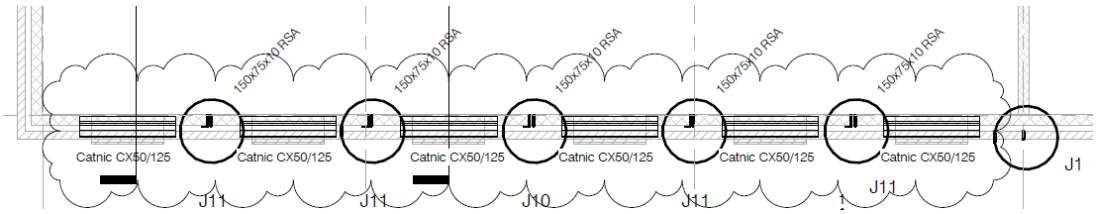

Figure 5-20: Steel sections within the building envelope

Condensation within the building envelope is seen developing in the plant room (see Figure 5-21). Above the area affected by condensation is a balcony in which a drainage system is situated, and therefore it was presumed that water sips through the building envelope through the drainage system.

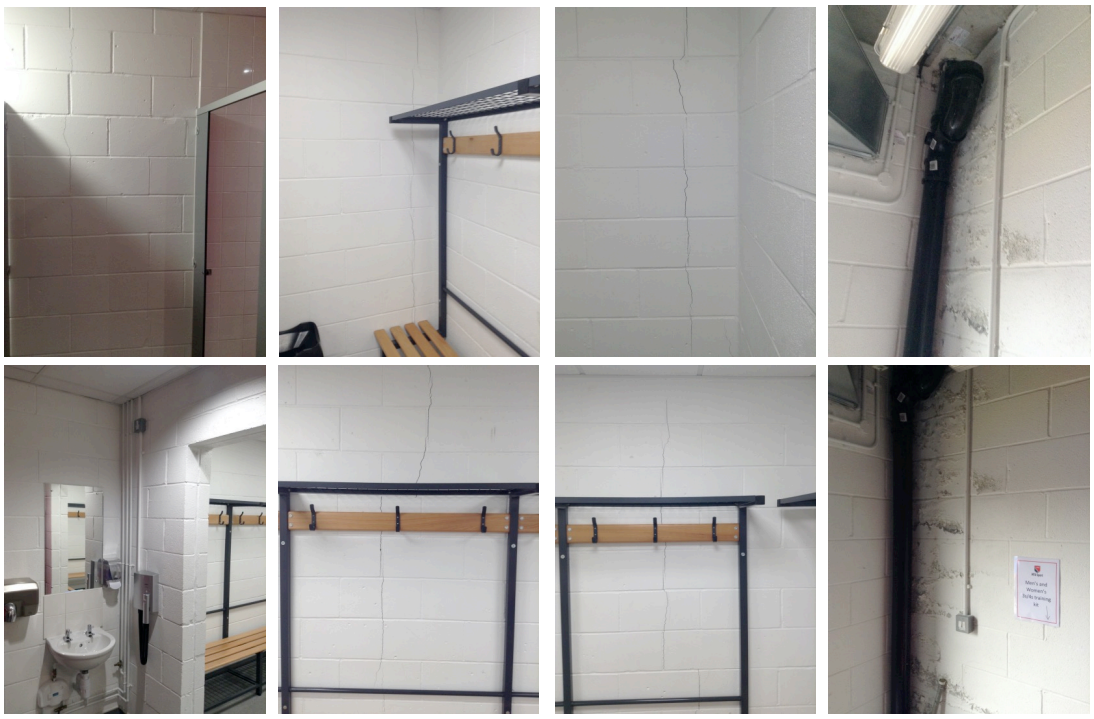

Figure 5-21 Defects found within the building envelope

Further defects noticed during the building audit were cracks on both internal partitions and external wall. Cracks on the internal partitions were all vertical cracks while that of the external were horizontal as mentioned above. Most of the vertical cracks noticed are observed to have started at the mortar joint (i.e. the weakest point) and then further into the blockwork. Depending on the location of the cracks, they can act as heat sinks. Further thermal images of cracks and defects can be found in *Appendix B1 and Appendix B2*.

5.3.2 Effect Of Thermal Bridges From Thermography Using Matlab

The effect of thermal bridges as identified by Martin et al. (2011) is still an issue that is not implemented correctly in calculations or sometimes neglected. Furthermore, Martin et al. (2011) identified that this is mainly due to the transfer of heat passing through the building envelope considered as one dimensional. To evaluate heat losses and gains generated through thermal bridges, certain factors have to be taken into consideration. These factors include; weather conditions, level of insulation, the thermal bridge constructive solution and the type of building have to be taken into consideration. Martin et al. (2011) identified that quantifying the heat loss and gain generated through thermal bridges is heavily dependent on the method used to implement its effect within the calculation of the building energy demand.

Linear thermal transmittance (used to represent the heat flow added by thermal bridges to surrounding elements) are features used to assess the effect of thermal bridges in transient

building simulation programs such as TRNSYS. Other models adopt different assumptions and therefore lead to different results. *Hence the need to know the real dynamic behaviour of thermal bridges*(Martin et al., 2011). To evaluate the effect of thermal bridges on the energy performance of buildings, Ge & Baba (2015) identified that the equivalent U-value method is the most used. The equivalent U-value method is used to adjust the insulation level of the one-dimensional multi-layered envelope component such that its thermal transmittance is equal to the effective overall U-value of the envelope detail with thermal bridges. Furthermore, the material properties of the multi-layered component are kept unchanged. The effect of thermal bridges on the overall thermal resistance is therefore taken into account, while the thermal inertia effect of the thermal bridge is ignored.

An image obtained by an infrared camera provides the temperature of each pixel hit by the radiation emitted from the object examined. Using MATLAB, the temperature profile of the affected areas regarded as thermal bridges were analysed. This was done to examine the extent to which unwanted heat loss or heat gain was present in the facility. To achieve this, the thermographic images were converted to matrices and imported into MATLAB. The program was then used to identify the point at which heat is lost or gained, and the temperature profile was obtained using a graph of temperature vs distance. Temperature factors are obtained using the equation below

$$f_{Rsi} = \frac{T_{si} - T_e}{T_i - T_e} \qquad \textit{Equation 5-1}$$

Where T_{si} is the surface wall temperature, T_e is the external temperature and T_i is the internal temperature.

In changing room 1, the effect of heat gain from the mortar joints was analysed. The analysed thermography image from MATLAB is shown in Figure 5-22 below. A line was drawn from the top of the image to the bottom, and this was used to obtain the temperature along the line. The distance of the line was calculated, and the temperature profile was drawn, as shown in Figure 5-22. It can be seen that at every mortar joint there was an increase in temperature of about 0.8°C. For the cracks, there was a temperature decrease of about 1.2°C in comparison to the temperature of the wall.

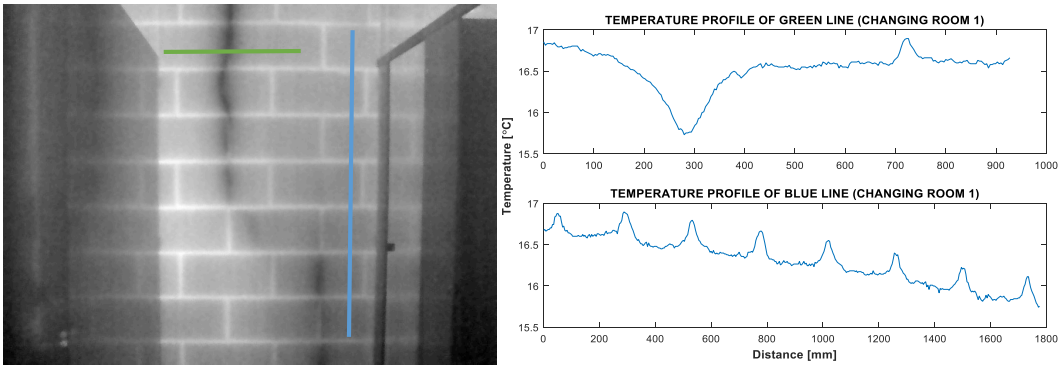

Figure 5-22: Processed Matlab thermography image and temperature profile of the wall in Changing room 1

Mortar joints were noticed to have a pattern of heat losses and gains within the building envelope. Changing rooms 5 and 6 were examined to have heat losses in the external wall (wall facing towards the north). A difference in the surface temperature of about 1.5°C was observed in comparison to wall surface temperature (see Figure 5-23).

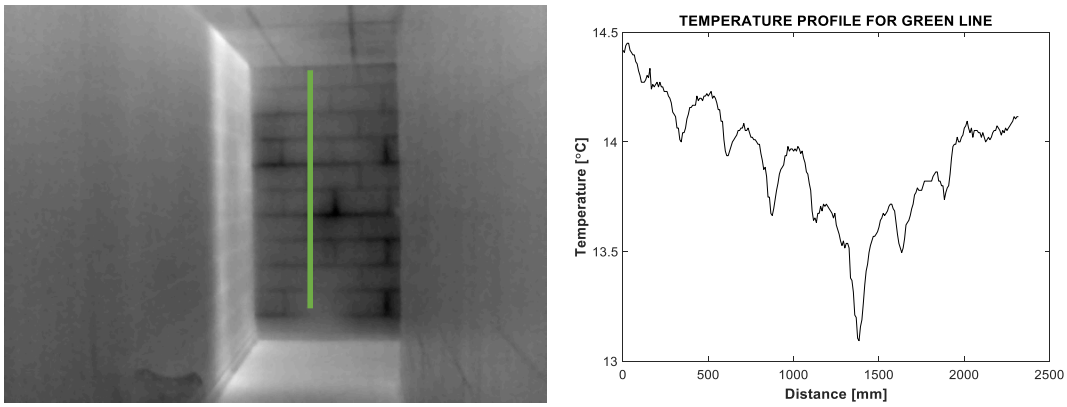

Figure 5-23: Temperature profile of the external wall in the changing room

In the main lounge, the temperature profile for the expansion joint was analysed. From the processed MATLAB image shown in Figure 5-24, the expansion joint is represented by the orange and red line. It can be noted from the graph that the difference in temperature between the block and expansion joint is about 1.2°C. The effect of the mortar joint just before the expansion joint can be observed from both sides in the graph. In Figure 5-24 (orange line), it was observed that the temperature within the expansion joint was unstable and there was a reduction in temperature where there is an intersection of mortar joint and the expansion joint. On the adjacent wall, the mortar joint was observed to influence the temperature with a reduction in temperature at each joint. The temperature reduction for both mortar and expansion joint was due to the wall being an external wall. The expansion joint was observed to be on both sides of the wall (internal and external), causing a pathway for the increase in temperature.

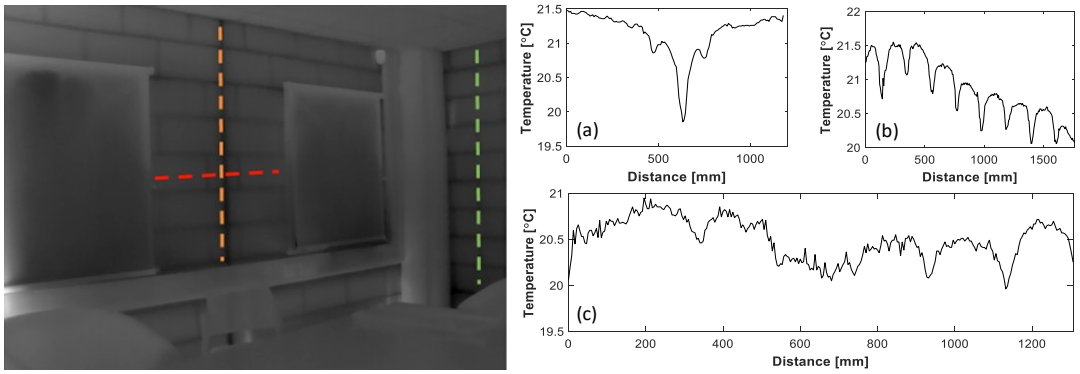

Figure 5-24: Thermal image (left) with red, green and blue lines which correspond to temperature profiles (right (a), (b) and (c), respectively).

The expansion joints from the main-lounge are four in number and therefore have a substantial amount of influence on the heat exchanges between the external and internal environment. A line was drawn across two of the expansion joints, and for the first expansion joint, a decrease of about 1.2°C was noticed while for the second expansion joint, a decrease of about 3°C was observed. Furthermore, a rise in temperature can be seen due to the radiator being on with a temperature of 55°C, but the expansion joint still influences the surface temperature of the wall by reducing (halving) the temperature by 3°C (see Figure 5-25).

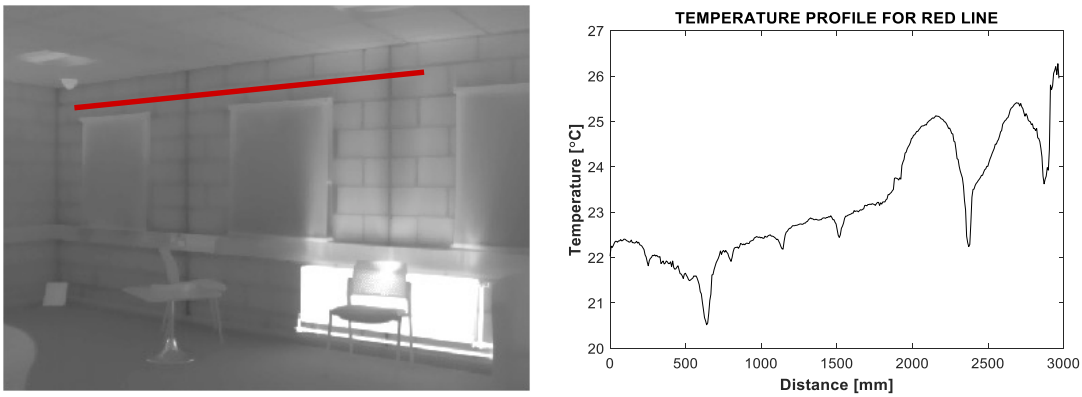

Figure 5-25: Temperature profile for expansion joints in main-lounge

Thermography images of the changing rooms were examined, and results revealed that heat was gained from the corner joints. An increase of about 1.1°C and 0.8°C were observed due to the corners from changing room 5 and 6, respectively (see Figure 5-26).

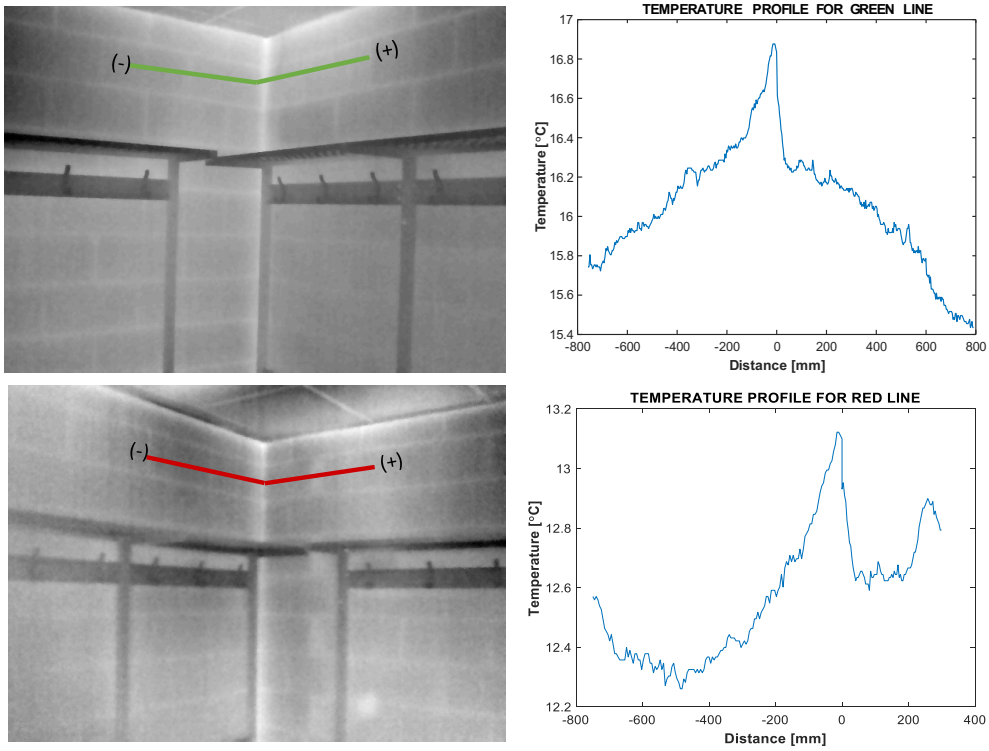

Figure 5-26: Temperature profile of the corner joint in changing rooms

5.3.3 Numerical Analysis of Thermal Bridges

The numerical analysis aims to obtain the heat flow through the thermal bridges and examine their effects. Locations of thermal bridges revealed in the thermography analysis are investigated. Finite element models, mimicking real-life scenarios, are created using 3-D solid elements in ANSYS (a finite element analysis software). Parameters measured such as internal and external temperature during the thermography were used as inputs in ANSYS. The convection heat transfer is applied to both the internal and external layers of the wall. Also, the heat transfer coefficient and the bulk temperatures are applied. These are set as constant variables to simulate the same conditions as obtained from the infrared thermography. Temperature profiles are obtained from simulations and compared with profiles generated from thermography.

For the main-lounge, the external wall in which five steel frames are situated was modelled numerically using ANSYS. Boundary conditions from the infrared thermography are used with the external temperature at the time of the experiment being 6.6°C and the internal temperature was 24.6°C. The values for convective heat transfer coefficient which are 0.13(m^2K/W) for the internal environment and 0.04 (m^2K/W) for the external environment were obtained from BS EN ISO 6949 (2007). Results reveal heat losses from the mortar joint and also the expansion joint with steel frames. The bricks were observed to have

about 1.5°C more than the mortar joints and about 2°C more than the expansion joint (see Figure 5-27).

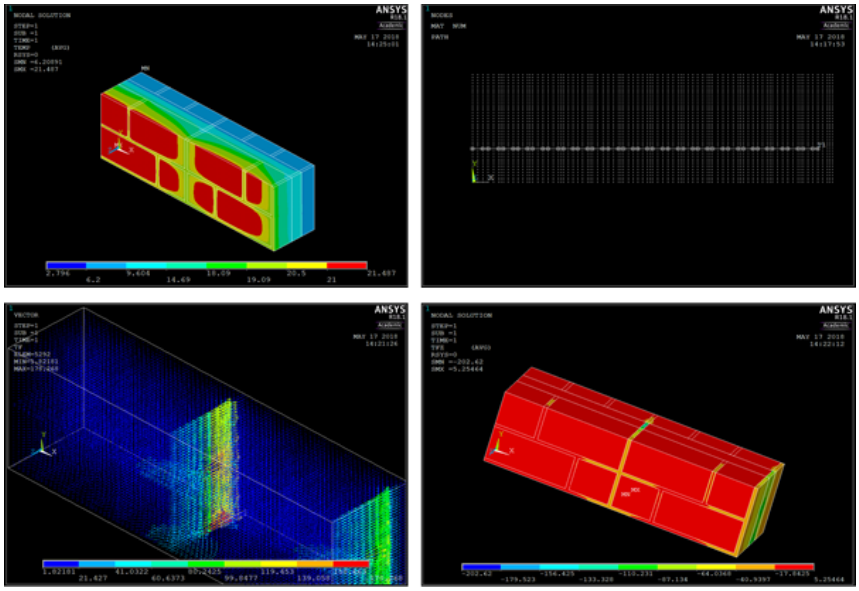

Figure 5-27: ANSYS simulation showing temperature distribution through the expansion and mortar joint (top left), nodes distribution (top right), heat flow vectors (bottom left) and heat flow distribution (bottom right)

The expansion joint located at the corner of the main-lounge was also modelled using ANSYS. The boundary conditions used was also from the infrared thermography. Results from the numerical analysis revealed that there is a significant surface temperature difference of about 2°C between the expansion joint and the brick.

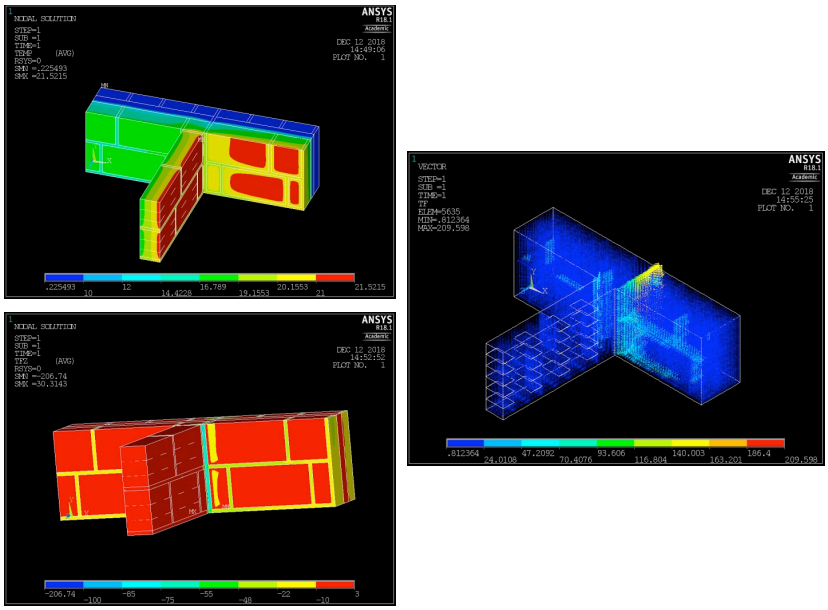

Figure 5-28: ANSYS simulation showing temperature distribution through the corner expansion joint (top left), heat flow distribution (bottom left) and heat flow vectors (right)

Using Path operations, the temperature profile of the wall was obtained. This was achieved by obtaining the temperature data and distance of the nodes. Figure 5-29 obtained from ANSYS shows the heat losses at the mortar joint and expansion joint.it can be observed that the most variation in surface temperature occurs due to the structural steel and followed by the mortar joint.

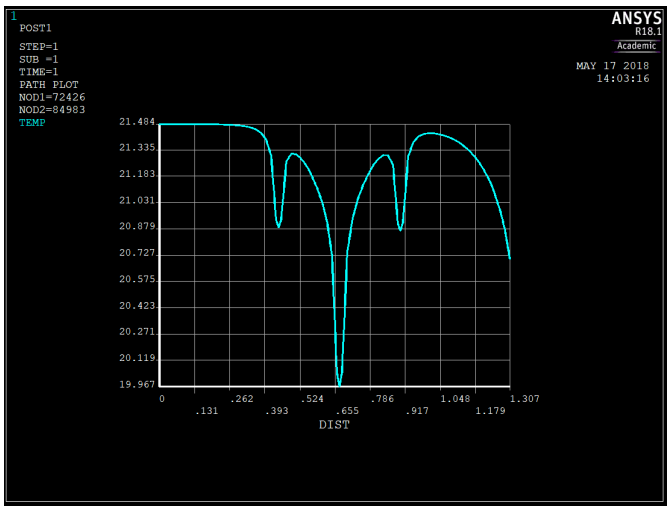

Figure 5-29: Temperature profile of expansion joint from ANSYS

5.3.4 Effect Of Thermal Bridges From Numerical Analysis Using ANSYS

Heat losses from the building envelope were observed from the results obtained in the thermography and numerical analysis. These losses were mainly due to expansion joints, corners, mortar joint and also cracks within the envelope.

Brick and block walls which are assumed to be a set of homogeneous layers revealed that the mortar joints connecting the bricks and blocks were behaving as a thermal bridge. This was also observed by Branco et al. 2004 in his study using the boundary element method. Mortar joints were presumed to be dry during the calibration process with thermal conductivity of $0.93W.m^{-1}.K^{-1}$. This was observed not to be in correlation with the infrared thermography result. Therefore, the thermal conductivity of the mortar joint was updated to $1.5W.m^{-1}.K^{-1}$ which specifies that of a moist mortar. Taking this assumption of the material property of real mortar joint, the FEA results correspond very well with the results obtained through the infrared thermography. The mortar joint was observed to behave as a repeated thermal bridge with a heat flux of -15W/m^2 as shown in Figure 5-46.

Expansion joints within a building envelope are very important as they allow for thermal contraction and expansion, which are caused by temperature changes. These joints have to be taken into consideration as they may pose to behave as thermal bridges. The expansion

joint alone were observed not to have contributed to the heat losses within the wall. Further investigation of the building envelop, and building plans led to the finding that within the expansion joints, there are structural steel members. Due to the high conductivity of the structural steel, they were observed to have contributed to the heat losses within the wall by decreasing the thermal resistivity, therefore creating a thermal bridge. It is assumed that the thermal bridge created by the structural steel member is due to breakage of insulation. The heat losses within the expansion joint were observed to be $27.54 W/m^2$ and $15.9 W/m^2$ for the mortar joints as shown in Figure 5-46.

In general, the mortar joints, cracks and expansion joint created weak points for air within the building envelope, thereby affecting the air changes per hour within the building and increasing infiltration. Due to the air changes being affected, this thereby affects the energy usage and performance of the building.

5.3.5 Comparison of numerical analysis with thermography

Steady-state numerical analysis was carried out by inputting the indoor and outdoor temperature. Using path operations in ANSYS post-processing, temperature profiles were calculated where the nodal distances and temperatures between each node were obtained. Thermal bridges are distinguishable in both numerical models and thermal images. Figure 5-30 shows the simulated and measured temperature profiles of the building joints. The plots show very good agreement between simulated and measured temperatures. Some deviations in temperatures are due to the material properties in the model being homogeneous and isotropic.

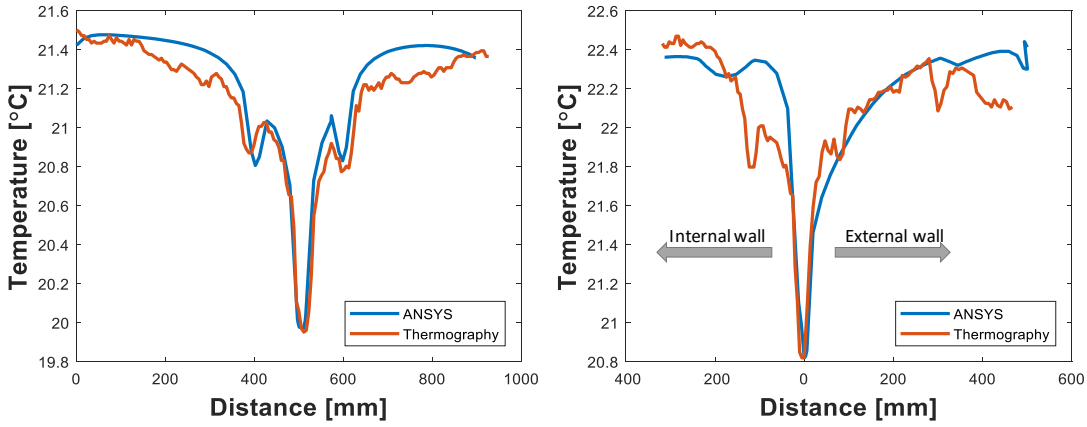

Figure 5-30: Comparison of temperature profile for expansion joint with steel (left) and corner expansion joint (right)

5.4 Computer Simulation

5.4.1 Monitored data

The monitoring system consists of four temperature and humidity sensors located at strategic places to avoid the influence of solar heat gains and heat gains due to appliances. Two sensors were installed at the main-lounge while the others at the changing rooms (upper floor (5) and ground floor (3)). Monthly readings were collected from the sensors for a period of 12-months (year) with 15 minutes interval from the 1st of July 2017 to the 1st of July 2018. Therefore, a total of 130,912 temperatures and humidity data were recorded. A sample of the results from Log Tag analyser can be found in *Appendix A2: Log Tag Results.*

Main-Lounge

The readings obtained from the sensor (1010095587) which was situated in the main lounge had an average temperature reading of 22.09°C with the lowest reading being 13.60 °C , the highest reading of 34.0 °C (see Figure 5-31) and a standard deviation of 3.25. The main lounge had an average relative humidity reading of 46.01%RH with the lowest reading being 23.10%RH, highest reading of 75.20%RH and a standard deviation of 3.3%RH for July.

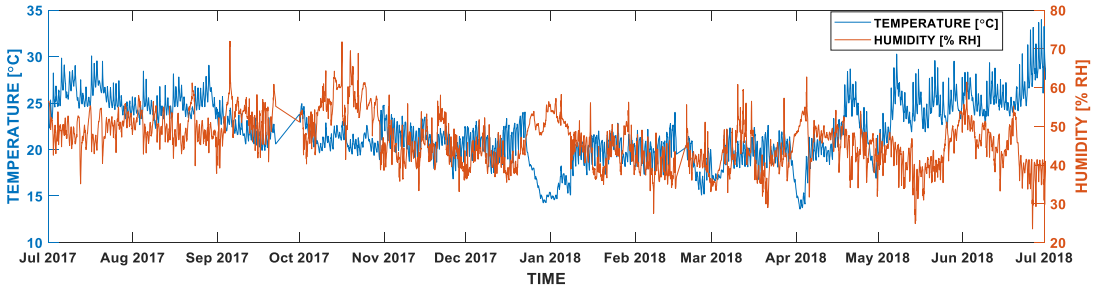

Figure 5-31: Temperature and Humidity result of sensor 1010095587 (main lounge)

During the 2017 winter period (October 2017- April 2018), a mean temperature and humidity reading of 20.1°C and 45.51%RH was recorded. A temperature within the period ranged from 28.7°C – 13.6°C while humidity readings were observed to be between 27.5-71.8%RH. The summer period of 2018 had a higher temperature of 34°C (occurred in June 2018) which is 4° C (July 2017 - 30° C) higher than the summer of 2017. It should be noted that the heating during the summer was switched off and the building was cooled using a passive measure (i.e. natural ventilation).

Changing Rooms

The readings obtained from the sensor (1010095588) and (1010095607), which were situated in changing room 3 and 5 respectively had an average temperature reading of 17.25°C and 19.75 °C. Changing room 3 had the lowest reading of 10.07°C with changing room 5 having the highest reading of 25.8 °C, as shown in Figure 5-32 and Figure 5-33 respectively. The average relative humidity reading of the changing rooms 3 and 5 were 51.08%RH and 46.29%RH respectively.

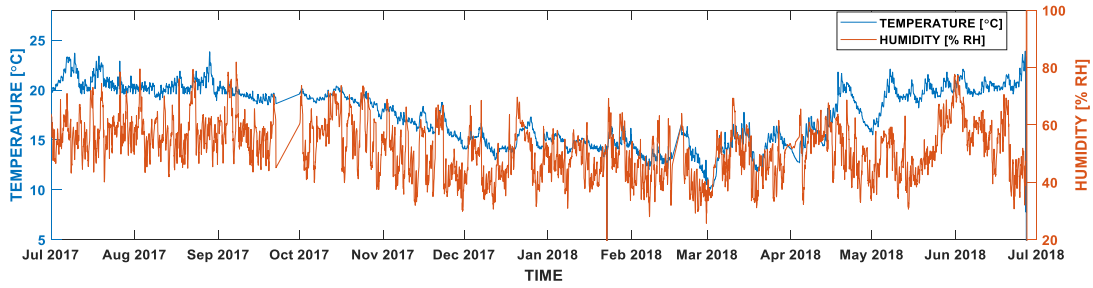

Figure 5-32: Temperature and Humidity result of sensor 1010095588 (Changing room 3)

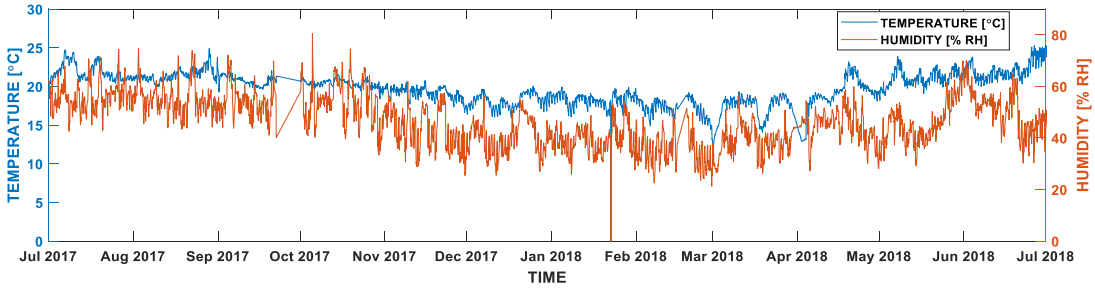

Figure 5-33: Temperature and Humidity result of sensor 1010095607 (Changing room 5)

Temperatures in the changing rooms were higher in the summer of 2018 when compared to that of 2017. In changing room 5, the maximum temperature occurred in June 2018 and was observed to be 25.8°C which is 1°C higher than the previous year. During the winter period, the lowest temperatures recorded occurred in March 2018, where temperatures in changing room 3 and 5 were 10.07°C and 12.10°C respectively.

Clubhouse Utility Data

The Clubhouse utility data was obtained through the university's estate department. The data collected by the estate department are the gas and electricity consumption, lightning consumption, PV generation and water consumption. These data span from March 2016 to date. Figure 5-34 shows the comparison between gas and electricity over the years (2016-2018). The electricity data is a combination of lightning consumption and electrical appliance

consumption data. The year 2016 has the highest gas consumption while 2018 has the highest electricity consumption in June.

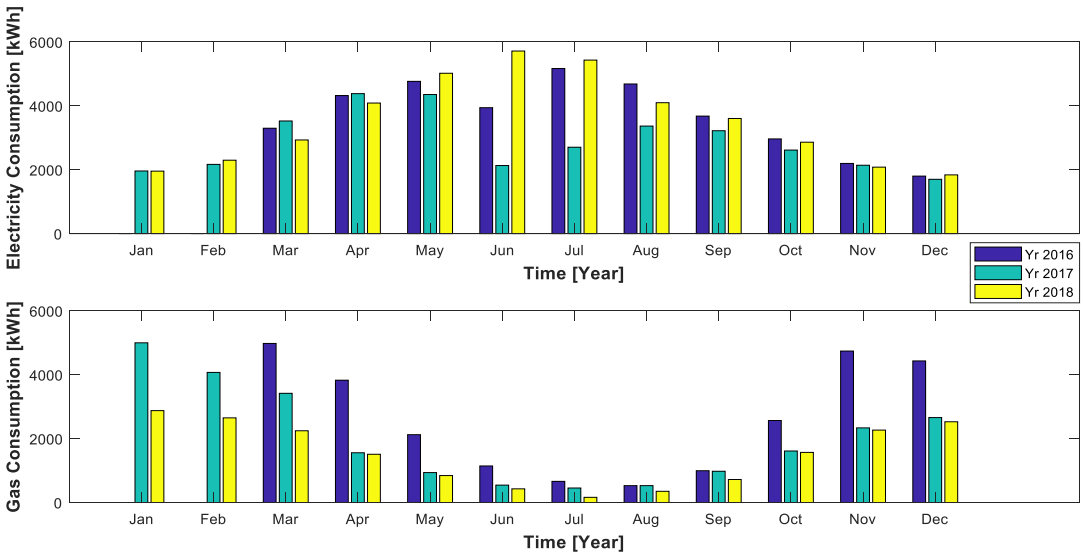

Figure 5-34: Gas and Electricity consumption of the clubhouse over the year 2016-2018

5.4.2 Energy simulation

The model of the case study is created using DesignBuilder, a graphic user interface created for the EnergyPlus simulation engine. Using floor plans, structural details, mechanical and electrical drawings from the building audit phase, an accurate model is built.

5.4.2.1 The Climate Data

In this research, UK Met office weather data for the year July 2017 to July 2018, Design Summer year weather data (DSY) and the EnergyPlus database of the International weather for energy calculations (IWEC) for Nottingham was chosen, which are made up of hourly collected data. This is because the research focuses on the whole building performance, summer performance and overheating assessments for the Clifton clubhouse.

A graphical representation of the UK Met office climatic weather data used for the simulation for the period of June 2017 to December 2017 is shown in Figure 5-35 (The graphical representation for January 2018-July 2018 can be found in *Appendix C2*). An average reading of 9.52°C and 5.47°C were recorded for the outside dry bulb temperature and the dew point temperature respectively. The wind speed was 4.25m/s with the average direction being south-western. The weather data has a solar attitude of 0.35°, solar azimuth 182.72°, direct normal solar 596.53kWh and a diffuse horizontal solar of 621.38kWh.

Future weather data from the Prometheus project was used for future prediction and in particular to assess overheating risks in the building. Outside dry bulb temperature is

predicted to rise in the future (see Figure 5-36) with an increase of about 3°C in 2080 (50th percentile) or 6°C in 2080 (90th Percentile) in comparison with the current weather data set. The Dew points temperature is also predicted to increase in the future by about 2°C from 2030 to 2080 (50th percentile).

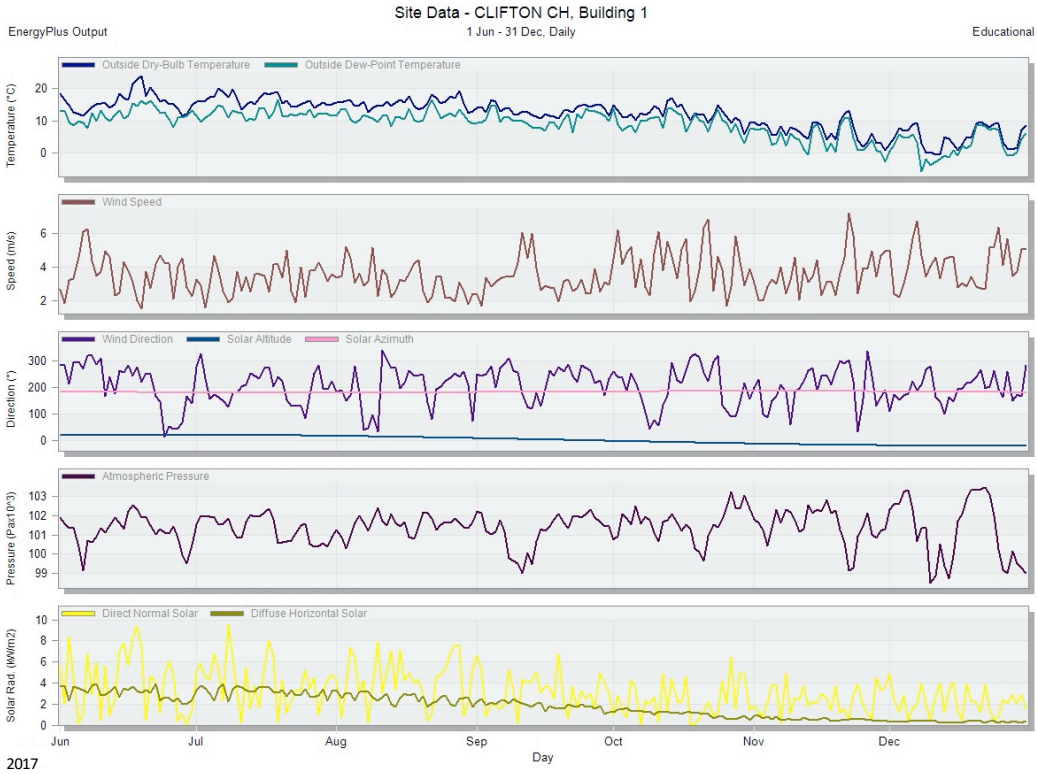

Figure 5-35: UK Met office weather data processed in DesignBuilder for June 2017 to December 2017

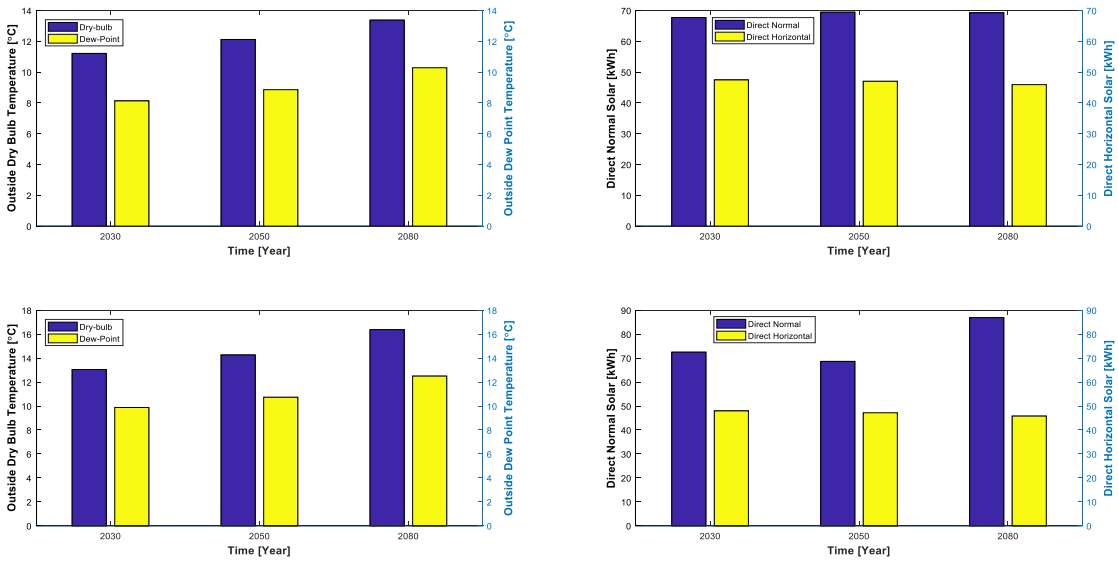

Figure 5-36: Graphical comparison of future weather data showing 50percentile (top) and 90 percentile (bottom)

Weather data such as wind speed and direction are predicted not have a significant change in the future. Wind direction is mostly in the south-western direction while the wind speed is with 4.06m/s and 4.45m/s. Other data such as direct normal and horizontal solar are also predicted to have an increase, but the only significant increase was predicted to occur with the direct normal solar in the worst-case scenario (90th percentile)

The Figure below shows the dry and wet bulb temperature of Nottingham from July 2017 to July 2018. The summer temperature (July) of 2018 was higher than the previous year, which was as a result of the heatwave experienced during the summer of 2018, as mentioned in (BBC, 2018).

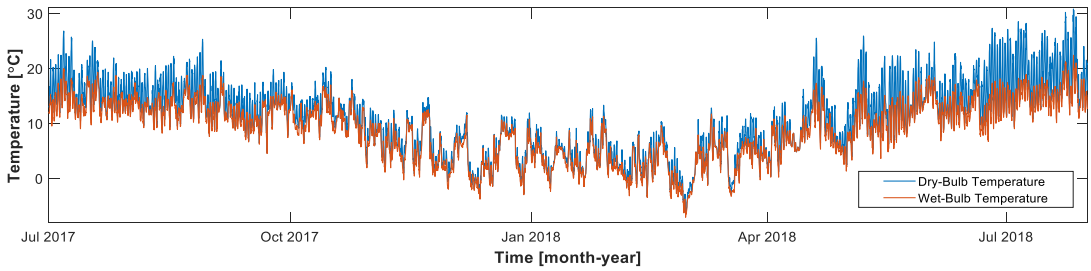

Figure 5-37: Temperature data of Nottingham from the UK Met Office

5.4.2.2 Type of building and activity

To describe how buildings and its system operates (Table 5-1), occupancy schedule is used in building energy simulation. This is used to demonstrate the character of the occupancy influence on total energy consumption of the building (Martinaitis et al., 2015). The occupancy for the Clifton clubhouse was described as a university changing facility. Therefore, the building is unoccupied during weekends, university closure days and holidays (July – September).

Table 5-1: Building Description

Building location	**Nottingham Trent University**	**Nottingham, United Kingdom**
Building type	Sports lounge	Changing facility
Floor area	Occupied floor area	450.9 m^2
Dimensions and height	Average floor height	3.5 m
	Window Height	1.0 m
	Door height	2.1 m
Construction and building envelope	External wall	102.50 mm Old Trafford Redbrick 75 mm Knauf Dritherm Cavity Slab 140 mm Thermalite Hi-Strength
	Roof	Solar panel Roofing sheets
	Partition	Hanson Evalast Paint Grade Aggregate
	Windows	Double glazed clear
Operating hours	Monday to Friday	8:00 hrs to 17:00 hrs
	Weekend	Closed
	Holiday	Closed after term time
Lights	Type	Surface mount
	Target Illuminance	200 lux
Activities	Occupancy schedule	University changing facilities with showers
	Activity	Changing facility with showers
Domestic hot water	Type	Gas boilers
Solar panel	Capacity	34 kW

5.4.2.3 Model Creation

The building model was developed using DesignBuilder. The model is divided into zones with each zone having different activities. A zone is defined as a group of rooms that have the same set of activities and temperature set points. The main activity of the building model was set to changing facilities with showers. Zones that are not heated nor cooled such as the lift area and roof were set as semi exterior unconditioned which means that the zones are set as unoccupied and activities, HVAC and lightning templates are set as none. Zones classification used in the clubhouse are listed below:

Table 5-2: Building zones, activities and setpoints for the clubhouse

Zones	Activity	Occupancy (people/m^2)	Temperature setpoints (°C)
Lounge	Hall/lecture theatre/assembly area	0.1750	23-19
Changing rooms	Changing room facilities with showers	0.1000	Heat recovery
Plant rooms	Light plant room	0.1000	No heating and cooling
Store	Storeroom	0.0250	No heating and cooling
Reception	Reception	0.1008	22-16
Toilets	Toilets	0.1124	22-18

Three HVAC systems are installed in the Clifton Clubhouse, which are Radiators, Heat recovery units (HRU) and Domestic hot water unit (DHW). A detailed HVAC system (see Figure 5-38) was modelled to simulate the system of the facility. For the HVAC system, the building was divided into three zone groups, namely, zone group 1, zone group 2 and zone group 3 (see Table 5-3)

The Heating system, which consists of a boiler and a radiator (Figure 5-38a), was first modelled and applied to the zone group 1, which comprises of the main-lounge and reception where heating is available. This system consists of a demand and supply side. The supply side of the system consists of the boiler, set-point manager and the supply pump. The boiler is fed by natural gas as the fuel type with the nominal efficiency set as 0.890. The set-point manager was set to schedule (in which it would operate based on the scheduled specified for each room that requires heating), and the hot water temperature into the radiators was set as 70°C.

The domestic hot water system (Figure 5-38b) was applied to zone group 2, which comprises of the changing rooms, shower rooms, toilets and main-lounge. The delivery set-point temperature was set to 55°C, which operates according to the schedule for each defined location. The supply section of the domestic hot water system consists of the water heater, set-point manager and the supply pump. The water heater was set to operate using natural gas with an efficiency of 0.90; this efficiency changes according to the load on the system.

The heat recovery unit (Figure 5-38c) was also modelled with an inlet and extraction fans in zone group 3 which comprises of the changing rooms and shower rooms. The supply section of the heat recovery unit consists of set-point manager, heating coil, extraction and supply fans. For the heat recovery, a plate heat exchanger was used with the heat recovery operations set as scheduled. The demand section consists of a direct air distribution unit which allows supplied air to be delivered from the air handling units to the zones without any level control or tempering.

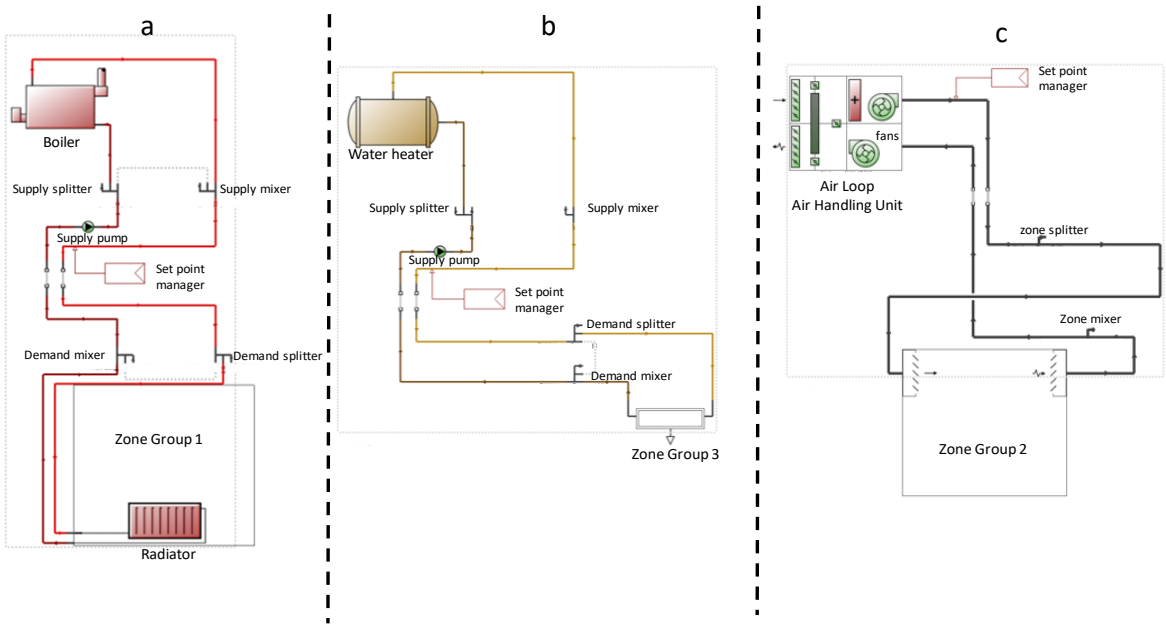

Figure 5-38: Modelled HVAC systems in DesignBuilder (a) Radiator and boiler (b) Domestic hot water system and (c) Heat recovery unit (HRU)

Table 5-3: Zone groups for HVAC systems and their locations

Zone Group	HVAC	Locations
Zone group 1	Radiators, Boilers and Natural Ventilation	Main-lounge and Reception
Zone group 2	Heat Recovery Units	Changing rooms and shower room (1,2,3,4,5 & 6), official changing rooms and toilets
Zone group 3	Domestic Hot water	All rooms except reception, stores, plant rooms and lift

5.4.2.4 The Simulation

Theodosiou & Papadopoulos 2008 conveyed the importance and the demand for convergence between the predicted and the actual building energy consumption. This has proven to be an essential factor during the design and construction process. The analysis performed in this study includes

- Creation of the 3D model with DesignBuilder using parameters obtained from building audit
- Annual simulation of the building
- Summer simulation of the building for overheating analysis

Results obtained from the EnergyPlus simulation in DesignBuilder for the entire building is shown in Figure 5-39. From the temperature graphs, an average operative, air and radiant temperature of 20.08°C, 19.97°C and 20.20°C was achieved respectively while the outside dry bulb temperature was 9.52°C on an average for the year. Heat losses due to external walls and external infiltration contributed the highest while zone sensible heating, general lightning and occupancy contributed to the heat gains into the facility. Further results can be found in *Appendix C: Computer Simulation* where the results are explained for each year.

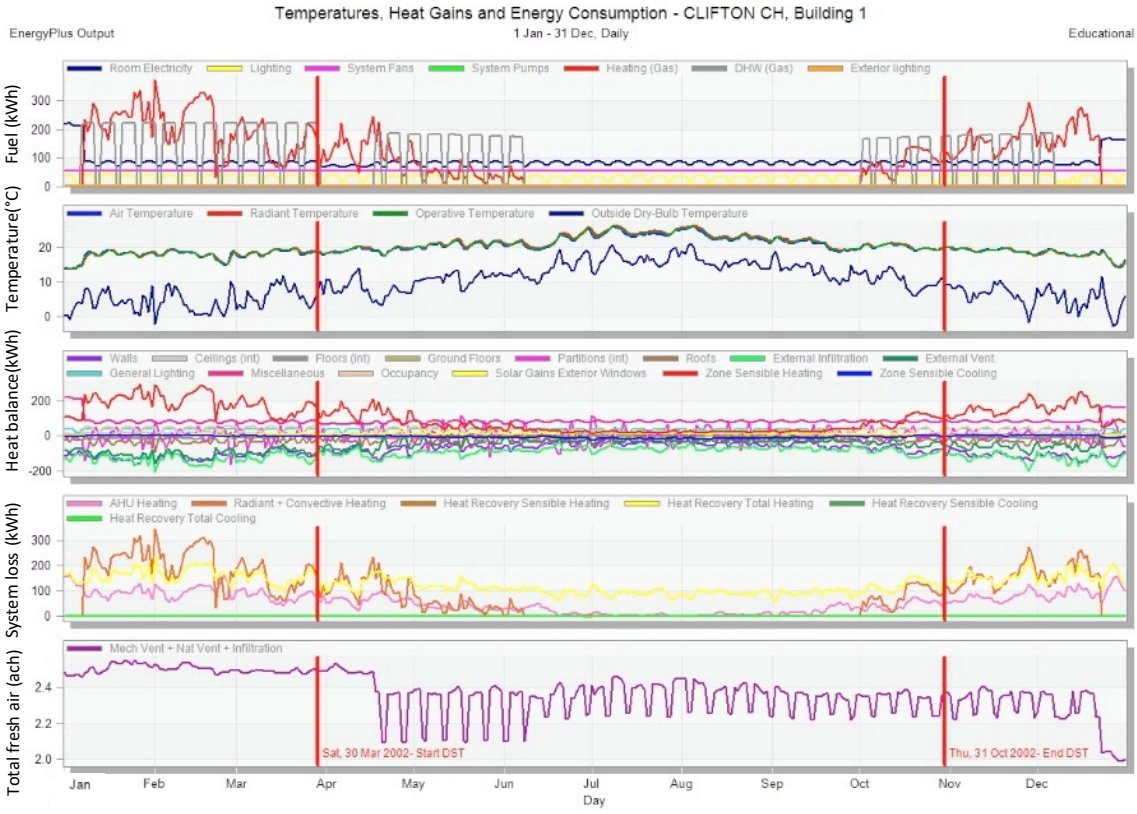

Figure 5-39: Energy simulation output

5.4.3 Model Calibration

In this section, observations from the infrared thermography, building audit and monitoring are used to calibrate the energy model to ensure that the model behaves as expected. A manual calibration method is used in this study, which depends on iterative intervention by the modeller. A list of variables, observations and how they affect the model are outlined below

5.4.3.1 Heating Times

The heating times of the clubhouse changes due to when the facility is used and dependent on the external weather conditions. With the use of the monitoring (in particular sensor) results, the internal temperatures were used as a guideline to understand the heating pattern of the clubhouse. In relation to this, a schedule was created to match the same heating pattern as that obtained from the sensor. This process was used to calibrate the heating system in the main lounge and the heat recovery unit for the changing rooms.

5.4.3.2 Hot water pipes

Hot water pipes from the changing rooms and shower rooms were identified during the thermography survey. The pipes being uninsulated means that they emit much heat to the facility. The pipes emit heat through radiation, convection and conduction in some cases as shown in section 5.3 above. The heat emitted from the hot water pipe through natural convection was calculated as $11.47 W/m^2$ and through radiation as $30.28 W/m^2$. The following equations were used;

$$Ra_L = \frac{g\beta(T_s - T_\infty)^3}{v^2} Pr \qquad \textit{Equation 5-2}$$

$$h = \frac{k}{D} Nu \qquad \textit{Equation 5-3}$$

$$Q = hA_s\dot{(}T_s - T_\infty) \qquad \textit{Equation 5-4}$$

$$Nu = CRa_L^n \qquad \textit{Equation 5-5}$$

$$Q_{rad} = \varepsilon\sigma A_s\dot{\left(}{T_s}^4 - {T_\infty}^4\right) \qquad \textit{Equation 5-6}$$

Where T_s is the surface temperature of the pipe. Ra_L is the Reynolds number, T_∞ is the room temperature, Pr is the Prandtl number, v is the kinematic viscosity, β is the coefficient of volume expansion, h is the average heat transfer coefficient of the surface, Q is the heat due to convection, Nu is the Nusselt number, A_s is the heat transfer surface area, ε is the Stefan-Boltzmann constant and C is a constant

In order to establish that the effect of the hot water pipe is accounted for, heat gain into the zone from the water outlet settings was switched on, and a miscellaneous heat gain into the building was added with the values of convection and radiation inputted and a schedule created for the hot water pipes.

5.4.3.3 Cracks

During the building audit, monitoring and infrared thermography phase, cracks were identified in the facility. Cracks are known to affect the energy performance of buildings and therefore need to be taken into account. Before the calibration process, the airtightness used in modelling the building was obtained from a previous air-tightness test in which the building had a $9.35m^3$ @ $50Pa$. Due to the presence of cracks in the facility and with the use of crack templates in DesignBuilder, the crack was set to medium.

5.4.4 Model Validation

For every computer simulation, model validation or verification has to be carried out. Model validation is understood to mean the extent at which a model produces results that represent the real-world behaviour, while model verification describes the extent at which a model produces results that are comparable with an alternative or standard method (Underwood, 2014). To estimate the energy performance of buildings, Rahman et al. (2010) stated that architectural, mechanical and electrical systems have to be modelled properly. Hence, model validation becomes an essential task to ensure accuracy in building energy predictions. Three methods are widely used as stated by Underwood (2014). They are:

- Empirical validation
- Analytical verification
- Inter-model comparison.

For this study, empirical validation method would be used. The Operative temperature results from DesignBuilder and Log tag sensors were collated and compared for all locations. Furthermore, The total gas consumption for the facility was also compared. The validation process can be done with monthly or hourly data, as stated by Rahman et al. (2010). In this study, the hourly data was used.

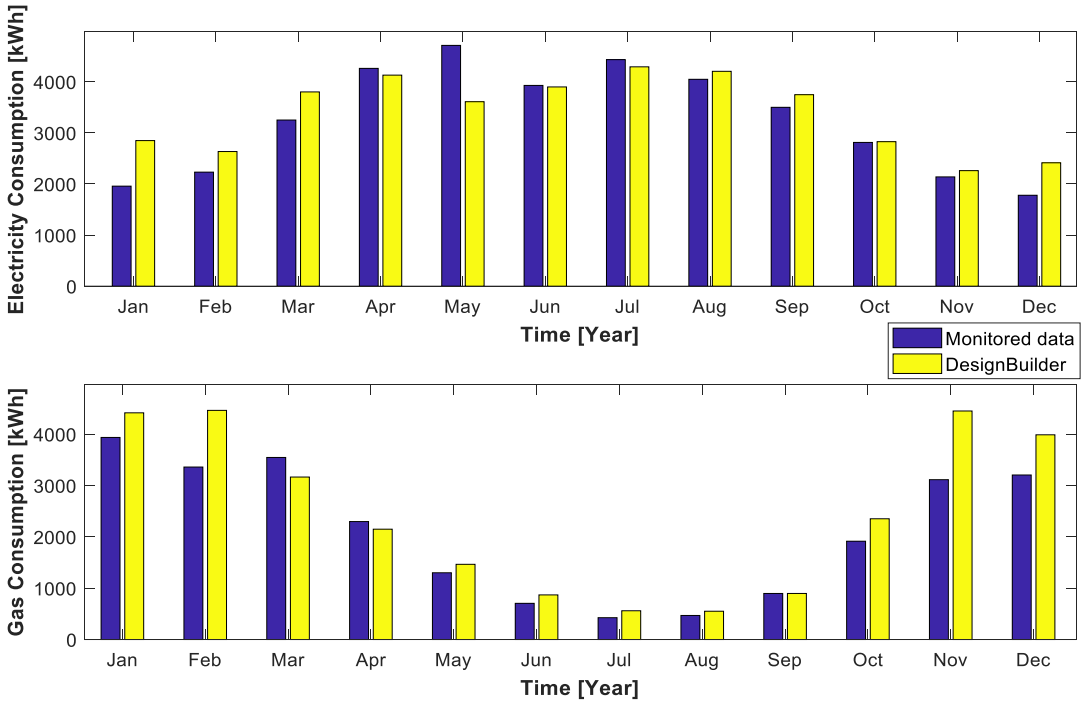

Figure 5-40: Gas and electricity consumption comparison

The results showed similar trends with some minimal discrepancies. The discrepancies may also be due to the influence of human behaviour and the preferences of occupants as also observed by Martinaitis et al. (2015). Furthermore, Li & Rezgui (2017) in his studies, observed that occupants are the main cause of the discrepancy between the simulated and measured data as they affect the energy consumption in buildings. This is because simulation software cannot quantify the uncertainty in human activities and their interaction with building elements which results in substantial prediction error.

The building uses natural ventilation in the main lounge which relies on occupant interaction and therefore leading to more discrepancies as observed by Hong et al. (2016) stating that low energy buildings that use passive energy measures such as natural ventilation, prediction errors become larger. Moreover, as shown in Figure 5-40, it can be noted that the actual gas consumption is slightly lower than the simulation results between May and July. The discrepancy can be explained due to the changes in schedule and occupancy rate in the building. The changes in the schedule and occupancy rate are because this period is meant for examinations and hence a decline in sports activities. It can also be noted that there is a decrease in the gas consumption for both results in July and August which is due to the summer holidays.

Discrepancies can also occur due to the study using the theoretical U-values, rather than the in-situ measured U-values of the building envelope as observed by various studies (Marshall

et al., 2017). U-values are often overestimated which may be due to the effect of environmental factors such as wind, moisture and ventilation.

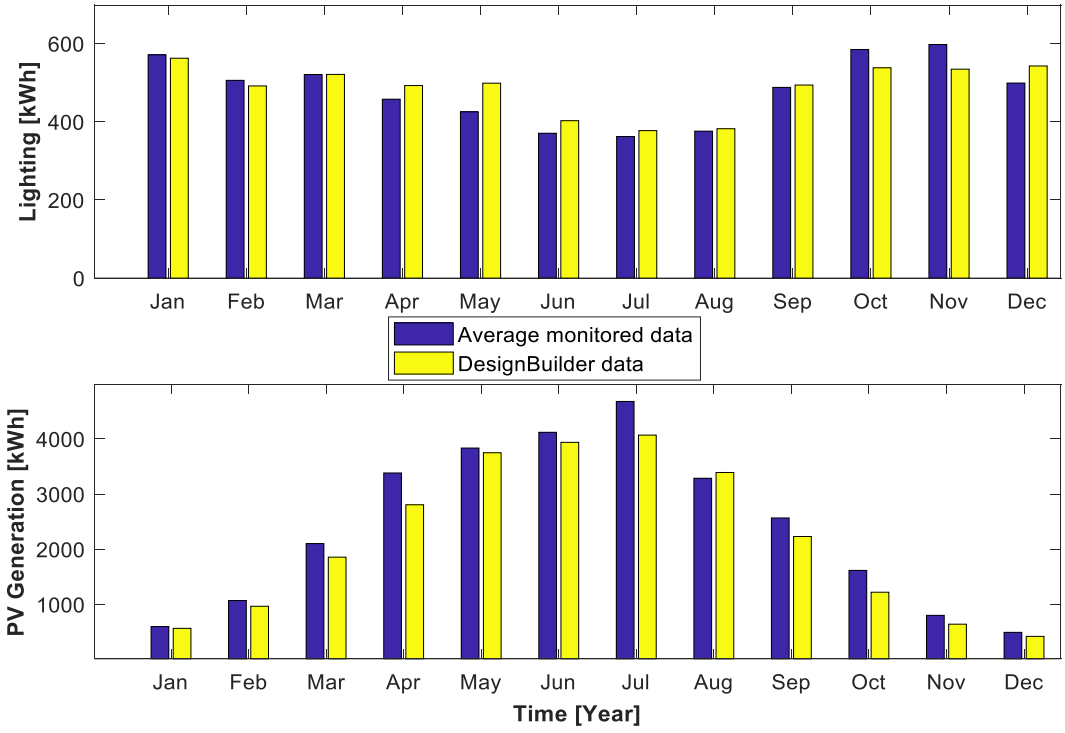

Figure 5-41: Lightning (top) and PV generation (bottom) comparison

Average lighting consumption data and photovoltaic generation data across the years 2016-2018 were compared to the modelled data (see Figure 5-41). From the comparison, the actual photovoltaic generation is always higher than the modelled data. This is assumed to be due to the 2018 summer weather. The 2018 summer period produced an average of 18% generation higher than the previous years of 2016 and 2017.

Figure 5-43 and Figure 5-45 shows the results from statistical analysis, where a positive mean bias error indicates that the predicted temperature (DesignBuilder) is higher than the actual temperature (sensor) and vice versa. The mean bias error is observed to be higher for the main-lounge in the summer period of 2018.

The RMSE, which is a measure of how close the predicted monthly temperature profile is to the actual profile, was relatively low. The RMSE ranges from 0.09 to 3.89 in the main lounge, while a range of 0.16 to 1.91 in changing room five. However, the CVRMSE, a ratio of RMSE to the range varies from 0.44% to 16.04% for the main-lounge and 0.84% to 8.96% in changing room five.

The reason why there are discrepancies in the summer period of 2018 is due to the heatwave experienced during that period. Furthermore, the main-lounge was cooled using natural ventilation which also added to the accumulation of error within that period. For the changing rooms, the error in the summer period of 2018 was relatively low as the rooms were equipped with HRU and therefore it was possible to calibrate the model using the HRU system.

From recommendations of ASHRAE Guideline 14 and reasons above, DesignBuilder model can be concluded to valid and capable of producing actual operating conditions of the Clifton clubhouse.

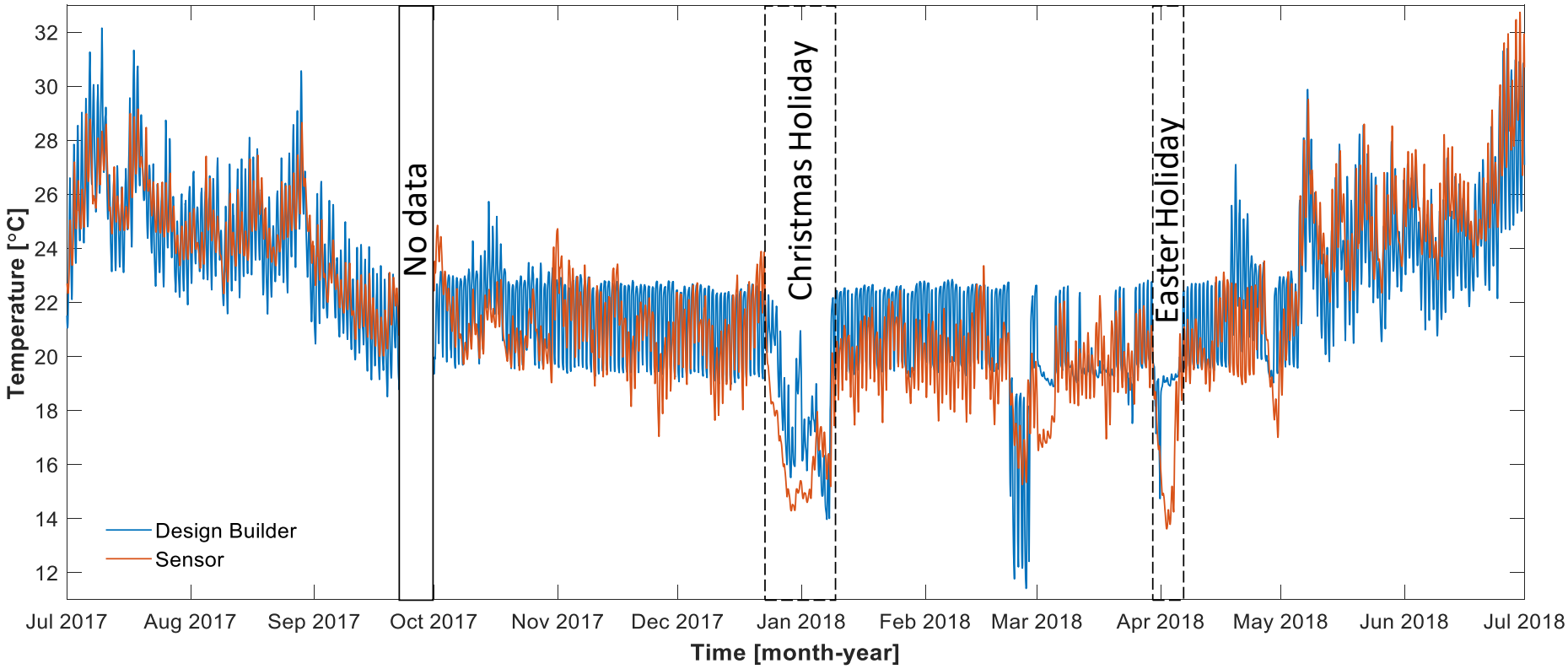

Figure 5-42: Comparison between DesignBuilder and sensor for main-lounge

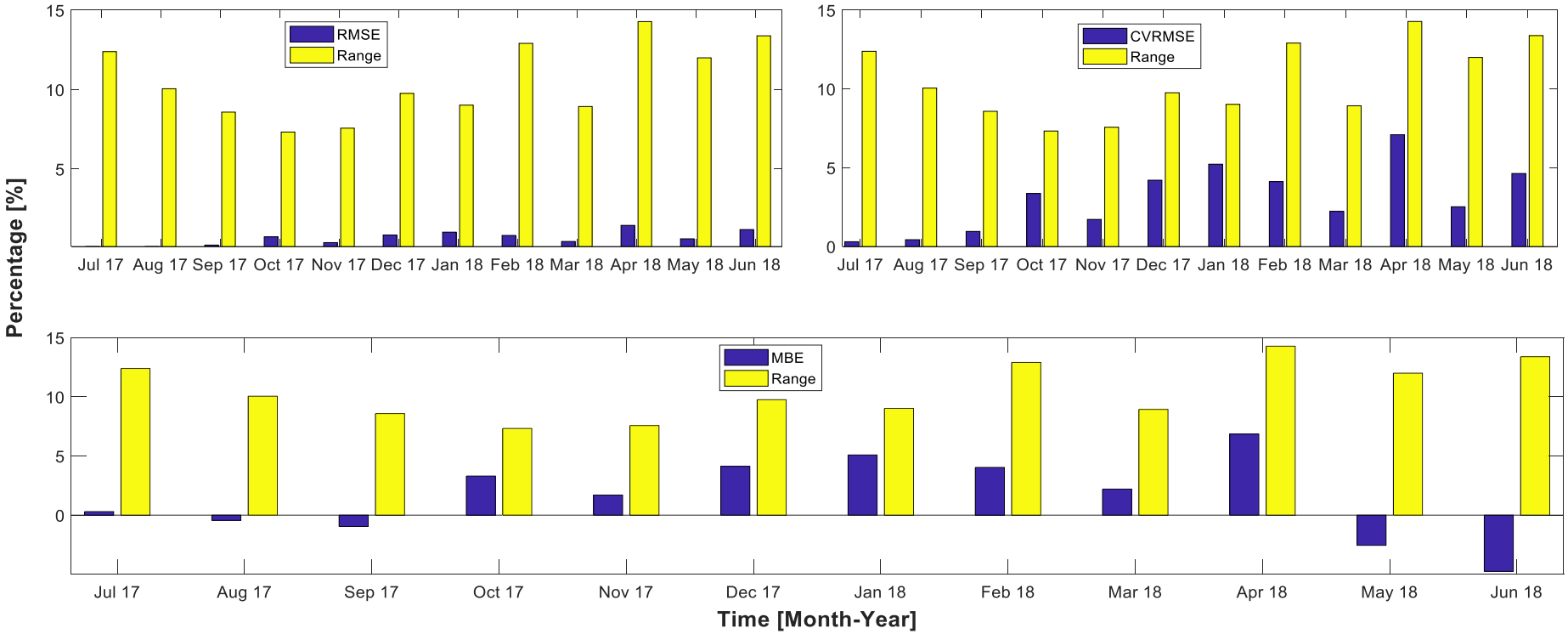

Figure 5-43: Statistical results for main-lounge

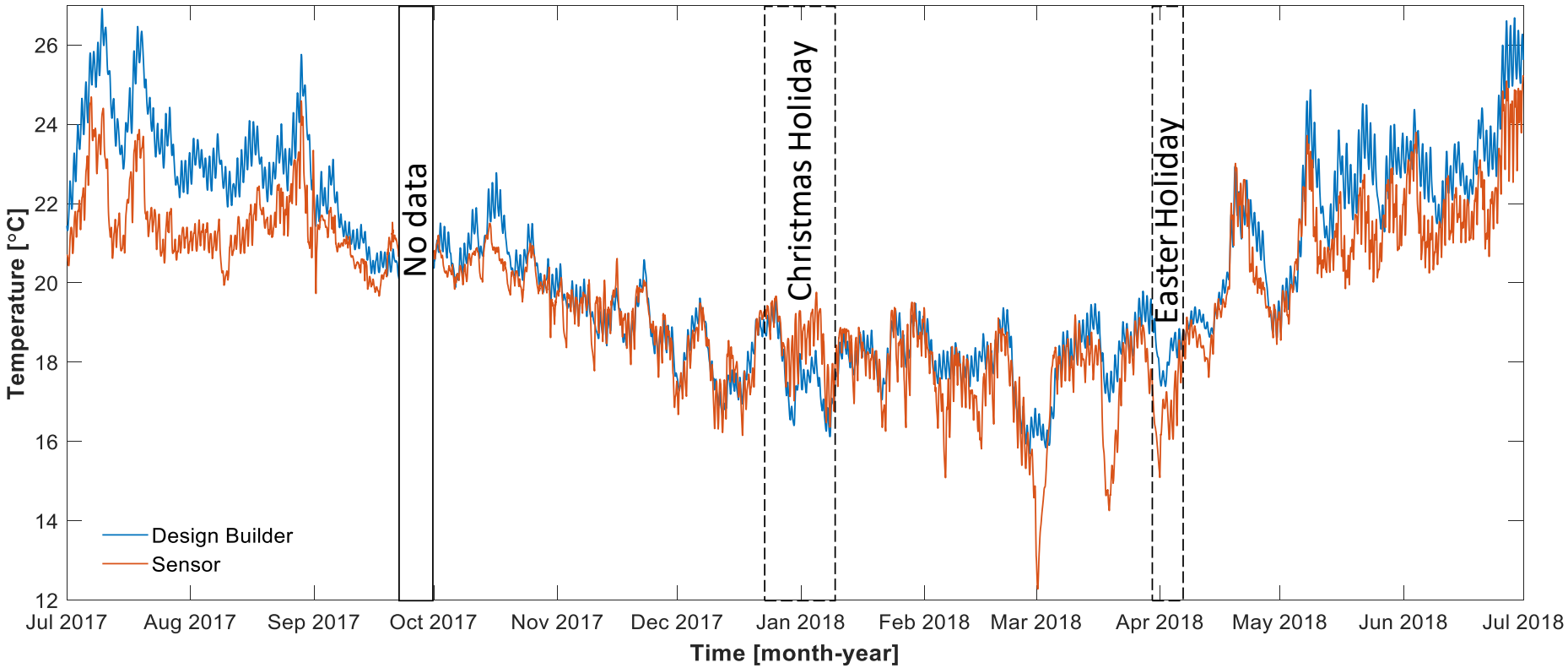

Figure 5-44: Comparison between DesignBuilder and sensor for changing room

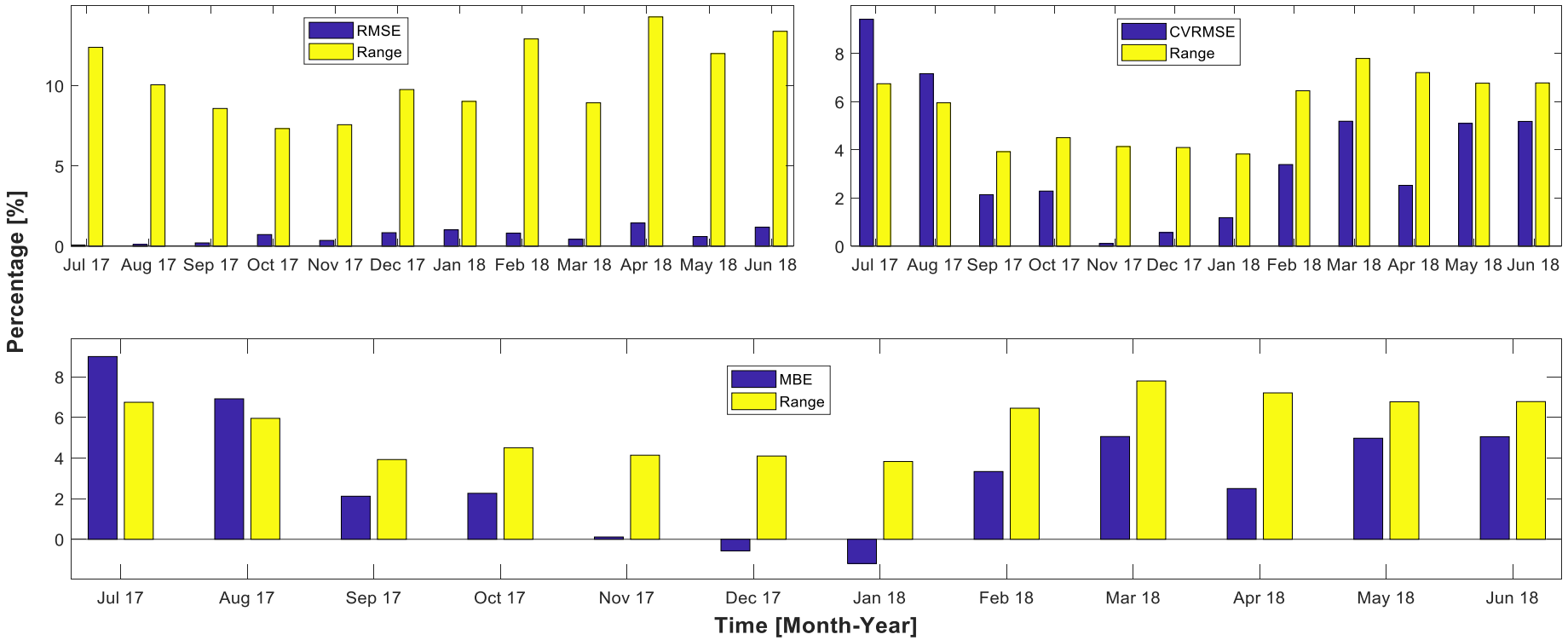

Figure 5-45: Statistical results for changing room

5.5 Effects of the thermal bridge on the energy performance of buildings

To calculate the effect of thermal bridges on energy consumption, the heat passing through the building envelope (represented by heat flux in W/m^2) is obtained from numerical analysis. From the heat flux profile, as shown in Figure 5-46, it can be observed that the heat flux through the expansion joint and mortar joint was 27.54W/m^2 and 15.9W/m^2 while that passing through the junction (Figure 5-46) is 55.1W/m^2.

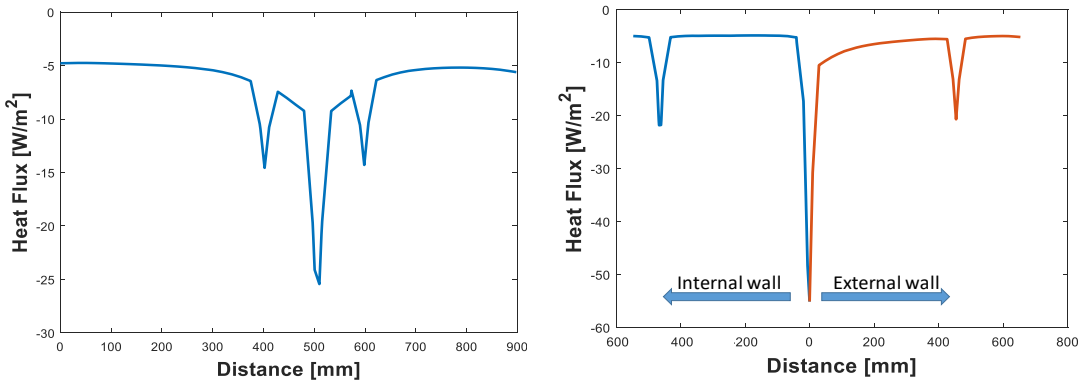

Figure 5-46: Heat flux profile of expansion joint (left) and corner (right)

From the thermographic survey and building plans, steel frames were observed to have created a thermal bridge. The detail of the affected envelope together with the thermal images are shown in Figure 5-48 and 46 below

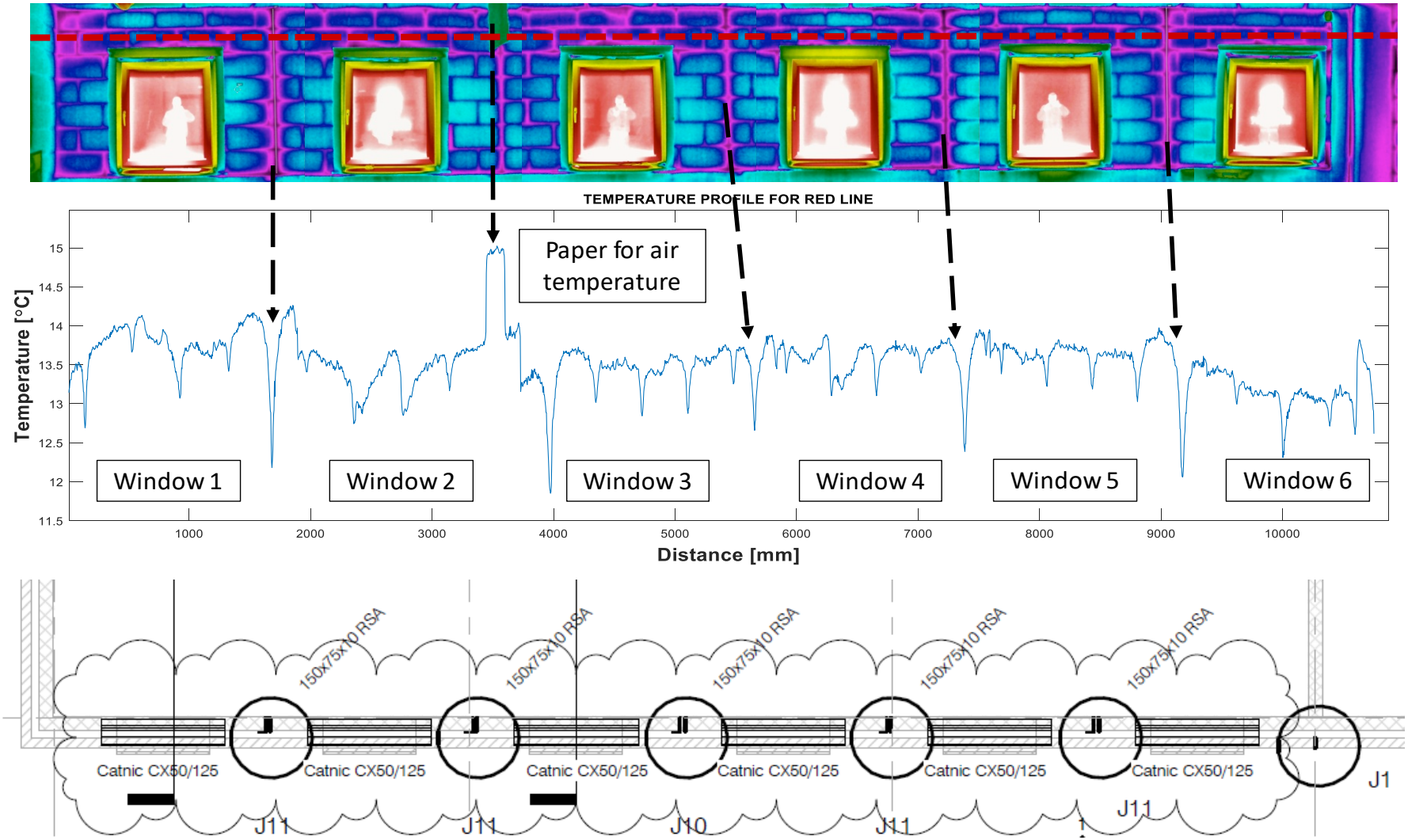

Figure 5-47: Wall affected by steel frames showing thermal image (top), temperature profile (mid) and steel section in plan (bottom)

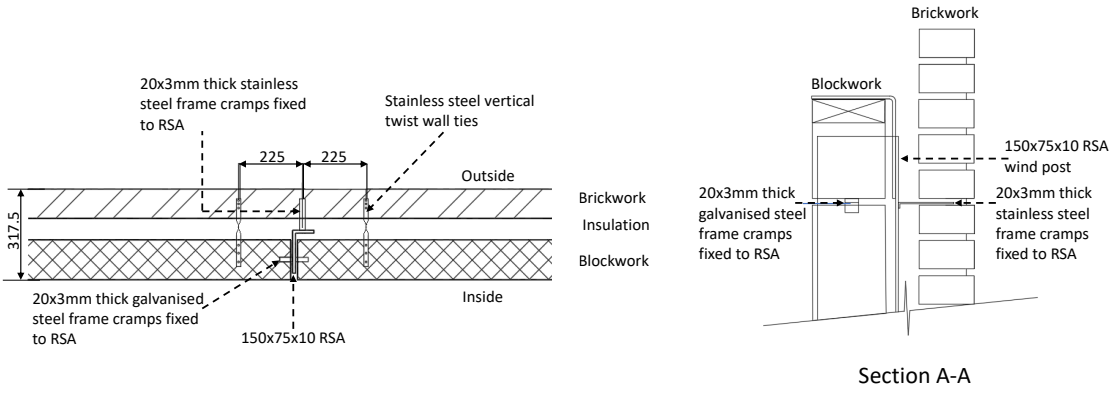

Figure 5-48: Section of steel (a) plan view and (b) elevation view

Steel frames within the building envelope are observed to have created a thermal bridge. Construction details from the building plans shown in Figure 5-48 reveal the position of the steel frames within the building envelope. The U-values and psi-values of the building envelope are calculated using Equations (4.6) to (4.11) (disclosed in Section 4.5). New U- and psi-values due to the presence of the steel frames and junctions Table 5-4 are used as input into the building energy model. This is done to compute the annual energy consumption with and without thermal bridges. Results revealed that the annual natural gas consumption increased by 16% when comparing models with and without thermal bridges (Figure 5-49 (top)). During the winter period, a difference of (25 %) between the models were revealed and on 5% difference was observed during July (summer). This can be associated with the difference in external and internal environment temperatures and the building occupancy. Models without thermal bridges are further observed to have a 10% and 2% reduction in heat losses during the winter and summer period respectively as shown in Figure 5-49 (bottom).

Table 5-4: Thermal bridge properties

Thermal Bridge Location	U-Value	New U-Value	Psi-Value
The thermal bridge created by Steel frame	0.32	0.52	0.256
Thermal bridge created by junction	0.32	0.32	0.678

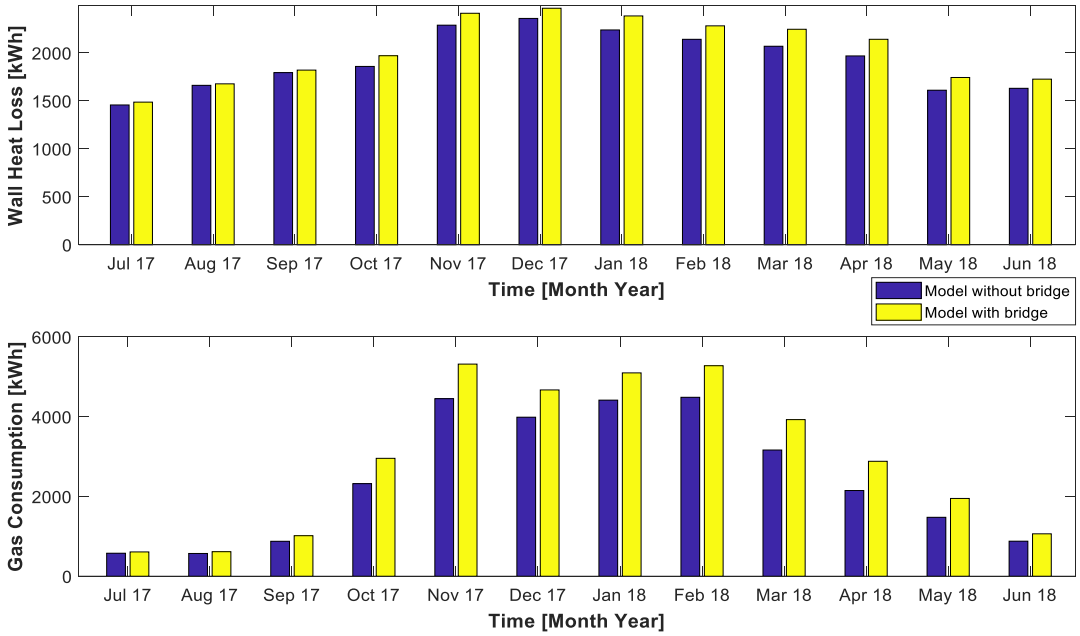

Figure 5-49: Gas consumption and wall heat loss with thermal bridge and without thermal bridge

5.6 Overheating Analysis

5.6.1 Effect of weather climates

Two different weather files are used to simulate the model, and these are the EnergyPlus IWEC weather data for Nottingham and the UK Met Office weather data. The IWEC is the result of the ASHRAE research project and are typical weather files suitable for use with building energy simulation programs. The EnergyPlus IWEC data provide average weather data for a period of 18years hourly weather data. Whereas the UK Met office weather data provides the current weather file which can be used for building energy simulation.

Figure 5-50 and Figure 5-51 shows the comparison between the sensors and the operative temperatures of both models (With IWEC data and UK Met Data) for the main-lounge and changing room respectively. It can be observed from both figures that the UK Met office data matches more closely with the sensor data especially during the summer period of 2018. The summer period of 2018 was an anomaly as temperatures rose beyond 30°C and the UK was without rainfall for weeks.

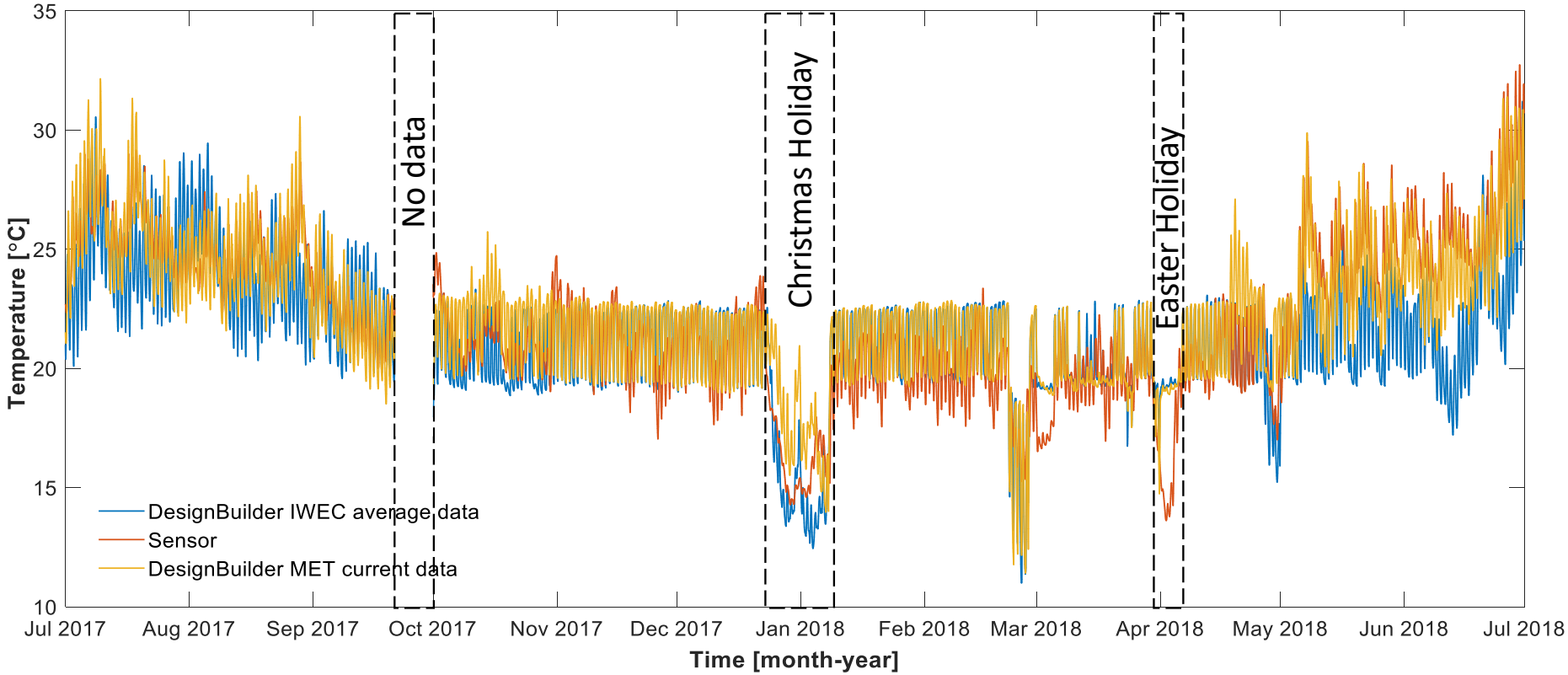

Figure 5-50: Operative temperature comparison for the sensor, EnergyPlus IWEC data and MET office data for the main-lounge

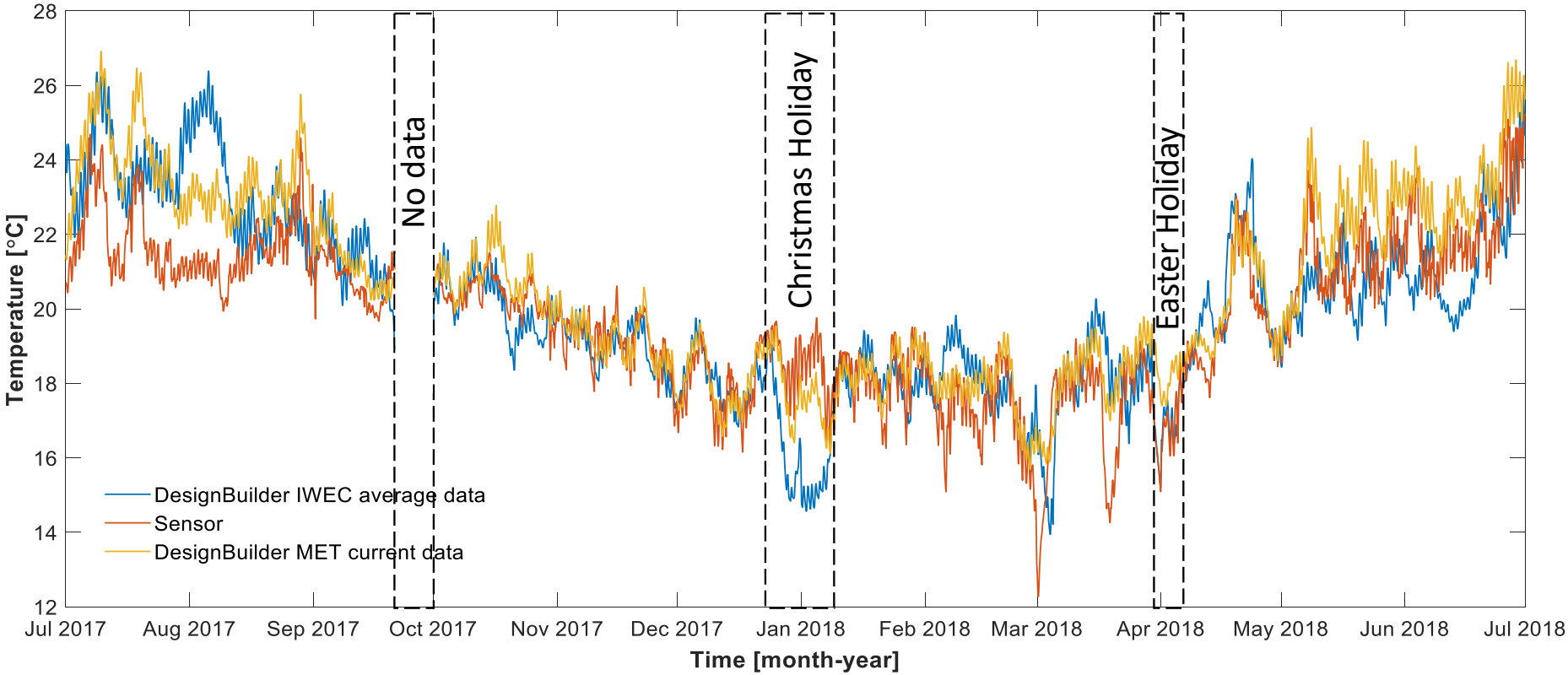

Figure 5-51: Operative temperature comparison for the sensor, EnergyPlus IWEC data and MET office data for the changing room

5.6.2 Influence of uninsulated hot water pipe

An infrared thermography survey on the Clifton Clubhouse was carried out on the 26th of November 2017 at 20:00hrs to avoid solar radiation and obtain the required temperature difference (between internal and external temperature). Thermal images are analysed to identify areas where there is unwanted heat gain into the facility. Unwanted heat gains were identified mainly at the changing rooms where there are exposed hot water pipes (Figure 5-52).

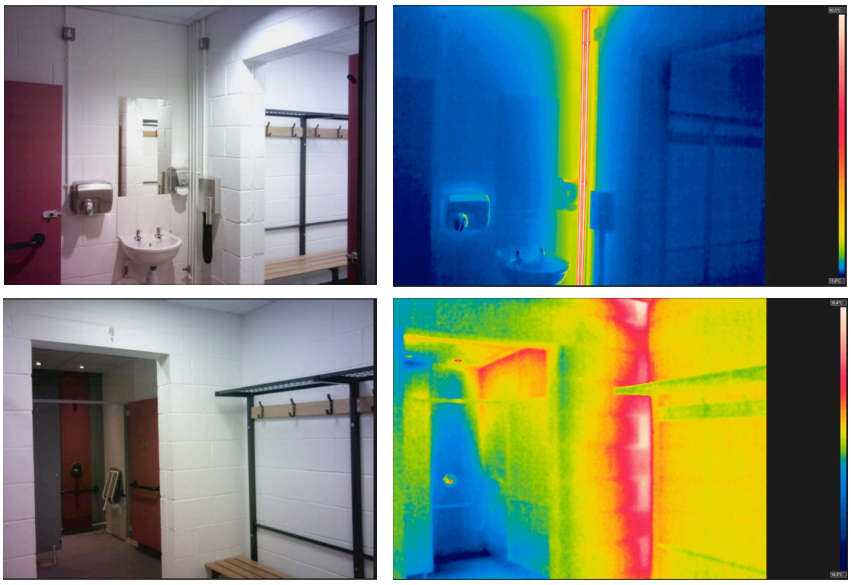

Figure 5-52: Digital (left) and thermal (right) image of hot water pipe in the shower room (top) and heat gain due to conduction into changing room (bottom)

Temperature ranges between 55-60°C were observed from the hot water pipe. Due to the main use of the facility (i.e. changing room with shower facilities), the schedule for the hot water pipe is on predominantly during term time. The influence of the domestic hot water pipes on indoor temperature can be observed in Figure 5-53. The pipes are observed to have a significant influence on the indoor temperature resulting in an increase of about 3-4°C in changing room 5.

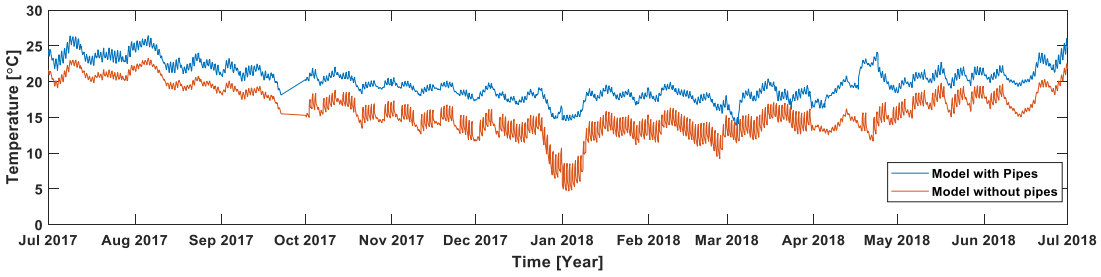

Figure 5-53: Influence of hot water pipes on indoor temperature

Convective and radiative heat transfer mechanism played a major role in the changing room with regards to the uninsulated hot water pipes. DesignBuilder's CFD analysis tool was used to evaluate the impact of the hot water pipe on temperature. Boundary conditions such as the vent for the heat recovery unit (four-way) and the uninsulated hot water pipe with 60°C were used. Results (see Figure 5-54) revealed that the air from the vents circulate towards the hot water pipe and together with the radiative impact increases the temperature in the changing rooms.

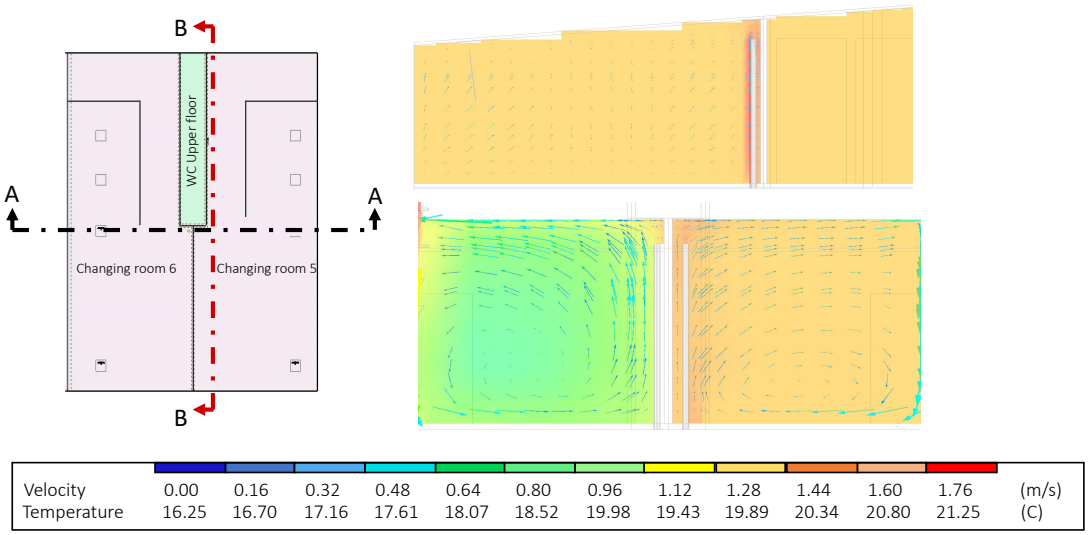

Figure 5-54: Section A-A (bottom) and B-B showing (top) showing the impact of uninsulated hot water pipe on temperature

5.6.3 Evaluation of overheating performance

The overheating assessment of the considered zones is presented in Table 5-5. From the table, it can be deduced that the clubhouse fails to fulfil the CIBSE TM52 overheating criteria in the future weather years. Changing rooms which do not have any means of cooling have been affected more by temperature increase. The increase in outside weather temperature together with the uninsulated hot water pipe, heat and humidity (increase in moisture) from the shower rooms contribute to the changing rooms failing. The main lounge, which has only natural ventilation as a means of cooling, has been affected less by the increase in temperature.

Table 5-5: CIBSE TM52 overheating assessment for years 2018, 2030 (50th Percentile), 2050 (50th Percentile) and 2080 (50th Percentile)

CIBSE TM52 OVERHEATING ASSESSMENT FOR THE CLUBHOUSE (the YEAR 2030 50TH PERCENTILE)

Block	Zone	Criterion 1 (%)	Criterion 2 (Khr)	Criterion 3 (hr)	Pass/Fail
1st Floor	Changing room 5	0.00	0.00	0.00	Pass
First Floor	Changing room 6	0.00	0.00	0.00	Pass
First Floor	Main lounge	0.70	8.50	0.00	Pass
G Floor	Changing room 1	0.00	0.00	0.00	Pass
Ground Floor	Changing room 3	0.00	0.00	0.00	Pass
Ground Floor	Changing room 4	0.00	0.00	0.00	Pass
Ground Floor	Main entrance	0.00	0.00	0.00	Pass

CIBSE TM52 OVERHEATING ASSESSMENT FOR THE CLUBHOUSE (the YEAR 2030 50TH PERCENTILE)

Block	Zone	Criterion 1 (%)	Criterion 2 (Khr)	Criterion 3 (hr)	Pass/Fail
First Floor	Changing room 5	0.00	0.00	0.00	Pass
First Floor	Changing room 6	0.00	0.00	0.00	Pass
First Floor	Main lounge	9.85	38.75	1.75	Fail
Ground Floor	Changing room 1	34.38	24.75	0.00	Fail
Ground Floor	Changing room 3	0.00	0.00	0.00	Pass
Ground Floor	Changing room 4	19.85	15.00	0.00	Fail
Ground Floor	Main entrance	1.46	4.00	0.00	Pass

CIBSE TM52 OVERHEATING ASSESSMENT FOR THE CLUBHOUSE (the YEAR 2050 50TH PERCENTILE)

Block	Zone	Criterion 1 (%)	Criterion 2 (Khr)	Criterion 3 (hr)	Pass/Fail
First Floor	Changing room 5	0.00	0.00	0.00	Pass
First Floor	Changing room 6	0.00	0.50	0.00	Pass
First Floor	Main lounge	17.98	66.50	16.00	Fail
Ground Floor	Changing room 1	47.80	26.25	0.00	Fail
Ground Floor	Changing room 3	0.00	2.50	0.00	Pass
Ground Floor	Changing room 4	43.56	24.25	0.00	Fail
Ground Floor	Main entrance	9.37	10.50	0.00	Fail

CIBSE TM52 OVERHEATING ASSESSMENT FOR THE CLUBHOUSE (the YEAR 2080 50TH PERCENTILE)

Block	Zone	Criterion 1 (%)	Criterion 2 (Khr)	Criterion 3 (hr)	Pass/Fail
First Floor	Changing room 5	0.45	1.00	0.00	Pass
First Floor	Changing room 6	1.23	2.75	0.00	Pass
First Floor	Main lounge	24.14	77.75	29.75	Fail
Ground Floor	Changing room 1	74.55	29.00	2.00	Fail
Ground Floor	Changing room 3	0.00	0.00	0.00	Pass
Ground Floor	Changing room 4	54.89	24.75	0.00	Fail
Ground Floor	Main entrance	12.30	12.75	0.00	Fail

Using the recommendations of CIBSE Guide A on overheating, the indoor temperature for the future weather was compared against the indoor temperature of the current year (see Figure 5-55). New buildings, refurbishments and adaptation strategies must conform to category II in BS EN 15251 as recommended. In free-running buildings, criterion II of BS EN 15251 sets a maximum acceptable temperature of 3°C above the comfort temperature for buildings in free-running mode. Temperature time histories of the main lounge showing the maximum acceptable temperature and the upper limit temperature for the year 2018, 2030, 2050 and 2080 were analysed (see Figure 5-56). The operative temperature in 2018,2030,2050 and 2080, suggests that the buildings thermal performance was unsatisfactory as T_{max} was exceeded for 12.16%, 25.66%, 37.18% and 45% respectively. Therefore the building fails under criteria I. This was not the case in 2018, although the operative temperature exceeds T_{max}, it was observed that it was for a couple hours resulting in 0.70% of the occupied hours. Therefore, the building satisfies criteria I in 2018. Higher operative temperatures occur mostly between July and September (Figure 5-55) which is also the period where the maximum temperature is mostly exceeded (see Figure 5-56).

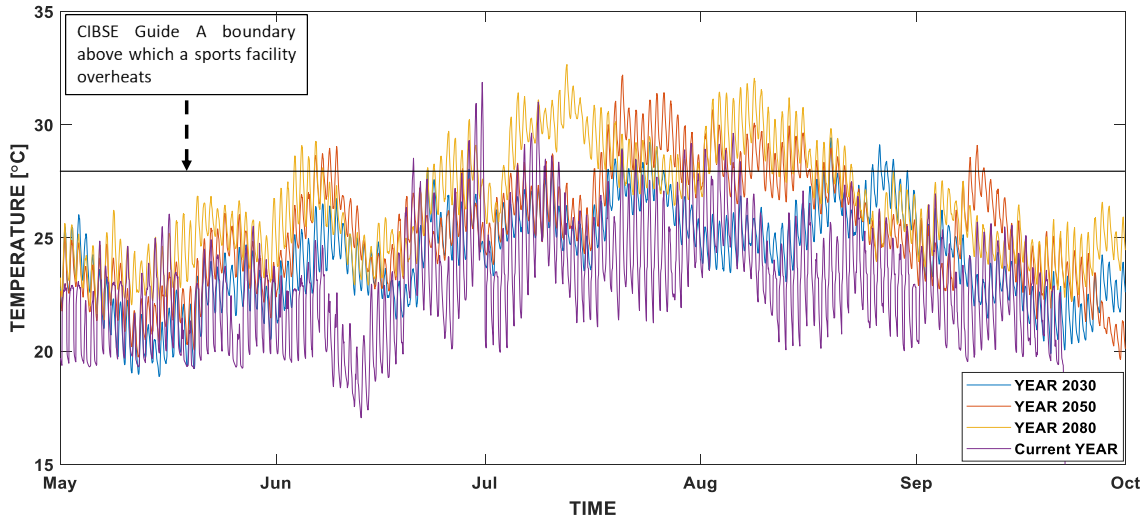

Figure 5-55: Indoor temperature of the main lounge for the current year (2018), 2030, 2050 and 2080 showing CIBSE guide A overheating boundary

In the current and future scenarios of 2030, 2050, and 2080, the operative temperature in the main-lounge exceeds the upper limit temperature (which covers the extremes of hot weather conditions) for 1.25hrs, 25.00hrs, 120.75hrs and 176.75hrs respectively. The operative temperature is within the comfort zone in 2018 and part of 2030 and 2050. However, the maximum acceptable temperature is also breached in all scenarios (Figure 5-56).

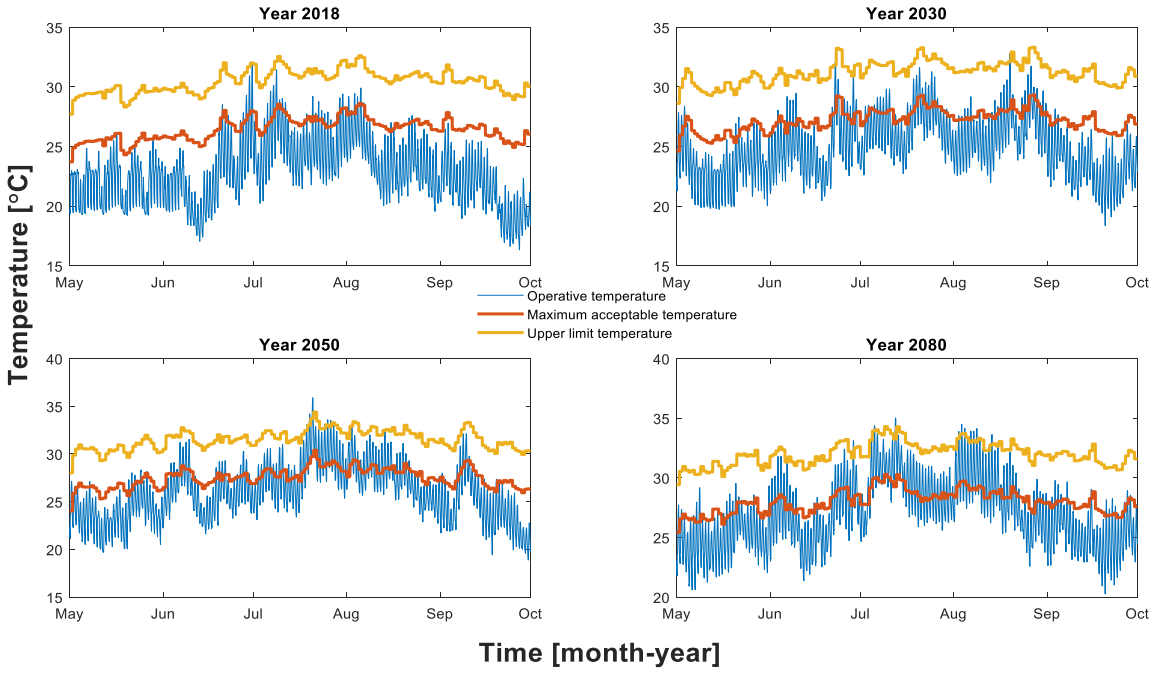

Figure 5-56: Maximum acceptable T_{max} and upper limit temperatures for 2018, 2030, 2050 and 2080

In the changing rooms, the operative temperature does not exceed the upper-limit temperature in all years using the 50th percentile data (Figure 5-57). However, using the 90th percentile, the upper limit is exceeded only in July 2080. For most of the analysed periods in all scenarios, the operative temperature is within the comfort temperature and does not exceed the maximum acceptable temperature (Figure 5-57).

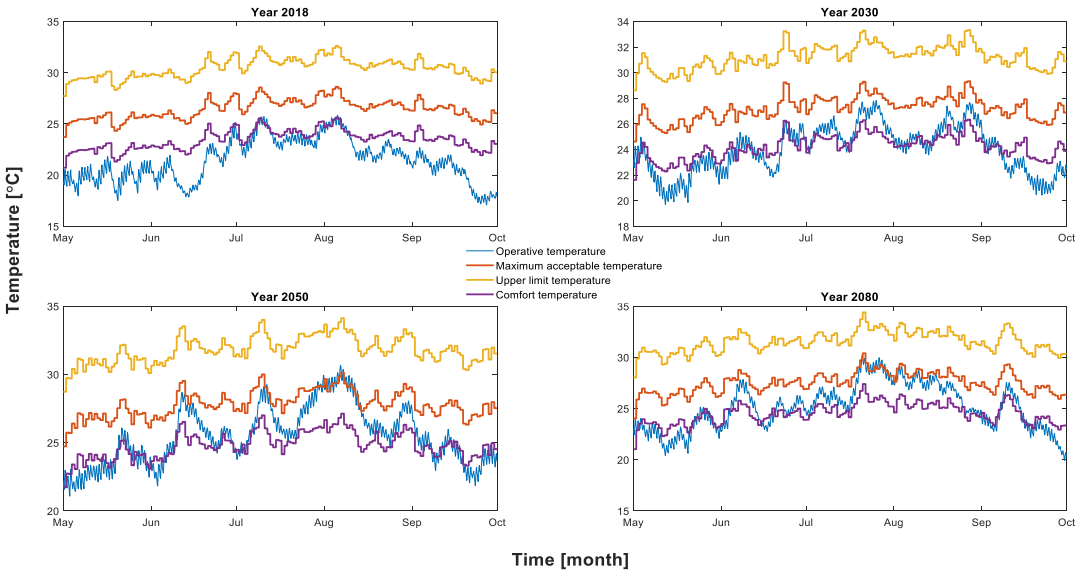

Figure 5-57: Maximum acceptable T_max and upper limit temperatures for 2018, 2030, 2050 and 2080 in the changing rooms

As mentioned in section 3 above, the changing rooms are equipped with a mechanical ventilation heat recovery unit with no cooling. However, a cooling effect takes place during the summer periods due to zone sensible heating as fresh air (not heated) from the heat recovery unit is being supplied into the changing rooms. Due to this effect, at some point in time, the external and internal temperature becomes equal (Figure 5-58). A building is not considered as overheating if the internal temperature is the same or lower than the external temperature.

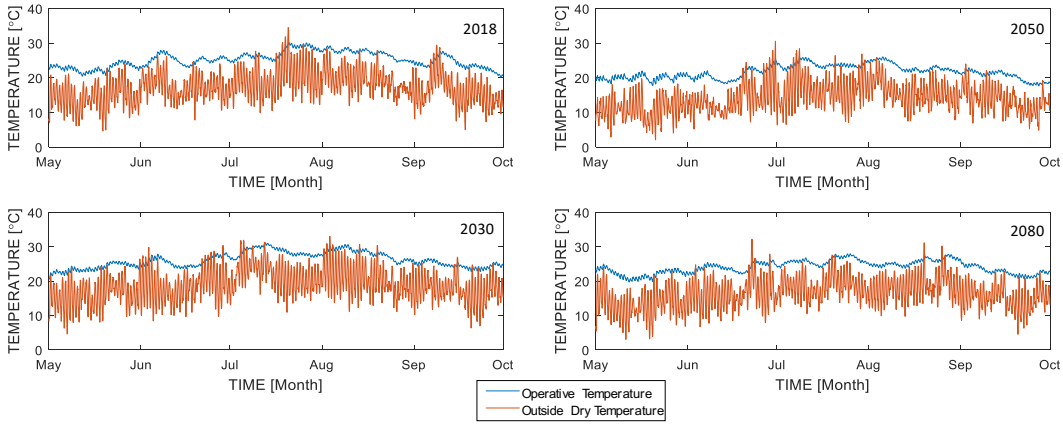

Figure 5-58: Outside and internal temperature of changing rooms

This is not the case in the main-lounge because, with natural ventilation, the air changes per hour into the lounge cannot be controlled or increased. From the model, an air change per hour of about 3.7ach is required to keep the changing rooms from overheating. In the main-lounge, an air change of about 1.8-2.0ach was achieved due to the natural ventilation. From a comfort perspective, the changing rooms fall within -2 and $+2$ (cool and warm) using the Fanger PMV thermal comfort scale (Figure 5-59). The main-lounge, however, falls into the hot zone ($+3$) predominantly in July for all scenarios

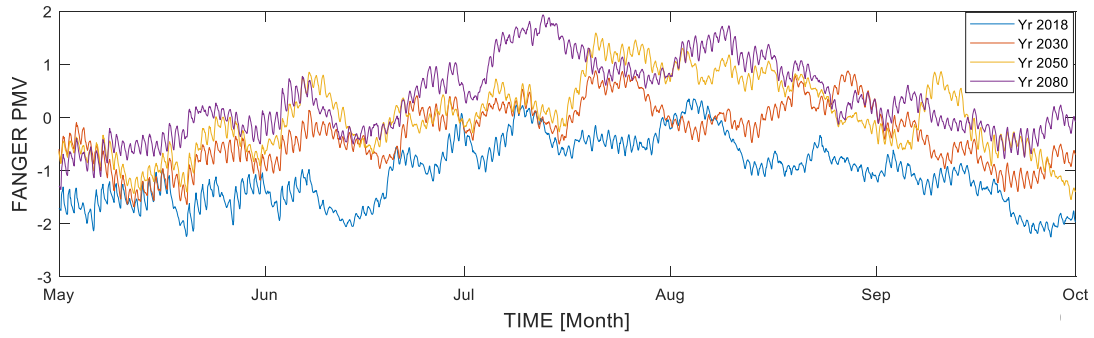

Figure 5-59: Fanger PMV of the changing rooms

Relative humidity data (for the period of 01-May 2018 to 02-July 2018) for the changing room was observed to be higher than that of the main-lounge (Figure 5-60). This is due to the increase in moisture from the shower rooms.

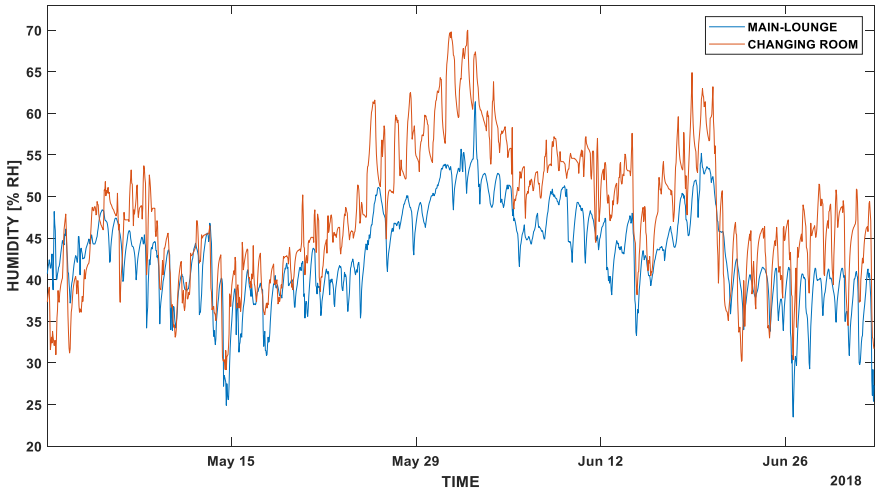

Figure 5-60: Monitored relative humidity for main-lounge and changing room

5.7 Summary

The Clifton clubhouse, which designed as a low energy building, is used as a case study to demonstrate the application of the proposed energy investigation framework. The thermography analysis identified and quantified thermal bridges using temperature profiles from thermal images and calibrating numerical models of part with thermal bridges. The building model is developed using DesignBuilder. The model is calibrated and validated using one year of collected temperature data from sensors. The framework was capable of identifying and evaluating the effects of thermal bridges on the building performance with a 25% increase in consumption in the winter periods. Effects of overheating are also analysed by providing inputting predicted future temperatures into the model. Results revealed that there is a high tendency of overheating in the future years of 2030 to 2080, especially in the main-lounge. Furthermore, results reveal that overheating risks in the changing rooms are very low except in the 90th percentile (2080) as a result of the availability of mechanical ventilation heat recovery system. In conclusion the Clifton clubhouse is observed to be underperforming based on the low energy standard it was built to achieve.

Chapter Contribution: Applications of the Energy Investigation Framework

The Energy investigation framework was used to assess the performance of a low energy building which was found to be underperforming. The framework provided the means to identify thermal bridges within the envelope and assess their effects on energy performance. As with the impact of climate change on buildings, the framework was used to evaluate the risk of overheating in the current and future years.

Chapter 6: Discussion

6.1 The Energy Investigation Framework

The Energy investigation framework is a process of analysing the energy use and consumption of buildings. It is a systematic combination of relevant energy analysis methods that provides an all-round investigation into the energy performance of buildings using energy simulation, infrared thermography and numerical analysis. This method allows for the detection and analysis of thermal bridges which affect the energy consumption of buildings by about 5-20% and 5-30% increase in annual heating load and heat losses respectively (Bianchi et al., 2014; Déqué et al., 2001; Gao et al., 2008; Kotti et al., 2017; Zalewski et al., 2010). Furthermore, the framework provides a platform for analysing the effect of other defects such as cracks and spaces within mortar joints on the energy performance of buildings. Studies such as (Borgstein et al., 2016; De Wilde, 2014) revealed the importance of bridging the gap between predicted and measured performance is central to the building industry as it would help in delivering buildings that are hefty towards change, engineered to adapt to change as well as maintaining a good performance in terms of occupants and climate. The framework aims to bridge the gap between predicted and measure performance and allows for the accurate future predictions of buildings to assess the performance of buildings under harsh weather conditions such as the risk of overheating.

A case of a low energy building with active (heat recovery) and passive (natural ventilation) was investigated using the proposed energy investigation frameworks. A low energy building is achieved by constructing a well-insulated building that is airtight which has balanced ventilation with a heat recovery system of high efficiency (Berggren & Wall, 2013). Therefore, when a building is designed on such principles, heat transfer occurs through the building element and thermal bridging. Furthermore, studies by (BrumĂ et al., 2016; Capozzoli et al., 2013; De Angelis & Serra, 2014; Déqué et al., 2000) all revealed that the increasing levels of insulation increase the weight of thermal bridges. In such a case, it is vital to understand and not to misjudge a thermal bridge, which may lead to energy systems being undersized, poor indoor climate, and most importantly energy costs that exceed expectations.

Using the energy investigation framework, a valid model of the Clifton clubhouse was created. Modelling is an essential tool used to identify and provide a solution to different problems. Models must be created to behave in the same manner as the real-life scenario. This was achieved using the systematic approach by collecting essential information from the

building audit and monitoring as well as information from the infrared thermography as specified in the framework. Information such as the cracks, heating patterns and the heat gain into the facility due to the uninsulated pipe were vital to ensuring the model behaves like the real building. Ascione et al. (2012) further stated that if buildings are considered to have defects such as thermal bridges and the building energy audit are carried out with sophisticated tools. They will not provide reliable results if the dispersing structures (not considering the defects) are not well modelled. Hence, the study aims at providing reliable results through the energy investigation framework by taking into account defects such as thermal bridges.

Building audit is important as they provide information on the building being studied. Ascione et al. (2012) conveyed the importance of accurate thermal investigations of buildings using adapted instruments and proper modelling criteria, above all in the presence of thermal bridges and discontinuities. From the building audit and monitoring and infrared thermography, defects such as cracks were predominantly identified and analysed. Cracks are seen as a means of infiltration and therefore lead to increasing air changes, which affects the airtightness and moisture levels of the building. Due to the increase of air changes, more energy has to be used for space heating in the facility. Other areas identified that increased the air changes per hour included mortar joints and doors. This was also evident after a previously conducted air-tightness test result revealed that the building was not air-tight. From the air-tightness results, penetrations from blockwork, door thresholds, roof and ceiling elements were revealed to have affected the airtightness. Infiltration is known to also cause mould and mildew growth, and this occurs when infiltrated air encounters colder regions of the building envelope and water vapour condenses. Studies such as Al-ajmi et al. (2008) show that door cracks and wall cracks account for an increase of about 19.7% in energy consumption.

The cracks, which may have formed due to the use of low-density blocks and building settlement, were observed to have an effect on the surface temperatures of the building envelope. A temperature difference of about 1°C-1.5°C which showed that the cracks were behaving as a heat sink within the envelope. Other cracks within the building envelop were identified and were observed to influence the surface temperatures but not as much as the crack in the main lounge. The cracks that were observed to influence the surface temperature were located only within the internal walls while cracks on the external wall

were observed not to influence the surface temperature. This is because of the insulating layer within the wall.

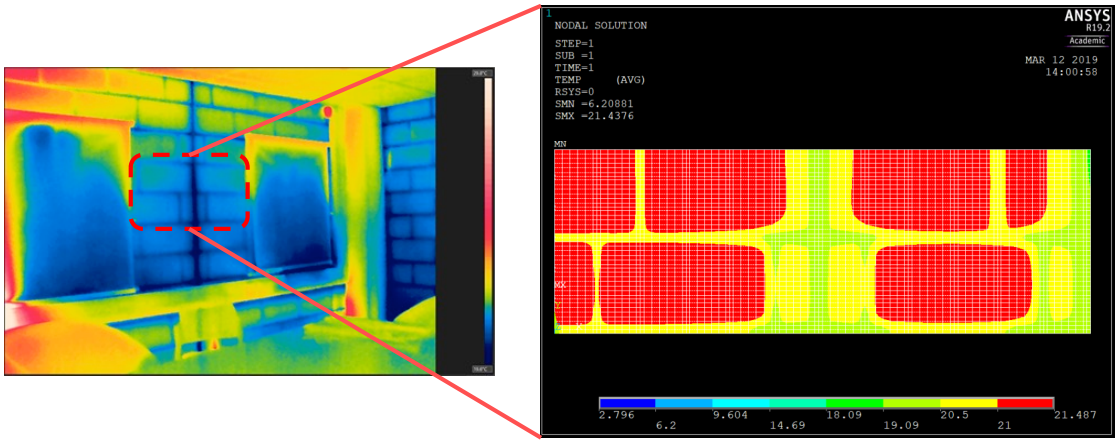

Figure 6-1: Heat loss due to structural element and mortar joints

Mortar joints were identified as a weakness (from a thermal perspective) in the energy performance of the Clifton clubhouse. Predominantly, heat losses from mortar joints (see Figure 6-1) were noticed throughout the building envelope using infrared thermography, and the effect was examined using numerical analysis. Al-sanea et al. (2012) strongly recommended that the effect of mortar joint must be removed as investigations revealed that increase in the height of mortar joints increases the peak, daily and yearly cooling and heating transmission load. Branco et al. (2004) also observed that the mortar strip between bricks behaved as a thermal bridge in which Ascione et al. (2013) stressed the relevance of the research in the EU as a great part of European buildings has walls with bricks. The literature on thermal bridging usually focus on bridges from the structural element and insufficient attention has been given to mortar joints (Zedan et al., 2016). Detachments between the mortar and masonry may produce an air layer thereby introducing additional thermal resistances and hence altering the distribution of the area with anomalies. This was also revealed to occur between plaster and masonry as noticed by De Freitas et al. (2014). Furthermore, it is assumed that the brick/block-wall acts as a homogeneous material, which is not the case, as seen in this study (section 5.3). This is as a result of the difference in thermal conductivity of the materials as the transmittance of a brick or block wall depends on the elements in which it is made up (mortar joints, number and shape of air cavities and material used in the bricks or blocks). Mortar joints cover about 4-10% of the total masonry wall area. Therefore, any heat loss due to mortar joint is not negligible, and hence the mortar joint has to be taken into account when investigating the energy performance of a building

There are different options to consider when building a brick/block wall to avoid or reduce the thermal bridging effect of the mortar joints. Juarez et al. 2012 examined the influence of horizontal joints on the thermal properties of single leaf walls lights clay blocks. The author observed that this could be achieved by using lightweight mortars that have a lower thermal conductivity or using thinner layers of bonding mortar in horizontal joints to minimise the amount of mortar used. Minimising the number of mortars leads to the reduction in the thickness of the layer and the extent of penetration hence minimises the thermal bridging effect in the joint. Regardless of the type of blocks used for construction, thinner joints bring about a 13% increase in thermal performance (Juárez et al., 2012). Zedan et al. (2016) proposed that the effect of thermal bridging resulting from mortar joints can be eliminated using a tongue and groove insulating building blocks. This provides continuity of the insulating layer and hence eliminates the bridging effects.

Structural elements are known to create thermal bridges either through different materials, geometry or a combination of different material and geometry. In this case, structural steel elements and expansion joints created thermal bridges within the envelope. With the structural steel elements being five in number (see Figure 6-2), a substantial heat loss (see Figure 6-1) was noticed together with heat loss from the movement joint. Steel having a high thermal conductivity plays a major role in heat losses within the envelope while the mortar around the movement joint creates the bridge between the internal and external environment. In previous studies, Kosney and Christian (1995) demonstrated that the thermal resistance of a concrete wall reinforced with steel profiles might diminish by around 48%. Therefore, the effect of steel on the building energy envelope is not new to the energy society.

Ties are also present among masonry wall, although the ties may not be visible, but they have high conductivity. It is assumed that they also influence the heat loss due through the mortar joint (see Figure 6-1). Angelis et al. 2014 observed that point thermal bridges characterise steel frame construction. The steel ties within the wall can cause this.

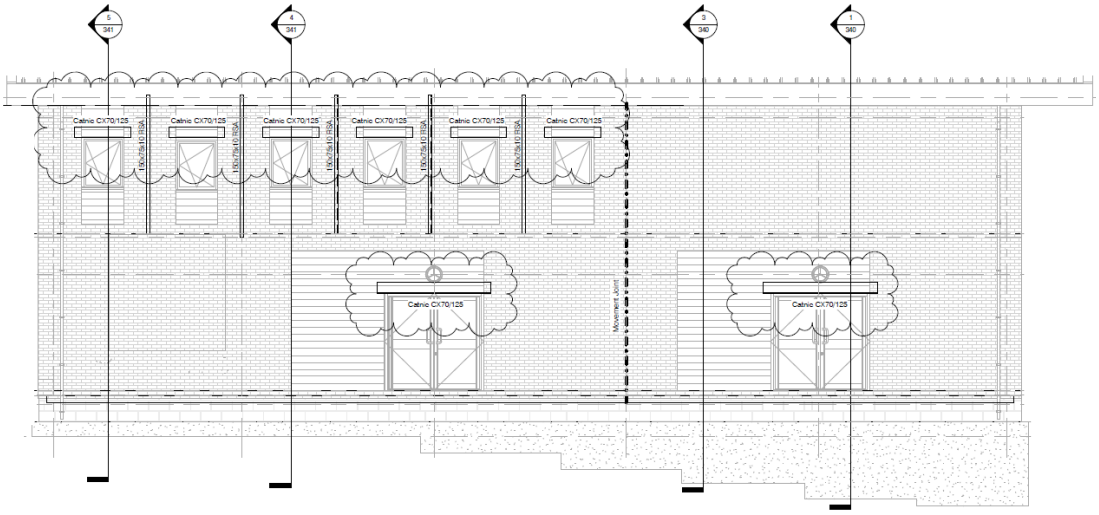

Figure 6-2: Elevation showing structural steel and lintels

The effect of the thermal bridging was evaluated using numerical analysis (ANSYS) as the bridges require a proper modelling in other to avoid problems such as mould growth and vapour condensation (Ascione et al., 2012). The heat fluxes observed at thermal bridge due to the steel members are 27.54W/m^2 , mortar joints as 15.9W/m^2 and due to the corner is 55.1W/m^2 . Prata et al (2018) experimented with a linear thermal bridge of a wooden building corner and revealed that the linear thermal bridge has a heat flux of 17.2W/m^2 under steady state conditions. The differences between the results is due to high thermal conductivity of steel in comparison with that of the wooden structure and the temperature difference between indoor and outdoor environments.

In the Design stages, thermal bridges are accounted for in the design of the low energy building (Clifton clubhouse). The use of continuous insulation was adopted and ensured in the design of the clubhouse. If care is not taken during the construction phase, thermal bridges can be created even if during the design phase, an ideal design was taken into account. Furthermore, from the case –study, thermal bridges identified were not seen during the design stages or may have been created unintentionally during construction. Therefore, care must be advised during the construction phase in other to avoid creating thermal bridging. This was also observed by Kuusk et al. (2017) where the author stated that possible changes in construction phases are not taken into account in energy calculation results as control mechanisms often stop at building permit phase.

Global warming has gained more emphasis due to the recent events in the current years 2010-2019. A record winter temperature was set in February with temperatures rising to 21.2°C for 2019 (Daniel, 2019) while the previous year (2018) had temperatures at -12°C in

some parts of the United Kingdom (BBC, 2018). Due to these uncertainties, buildings should be assessed so that to ensure that they provide the necessary comfort. Using the energy investigation framework, the risk of overheating was assessed in the clubhouse using future weather data from the Prometheus project. Results revealed that the clubhouse has a high tendency to overheat. The main concern was that of the main lounge in which it is cooled only through natural ventilation. The temperature within the main lounge was as high as 32°C in July of 2018 and 33°C in 2080 from the future prediction. In 2018, the UK experienced heatwave between the months of May-September and the sensors within the building recorded temperatures as high as 31°C.

Changing rooms, on the other hand, tend to overheat but not as high as the main lounge. Due to the presence of mechanical ventilation (heat recovery unit), zone sensible cooling comes into play in the changing rooms, and therefore temperatures are not as high as that of the main lounge. A factor that may contribute to the changing rooms overheating is the influence of the hot water pipes. Energy investigation framework provided the platform to investigate the influence of uninsulated hot-water pipes in the building energy. The hot water pipes are uninsulated and operate at a temperature of about 60° C. With the help of heat transfer mechanisms; radiation from the pipe and convection due to the inlet ventilation from the heat recovery unit, heat is gained into the changing rooms. This resulted in an increase in temperature by about 2.5°C. Although some may argue that, the heat gain is welcomed during the heating period (winter). This is not the case during the summer period as the pipes will still be in operation during the period. Hence the pipes may lead to overheating.

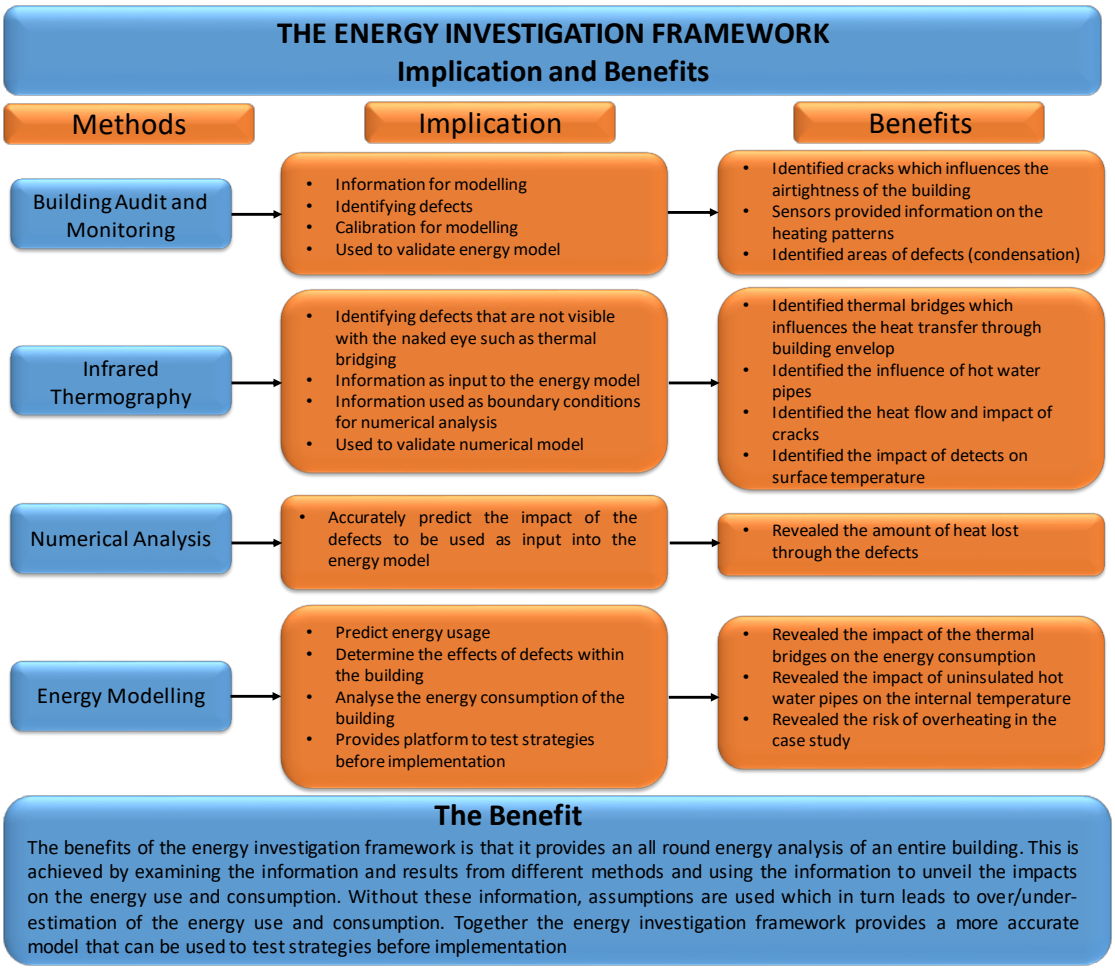

Figure 6-3: implication and benefits of the energy investigation framework

The clubhouse built as a low energy building with both passive and active measures was observed to have heat losses within the envelope caused by cracks, structural steel, mortar joints and internal to external wall junctions. The structural steel and internal to external wall junctions created linear thermal bridges along with the building envelope thereby decreasing the thermal resistance of the envelope and increasing the heat flow. The linear thermal bridges were observed to have affected the gas consumption of the clubhouse by an extra 15% consumption.

Using the recommendation of De Wilde (2014) on the bridging the performance gap, as mentioned in section 4.4.3. Ignoring the effect of thermal bridges on the overall energy performance of buildings can be regarded as contributing to model uncertainties hence errors. Therefore, the correct implementation of thermal bridges is required to bridge the performance gap as implemented in this study using the energy investigation framework. The energy investigation framework results were also used as feedback to the clients (in this

case NTU Estates department) regarding the performance of the building in use. Furthermore, observations were used to improve other properties.

Buildings are unique; therefore, all buildings differ in their configurations, material used and method of construction. Solutions to avoid thermal bridges is quite subjective depending on the nature of the building and thermal bridge. Solutions may range from the increase in insulation from both exterior and interior environment, use of thermal breaks etc. Therefore, in this case, a general solution is not provided.

Chapter 7: Conclusion and Contribution to the knowledge

7.1 Introduction

In the previous chapters of this thesis, a framework for energy investigation was developed using relevant energy analysis methods. The application of the framework was validated using a low energy building as a case study. This chapter concludes the thesis by providing the following

- Summary of Research
- Achievements of the research based on the set objectives
- Contribution to Knowledge and Practice
- Limitations and recommendations for future work

7.2 Summary of Research

In recent years, there has been much debate regarding the temperature rising in the future. These have led to researcher pondering about ways to reduce the greenhouse gas emissions and climate leading to a risk of overheating or hothouse effect. Extreme weather events, which have been linked to climate change, cost thousands of lives and caused huge damage throughout the world in 2018. The European Union and the United Kingdom have a pledge called the Climate Change Act to reduce greenhouse gas emissions by 80% in comparison with the 1990 baseline. The building sector is seen as a large contributor to the greenhouse gas emission, hence the continuous development in terms of initiatives such as REMOURBAN Project and development of energy-efficient buildings such as low energy buildings and zero energy buildings. For the energy-efficient buildings, not all perform as expected.

The main aim of this thesis was to create a framework for investigating the energy performance of buildings with a focus on the effect of thermal bridges in the energy performance of buildings and risk of overheating in modern low energy buildings. A recently built low energy building at Nottingham Trent University was chosen as a case study. The energy investigation framework was applied to assess the performance of the building in which it was revealed to be underperforming. The reasons why the building was not performing were revealed through the framework. Thermal bridges were identified as one of the main factors affecting the building. Other defects included the envelope not being air-tight as cracks increase the air changes per hour.

Overheating is a major concern in buildings as temperature are on the rise due to the effects of Global warming and climate change. The Energy investigation framework was used to assess the risk of overheating in a low energy building. Through the framework, the effects of mechanical ventilation, natural ventilation and uninsulated pipes on overheating were evaluated.

7.3 Achievements of aims and objectives

The achievement of the set objectives are as follows

Objective 1: Create a framework for the overall investigation of energy performance in buildings: The building energy investigation framework provides a guide on how to conduct a building performance analysis and evaluation. The framework is a systematic combination of relevant energy analysis and numerical methods. Four phases were created to form the energy investigation framework where a systematic transfer of information occurs within the phases. The validation and calibration of models of building parts with thermal bridges and building energy simulation models are useful when evaluating current building performances, accounting for possible energy savings (by minimising effects of thermal bridges) and predicting the future performance of the building. Using the proposed framework, areas that influence the energy consumption of a building such as cracks, thermal bridges and hot water pipes can be characterised.

Objective 2: Modelling and investigating the existing building structure using a building energy simulation program: Investigative research into the existing structure was achieved using thermography. The thermography was used to obtain boundary conditions and specific information relating to the building energy use. These were used as inputs for the building energy model using DesignBuilder. The model was compared to monitored data which were in good agreement.

Objective 3: Modelling of thermal bridges within the building using finite element analysis software: Thermal bridges were identified using infrared thermography. The affected area was further modelled using finite element analyses program (ANSYS) with the same conditions observed during the thermography survey. Observations from the thermography survey were used as boundary conditions while the results were used to verify the numerical model by comparing the temperature profile. From this, the impact of the thermal bridge (heat flux) on the building envelope was evaluated.

Objective 4: Investigating the effect of thermal bridging on the existing structure: Mortar and expansion joints and cracks create weak areas for air within the building envelope, thereby affecting the air exchange within the building and increasing infiltration, hence increasing the energy usage. In the case study, heat losses through thermal bridges in expansion joints with steel frame cramps, mortars and cracks increased the gas consumption by 15% and 5% during the winter and summer periods, respectively. The heat flow through the clubhouse walls increased by about 14% and 6% in winter and summer, respectively. Furthermore, eliminating thermal bridges resulting from cracks and joints could save up to 15% on the gas consumption bill.

Objective 5: Assess the risk of overheating in buildings: With global warming being a hot topic of discussion accurate building energy models can help to evaluate the effects of overheating. The case study revealed that under the two-current method of overheating assessment (CIBSE Guide A and TM52), the clubhouse is in a high risk of overheating in future. Furthermore, the hot water pipes are observed to influence the temperature in the clubhouse. This information is useful at the design stage and could help foresee potential overheating of the building.

7.4 Contribution to knowledge

In section 1.1, the identified problem, different studies have been carried out on improving the energy performance of buildings, but only a few studies have been done on the effect of thermal bridges on the whole building and the impact of thermal bridges in building energy demand is not properly calculated as stated by Ge & Baba (2015) and Martin et al. (2012)respectively. Furthermore, in a recent study by Kuusk et al. (2017), it was revealed that the energy losses through thermal bridges are not sufficiently taken into account as many EU countries adopt simplified approach or use default values in energy calculation software. This study will take into account the effect of thermal bridges overall building with the use of ANSYS to study the thermal bridge and DesignBuilder to simulate the performance of the facility.

The energy investigation framework: There are different methods of energy analysis such as infrared thermography, numerical analysis and the use of building energy simulation programs. Individually these methods provide information on the specific energy use and consumption. The energy investigation framework was developed to combine and use information from the individual methods for an all-round energy investigation. Assessors can use this, as a study by Kuusk et al. (2017) pointed out that the energy performance of new

and renovated buildings (in Belgium) is assessed at the moment of completion of works. In a study by Ascione et al. (2012), the importance of accurate modelling is stressed. They stated that if buildings are considered to have patchy elements with many thermal bridges and the building energy audit are carried out with sophisticated energy simulators, and they will not provide reliable results if the dispersing structures are not well modelled. The energy investigation framework aims to address this by providing an innovative use of the methods collectively to provide accurate models closer to reality and abscond the use of assumptions which leads to inaccurate interpretations and under/over-estimation of energy use, and consumption hence results in the reduction of the performance gap.

Effect of overheating in building: The risk of overheating in buildings around Europe has been undermined in recent years. With recent weather events and trends in global warming that have been occurring in recent, building need to adapt to the uncertainties of the weather. Assessing the risk of overheating in buildings should be mandatory as temperatures are predicted to rise in the future. The assessment of the risk of overheating is not new; this study aimed at stressing the need for accurate models in other to assess the risk of overheating in buildings.

Effect of thermal bridging (Review on thermal bridge effects and calculation methods): The effect of the thermal bridge is known to the industry, but it is underestimated. Therefore, this study analysed the effect of thermal bridging in conjunction with other building energy effects. With the statements made by (Ge & Baba, 2015; Kuusk et al., 2017; Martin et al., 2012), the energy investigation framework provides the steps to take into account thermal bridging when performing energy simulations accurately. Furthermore, extensive literature was achieved during this study, which conveys the effect of thermal bridges across different types of building and wall configurations. The literature also conveys different methods (from simplified or detailed methods) in which thermal bridges can be analysed.

From the literature review, authors differently due to either the causes or their effects classified thermal bridges. A combined classification of thermal bridges was achieved using the causes, effect and type of heat flow of the thermal bridge

Contribution to practise

Through retrofitting intervention, a reduction of 50% of building energy consumption can be achieved. Monitoring tools for energy which is part of the REMOURBAN project involves developing and deploying monitoring tools to achieve performances related to energy efficiency and financial viability. The Energy Investigative Framework can be (will be used) used as a means of monitoring the interventions of the REMOURBAN projects. Through the framework, identification and the effect of thermal bridges (if any) can be examined. The retrofitted buildings are expected to achieve thermal comfort in the present and future weather conditions. Therefore, with the use of the framework, the risk of overheating of the properties can be assessed.

Furthermore, technical reports have been published for the REMOURBAN project, these are outlined below;

- D5.4: Replicability Plan for each follower city. Annex A2: Gastronomia feasibility study in Seraing. Renewable energy solutions for a heating system. July 2019, Co-Authored Technical Reports on REMOURBAN Project, European Union 2020
- D4.14: Report of the specific evaluation procedures deployment. Analysis of Performance. June 2020, Co-Authored Technical Reports on REMOURBAN Project, European Union 2020

References

Abel, E. (1994). Low-energy buildings. *Energy & Buildings*, *21*, 169–174.

Aguilar, F., Solano, J. P., & Vicente, P. G. (2014). Transient modeling of high-inertial thermal bridges in buildings using the equivalent thermal wall method. *Applied Thermal Engineering*, *67*(1–2), 370–377. https://doi.org/10.1016/j.applthermaleng.2014.03.058

Ahmad, M. W., Mourshed, M., Mundow, D., Sisinni, M., & Rezgui, Y. (2016). Building energy metering and environmental monitoring - A state-of-the-art review and directions for future research. *Energy and Buildings*, *120*, 85–102. https://doi.org/10.1016/j.enbuild.2016.03.059

Al-Homoud, M. S. (2005). Performance characteristics and practical applications of common building thermal insulation materials. *Building and Environment*, *40*(3), 353–366. https://doi.org/10.1016/j.buildenv.2004.05.013

Al-Sanea, S. A., & Zedan, M. F. (2012). Effect of thermal bridges on transmission loads and thermal resistance of building walls under dynamic conditions. *Applied Energy*, *98*, 584–593. https://doi.org/10.1016/j.apenergy.2012.04.038

Andarini, R. (2014). The role of building thermal simulation for energy efficient building design. *Energy Procedia*, *47*, 217–226. https://doi.org/10.1016/j.egypro.2014.01.217

Anderson, B. (2006). *BRE 443: Conventions for U-value calculations*.

Asadi, I., Shafigh, P., Abu Hassan, Z. F. Bin, & Mahyuddin, N. B. (2018). Thermal conductivity of concrete-A review. *Journal of Building Engineering*, *20*, 81–93. https://doi.org/.1037//0033-2909.I26.1.78

Ascione, F., Bianco, N., De Masi, R. F., De'Rossi, F., & Vanoli, G. P. (2013). Simplified state space representation for evaluating thermal bridges in building: Modelling, application and validation of a methodology. *Applied Thermal Engineering*, *61*(2), 344–354. https://doi.org/10.1016/j.applthermaleng.2013.07.052

Ascione, F., Bianco, N., De Masi, R. F., Mauro, G. M., Musto, M., & Vanoli, G. P. (2014). Experimental validation of a numerical code by thin film heat flux sensors for the resolution of thermal bridges in dynamic conditions. *Applied Energy*, *124*, 213–222. https://doi.org/10.1016/j.apenergy.2014.03.014

Ascione, F., Bianco, N., De Rossi, F., Turni, G., & Vanoli, G. P. (2012). Different methods for the modelling of thermal bridges into energy simulation programs: Comparisons of accuracy for flat heterogeneous roofs in Italian climates. *Applied Energy*, *97*, 405–418. https://doi.org/10.1016/j.apenergy.2012.01.022

Ascione, F., De Masi, R. F., de Rossi, F., Ruggiero, S., & Vanoli, G. P. (2016). Optimization of building envelope design for nZEBs in Mediterranean climate: Performance analysis of residential case study. *Applied Energy*, *183*, 938–957. https://doi.org/10.1016/j.apenergy.2016.09.027

Asdrubali, F., Baldinelli, G., & Bianchi, F. (2012). A quantitative methodology to evaluate thermal bridges in buildings. *Applied Energy*, *97*, 365–373.

https://doi.org/10.1016/j.apenergy.2011.12.054

Azar, E., & Menassa, C. C. (2012). A comprehensive analysis of the impact of occupancy parameters in energy simulation of office buildings. *Energy and Buildings*, *55*, 841–853. https://doi.org/10.1016/j.enbuild.2012.10.002

Baba, F., & Ge, H. (2016). Dynamic effect of balcony thermal bridges on the energy performance of a high-rise residential building in Canada. *Energy and Buildings*, *116*, 78–88. https://doi.org/10.1016/j.enbuild.2015.12.044

Balaras, C. A., & Argiriou, A. A. (2002). Infrared thermography for building diagnostics. *Energy and Buildings*, *34*(2), 171–183. https://doi.org/10.1016/S0378-7788(01)00105-0

Baldinelli, G., Bianchi, F., Rotili, A., Costarelli, D., Seracini, M., Vinti, G., Asdrubali, F., & Evangelisti, L. (2018). A model for the improvement of thermal bridges quantitative assessment by infrared thermography. *Applied Energy*, *211*(August 2017), 854–864. https://doi.org/10.1016/j.apenergy.2017.11.091

BBC. (n.d.). *Heatwave: 2018 was the joint hottest summer for UK - BBC News*. Retrieved October 23, 2018, from https://www.bbc.co.uk/news/uk-45399134

BBC. (2018). *Europe freezes as "Beast from the East" arrives - BBC News*. https://www.bbc.co.uk/news/world-europe-43218229

Bergero, S., Cavalletti, P., & Chiari, A. (2017). Energy refurbishment in existing buildings: Thermal bridge correction according to DM 26/06/2015 limit values. *Energy Procedia*, *140*(May), 127–140. https://doi.org/10.1016/j.egypro.2017.11.129

Berggren, B., & Wall, M. (2013). Calculation of thermal bridges in (Nordic) building envelopes - Risk of performance failure due to inconsistent use of methodology. *Energy and Buildings*, *65*, 331–339. https://doi.org/10.1016/j.enbuild.2013.06.021

Bianchi, F., Pisello, A. L., Baldinelli, G., & Asdrubali, F. (2014). Infrared thermography assessment of thermal bridges in building envelope: Experimental validation in a test room setup. *Sustainability (Switzerland)*, *6*(10), 7107–7120. https://doi.org/10.3390/su6107107

Bingel, P., & Bown, A. (2009). Sustainability of masonry in construction. *Sustainability of Construction Materials*, 82–119. https://doi.org/10.1533/9781845695842.82

Borgstein, E. ., Lamberts, R., & Hensen, J. L. . (2016). Evaluating energy performance in non domestic buildings: A review. *Energy and Buildings*, *128*.

Branco, F., Tadeu, A., & Simoes, N. (2004). Heat conduction across double brick walls via BEM. *Building and Environment*, *39*(1), 51–58. https://doi.org/10.1016/j.buildenv.2003.08.005

BrumĂ, B., Moga, L., & Moga, I. (2016). Aspects Regarding Dynamic Calculation of Plan Building Elements Having Thermal Bridges. *Energy Procedia*, *85*(November 2015), 77–84. https://doi.org/10.1016/j.egypro.2015.12.276

Brundtland. (1987). *Our common future: Report of the World Commission on Environment and Development* (UN General Assembly document A/42/427 (Ed.)). Oxford University Press.

BS EN ISO 10211 : 2017 BSI Standards Publication Thermal bridges in building construction - Heat flows and surface temperatures - Detailed calculations. (2017).

BSI. (2007). BS EN ISO 6946:2007 - Building components and building elements. Thermal resistance and thermal transmittance. Calculation method. *British Standards Institution*. https://doi.org/10.3403/30127651

Capozzoli, A., Gorrino, A., & Corrado, V. (2013). A building thermal bridges sensitivity analysis. *Applied Energy*, *107*, 229–243. https://doi.org/10.1016/j.apenergy.2013.02.045

Cappelletti, F., Gasparella, A., Romagnoni, P., & Baggio, P. (2011). Analysis of the influence of installation thermal bridges on windows performance: The case of clay block walls. *Energy and Buildings*, *43*(6), 1435–1442. https://doi.org/10.1016/j.enbuild.2011.02.004

CIBSE. (2006). Environment Design. In *Freelancer's Guide to Corporate Event Design: From Technology Fundamentals to Scenic and Environmental Design*. https://doi.org/10.1016/B978-0-240-81224-3.00016-9

CIBSE. (2015). *Building performance modelling AM11*.

Clarke, J. A. (2001). *Energy Simulation in Building Design* (H. Butterworth (Ed.); 2nd ed.).

Coakley, D., Raftery, P., & Keane, M. (2014). A review of methods to match building energy simulation models to measured data. *Renewable and Sustainable Energy Reviews*, *37*, 123–141. https://doi.org/10.1016/j.rser.2014.05.007

Daniel, T. (2019). *Freak weather "will make life harder for business" - BBC News*. https://www.bbc.co.uk/news/business-47400729?intlink_from_url=https://www.bbc.co.uk/news/topics/clw2rl7ekd6t/uk-heatwave&link_location=live-reporting-story

Danish, S. S. M., Senjyu, T., Ibrahimi, M. A., Ahmadi, M., & Howlader, M. A. (2019). A managed framework for energy-efficient building. *Journal of Building Engineering*, *21*, 120–128.

De Angelis, E., & Serra, E. (2014). Light steel-frame walls: Thermal insulation performances and thermal bridges. *Energy Procedia*, *45*, 362–371. https://doi.org/10.1016/j.egypro.2014.01.039

De Freitas, S. S., De Freitas, V. P., & Barreira, E. (2014). Detection of façade plaster detachments using infrared thermography - A nondestructive technique. *Construction and Building Materials*, *70*, 80–87. https://doi.org/10.1016/j.conbuildmat.2014.07.094

De Wilde, P. (2014). The gap between predicted and measured energy performance of buildings: A framework for investigation. *Automation in Construction*, *41*, 40–49. https://doi.org/10.1016/j.autcon.2014.02.009

De Wit, S. (2004). Advanced Building Simulation. In A. M. Malkawi & G. Augenbroe (Eds.), *Advanced building simulation* (1st ed., pp. 25–59). Spon Press.

Deng, S., Wang, R. Z., & Dai, Y. J. (2014). How to evaluate performance of net zero energy building - A literature research. *EnergyEnergy*, *71*, 1–16.

Déqué, F., Ollivier, F., & Poblador, A. (2000). Grey boxes used to represent buildings with a

minimum number of geometric and thermal parameters. *Energy and Buildings*, *31*(1), 29–35. https://doi.org/10.1016/S0378-7788(98)00074-7

Déqué, F., Ollivier, F., & Roux, J. . (2001). Effect of 2D modelling of thermal bridges on the energy performance of buildings. *Energy and Buildings*, *33*(6), 583–587. https://doi.org/10.1016/S0378-7788(00)00128-6

DesignBuilder. (2019). *Calculation Options*. https://designbuilder.co.uk/helpv1/Content/Calculation_Options.htm

Dikarev, K., Berezyuk, A., Kuzmenko, O., & Skokova, A. (2016). Experimental and Numerical Thermal Analysis of Joint Connection “floor Slab - Balcony Slabe” with Integrated Thermal Break. *Energy Procedia*, *85*(November 2015), 184–192. https://doi.org/10.1016/j.egypro.2015.12.325

Din, A. ., & Brotas, L. (2017). The Impacts of Overheating Mitigation within the Life Cycle Carbon of Dwellings under UK Future Climate. *Procedia Environmental Sciences*, *38*, 21.

Djongyang, N., Tchinda, R., & Njomo, D. (2010). Thermal comfort: A review paper. *Renewable and Sustainable Energy Reviews*, *14*(9), 2626–2640. https://doi.org/10.1016/j.rser.2010.07.040

Dodoo, A., Gustavsson, L., & Sathre, R. (2011). Primary energy implications of ventilation heat recovery in residential buildings. *Energy and Buildings*, *43*(7), 1566–1572. https://doi.org/10.1016/j.enbuild.2011.02.019

Dols, W. S., Emmerich, S. J., & Polidoro, B. J. (2016). Coupling the multizone airflow and contaminant transport software CONTAM with EnergyPlus using co-simulation. *Building Simulation*, *9*(4), 469–479. https://doi.org/10.1007/s12273-016-0279-2

Doran, S, M., & Gorgolewski, M, T. (2012). *BRE DIGEST 465: U-Values for light steel-frame construction*. *37*, 257–268.

Dumitrescu, L., Baran, I., & Pescaru, R. A. (2017). The Influence of Thermal Bridges in the Process of Buildings Thermal Rehabilitation. *Procedia Engineering*, *181*, 682–689. https://doi.org/10.1016/j.proeng.2017.02.450

Elshafei, G., Negm, A., Bady, M., Suzuki, M., & Ibrahim, M. G. (2017). Numerical and Experimental Investigations of the Impacts of Window Parameters on Indoor Natural Ventilation in a Residential Building. *Energy and Buildings*, *141*, 321–332. https://doi.org/10.1016/j.enbuild.2017.02.055

Etheridge, D. (2011). *Natural Ventilation of Buildings: Theory, Measurement and Design* (2nd ed.). John Wiley & Sons, Incorporated.

European Commission. (2010). Directive 2010/31/EU. *Official Journal of the European Union*, 13–35.

Evola, G., Margani, G., & Marletta, L. (2011). Energy and cost evaluation of thermal bridge correction in Mediterranean climate. *Energy and Buildings*, *43*(9), 2385–2393. https://doi.org/10.1016/j.enbuild.2011.05.028

Fantucci, S., Isaia, F., Serra, V., & Dutto, M. (2017). Insulating coat to prevent mold growth in thermal bridges. *Energy Procedia*, *134*, 414–422.

https://doi.org/10.1016/j.egypro.2017.09.591

Feng, H., & Hewage, K. (2014). Energy saving performance of green vegetation on LEED certified buildings. *Energy and Buildings*, *75*, 281–289. https://doi.org/10.1016/j.enbuild.2013.10.039

Flir. (2017). *Flir Manual*. https://www.flir.com/globalassets/imported-assets/document/flir-ets320-user-manual.pdf

Fokaides, P. A., Christoforou, E., Ilic, M., & Papadopoulos, A. (2016). Performance of a Passive House under subtropical climatic conditions. *Energy and Buildings*, *133*, 14–31. https://doi.org/10.1016/j.enbuild.2016.09.060

Fosas, D., Coley, D. A., Natarajan, S., Herrera, M., Fosas de Pando, M., & Ramallo-Gonzalez, A. (2018). Mitigation versus adaptation: Does insulating dwellings increase overheating risk? *Building and Environment*, *143*(May), 740–759. https://doi.org/10.1016/j.buildenv.2018.07.033

Fox, M., Coley, D., Goodhew, S., & De Wilde, P. (2014). Thermography methodologies for detecting energy related building defects. *Renewable and Sustainable Energy Reviews*, *40*, 296–310. https://doi.org/10.1016/j.rser.2014.07.188

Fumo, N. (2014). A review on the basics of building energy estimation. *Renewable and Sustainable Energy Reviews*, *31*, 53–60. https://doi.org/10.1016/j.rser.2013.11.040

G,R, L. (2003). *Mesh Free Methods*. CRC Press.

Gao, Y., Roux, J. J., Zhao, L. H., & Jiang, Y. (2008). Dynamical building simulation: A low order model for thermal bridges losses. *Energy and Buildings*, *40*(12), 2236–2243. https://doi.org/10.1016/j.enbuild.2008.07.003

Garrido, I., Lagüela, S., Arias, P., & Balado, J. (2018). Thermal-based analysis for the automatic detection and characterization of thermal bridges in buildings. *Energy and Buildings*, *158*, 1358–1367. https://doi.org/10.1016/j.enbuild.2017.11.031

Ge, H., & Baba, F. (2015). Dynamic effect of thermal bridges on the energy performance of a low-rise residential building. *Energy and Buildings*, *105*, 106–118. https://doi.org/10.1016/j.enbuild.2015.07.023

Ge, H., & Baba, F. (2017). Effect of dynamic modeling of thermal bridges on the energy performance of residential buildings with high thermal mass for cold climates. *Sustainable Cities and Society*, *34*(June), 250–263. https://doi.org/10.1016/j.scs.2017.06.016

Green, E., Hope, T., & Yates, A. (2015). *Sustainable Buildings*. ICE Publishing. www.icevirtuallibrary.com

Grinzato, E. (2012). State of the Art and Perspective of Infrared Thermography Apllied to Building Science. In *Infrared Thermography: Recent advances and future trends* (pp. 200–230). Bentham Science Publications.

Gupta, R., & Gregg, M. (2018). Assessing energy use and overheating risk in net zero energy dwellings in UK. *Energy and Buildings*, *158*, 897–905.

Harish, V. S. K. ., & Kumar, A. (2016). A review on modelling and simmulation of building energy systems. *Renewable and Sustainable Energy Reviews*, *56*.

Hensen, J. (2004). Integrated building airflow simulation. In A. M. Malkawi & G. Augenbroe (Eds.), *Advanced building simulation* (pp. 87–118). Spon Press.

HSE. (2019). *Health and Safety Executive*. http://www.hse.gov.uk/temperature/thermal/factors.htm

Hui, S. C. M. (2001). Low energy building design in high density urban cities. *Renewable Energy*, *24*(3–4), 627–640. https://doi.org/10.1016/S0960-1481(01)00049-0

Jelle, B. P. (2011). Traditional, state-of-the-art and future thermal building insulation materials and solutions - Properties, requirements and possibilities. *Energy and Buildings*, *43*(10), 2549–2563. https://doi.org/10.1016/j.enbuild.2011.05.015

Juárez, M. C., Morales, M. P., Muñoz, P., & Mendívil, M. A. (2012). Influence of horizontal joint on the thermal properties of single-leaf walls with lightweight clay blocks. *Energy and Buildings*, *49*, 362–366. https://doi.org/10.1016/j.enbuild.2012.02.033

Kämpf, J. H. (2009). *On the Modelling and Optimisation of Urban Energy Fluxes*. *4548*, 171. https://doi.org/10.5075/epfl-thesis-4548

Karlsson, F., & Moshfegh, B. (2013). A Low-Energy Building Project in Sweden - the Lindås Pilot Project. In *Sustainability, Energy and Architecture: Case Studies in Realizing Green Buildings*. Elsevier. https://doi.org/10.1016/B978-0-12-397269-9.00012-8

Khatib, J. M. (2009). Introduction. *Sustainability of Construction Materials*. https://doi.org/10.1016/B978-1-84569-349-7.50015-1

Konis, K., Gamas, A., & Kensek, K. (2016). Passive performance and building form: An optimization framework for early-stage design support. *Solar Energy*, *125*, 161–179. https://doi.org/10.1016/j.solener.2015.12.020

Kothandaraman, C. . (2006). *Fundamemtals of Heat and Mass transfer* (Revised 3r). New Age International.

Kotti, S., Teli, D., & James, P. A. B. (2017). *Quantifying Thermal Bridge Effects and Assessing Retrofit Solutions in a Greek Residential Building*. *38*, 306–313.

Kuusk, K., Kurnitski, J., & Kalamees, T. (2017). Calculation and compliance procedures of thermal bridges in energy calculations in various European countries. *Energy Procedia*, *132*, 27–32. https://doi.org/10.1016/j.egypro.2017.09.626

Kylili, A., Fokaides, P. A., Christou, P., & Kalogirou, S. A. (2014). Infrared thermography (IRT) applications for building diagnostics: A review. *Applied Energy*, *134*, 531–549. https://doi.org/10.1016/j.apenergy.2014.08.005

Lapinskiene, V., & Martinaitis, V. (2013). The framework of an optimization model for building envelope. *Procedia Engineering*, *57*, 670–677. https://doi.org/10.1016/j.proeng.2013.04.085

Larbi, A. Ben. (2005). Statistical modelling of heat transfer for thermal bridges of buildings. *Energy and Buildings*, *37*(9), 945–951. https://doi.org/10.1016/j.enbuild.2004.12.013

Li, D. H. W., Yang, L., & Lam, J. C. (2013). Zero energy buildings and sustainable development implications - A review. *Energy*, *54*, 1–10. https://doi.org/10.1016/j.energy.2013.01.070

Li, X. Q., Chen, Y., Spitler, J. D., & Fisher, D. (2009). Applicability of calculation methods for conduction transfer function of building constructions. *International Journal of Thermal Sciences*, *48*(7), 1441–1451. https://doi.org/10.1016/j.ijthermalsci.2008.11.006

Li, Y., & Rezgui, Y. (2017). A novel concept to measure envelope thermal transmittance and air infiltration using a combined simulation and experimental approach. *Energy and Buildings*, *140*, 380–387. https://doi.org/10.1016/j.enbuild.2017.02.036

Liang, X., Wang, Y., Zhang, Y., Jiang, J., Chen, H., Zhang, X., Guo, H., & Roskilly, T. (2017). Analysis and Optimization on Energy Performance of a Rural House in Northern China Using Passive Retrofitting. *Energy Procedia*, *105*, 3023–3030. https://doi.org/10.1016/j.egypro.2017.03.618

Lo, E., Ma, Z., Borelli, D., & Schenone, C. (2017). Residential building retrofit through numerical simulation : a case study. *Energy Procedia*, *111*(September 2016), 91–100. https://doi.org/10.1016/j.egypro.2017.03.011

Lowe, J. A., Mcdonald, R. E., Mcinnes, R. N., Mcsweeney, C. F., Mitchell, J. F. B., Rostron, J. W., Thornton, H. E., Tucker, S., & Yamazaki, K. (2018). *UKCP18 Land Projections : Science Report November 2018*. *November*.

Maile, T., Fischer, M., & Bazjanac, V. (2007). Building Energy Performance Simulation Tools - a Life-Cycle and Interoperable Perspective. *Center for Integrated Facility Engineering*, *December*, 1–49. cife.stanford.edu/sites/default/files/WP107.pdf

Mao, G., & Johannesson, G. (1997). Dynamic calculation of thermal bridges. *Energy and Buildings*, *26*(3), 233–240. https://doi.org/10.1016/S0378-7788(97)00005-4

Mardiana-Idayu, A., & Riffat, S. B. (2012). Review on heat recovery technologies for building applications. *Renewable and Sustainable Energy Reviews*, *16*(2), 1241–1255. https://doi.org/10.1016/j.rser.2011.09.026

Marshall, A., Fitton, R., Swan, W., Farmer, D., Johnston, D., Benjaber, M., & Ji, Y. (2017). Domestic building fabric performance: Closing the gap between the in situ measured and modelled performance. *Energy and Buildings Buildings*, *150*, 307–317.

Martin, K., Erkoreka, A., Flores, I., Odriozola, M., & Sala, J. M. (2011). Problems in the calculation of thermal bridges in dynamic conditions. *Energy and Buildings*, *43*(2–3), 529–535. https://doi.org/10.1016/j.enbuild.2010.10.018

Martin, K., Escudero, C., Erkoreka, A., Flores, I., & Sala, J. M. (2012). Equivalent wall method for dynamic characterisation of thermal bridges. *Energy and Buildings*, *55*, 704–714. https://doi.org/10.1016/j.enbuild.2012.08.024

Martinaitis, V., Zavadskas, E. K., Motuzienė, V., & Vilutienė, T. (2015). Importance of occupancy information when simulating energy demand of energy efficient house: A case study. *Energy and Buildings*, *101*, 64–75. https://doi.org/10.1016/j.enbuild.2015.04.031

Mayer, R., Enache-Pommer, E., Parsons, G., Mazor, M., Hansbro, J., Lastovica, J., Buck, C., & Maurer, M. (2014). Finite element thermal modeling and correlation of various building wall assembly systems. *Energy and Buildings*, *75*, 410–418. https://doi.org/10.1016/j.enbuild.2013.11.034

McGrath, M. (2018a). *Climate change: Huge costs of warming impacts in 2018 - BBC News*. BBC. https://www.bbc.co.uk/news/science-environment-46637102

McGrath, M. (2018b). *Climate change: Warming made UK heatwave 30 times more likely - BBC News*. BBC. https://www.bbc.co.uk/news/science-environment-46462014

McMullan, R. (2018). *Environmental Science in Building* (8th ed.). Palgrave.

Najjar, M. K., Figueiredo, K., Hammad, A. W. A., Tam, V. W. Y., Evangelista, A. C. J., & Haddad, A. (2019). A framework to estimate heat energy loss in building operation. In *Journal of Cleaner Production* (Vol. 235, pp. 789–800). https://doi.org/10.1016/j.jclepro.2019.07.026

Nicol, J. F., & Humphreys, M. A. (2002). Adaptive thermal comfort and sustainable thermal standards for buildings. *Energy and Buildings*, *34*(6), 563–572. https://doi.org/10.1016/S0378-7788(02)00006-3

O'Grady, M., Lechowska, A. A., & Harte, A. M. (2017a). Infrared thermography technique as an in-situ method of assessing heat loss through thermal bridging. *Energy and Buildings*, *135*, 20–32. https://doi.org/10.1016/j.enbuild.2016.11.039

O'Grady, M., Lechowska, A. A., & Harte, A. M. (2017b). Quantification of heat losses through building envelope thermal bridges influenced by wind velocity using the outdoor infrared thermography technique. *Applied Energy*, *208*(September), 1038–1052. https://doi.org/10.1016/j.apenergy.2017.09.047

Papadopoulos, A. M. (2005). State of the art in thermal insulation materials and aims for future developments. *Energy and Buildings*, *37*(1), 77–86. https://doi.org/10.1016/j.enbuild.2004.05.006

Pi, Y., & Yu, T. (2015). The Manual of Low Energy Office Design. *Procedia Engineering*, *121*(2012), 1962–1968. https://doi.org/10.1016/j.proeng.2015.09.188

Porritt, S. M., Cropper, P. C., Shao, L., & Goodier, C. I. (2012). Ranking of interventions to reduce dwelling overheating during heat waves. *Energy and Buildings*, *55*, 16–27. https://doi.org/10.1016/j.enbuild.2012.01.043

Porritt, S., Shao, L., Cropper, P., & Goodier, C. (2011). Adapting dwellings for heat waves. *Sustainable Cities and Society*, *1*(2), 81–90. https://doi.org/10.1016/j.scs.2011.02.004

Prata, J., Simões, N., & Tadeu, A. (2018). Heat transfer measurements of a linear thermal bridge in a wooden building corner. *Energy and Buildings*, *158*, 194–208. https://doi.org/10.1016/j.enbuild.2017.09.073

Quinten, J., & Feldheim, V. (2016). Dynamic modelling of multidimensional thermal bridges in building envelopes: Review of existing methods, application and new mixed method. *Energy and Buildings*, *110*, 284–293. https://doi.org/10.1016/j.enbuild.2015.11.003

Rahman, M. M., Rasul, M. G., & Khan, M. M. K. (2010). Energy conservation measures in an institutional building in sub-tropical climate in Australia. *Applied Energy*, *87*(10), 2994–3004. https://doi.org/10.1016/j.apenergy.2010.04.005

Rahman, M., Rasul, M., & Khan, M. M. K. (2008). Energy conservation measures in an institutional building by dynamic simulation using DesignBuilder. *Proceedings of the*

3rd IASME/WSEAS International Conference on Energy & Environment (EE '08), Paper, *565–266*, 192–197.

Ramallo Gonzalez, A. P., Eames, M. E., & Coley, D. A. (2013). Lumped parameter models for building thermal modelling: An analytic approach to simplifying complex multi-layered constructions. *Energy and Buildings*, *60*, 174–184. https://doi.org/10.1016/j.enbuild.2013.01.014

Rodriguez Jara, E., Sanchez de la Flor, F. J., Allvarez Dominguez, S., Molina Felix, J. L., & Salmeron Lissen, J. M. (2016). A new analytical approach for simplified thermal modelling of buildings: Self-Adjusting RC-network model. *Energy and Buildings*, *130*, 85–97. https://doi.org/10.1016/j.enbuild.2016.08.039

Royapoor, M., & Roskilly, T. (2015). Building model calibration using energy and environmental data. *Energy and Buildings*, *94*, 109–120. https://doi.org/10.1016/j.enbuild.2015.02.050

Sarbu, I., & Sebarchievici, C. (2017). Solar Water and Space-Heating Systems. In *Solar Heating and Cooling Systems*. https://doi.org/10.1016/b978-0-12-811662-3.00005-0

Savastano, H., Santos, S. F., & Agopyan, V. (2009). Sustainability of vegetable fibres in construction. In *Sustainability of Construction Materials* (Issue c). Woodhead Publishing Limited. https://doi.org/10.1533/9781845695842.55

Schöck. (2015). *Thermal Bridging Guide*. *June*. http://www.schoeck.co.uk/upload/files/download/Thermal_Bridging_Guide_Schoeck_Isokorb_[5993].pdf

Shurcliff, W. A. (1988). Air-To-Air Heat-Exchangers for Houses. *Annual Review of Energy*, *13*(1), 1–22. https://doi.org/10.1146/annurev.eg.13.110188.000245

Sierra, F., Bai, J., & Maksoud, T. (2015). Impact of the simplification of the methodology used to assess the thermal bridge of the head of an opening. *Energy and Buildings*, *87*, 342–347. https://doi.org/10.1016/j.enbuild.2014.11.049

Sierra, Francisco, Gething, B., Bai, J., & Maksoud, T. (2017). Impact of the position of the window in the reveal of a cavity wall on the heat loss and the internal surface temperature of the head of an opening with a steel lintel. *Energy and Buildings*, *142*, 23–30. https://doi.org/10.1016/j.enbuild.2017.02.037

Stazi, F., Tomassoni, E., & Costanzo, D. P. (2017). Super insulated wooden envelopes in Mediterranean climate: Summer overheating, thermal comfort optimaization, environmental imapct on an Italian case study. *Energy and Buildings*, *138*, 716–732.

Tadeu, A., Simões, I., Simões, N., & Prata, J. (2011). Simulation of dynamic linear thermal bridges using a boundary element method model in the frequency domain. *Energy and Buildings*, *43*(12), 3685–3695. https://doi.org/10.1016/j.enbuild.2011.10.001

Taleb, H. M. (2014). Using passive cooling strategies to improve thermal performance and reduce energy consumption of residential buildings in U.A.E. buildings. *Frontiers of Architectural Research*, *3*(2), 154–165. https://doi.org/10.1016/j.foar.2014.01.002

Taleb, H. M., & Sharples, S. (2011). Developing sustainable residential buildings in Saudi Arabia: A case study. *Applied Energy*, *88*(1), 383–391. https://doi.org/10.1016/j.apenergy.2010.07.029

Taylor, T., Counsell, J., & Gill, S. (2014). Combining thermography and computer simulation to identify and assess insulation defects in the construction of building façades. *Energy and Buildings*, *76*, 130–142. https://doi.org/10.1016/j.enbuild.2014.02.080

Theodosiou, T. G., & Papadopoulos, A. M. (2008). The impact of thermal bridges on the energy demand of buildings with double brick wall constructions. *Energy and Buildings*, *40*(11), 2083–2089. https://doi.org/10.1016/j.enbuild.2008.06.006

Theodosiou, T., Tsikaloudaki, K., & Bikas, D. (2017). Analysis of the Thermal Bridging Effect on Ventilated Facades. *Procedia Environmental Sciences*, *38*, 397–404. https://doi.org/10.1016/j.proenv.2017.03.121

Theodosiou, Theodoros G., Tsikaloudaki, A. G., Kontoleon, K. J., & Bikas, D. K. (2015). Thermal bridging analysis on cladding systems for building facades. *Energy and Buildings*, *109*, 377–384. https://doi.org/10.1016/j.enbuild.2015.10.037

Thompson, M. K., & Thompson, J. M. (2017). Introduction to ANSYS and Finite Element Modeling. *ANSYS Mechanical APDL for Finite Element Analysis*, 1–9. https://doi.org/10.1016/B978-0-12-812981-4.00001-0

Totten, P. E., O'Brien, S. M., & Pazera, M. (2008). The Effects of Thermal Bridging at Interface Conditions. *Building Enclosure Science and Technology (BEST 1) Conference*, 12.

Tronchin, L., & Fabbri, K. (2008). Energy performance building evaluation in Mediterranean countries: Comparison between software simulations and operating rating simulation. *Energy and Buildings*, *40*(7), 1176–1187. https://doi.org/10.1016/j.enbuild.2007.10.012

Underwood, C. P. (2014). An improved lumped parameter method for building thermal modelling. *Energy and Buildings*, *79*, 191–201. https://doi.org/10.1016/j.enbuild.2014.05.001

Wang, H., & Zhai, Z. (John). (2016). Advances in building simulation and computational techniques: A review between 1987 and 2014. *Energy and Buildings*, *128*, 319–335. https://doi.org/10.1016/j.enbuild.2016.06.080

Wang, L., & Wong, N. H. (2008). Coupled simulations for naturally ventilated residential buildings. *Automation in Construction*, *17*(4), 386–398. https://doi.org/10.1016/j.autcon.2007.06.004

Wasilowski, H. a, & Reinhart, C. F. (2009). Modelling na Existing Building in Designbuilder / EnergyPlus Custom Versus Default Inputs. *Eleventh International IBPSA Conference*, 1252–1259.

Weerasuriya, A. U., Zhang, X., Gan, V. J. L., & Tan, Y. (2019). A holistic framework to utilize natural ventilation to optimize energy performance of residential high-rise buildings. In *Building and Environment* (Vol. 153, pp. 218–232). https://doi.org/10.1016/j.buildenv.2019.02.027

Wells, L., Rismanchi, B., & Aye, L. (2018). A review of Net Zero Energy Buildings with reflections on the Australian context. *Energy*, *158*, 616–628. https://doi.org/.1037//0033-2909.I26.1.78

World Metrological Organisation. (2018). *The State of the Global Climate in 2018*. *October*.

https://public.wmo.int/en/our-mandate/climate/wmo-statement-state-of-global-climate

Yang, L., Yan, H., & Lam, J. C. (2014). Thermal comfort and building energy consumption implications - A review. *Applied Energy*, *115*, 164–173. https://doi.org/10.1016/j.apenergy.2013.10.062

Yu, S., Cui, Y., Xu, X., & Feng, G. (2015). Impact of Civil Envelope on Energy Consumption based on EnergyPlus. *Procedia Engineering*, *121*, 1528–1534. https://doi.org/10.1016/j.proeng.2015.09.130

Zalewski, L., Lassue, S., Rousse, D., & Boukhalfa, K. (2010). Experimental and numerical characterization of thermal bridges in prefabricated building walls. *Energy Conversion and Management*, *51*(12), 2869–2877. https://doi.org/10.1016/j.enconman.2010.06.026

Zedan, M. F., Al-Sanea, S., Al-Mujahid, A., & Al-Suhaibani, Z. (2016). Effect of Thermal Bridges in Insulated Walls on Air-Conditioning Loads Using Whole Building Energy Analysis. *Sustainability (Switzerland)*, *8*(6), 1–20. https://doi.org/10.3390/su8060560

Zhai, Z. J., & Chen, Q. Y. (2005). Performance of coupled building energy and CFD simulations. *Energy and Buildings*, *37*(4), 333–344. https://doi.org/10.1016/j.enbuild.2004.07.001

Appendix A: Clifton Clubhouse Monitoring

This section provides results on the monitoring of Clifton clubhouse sports centre. Temperature and humidity of the clubhouse were monitored for a period of 1 year between July 2017 and July 2018. This period covered the winter and summer periods of the clubhouse. Log Tag Haxo 8 was used for the monitoring which stores up to 8000 sets of data. The sensors were programmed to record data at 15-20 minutes interval, and the software Log Tag Analyser was used to download the results. The analyser produces the results in the form of a report (in PDF format) and spread-sheet (in .csv format).

Three rooms were monitored in the clubhouse, namely the main-lounge (first floor), changing room five (first floor) and changing room three (ground-floor). In this section, sample results from the Log tag sensors and building plans are provided.

Appendix A1: Building Plan

First Floor Plan

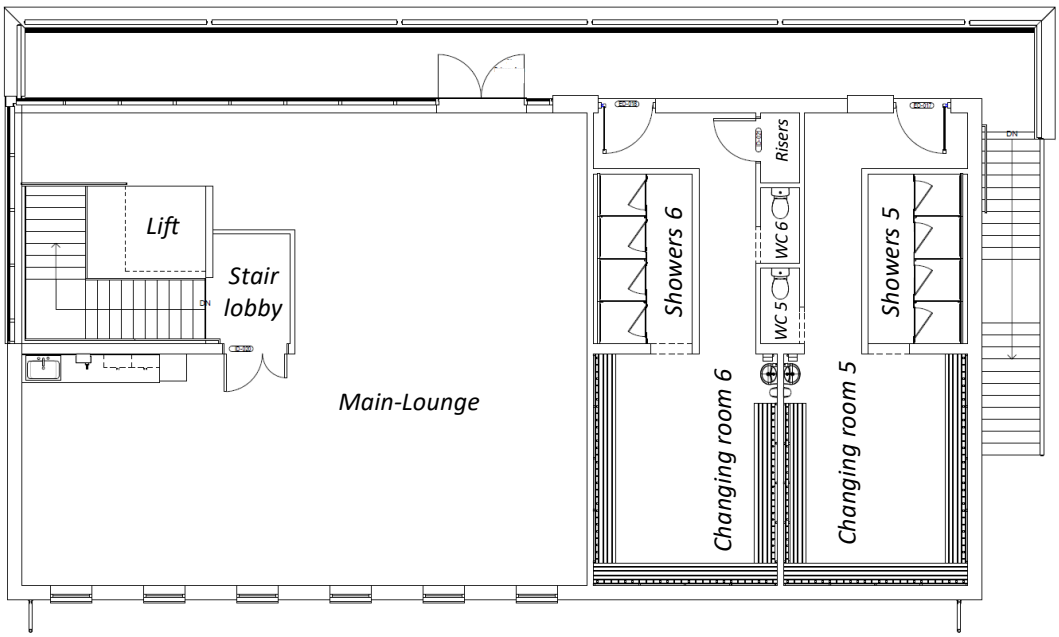

Ground Floor Plan

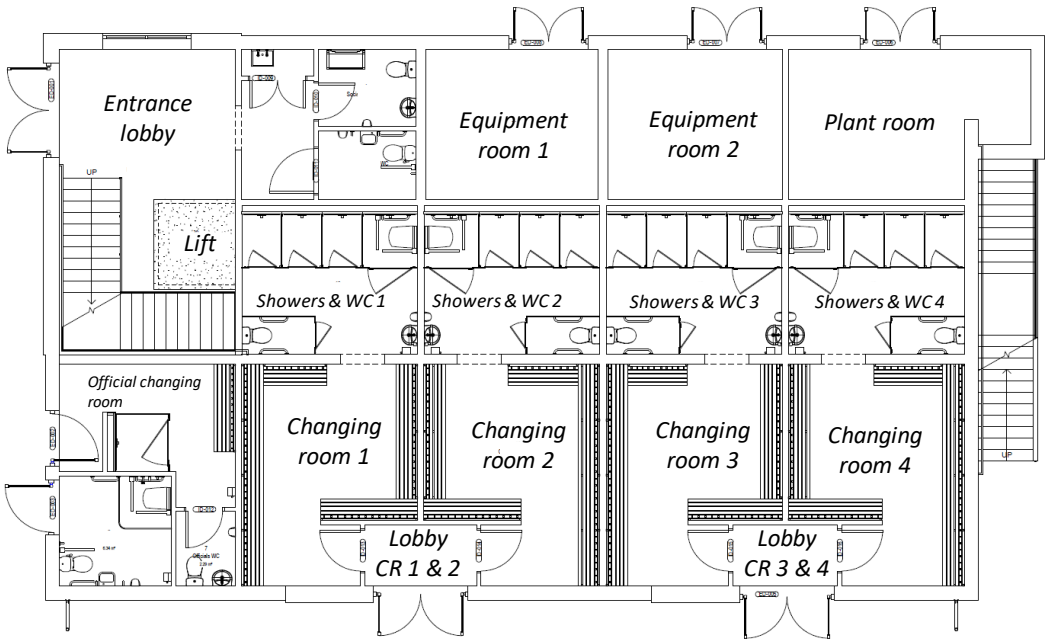

Appendix A2: Log Tag Results

LogTag

Recorder has been downloaded 26/07/2017 11:01:34 (UTC +00:00, daylight time)

Alarm Status

Low	OK
High	Fail

Recorder Info

Serial #: **1010095587** Model: **HAXO-8** Battery: **OK** Trip #: **1**

User ID: **5587**

Recorder Configuration

Start type: **Date/Time start**

Start delay: **None**

Interval: **15 Minutes**

Temperature alarms

Lower: **-18.9 °C after 2 Consecutive**

Humidity alarms

Lower: **0.0 %RH after 2 Consecutive**

Recorded Data

First reading: **01/07/2017 00:00:00**

Last reading: **26/07/2017 11:00:00**

Elapsed Time: **25 Days, 11 Hours** Total readings: **2445**

First evaluated: **01/07/2017 00:00:00**

Last evaluated: **26/07/2017 11:00:00**

Temperature statistics

Lowest: **22.3 °C**

@ 01/07/2017 05:15:00

Highest: **30.2 °C**

Humidity statistics

Lowest :**34.7 %RH**

@ 12/07/2017 19:15:00

Highest :**56.5 %RH**

Low Alarm

Temperature Triggered: **(none)**

Time below: **(none)**

High Alarm

Temperature Triggered: **@ 01/07/2017 00:15:00**

Time above: **25 Days, 11 Hours**

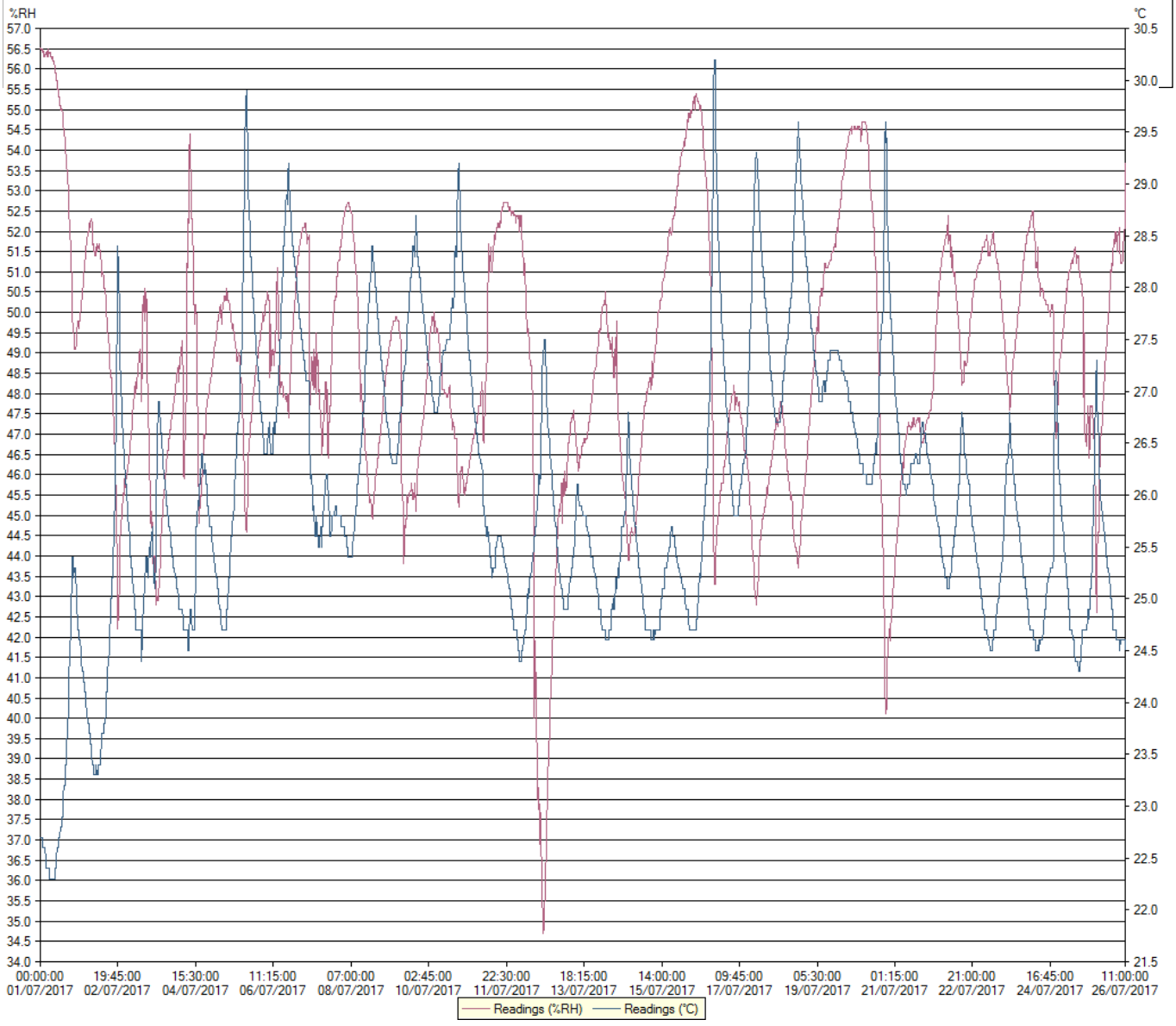

Chart

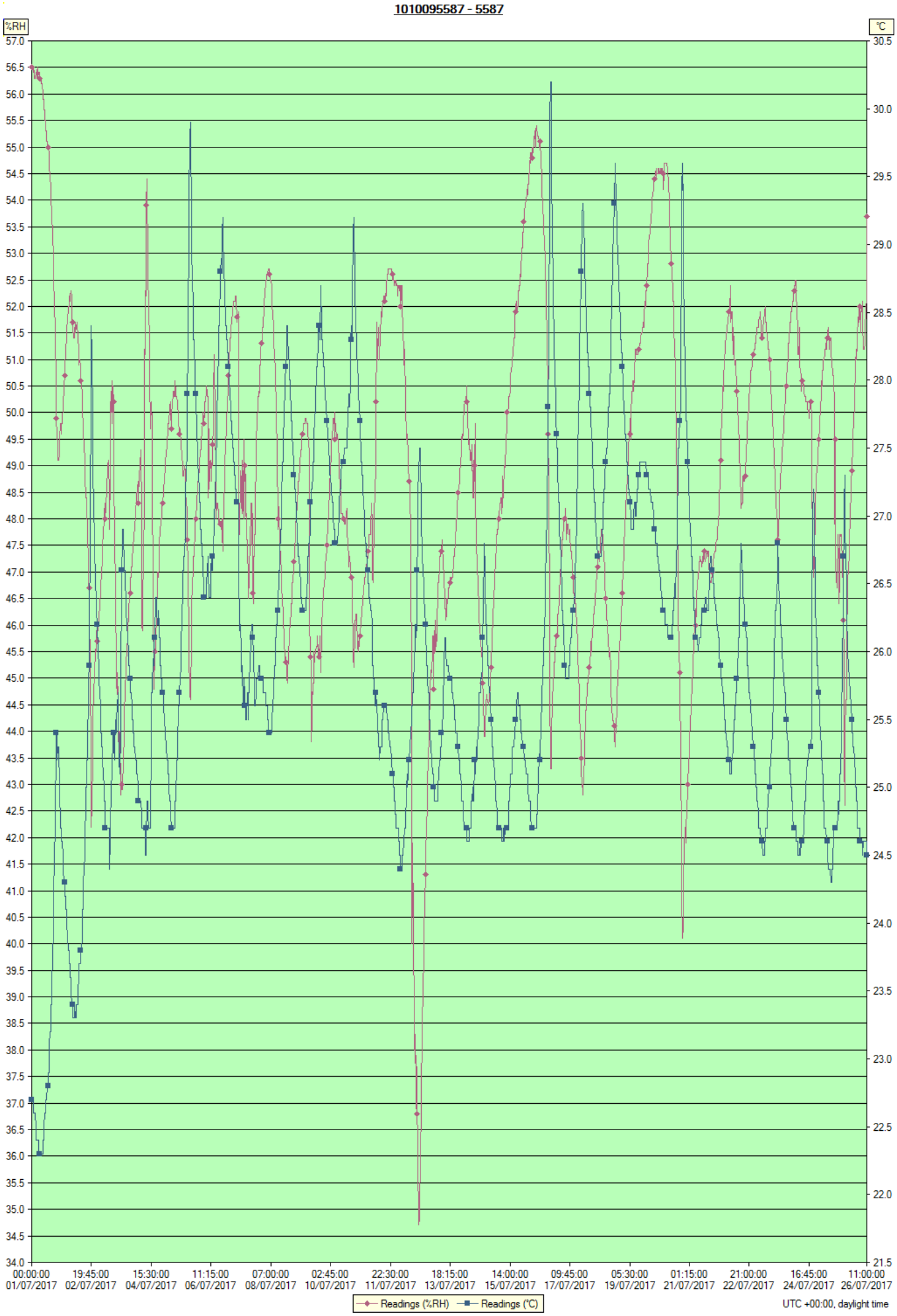
1010095587 - 5587
%RH
°C
57.0
56.5
56.0
55.5
55.0
54.5
54.0
53.5
53.0
52.5
52.0
51.5
51.0
50.5
50.0
49.5
49.0
48.5
48.0
47.5
47.0
46.5
46.0
45.5
45.0
44.5
44.0
43.5
43.0
42.5
42.0
41.5
41.0
40.5
40.0
39.5
39.0
38.5
38.0
37.5
37.0
36.5
36.0
35.5
35.0
34.5
34.0
30.5
30.0
29.5
29.0
28.5
28.0
27.5
27.0
26.5
26.0
25.5
25.0
24.5
24.0
23.5
23.0
22.5
22.0
21.5
00:00:00 01/07/2017
19:45:00 02/07/2017
15:30:00 04/07/2017
11:15:00 06/07/2017
07:00:00 08/07/2017
02:45:00 10/07/2017
22:30:00 11/07/2017
18:15:00 13/07/2017
14:00:00 15/07/2017
09:45:00 17/07/2017
05:30:00 19/07/2017
01:15:00 21/07/2017
21:00:00 22/07/2017
16:45:00 24/07/2017
11:00:00 26/07/2017
Readings (%RH)
Readings (°C)
UTC +00:00, daylight time

Index	Date	Time	%RH	°C
1	01/07/2017	00:00:00	56.5	22.7
2	01/07/2017	00:15:00	56.5	22.7
3	01/07/2017	00:30:00	56.5	22.7
4	01/07/2017	00:45:00	56.5	22.7
5	01/07/2017	01:00:00	56.4	22.7
6	01/07/2017	01:15:00	56.5	22.7
7	01/07/2017	01:30:00	56.5	22.6
8	01/07/2017	01:45:00	56.4	22.6
9	01/07/2017	02:00:00	56.3	22.6
10	01/07/2017	02:15:00	56.3	22.6
11	01/07/2017	02:30:00	56.3	22.6
12	01/07/2017	02:45:00	56.3	22.6
13	01/07/2017	03:00:00	56.4	22.5
14	01/07/2017	03:15:00	56.4	22.5
15	01/07/2017	03:30:00	56.4	22.4
16	01/07/2017	03:45:00	56.3	22.4
17	01/07/2017	04:00:00	56.4	22.4
18	01/07/2017	04:15:00	56.5	22.4
19	01/07/2017	04:30:00	56.5	22.4
20	01/07/2017	04:45:00	56.3	22.4
21	01/07/2017	05:00:00	56.4	22.4
22	01/07/2017	05:15:00	56.4	22.3
23	01/07/2017	05:30:00	56.4	22.3
24	01/07/2017	05:45:00	56.4	22.3
25	01/07/2017	06:00:00	56.3	22.3
26	01/07/2017	06:15:00	56.3	22.3
27	01/07/2017	06:30:00	56.3	22.3
28	01/07/2017	06:45:00	56.2	22.3
29	01/07/2017	07:00:00	56.3	22.3
30	01/07/2017	07:15:00	56.2	22.3
31	01/07/2017	07:30:00	56.2	22.3
32	01/07/2017	07:45:00	56.2	22.3
33	01/07/2017	08:00:00	56.0	22.3
34	01/07/2017	08:15:00	55.9	22.3
35	01/07/2017	08:30:00	55.9	22.4
36	01/07/2017	08:45:00	55.9	22.4
37	01/07/2017	09:00:00	55.9	22.4
38	01/07/2017	09:15:00	55.7	22.5
39	01/07/2017	09:30:00	55.7	22.6
40	01/07/2017	09:45:00	55.5	22.6
41	01/07/2017	10:00:00	55.5	22.6
42	01/07/2017	10:15:00	55.5	22.6
43	01/07/2017	10:30:00	55.3	22.7
44	01/07/2017	10:45:00	55.3	22.7
45	01/07/2017	11:00:00	55.2	22.7
46	01/07/2017	11:15:00	55.0	22.8
47	01/07/2017	11:30:00	55.1	22.8
48	01/07/2017	11:45:00	55.1	22.8
49	01/07/2017	12:00:00	55.0	22.8
50	01/07/2017	12:15:00	55.0	22.9
51	01/07/2017	12:30:00	54.9	22.9
52	01/07/2017	12:45:00	54.6	23.1
53	01/07/2017	13:00:00	54.6	23.1
54	01/07/2017	13:15:00	54.5	23.2
55	01/07/2017	13:30:00	54.4	23.2
56	01/07/2017	13:45:00	54.3	23.2
57	01/07/2017	14:00:00	54.2	23.3
58	01/07/2017	14:15:00	54.0	23.4
59	01/07/2017	14:30:00	53.8	23.4
60	01/07/2017	14:45:00	53.7	23.5
61	01/07/2017	15:00:00	53.6	23.6
62	01/07/2017	15:15:00	53.5	23.7
63	01/07/2017	15:30:00	53.3	23.8
64	01/07/2017	15:45:00	53.0	23.9
65	01/07/2017	16:00:00	52.7	24.1
66	01/07/2017	16:15:00	52.4	24.3
67	01/07/2017	16:30:00	52.2	24.4
68	01/07/2017	16:45:00	52.0	24.5
69	01/07/2017	17:00:00	51.6	24.7
70	01/07/2017	17:15:00	51.4	24.7
71	01/07/2017	17:30:00	51.2	24.9
72	01/07/2017	17:45:00	50.8	25.2
73	01/07/2017	18:00:00	49.9	25.4
74	01/07/2017	18:15:00	49.6	25.4
75	01/07/2017	18:30:00	49.5	25.3
76	01/07/2017	18:45:00	49.6	25.2
77	01/07/2017	19:00:00	49.4	25.3
78	01/07/2017	19:15:00	49.1	25.3
79	01/07/2017	19:30:00	49.1	25.3
80	01/07/2017	19:45:00	49.1	25.2
81	01/07/2017	20:00:00	49.1	25.2
82	01/07/2017	20:15:00	49.2	25.1
83	01/07/2017	20:30:00	49.5	25.0
84	01/07/2017	20:45:00	49.5	24.9
85	01/07/2017	21:00:00	49.8	24.8
86	01/07/2017	21:15:00	49.8	24.7
87	01/07/2017	21:30:00	49.6	24.7
88	01/07/2017	21:45:00	49.6	24.7
89	01/07/2017	22:00:00	49.8	24.6
90	01/07/2017	22:15:00	49.8	24.6
91	01/07/2017	22:30:00	49.9	24.6
92	01/07/2017	22:45:00	50.1	24.5
93	01/07/2017	23:00:00	50.2	24.4
94	01/07/2017	23:15:00	50.2	24.4
95	01/07/2017	23:30:00	50.4	24.3
96	01/07/2017	23:45:00	50.5	24.3
97	02/07/2017	00:00:00	50.7	24.3
98	02/07/2017	00:15:00	50.9	24.2
99	02/07/2017	00:30:00	50.9	24.2
100	02/07/2017	00:45:00	51.1	24.2
101	02/07/2017	01:00:00	51.2	24.1
102	02/07/2017	01:15:00	51.4	24.1
103	02/07/2017	01:30:00	51.5	24.1
104	02/07/2017	01:45:00	51.6	24.0
105	02/07/2017	02:00:00	51.7	23.9
106	02/07/2017	02:15:00	51.7	23.9
107	02/07/2017	02:30:00	51.8	23.9
108	02/07/2017	02:45:00	51.9	23.8
109	02/07/2017	03:00:00	52.0	23.8
110	02/07/2017	03:15:00	52.0	23.8
111	02/07/2017	03:30:00	52.1	23.7
112	02/07/2017	03:45:00	52.2	23.7
113	02/07/2017	04:00:00	52.1	23.7
114	02/07/2017	04:15:00	52.2	23.6
115	02/07/2017	04:30:00	52.3	23.6
116	02/07/2017	04:45:00	52.3	23.6
117	02/07/2017	05:00:00	52.3	23.5
118	02/07/2017	05:15:00	52.2	23.4
119	02/07/2017	05:30:00	51.7	23.4
120	02/07/2017	05:45:00	51.6	23.4
121	02/07/2017	06:00:00	51.7	23.4
122	02/07/2017	06:15:00	51.6	23.3
123	02/07/2017	06:30:00	51.4	23.3
124	02/07/2017	06:45:00	51.5	23.3
125	02/07/2017	07:00:00	51.4	23.3
126	02/07/2017	07:15:00	51.6	23.3
127	02/07/2017	07:30:00	51.5	23.4
128	02/07/2017	07:45:00	51.7	23.3
129	02/07/2017	08:00:00	51.5	23.3
130	02/07/2017	08:15:00	51.5	23.3
131	02/07/2017	08:30:00	51.6	23.3
132	02/07/2017	08:45:00	51.6	23.4
133	02/07/2017	09:00:00	51.7	23.4
134	02/07/2017	09:15:00	51.7	23.4
135	02/07/2017	09:30:00	51.6	23.4
136	02/07/2017	09:45:00	51.5	23.4
137	02/07/2017	10:00:00	51.4	23.5
138	02/07/2017	10:15:00	51.2	23.6
139	02/07/2017	10:30:00	50.9	23.6
140	02/07/2017	10:45:00	50.9	23.7
141	02/07/2017	11:00:00	51.0	23.7
142	02/07/2017	11:15:00	51.0	23.7
143	02/07/2017	11:30:00	50.9	23.7
144	02/07/2017	11:45:00	50.8	23.8
145	02/07/2017	12:00:00	50.6	23.8
146	02/07/2017	12:15:00	50.6	23.8
147	02/07/2017	12:30:00	50.5	23.8
148	02/07/2017	12:45:00	50.4	23.9
149	02/07/2017	13:00:00	50.2	24.0
150	02/07/2017	13:15:00	50.0	24.1
151	02/07/2017	13:30:00	49.8	24.1
152	02/07/2017	13:45:00	49.6	24.2
153	02/07/2017	14:00:00	49.6	24.3
154	02/07/2017	14:15:00	49.4	24.4

Index	Date	Time	%RH	°C
155	02/07/2017	14:30:00	49.3	24.4
156	02/07/2017	14:45:00	49.2	24.5
157	02/07/2017	15:00:00	49.1	24.6
158	02/07/2017	15:15:00	48.7	24.7
159	02/07/2017	15:30:00	48.5	24.8
160	02/07/2017	15:45:00	48.4	25.0
161	02/07/2017	16:00:00	48.4	25.0
162	02/07/2017	16:15:00	48.3	25.1
163	02/07/2017	16:30:00	48.1	25.2
164	02/07/2017	16:45:00	47.9	25.2
165	02/07/2017	17:00:00	47.6	25.4
166	02/07/2017	17:15:00	47.3	25.6
167	02/07/2017	17:30:00	46.9	25.8
168	02/07/2017	17:45:00	46.8	25.8
169	02/07/2017	18:00:00	46.7	25.9
170	02/07/2017	18:15:00	46.3	26.1
171	02/07/2017	18:30:00	46.0	26.3
172	02/07/2017	18:45:00	45.5	26.7
173	02/07/2017	19:00:00	44.8	27.2
174	02/07/2017	19:15:00	43.8	27.7
175	02/07/2017	19:30:00	42.9	28.2
176	02/07/2017	19:45:00	42.2	28.4
177	02/07/2017	20:00:00	42.6	28.2
178	02/07/2017	20:15:00	42.8	28.1
179	02/07/2017	20:30:00	43.3	27.8
180	02/07/2017	20:45:00	43.7	27.5
181	02/07/2017	21:00:00	44.2	27.3
182	02/07/2017	21:15:00	44.8	27.1
183	02/07/2017	21:30:00	44.8	27.0
184	02/07/2017	21:45:00	45.0	26.9
185	02/07/2017	22:00:00	45.1	26.8
186	02/07/2017	22:15:00	45.2	26.7
187	02/07/2017	22:30:00	45.4	26.6
188	02/07/2017	22:45:00	45.5	26.5
189	02/07/2017	23:00:00	45.6	26.4
190	02/07/2017	23:15:00	45.5	26.4
191	02/07/2017	23:30:00	45.9	26.3
192	02/07/2017	23:45:00	45.9	26.2
193	03/07/2017	00:00:00	45.7	26.2
194	03/07/2017	00:15:00	45.9	26.1
195	03/07/2017	00:30:00	45.9	26.1
196	03/07/2017	00:45:00	46.0	26.0
197	03/07/2017	01:00:00	46.1	25.9
198	03/07/2017	01:15:00	46.1	25.8
199	03/07/2017	01:30:00	46.2	25.8
200	03/07/2017	01:45:00	46.3	25.7
201	03/07/2017	02:00:00	46.4	25.7
202	03/07/2017	02:15:00	46.6	25.6
203	03/07/2017	02:30:00	46.6	25.5
204	03/07/2017	02:45:00	46.8	25.4
205	03/07/2017	03:00:00	46.9	25.4
206	03/07/2017	03:15:00	47.0	25.3
207	03/07/2017	03:30:00	47.2	25.3
208	03/07/2017	03:45:00	47.3	25.2
209	03/07/2017	04:00:00	47.5	25.2
210	03/07/2017	04:15:00	47.7	25.1
211	03/07/2017	04:30:00	47.8	25.1
212	03/07/2017	04:45:00	47.9	25.0
213	03/07/2017	05:00:00	48.0	25.0
214	03/07/2017	05:15:00	48.1	24.9
215	03/07/2017	05:30:00	48.3	24.9
216	03/07/2017	05:45:00	48.1	24.9
217	03/07/2017	06:00:00	48.0	24.7
218	03/07/2017	06:15:00	48.2	24.7
219	03/07/2017	06:30:00	48.3	24.7
220	03/07/2017	06:45:00	48.5	24.7
221	03/07/2017	07:00:00	48.6	24.7
222	03/07/2017	07:15:00	48.7	24.7
223	03/07/2017	07:30:00	48.8	24.7
224	03/07/2017	07:45:00	49.0	24.7
225	03/07/2017	08:00:00	49.1	24.7
226	03/07/2017	08:15:00	48.9	24.7
227	03/07/2017	08:30:00	48.9	24.7
228	03/07/2017	08:45:00	48.6	24.7
229	03/07/2017	09:00:00	47.8	24.4
230	03/07/2017	09:15:00	48.9	24.6
231	03/07/2017	09:30:00	49.5	24.7

Index	Date	Time	%RH	°C
232	03/07/2017	09:45:00	50.2	24.8
233	03/07/2017	10:00:00	50.0	24.9
234	03/07/2017	10:15:00	50.4	25.0
235	03/07/2017	10:30:00	50.4	25.1
236	03/07/2017	10:45:00	50.6	25.1
237	03/07/2017	11:00:00	49.8	25.2
238	03/07/2017	11:15:00	50.5	25.3
239	03/07/2017	11:30:00	50.0	25.4
240	03/07/2017	11:45:00	50.5	25.4
241	03/07/2017	12:00:00	50.2	25.4
242	03/07/2017	12:15:00	48.4	25.3
243	03/07/2017	12:30:00	48.1	25.2
244	03/07/2017	12:45:00	47.6	25.3
245	03/07/2017	13:00:00	47.6	25.3
246	03/07/2017	13:15:00	46.7	25.5
247	03/07/2017	13:30:00	46.4	25.4
248	03/07/2017	13:45:00	45.3	25.4
249	03/07/2017	14:00:00	44.9	25.4
250	03/07/2017	14:15:00	44.9	25.5
251	03/07/2017	14:30:00	44.7	25.6
252	03/07/2017	14:45:00	45.1	25.6
253	03/07/2017	15:00:00	44.6	25.7
254	03/07/2017	15:15:00	43.9	25.6
255	03/07/2017	15:30:00	43.9	25.5
256	03/07/2017	15:45:00	43.7	25.3
257	03/07/2017	16:00:00	44.0	25.2
258	03/07/2017	16:15:00	43.2	25.1
259	03/07/2017	16:30:00	43.5	25.2
260	03/07/2017	16:45:00	44.0	25.2
261	03/07/2017	17:00:00	42.8	25.3
262	03/07/2017	17:15:00	43.0	25.6
263	03/07/2017	17:30:00	43.1	26.0
264	03/07/2017	17:45:00	42.9	26.3
265	03/07/2017	18:00:00	43.0	26.6
266	03/07/2017	18:15:00	42.9	26.8
267	03/07/2017	18:30:00	42.9	26.9
268	03/07/2017	18:45:00	43.1	26.8
269	03/07/2017	19:00:00	43.3	26.9
270	03/07/2017	19:15:00	43.5	26.8
271	03/07/2017	19:30:00	43.9	26.7
272	03/07/2017	19:45:00	44.2	26.7
273	03/07/2017	20:00:00	44.4	26.6
274	03/07/2017	20:15:00	44.7	26.6
275	03/07/2017	20:30:00	44.9	26.5
276	03/07/2017	20:45:00	45.0	26.4
277	03/07/2017	21:00:00	45.1	26.4
278	03/07/2017	21:15:00	45.3	26.3
279	03/07/2017	21:30:00	45.5	26.2
280	03/07/2017	21:45:00	45.6	26.2
281	03/07/2017	22:00:00	45.7	26.1
282	03/07/2017	22:15:00	45.9	26.1
283	03/07/2017	22:30:00	46.0	26.1
284	03/07/2017	22:45:00	46.1	26.0
285	03/07/2017	23:00:00	46.2	26.0
286	03/07/2017	23:15:00	46.3	25.9
287	03/07/2017	23:30:00	46.5	25.9
288	03/07/2017	23:45:00	46.6	25.8
289	04/07/2017	00:00:00	46.6	25.8
290	04/07/2017	00:15:00	46.8	25.8
291	04/07/2017	00:30:00	46.9	25.7
292	04/07/2017	00:45:00	46.9	25.7
293	04/07/2017	01:00:00	47.1	25.7
294	04/07/2017	01:15:00	47.1	25.6
295	04/07/2017	01:30:00	47.2	25.6
296	04/07/2017	01:45:00	47.3	25.5
297	04/07/2017	02:00:00	47.4	25.5
298	04/07/2017	02:15:00	47.5	25.4
299	04/07/2017	02:30:00	47.6	25.4
300	04/07/2017	02:45:00	47.6	25.4
301	04/07/2017	03:00:00	47.7	25.3
302	04/07/2017	03:15:00	47.8	25.3
303	04/07/2017	03:30:00	47.9	25.3
304	04/07/2017	03:45:00	48.0	25.2
305	04/07/2017	04:00:00	48.1	25.2
306	04/07/2017	04:15:00	48.2	25.2
307	04/07/2017	04:30:00	48.3	25.2
308	04/07/2017	04:45:00	48.3	25.1

Index	Date	Time	%RH	°C
309	04/07/2017	05:00:00	48.5	25.1
310	04/07/2017	05:15:00	48.5	25.1
311	04/07/2017	05:30:00	48.6	25.1
312	04/07/2017	05:45:00	48.7	25.0
313	04/07/2017	06:00:00	48.3	24.9
314	04/07/2017	06:15:00	48.5	24.9
315	04/07/2017	06:30:00	48.7	24.9
316	04/07/2017	06:45:00	48.8	24.9
317	04/07/2017	07:00:00	49.0	24.9
318	04/07/2017	07:15:00	49.0	24.9
319	04/07/2017	07:30:00	49.1	24.9
320	04/07/2017	07:45:00	49.2	24.9
321	04/07/2017	08:00:00	49.3	24.9
322	04/07/2017	08:15:00	48.1	24.8
323	04/07/2017	08:30:00	46.2	24.7
324	04/07/2017	08:45:00	46.0	24.7
325	04/07/2017	09:00:00	45.9	24.7
326	04/07/2017	09:15:00	46.6	24.7
327	04/07/2017	09:30:00	47.1	24.7
328	04/07/2017	09:45:00	47.1	24.7
329	04/07/2017	10:00:00	47.3	24.7
330	04/07/2017	10:15:00	48.3	24.7
331	04/07/2017	10:30:00	49.3	24.7
332	04/07/2017	10:45:00	51.2	24.7
333	04/07/2017	11:00:00	51.1	24.7
334	04/07/2017	11:15:00	52.3	24.5
335	04/07/2017	11:30:00	52.2	24.5
336	04/07/2017	11:45:00	52.9	24.6
337	04/07/2017	12:00:00	53.9	24.7
338	04/07/2017	12:15:00	54.4	24.8
339	04/07/2017	12:30:00	53.9	24.9
340	04/07/2017	12:45:00	53.2	24.9
341	04/07/2017	13:00:00	52.9	24.9
342	04/07/2017	13:15:00	52.9	24.8
343	04/07/2017	13:30:00	51.7	24.7
344	04/07/2017	13:45:00	52.3	24.7
345	04/07/2017	14:00:00	51.0	24.7
346	04/07/2017	14:15:00	50.2	24.7
347	04/07/2017	14:30:00	50.5	24.7
348	04/07/2017	14:45:00	49.9	24.7
349	04/07/2017	15:00:00	49.7	24.9
350	04/07/2017	15:15:00	50.2	25.2
351	04/07/2017	15:30:00	50.0	25.4
352	04/07/2017	15:45:00	50.1	25.7
353	04/07/2017	16:00:00	49.9	25.7
354	04/07/2017	16:15:00	48.2	25.8
355	04/07/2017	16:30:00	48.5	25.8
356	04/07/2017	16:45:00	46.9	25.9
357	04/07/2017	17:00:00	45.9	25.9
358	04/07/2017	17:15:00	45.5	26.0
359	04/07/2017	17:30:00	45.1	25.9
360	04/07/2017	17:45:00	44.8	26.1
361	04/07/2017	18:00:00	45.5	26.1
362	04/07/2017	18:15:00	45.4	26.1
363	04/07/2017	18:30:00	45.5	26.4
364	04/07/2017	18:45:00	45.5	26.4
365	04/07/2017	19:00:00	45.8	26.4
366	04/07/2017	19:15:00	46.1	26.4
367	04/07/2017	19:30:00	46.4	26.3
368	04/07/2017	19:45:00	46.6	26.2
369	04/07/2017	20:00:00	46.8	26.2
370	04/07/2017	20:15:00	47.0	26.2
371	04/07/2017	20:30:00	46.9	26.2
372	04/07/2017	20:45:00	46.9	26.3
373	04/07/2017	21:00:00	47.1	26.2
374	04/07/2017	21:15:00	47.4	26.2
375	04/07/2017	21:30:00	47.6	26.1
376	04/07/2017	21:45:00	47.7	26.1
377	04/07/2017	22:00:00	47.8	26.0
378	04/07/2017	22:15:00	47.8	25.9
379	04/07/2017	22:30:00	47.9	25.9
380	04/07/2017	22:45:00	48.0	25.8
381	04/07/2017	23:00:00	48.0	25.8
382	04/07/2017	23:15:00	48.0	25.8
383	04/07/2017	23:30:00	48.2	25.7
384	04/07/2017	23:45:00	48.3	25.7
385	05/07/2017	00:00:00	48.3	25.7

Index	Date	Time	%RH	°C
386	05/07/2017	00:15:00	48.5	25.7
387	05/07/2017	00:30:00	48.6	25.6
388	05/07/2017	00:45:00	48.6	25.6
389	05/07/2017	01:00:00	48.7	25.5
390	05/07/2017	01:15:00	48.8	25.5
391	05/07/2017	01:30:00	48.9	25.4
392	05/07/2017	01:45:00	49.0	25.4
393	05/07/2017	02:00:00	49.1	25.4
394	05/07/2017	02:15:00	49.2	25.3
395	05/07/2017	02:30:00	49.2	25.3
396	05/07/2017	02:45:00	49.4	25.2
397	05/07/2017	03:00:00	49.5	25.2
398	05/07/2017	03:15:00	49.5	25.2
399	05/07/2017	03:30:00	49.6	25.2
400	05/07/2017	03:45:00	49.7	25.1
401	05/07/2017	04:00:00	49.8	25.1
402	05/07/2017	04:15:00	49.8	25.1
403	05/07/2017	04:30:00	49.9	25.0
404	05/07/2017	04:45:00	50.0	24.9
405	05/07/2017	05:00:00	50.1	24.9
406	05/07/2017	05:15:00	50.1	24.9
407	05/07/2017	05:30:00	50.2	24.9
408	05/07/2017	05:45:00	50.0	24.8
409	05/07/2017	06:00:00	49.7	24.7
410	05/07/2017	06:15:00	49.8	24.7
411	05/07/2017	06:30:00	50.0	24.7
412	05/07/2017	06:45:00	50.1	24.7
413	05/07/2017	07:00:00	50.2	24.7
414	05/07/2017	07:15:00	50.3	24.7
415	05/07/2017	07:30:00	50.3	24.7
416	05/07/2017	07:45:00	50.4	24.7
417	05/07/2017	08:00:00	50.3	24.7
418	05/07/2017	08:15:00	50.4	24.7
419	05/07/2017	08:30:00	50.4	24.7
420	05/07/2017	08:45:00	50.3	24.8
421	05/07/2017	09:00:00	50.6	24.9
422	05/07/2017	09:15:00	50.4	24.9
423	05/07/2017	09:30:00	50.4	24.9
424	05/07/2017	09:45:00	50.3	25.0
425	05/07/2017	10:00:00	50.3	25.1
426	05/07/2017	10:15:00	50.3	25.2
427	05/07/2017	10:30:00	50.2	25.2
428	05/07/2017	10:45:00	50.2	25.3
429	05/07/2017	11:00:00	50.1	25.4
430	05/07/2017	11:15:00	50.0	25.5
431	05/07/2017	11:30:00	49.8	25.6
432	05/07/2017	11:45:00	49.7	25.6
433	05/07/2017	12:00:00	49.6	25.7
434	05/07/2017	12:15:00	49.6	25.7
435	05/07/2017	12:30:00	49.7	25.8
436	05/07/2017	12:45:00	49.6	25.8
437	05/07/2017	13:00:00	49.5	25.9
438	05/07/2017	13:15:00	49.5	26.0
439	05/07/2017	13:30:00	49.4	26.1
440	05/07/2017	13:45:00	49.2	26.2
441	05/07/2017	14:00:00	49.2	26.3
442	05/07/2017	14:15:00	49.0	26.4
443	05/07/2017	14:30:00	48.9	26.5
444	05/07/2017	14:45:00	48.8	26.6
445	05/07/2017	15:00:00	48.8	26.6
446	05/07/2017	15:15:00	48.8	26.7
447	05/07/2017	15:30:00	48.8	26.7
448	05/07/2017	15:45:00	49.0	26.7
449	05/07/2017	16:00:00	49.0	26.7
450	05/07/2017	16:15:00	48.9	26.9
451	05/07/2017	16:30:00	48.7	27.0
452	05/07/2017	16:45:00	48.4	27.2
453	05/07/2017	17:00:00	48.3	27.3
454	05/07/2017	17:15:00	48.4	27.3
455	05/07/2017	17:30:00	48.1	27.5
456	05/07/2017	17:45:00	47.9	27.7
457	05/07/2017	18:00:00	47.6	27.9
458	05/07/2017	18:15:00	47.2	28.2
459	05/07/2017	18:30:00	46.6	28.6
460	05/07/2017	18:45:00	46.1	28.9
461	05/07/2017	19:00:00	45.6	29.2
462	05/07/2017	19:15:00	45.2	29.4

Index	Date	Time	%RH	°C
463	05/07/2017	19:30:00	45.0	29.7
464	05/07/2017	19:45:00	44.8	29.8
465	05/07/2017	20:00:00	44.7	29.8
466	05/07/2017	20:15:00	44.6	29.9
467	05/07/2017	20:30:00	45.0	29.6
468	05/07/2017	20:45:00	45.4	29.4
469	05/07/2017	21:00:00	45.9	29.1
470	05/07/2017	21:15:00	46.5	28.9
471	05/07/2017	21:30:00	46.6	28.8
472	05/07/2017	21:45:00	46.8	28.7
473	05/07/2017	22:00:00	47.0	28.6
474	05/07/2017	22:15:00	47.2	28.4
475	05/07/2017	22:30:00	47.3	28.3
476	05/07/2017	22:45:00	47.3	28.3
477	05/07/2017	23:00:00	47.5	28.2
478	05/07/2017	23:15:00	47.6	28.1
479	05/07/2017	23:30:00	47.7	28.0
480	05/07/2017	23:45:00	47.9	27.9
481	06/07/2017	00:00:00	48.0	27.9
482	06/07/2017	00:15:00	48.1	27.8
483	06/07/2017	00:30:00	48.2	27.7
484	06/07/2017	00:45:00	48.3	27.7
485	06/07/2017	01:00:00	48.4	27.6
486	06/07/2017	01:15:00	48.5	27.5
487	06/07/2017	01:30:00	48.6	27.5
488	06/07/2017	01:45:00	48.7	27.4
489	06/07/2017	02:00:00	48.7	27.3
490	06/07/2017	02:15:00	48.8	27.3
491	06/07/2017	02:30:00	48.9	27.2
492	06/07/2017	02:45:00	49.0	27.2
493	06/07/2017	03:00:00	49.1	27.1
494	06/07/2017	03:15:00	49.2	27.1
495	06/07/2017	03:30:00	49.3	26.9
496	06/07/2017	03:45:00	49.3	26.9
497	06/07/2017	04:00:00	49.4	26.8
498	06/07/2017	04:15:00	49.5	26.8
499	06/07/2017	04:30:00	49.6	26.8
500	06/07/2017	04:45:00	49.7	26.7
501	06/07/2017	05:00:00	49.8	26.7
502	06/07/2017	05:15:00	49.9	26.6
503	06/07/2017	05:30:00	50.0	26.6
504	06/07/2017	05:45:00	49.9	26.5
505	06/07/2017	06:00:00	49.8	26.4
506	06/07/2017	06:15:00	50.0	26.4
507	06/07/2017	06:30:00	50.0	26.4
508	06/07/2017	06:45:00	50.2	26.4
509	06/07/2017	07:00:00	50.2	26.4
510	06/07/2017	07:15:00	50.2	26.4
511	06/07/2017	07:30:00	50.2	26.4
512	06/07/2017	07:45:00	50.4	26.4
513	06/07/2017	08:00:00	50.5	26.5
514	06/07/2017	08:15:00	50.4	26.6
515	06/07/2017	08:30:00	50.4	26.6
516	06/07/2017	08:45:00	50.3	26.6
517	06/07/2017	09:00:00	50.3	26.7
518	06/07/2017	09:15:00	48.4	26.6
519	06/07/2017	09:30:00	48.7	26.4
520	06/07/2017	09:45:00	49.7	26.4
521	06/07/2017	10:00:00	49.5	26.4
522	06/07/2017	10:15:00	48.7	26.4
523	06/07/2017	10:30:00	49.0	26.4
524	06/07/2017	10:45:00	49.0	26.4
525	06/07/2017	11:00:00	49.1	26.6
526	06/07/2017	11:15:00	49.1	26.6
527	06/07/2017	11:30:00	48.8	26.7
528	06/07/2017	11:45:00	48.7	26.6
529	06/07/2017	12:00:00	49.4	26.7
530	06/07/2017	12:15:00	49.0	26.6
531	06/07/2017	12:30:00	49.4	26.7
532	06/07/2017	12:45:00	49.7	26.7
533	06/07/2017	13:00:00	50.3	26.7
534	06/07/2017	13:15:00	50.4	26.8
535	06/07/2017	13:30:00	51.1	26.9
536	06/07/2017	13:45:00	50.7	27.0
537	06/07/2017	14:00:00	50.2	27.1
538	06/07/2017	14:15:00	50.4	27.1
539	06/07/2017	14:30:00	49.8	27.2

Index	Date	Time	%RH	°C
540	06/07/2017	14:45:00	48.8	27.3
541	06/07/2017	15:00:00	48.0	27.4
542	06/07/2017	15:15:00	48.3	27.6
543	06/07/2017	15:30:00	48.3	27.7
544	06/07/2017	15:45:00	48.3	27.8
545	06/07/2017	16:00:00	48.3	27.9
546	06/07/2017	16:15:00	48.3	28.0
547	06/07/2017	16:30:00	48.1	28.2
548	06/07/2017	16:45:00	47.9	28.4
549	06/07/2017	17:00:00	48.0	28.4
550	06/07/2017	17:15:00	48.0	28.4
551	06/07/2017	17:30:00	48.0	28.5
552	06/07/2017	17:45:00	47.9	28.7
553	06/07/2017	18:00:00	47.9	28.8
554	06/07/2017	18:15:00	47.9	28.8
555	06/07/2017	18:30:00	47.8	28.9
556	06/07/2017	18:45:00	47.8	28.9
557	06/07/2017	19:00:00	47.9	28.9
558	06/07/2017	19:15:00	48.0	28.8
559	06/07/2017	19:30:00	47.7	29.1
560	06/07/2017	19:45:00	47.4	29.2
561	06/07/2017	20:00:00	47.6	29.1
562	06/07/2017	20:15:00	47.8	29.0
563	06/07/2017	20:30:00	48.2	28.9
564	06/07/2017	20:45:00	48.4	28.8
565	06/07/2017	21:00:00	48.6	28.7
566	06/07/2017	21:15:00	48.7	28.7
567	06/07/2017	21:30:00	49.0	28.6
568	06/07/2017	21:45:00	49.4	28.5
569	06/07/2017	22:00:00	49.5	28.4
570	06/07/2017	22:15:00	49.6	28.4
571	06/07/2017	22:30:00	49.8	28.4
572	06/07/2017	22:45:00	49.9	28.3
573	06/07/2017	23:00:00	50.1	28.3
574	06/07/2017	23:15:00	50.2	28.2
575	06/07/2017	23:30:00	50.4	28.2
576	06/07/2017	23:45:00	50.5	28.1
577	07/07/2017	00:00:00	50.7	28.1
578	07/07/2017	00:15:00	50.8	28.1
579	07/07/2017	00:30:00	51.0	28.0
580	07/07/2017	00:45:00	51.1	28.0
581	07/07/2017	01:00:00	51.2	27.9
582	07/07/2017	01:15:00	51.4	27.9
583	07/07/2017	01:30:00	51.4	27.8
584	07/07/2017	01:45:00	51.5	27.8
585	07/07/2017	02:00:00	51.6	27.7
586	07/07/2017	02:15:00	51.7	27.7
587	07/07/2017	02:30:00	51.7	27.6
588	07/07/2017	02:45:00	51.9	27.6
589	07/07/2017	03:00:00	51.9	27.6
590	07/07/2017	03:15:00	52.0	27.5
591	07/07/2017	03:30:00	52.0	27.5
592	07/07/2017	03:45:00	52.1	27.4
593	07/07/2017	04:00:00	52.1	27.4
594	07/07/2017	04:15:00	52.1	27.3
595	07/07/2017	04:30:00	52.1	27.3
596	07/07/2017	04:45:00	52.1	27.3
597	07/07/2017	05:00:00	52.2	27.2
598	07/07/2017	05:15:00	52.2	27.2
599	07/07/2017	05:30:00	52.2	27.2
600	07/07/2017	05:45:00	52.1	27.1
601	07/07/2017	06:00:00	51.8	27.1
602	07/07/2017	06:15:00	51.7	27.1
603	07/07/2017	06:30:00	51.8	27.1
604	07/07/2017	06:45:00	51.8	27.1
605	07/07/2017	07:00:00	51.8	27.1
606	07/07/2017	07:15:00	51.9	27.1
607	07/07/2017	07:30:00	50.0	26.9
608	07/07/2017	07:45:00	47.4	26.6
609	07/07/2017	08:00:00	48.0	26.2
610	07/07/2017	08:15:00	48.1	26.2
611	07/07/2017	08:30:00	48.5	26.1
612	07/07/2017	08:45:00	48.9	26.2
613	07/07/2017	09:00:00	48.8	26.2
614	07/07/2017	09:15:00	48.8	26.0
615	07/07/2017	09:30:00	48.2	25.9
616	07/07/2017	09:45:00	49.1	25.8

Index	Date	Time	%RH	°C
617	07/07/2017	10:00:00	48.1	25.8
618	07/07/2017	10:15:00	48.7	25.9
619	07/07/2017	10:30:00	48.9	25.6
620	07/07/2017	10:45:00	48.3	25.7
621	07/07/2017	11:00:00	48.0	25.6
622	07/07/2017	11:15:00	49.5	25.8
623	07/07/2017	11:30:00	48.9	25.8
624	07/07/2017	11:45:00	48.7	25.7
625	07/07/2017	12:00:00	49.0	25.6
626	07/07/2017	12:15:00	48.9	25.6
627	07/07/2017	12:30:00	48.8	25.6
628	07/07/2017	12:45:00	48.1	25.5
629	07/07/2017	13:00:00	48.0	25.5
630	07/07/2017	13:15:00	48.1	25.6
631	07/07/2017	13:30:00	47.8	25.6
632	07/07/2017	13:45:00	47.4	25.6
633	07/07/2017	14:00:00	47.6	25.7
634	07/07/2017	14:15:00	46.7	25.6
635	07/07/2017	14:30:00	46.5	25.5
636	07/07/2017	14:45:00	46.9	25.7
637	07/07/2017	15:00:00	46.7	25.7
638	07/07/2017	15:15:00	46.9	25.8
639	07/07/2017	15:30:00	47.7	25.9
640	07/07/2017	15:45:00	47.5	25.9
641	07/07/2017	16:00:00	47.7	26.0
642	07/07/2017	16:15:00	48.0	26.0
643	07/07/2017	16:30:00	48.3	26.1
644	07/07/2017	16:45:00	48.3	26.2
645	07/07/2017	17:00:00	48.0	26.2
646	07/07/2017	17:15:00	47.5	26.2
647	07/07/2017	17:30:00	48.1	26.2
648	07/07/2017	17:45:00	47.5	26.2
649	07/07/2017	18:00:00	46.6	26.1
650	07/07/2017	18:15:00	46.4	26.0
651	07/07/2017	18:30:00	47.1	25.9
652	07/07/2017	18:45:00	47.5	25.8
653	07/07/2017	19:00:00	47.3	25.8
654	07/07/2017	19:15:00	47.7	25.6
655	07/07/2017	19:30:00	47.7	25.6
656	07/07/2017	19:45:00	48.2	25.6
657	07/07/2017	20:00:00	49.2	25.7
658	07/07/2017	20:15:00	49.6	25.7
659	07/07/2017	20:30:00	49.6	25.8
660	07/07/2017	20:45:00	49.7	25.8
661	07/07/2017	21:00:00	49.9	25.8
662	07/07/2017	21:15:00	50.1	25.8
663	07/07/2017	21:30:00	50.1	25.8
664	07/07/2017	21:45:00	50.2	25.8
665	07/07/2017	22:00:00	50.4	25.9
666	07/07/2017	22:15:00	50.3	25.9
667	07/07/2017	22:30:00	50.4	25.9
668	07/07/2017	22:45:00	50.5	25.9
669	07/07/2017	23:00:00	50.9	25.8
670	07/07/2017	23:15:00	50.9	25.8
671	07/07/2017	23:30:00	51.0	25.8
672	07/07/2017	23:45:00	51.2	25.8
673	08/07/2017	00:00:00	51.3	25.8
674	08/07/2017	00:15:00	51.3	25.8
675	08/07/2017	00:30:00	51.3	25.8
676	08/07/2017	00:45:00	51.3	25.8
677	08/07/2017	01:00:00	51.6	25.8
678	08/07/2017	01:15:00	51.6	25.8
679	08/07/2017	01:30:00	51.7	25.7
680	08/07/2017	01:45:00	51.9	25.7
681	08/07/2017	02:00:00	51.9	25.7
682	08/07/2017	02:15:00	52.1	25.7
683	08/07/2017	02:30:00	52.2	25.7
684	08/07/2017	02:45:00	52.3	25.7
685	08/07/2017	03:00:00	52.4	25.7
686	08/07/2017	03:15:00	52.5	25.6
687	08/07/2017	03:30:00	52.5	25.6
688	08/07/2017	03:45:00	52.5	25.6
689	08/07/2017	04:00:00	52.6	25.6
690	08/07/2017	04:15:00	52.6	25.6
691	08/07/2017	04:30:00	52.6	25.6
692	08/07/2017	04:45:00	52.6	25.5
693	08/07/2017	05:00:00	52.7	25.5

Index	Date	Time	%RH	°C
694	08/07/2017	05:15:00	52.7	25.5
695	08/07/2017	05:30:00	52.7	25.4
696	08/07/2017	05:45:00	52.7	25.4
697	08/07/2017	06:00:00	52.6	25.4
698	08/07/2017	06:15:00	52.6	25.4
699	08/07/2017	06:30:00	52.6	25.4
700	08/07/2017	06:45:00	52.5	25.4
701	08/07/2017	07:00:00	52.5	25.4
702	08/07/2017	07:15:00	52.5	25.4
703	08/07/2017	07:30:00	52.4	25.4
704	08/07/2017	07:45:00	52.2	25.5
705	08/07/2017	08:00:00	52.0	25.5
706	08/07/2017	08:15:00	51.9	25.6
707	08/07/2017	08:30:00	51.8	25.6
708	08/07/2017	08:45:00	51.7	25.7
709	08/07/2017	09:00:00	51.5	25.7
710	08/07/2017	09:15:00	51.3	25.8
711	08/07/2017	09:30:00	51.1	25.8
712	08/07/2017	09:45:00	51.0	25.9
713	08/07/2017	10:00:00	50.9	25.9
714	08/07/2017	10:15:00	50.7	26.0
715	08/07/2017	10:30:00	50.5	26.1
716	08/07/2017	10:45:00	50.3	26.1
717	08/07/2017	11:00:00	50.2	26.1
718	08/07/2017	11:15:00	50.1	26.2
719	08/07/2017	11:30:00	49.1	26.2
720	08/07/2017	11:45:00	49.2	26.3
721	08/07/2017	12:00:00	48.0	26.3
722	08/07/2017	12:15:00	47.8	26.4
723	08/07/2017	12:30:00	48.4	26.4
724	08/07/2017	12:45:00	48.1	26.5
725	08/07/2017	13:00:00	47.9	26.6
726	08/07/2017	13:15:00	47.8	26.6
727	08/07/2017	13:30:00	47.6	26.7
728	08/07/2017	13:45:00	47.4	26.8
729	08/07/2017	14:00:00	47.4	26.8
730	08/07/2017	14:15:00	47.2	26.9
731	08/07/2017	14:30:00	47.1	26.9
732	08/07/2017	14:45:00	46.9	27.1
733	08/07/2017	15:00:00	46.7	27.2
734	08/07/2017	15:15:00	46.5	27.3
735	08/07/2017	15:30:00	46.4	27.4
736	08/07/2017	15:45:00	46.3	27.4
737	08/07/2017	16:00:00	46.0	27.5
738	08/07/2017	16:15:00	46.0	27.6
739	08/07/2017	16:30:00	45.9	27.7
740	08/07/2017	16:45:00	45.8	27.7
741	08/07/2017	17:00:00	45.7	27.8
742	08/07/2017	17:15:00	45.4	27.9
743	08/07/2017	17:30:00	45.3	28.0
744	08/07/2017	17:45:00	45.3	28.1
745	08/07/2017	18:00:00	45.3	28.1
746	08/07/2017	18:15:00	45.4	28.1
747	08/07/2017	18:30:00	45.2	28.2
748	08/07/2017	18:45:00	45.0	28.4
749	08/07/2017	19:00:00	44.9	28.4
750	08/07/2017	19:15:00	45.1	28.3
751	08/07/2017	19:30:00	45.2	28.3
752	08/07/2017	19:45:00	45.3	28.2
753	08/07/2017	20:00:00	45.5	28.2
754	08/07/2017	20:15:00	45.7	28.1
755	08/07/2017	20:30:00	45.7	28.1
756	08/07/2017	20:45:00	45.9	28.0
757	08/07/2017	21:00:00	46.0	28.0
758	08/07/2017	21:15:00	46.1	27.9
759	08/07/2017	21:30:00	46.2	27.8
760	08/07/2017	21:45:00	46.3	27.8
761	08/07/2017	22:00:00	46.4	27.7
762	08/07/2017	22:15:00	46.4	27.7
763	08/07/2017	22:30:00	46.6	27.6
764	08/07/2017	22:45:00	46.8	27.6
765	08/07/2017	23:00:00	46.8	27.5
766	08/07/2017	23:15:00	46.9	27.5
767	08/07/2017	23:30:00	47.0	27.4
768	08/07/2017	23:45:00	47.1	27.4
769	09/07/2017	00:00:00	47.2	27.3
770	09/07/2017	00:15:00	47.3	27.3

Index	Date	Time	%RH	°C
771	09/07/2017	00:30:00	47.4	27.2
772	09/07/2017	00:45:00	47.7	27.2
773	09/07/2017	01:00:00	47.8	27.1
774	09/07/2017	01:15:00	47.9	27.1
775	09/07/2017	01:30:00	48.0	27.1
776	09/07/2017	01:45:00	48.1	27.0
777	09/07/2017	02:00:00	48.2	26.9
778	09/07/2017	02:15:00	48.3	26.9
779	09/07/2017	02:30:00	48.4	26.8
780	09/07/2017	02:45:00	48.5	26.8
781	09/07/2017	03:00:00	48.5	26.8
782	09/07/2017	03:15:00	48.7	26.7
783	09/07/2017	03:30:00	48.7	26.7
784	09/07/2017	03:45:00	48.8	26.7
785	09/07/2017	04:00:00	48.9	26.6
786	09/07/2017	04:15:00	49.0	26.6
787	09/07/2017	04:30:00	49.1	26.6
788	09/07/2017	04:45:00	49.2	26.5
789	09/07/2017	05:00:00	49.3	26.4
790	09/07/2017	05:15:00	49.3	26.4
791	09/07/2017	05:30:00	49.4	26.4
792	09/07/2017	05:45:00	49.5	26.4
793	09/07/2017	06:00:00	49.6	26.3
794	09/07/2017	06:15:00	49.6	26.3
795	09/07/2017	06:30:00	49.7	26.3
796	09/07/2017	06:45:00	49.8	26.3
797	09/07/2017	07:00:00	49.8	26.3
798	09/07/2017	07:15:00	49.8	26.3
799	09/07/2017	07:30:00	49.8	26.3
800	09/07/2017	07:45:00	49.8	26.3
801	09/07/2017	08:00:00	49.8	26.3
802	09/07/2017	08:15:00	49.9	26.3
803	09/07/2017	08:30:00	49.9	26.3
804	09/07/2017	08:45:00	49.9	26.4
805	09/07/2017	09:00:00	49.9	26.4
806	09/07/2017	09:15:00	49.8	26.4
807	09/07/2017	09:30:00	49.8	26.4
808	09/07/2017	09:45:00	49.8	26.6
809	09/07/2017	10:00:00	49.7	26.6
810	09/07/2017	10:15:00	49.6	26.7
811	09/07/2017	10:30:00	49.5	26.7
812	09/07/2017	10:45:00	49.4	26.8
813	09/07/2017	11:00:00	49.3	26.8
814	09/07/2017	11:15:00	47.6	26.8
815	09/07/2017	11:30:00	45.9	26.8
816	09/07/2017	11:45:00	45.7	26.9
817	09/07/2017	12:00:00	45.4	27.1
818	09/07/2017	12:15:00	45.3	27.1
819	09/07/2017	12:30:00	45.0	27.2
820	09/07/2017	12:45:00	43.8	27.2
821	09/07/2017	13:00:00	44.2	27.2
822	09/07/2017	13:15:00	44.6	27.2
823	09/07/2017	13:30:00	44.9	27.3
824	09/07/2017	13:45:00	44.7	27.3
825	09/07/2017	14:00:00	44.8	27.4
826	09/07/2017	14:15:00	45.0	27.4
827	09/07/2017	14:30:00	45.1	27.5
828	09/07/2017	14:45:00	45.5	27.6
829	09/07/2017	15:00:00	45.3	27.7
830	09/07/2017	15:15:00	45.4	27.7
831	09/07/2017	15:30:00	45.5	27.8
832	09/07/2017	15:45:00	45.5	27.9
833	09/07/2017	16:00:00	45.5	27.9
834	09/07/2017	16:15:00	45.6	28.0
835	09/07/2017	16:30:00	45.6	28.1
836	09/07/2017	16:45:00	45.6	28.1
837	09/07/2017	17:00:00	45.8	28.1
838	09/07/2017	17:15:00	45.8	28.1
839	09/07/2017	17:30:00	45.5	28.3
840	09/07/2017	17:45:00	45.4	28.4
841	09/07/2017	18:00:00	45.4	28.4
842	09/07/2017	18:15:00	45.4	28.4
843	09/07/2017	18:30:00	45.5	28.4
844	09/07/2017	18:45:00	45.6	28.3
845	09/07/2017	19:00:00	45.8	28.3
846	09/07/2017	19:15:00	45.1	28.7
847	09/07/2017	19:30:00	45.3	28.7

Index	Date	Time	%RH	°C
848	09/07/2017	19:45:00	45.4	28.6
849	09/07/2017	20:00:00	45.6	28.5
850	09/07/2017	20:15:00	45.9	28.4
851	09/07/2017	20:30:00	46.0	28.3
852	09/07/2017	20:45:00	46.3	28.3
853	09/07/2017	21:00:00	46.4	28.2
854	09/07/2017	21:15:00	46.5	28.2
855	09/07/2017	21:30:00	46.6	28.1
856	09/07/2017	21:45:00	46.6	28.1
857	09/07/2017	22:00:00	46.8	28.1
858	09/07/2017	22:15:00	46.8	28.0
859	09/07/2017	22:30:00	46.9	27.9
860	09/07/2017	22:45:00	47.0	27.9
861	09/07/2017	23:00:00	47.1	27.9
862	09/07/2017	23:15:00	47.3	27.8
863	09/07/2017	23:30:00	47.3	27.8
864	09/07/2017	23:45:00	47.4	27.7
865	10/07/2017	00:00:00	47.5	27.7
866	10/07/2017	00:15:00	47.6	27.7
867	10/07/2017	00:30:00	47.8	27.6
868	10/07/2017	00:45:00	47.9	27.6
869	10/07/2017	01:00:00	48.1	27.5
870	10/07/2017	01:15:00	48.2	27.5
871	10/07/2017	01:30:00	48.3	27.5
872	10/07/2017	01:45:00	48.4	27.4
873	10/07/2017	02:00:00	48.7	27.4
874	10/07/2017	02:15:00	48.7	27.3
875	10/07/2017	02:30:00	48.8	27.3
876	10/07/2017	02:45:00	49.0	27.3
877	10/07/2017	03:00:00	49.1	27.2
878	10/07/2017	03:15:00	49.3	27.2
879	10/07/2017	03:30:00	49.5	27.2
880	10/07/2017	03:45:00	49.5	27.1
881	10/07/2017	04:00:00	49.6	27.1
882	10/07/2017	04:15:00	49.7	27.1
883	10/07/2017	04:30:00	49.8	27.0
884	10/07/2017	04:45:00	49.9	27.0
885	10/07/2017	05:00:00	49.8	26.9
886	10/07/2017	05:15:00	49.9	26.9
887	10/07/2017	05:30:00	49.9	26.9
888	10/07/2017	05:45:00	50.0	26.8
889	10/07/2017	06:00:00	49.5	26.8
890	10/07/2017	06:15:00	49.8	26.8
891	10/07/2017	06:30:00	49.8	26.8
892	10/07/2017	06:45:00	49.5	26.8
893	10/07/2017	07:00:00	49.5	26.8
894	10/07/2017	07:15:00	49.5	26.8
895	10/07/2017	07:30:00	49.6	26.8
896	10/07/2017	07:45:00	49.6	26.8
897	10/07/2017	08:00:00	49.5	26.8
898	10/07/2017	08:15:00	49.5	26.9
899	10/07/2017	08:30:00	49.3	26.9
900	10/07/2017	08:45:00	49.2	27.0
901	10/07/2017	09:00:00	49.1	27.1
902	10/07/2017	09:15:00	48.9	27.1
903	10/07/2017	09:30:00	48.6	27.2
904	10/07/2017	09:45:00	48.6	27.2
905	10/07/2017	10:00:00	48.5	27.2
906	10/07/2017	10:15:00	48.3	27.3
907	10/07/2017	10:30:00	48.1	27.3
908	10/07/2017	10:45:00	48.1	27.4
909	10/07/2017	11:00:00	48.1	27.4
910	10/07/2017	11:15:00	48.1	27.4
911	10/07/2017	11:30:00	48.0	27.4
912	10/07/2017	11:45:00	48.1	27.4
913	10/07/2017	12:00:00	48.0	27.4
914	10/07/2017	12:15:00	48.0	27.4
915	10/07/2017	12:30:00	48.0	27.5
916	10/07/2017	12:45:00	47.9	27.5
917	10/07/2017	13:00:00	47.9	27.5
918	10/07/2017	13:15:00	47.9	27.5
919	10/07/2017	13:30:00	47.9	27.5
920	10/07/2017	13:45:00	48.0	27.5
921	10/07/2017	14:00:00	48.0	27.5
922	10/07/2017	14:15:00	48.1	27.5
923	10/07/2017	14:30:00	48.2	27.5
924	10/07/2017	14:45:00	47.9	27.5

Index	Date	Time	%RH	°C
925	10/07/2017	15:00:00	47.7	27.6
926	10/07/2017	15:15:00	47.6	27.7
927	10/07/2017	15:30:00	47.5	27.8
928	10/07/2017	15:45:00	47.3	27.8
929	10/07/2017	16:00:00	47.1	27.9
930	10/07/2017	16:15:00	47.2	27.9
931	10/07/2017	16:30:00	47.2	27.8
932	10/07/2017	16:45:00	47.3	27.8
933	10/07/2017	17:00:00	47.1	28.0
934	10/07/2017	17:15:00	47.1	28.1
935	10/07/2017	17:30:00	46.9	28.3
936	10/07/2017	17:45:00	46.9	28.4
937	10/07/2017	18:00:00	46.9	28.3
938	10/07/2017	18:15:00	46.9	28.3
939	10/07/2017	18:30:00	46.5	28.7
940	10/07/2017	18:45:00	46.1	28.8
941	10/07/2017	19:00:00	46.0	28.9
942	10/07/2017	19:15:00	45.7	29.0
943	10/07/2017	19:30:00	45.4	29.1
944	10/07/2017	19:45:00	45.2	29.2
945	10/07/2017	20:00:00	45.4	29.0
946	10/07/2017	20:15:00	45.7	28.9
947	10/07/2017	20:30:00	45.9	28.7
948	10/07/2017	20:45:00	46.1	28.6
949	10/07/2017	21:00:00	46.1	28.5
950	10/07/2017	21:15:00	46.2	28.4
951	10/07/2017	21:30:00	46.2	28.3
952	10/07/2017	21:45:00	46.0	28.3
953	10/07/2017	22:00:00	46.1	28.2
954	10/07/2017	22:15:00	45.7	28.1
955	10/07/2017	22:30:00	45.6	28.1
956	10/07/2017	22:45:00	45.5	28.0
957	10/07/2017	23:00:00	45.6	27.9
958	10/07/2017	23:15:00	45.7	27.9
959	10/07/2017	23:30:00	45.6	27.8
960	10/07/2017	23:45:00	45.8	27.8
961	11/07/2017	00:00:00	45.8	27.7
962	11/07/2017	00:15:00	45.9	27.7
963	11/07/2017	00:30:00	45.9	27.6
964	11/07/2017	00:45:00	46.0	27.5
965	11/07/2017	01:00:00	46.1	27.5
966	11/07/2017	01:15:00	46.1	27.4
967	11/07/2017	01:30:00	46.2	27.4
968	11/07/2017	01:45:00	46.3	27.3
969	11/07/2017	02:00:00	46.4	27.3
970	11/07/2017	02:15:00	46.5	27.2
971	11/07/2017	02:30:00	46.5	27.2
972	11/07/2017	02:45:00	46.6	27.1
973	11/07/2017	03:00:00	46.7	27.1
974	11/07/2017	03:15:00	46.8	27.0
975	11/07/2017	03:30:00	46.9	26.9
976	11/07/2017	03:45:00	46.9	26.9
977	11/07/2017	04:00:00	46.9	26.8
978	11/07/2017	04:15:00	47.0	26.8
979	11/07/2017	04:30:00	47.0	26.8
980	11/07/2017	04:45:00	47.1	26.7
981	11/07/2017	05:00:00	47.1	26.7
982	11/07/2017	05:15:00	47.2	26.7
983	11/07/2017	05:30:00	47.2	26.6
984	11/07/2017	05:45:00	47.3	26.6
985	11/07/2017	06:00:00	47.4	26.6
986	11/07/2017	06:15:00	47.4	26.5
987	11/07/2017	06:30:00	47.5	26.5
988	11/07/2017	06:45:00	47.6	26.4
989	11/07/2017	07:00:00	47.7	26.4
990	11/07/2017	07:15:00	47.7	26.4
991	11/07/2017	07:30:00	47.7	26.4
992	11/07/2017	07:45:00	47.7	26.3
993	11/07/2017	08:00:00	47.7	26.3
994	11/07/2017	08:15:00	48.0	26.3
995	11/07/2017	08:30:00	48.1	26.3
996	11/07/2017	08:45:00	48.3	26.3
997	11/07/2017	09:00:00	47.9	26.2
998	11/07/2017	09:15:00	47.5	26.1
999	11/07/2017	09:30:00	46.9	25.9
1000	11/07/2017	09:45:00	46.8	25.9
1001	11/07/2017	10:00:00	47.3	25.8

Index	Date	Time	%RH	°C
1002	11/07/2017	10:15:00	47.6	25.8
1003	11/07/2017	10:30:00	47.8	25.7
1004	11/07/2017	10:45:00	48.1	25.7
1005	11/07/2017	11:00:00	48.5	25.7
1006	11/07/2017	11:15:00	48.6	25.6
1007	11/07/2017	11:30:00	48.9	25.6
1008	11/07/2017	11:45:00	49.7	25.6
1009	11/07/2017	12:00:00	50.2	25.7
1010	11/07/2017	12:15:00	51.3	25.6
1011	11/07/2017	12:30:00	51.7	25.6
1012	11/07/2017	12:45:00	51.2	25.6
1013	11/07/2017	13:00:00	51.0	25.5
1014	11/07/2017	13:15:00	51.2	25.4
1015	11/07/2017	13:30:00	51.6	25.4
1016	11/07/2017	13:45:00	51.6	25.3
1017	11/07/2017	14:00:00	51.5	25.3
1018	11/07/2017	14:15:00	51.0	25.3
1019	11/07/2017	14:30:00	51.2	25.2
1020	11/07/2017	14:45:00	51.3	25.3
1021	11/07/2017	15:00:00	51.6	25.3
1022	11/07/2017	15:15:00	51.6	25.3
1023	11/07/2017	15:30:00	51.7	25.3
1024	11/07/2017	15:45:00	51.9	25.3
1025	11/07/2017	16:00:00	51.8	25.3
1026	11/07/2017	16:15:00	51.9	25.4
1027	11/07/2017	16:30:00	51.9	25.5
1028	11/07/2017	16:45:00	52.1	25.5
1029	11/07/2017	17:00:00	52.1	25.5
1030	11/07/2017	17:15:00	52.1	25.6
1031	11/07/2017	17:30:00	52.1	25.6
1032	11/07/2017	17:45:00	52.2	25.6
1033	11/07/2017	18:00:00	52.1	25.6
1034	11/07/2017	18:15:00	52.2	25.6
1035	11/07/2017	18:30:00	52.1	25.6
1036	11/07/2017	18:45:00	52.1	25.6
1037	11/07/2017	19:00:00	52.2	25.6
1038	11/07/2017	19:15:00	52.3	25.6
1039	11/07/2017	19:30:00	52.2	25.6
1040	11/07/2017	19:45:00	52.5	25.6
1041	11/07/2017	20:00:00	52.5	25.5
1042	11/07/2017	20:15:00	52.6	25.5
1043	11/07/2017	20:30:00	52.6	25.5
1044	11/07/2017	20:45:00	52.7	25.4
1045	11/07/2017	21:00:00	52.7	25.4
1046	11/07/2017	21:15:00	52.7	25.4
1047	11/07/2017	21:30:00	52.7	25.4
1048	11/07/2017	21:45:00	52.7	25.3
1049	11/07/2017	22:00:00	52.7	25.3
1050	11/07/2017	22:15:00	52.7	25.3
1051	11/07/2017	22:30:00	52.7	25.3
1052	11/07/2017	22:45:00	52.7	25.3
1053	11/07/2017	23:00:00	52.7	25.2
1054	11/07/2017	23:15:00	52.6	25.2
1055	11/07/2017	23:30:00	52.6	25.2
1056	11/07/2017	23:45:00	52.6	25.1
1057	12/07/2017	00:00:00	52.6	25.1
1058	12/07/2017	00:15:00	52.5	25.1
1059	12/07/2017	00:30:00	52.5	25.1
1060	12/07/2017	00:45:00	52.6	25.0
1061	12/07/2017	01:00:00	52.4	25.0
1062	12/07/2017	01:15:00	52.5	24.9
1063	12/07/2017	01:30:00	52.5	24.9
1064	12/07/2017	01:45:00	52.5	24.9
1065	12/07/2017	02:00:00	52.5	24.8
1066	12/07/2017	02:15:00	52.4	24.8
1067	12/07/2017	02:30:00	52.4	24.7
1068	12/07/2017	02:45:00	52.5	24.7
1069	12/07/2017	03:00:00	52.4	24.7
1070	12/07/2017	03:15:00	52.4	24.7
1071	12/07/2017	03:30:00	52.4	24.7
1072	12/07/2017	03:45:00	52.2	24.7
1073	12/07/2017	04:00:00	52.3	24.7
1074	12/07/2017	04:15:00	52.4	24.7
1075	12/07/2017	04:30:00	52.4	24.6
1076	12/07/2017	04:45:00	52.4	24.6
1077	12/07/2017	05:00:00	52.3	24.6
1078	12/07/2017	05:15:00	52.4	24.5

Index	Date	Time	%RH	°C
1079	12/07/2017	05:30:00	52.4	24.5
1080	12/07/2017	05:45:00	52.3	24.5
1081	12/07/2017	06:00:00	52.0	24.4
1082	12/07/2017	06:15:00	52.2	24.4
1083	12/07/2017	06:30:00	52.4	24.4
1084	12/07/2017	06:45:00	52.4	24.4
1085	12/07/2017	07:00:00	52.0	24.4
1086	12/07/2017	07:15:00	51.9	24.5
1087	12/07/2017	07:30:00	51.7	24.5
1088	12/07/2017	07:45:00	51.5	24.5
1089	12/07/2017	08:00:00	51.2	24.6
1090	12/07/2017	08:15:00	51.2	24.6
1091	12/07/2017	08:30:00	51.0	24.6
1092	12/07/2017	08:45:00	50.8	24.7
1093	12/07/2017	09:00:00	51.2	24.7
1094	12/07/2017	09:15:00	50.2	24.7
1095	12/07/2017	09:30:00	50.2	24.7
1096	12/07/2017	09:45:00	49.9	24.8
1097	12/07/2017	10:00:00	49.8	24.9
1098	12/07/2017	10:15:00	49.8	24.9
1099	12/07/2017	10:30:00	49.5	25.0
1100	12/07/2017	10:45:00	49.6	25.1
1101	12/07/2017	11:00:00	49.6	25.0
1102	12/07/2017	11:15:00	49.2	25.1
1103	12/07/2017	11:30:00	49.1	25.1
1104	12/07/2017	11:45:00	49.0	25.2
1105	12/07/2017	12:00:00	48.7	25.2
1106	12/07/2017	12:15:00	48.8	25.2
1107	12/07/2017	12:30:00	48.6	25.3
1108	12/07/2017	12:45:00	48.4	25.3
1109	12/07/2017	13:00:00	48.2	25.3
1110	12/07/2017	13:15:00	48.0	25.4
1111	12/07/2017	13:30:00	47.9	25.4
1112	12/07/2017	13:45:00	44.2	25.5
1113	12/07/2017	14:00:00	43.0	25.6
1114	12/07/2017	14:15:00	40.0	25.6
1115	12/07/2017	14:30:00	41.0	25.6
1116	12/07/2017	14:45:00	41.9	25.7
1117	12/07/2017	15:00:00	40.4	25.7
1118	12/07/2017	15:15:00	39.7	25.7
1119	12/07/2017	15:30:00	39.8	25.8
1120	12/07/2017	15:45:00	39.0	25.9
1121	12/07/2017	16:00:00	39.3	25.9
1122	12/07/2017	16:15:00	38.0	25.9
1123	12/07/2017	16:30:00	38.3	26.1
1124	12/07/2017	16:45:00	37.8	26.2
1125	12/07/2017	17:00:00	37.7	26.2
1126	12/07/2017	17:15:00	36.9	26.1
1127	12/07/2017	17:30:00	37.9	26.1
1128	12/07/2017	17:45:00	37.5	26.2
1129	12/07/2017	18:00:00	36.8	26.6
1130	12/07/2017	18:15:00	36.4	26.8
1131	12/07/2017	18:30:00	35.9	26.9
1132	12/07/2017	18:45:00	35.7	27.2
1133	12/07/2017	19:00:00	35.0	27.3
1134	12/07/2017	19:15:00	34.7	27.3
1135	12/07/2017	19:30:00	34.8	27.5
1136	12/07/2017	19:45:00	34.8	27.5
1137	12/07/2017	20:00:00	35.3	27.5
1138	12/07/2017	20:15:00	35.7	27.5
1139	12/07/2017	20:30:00	36.1	27.3
1140	12/07/2017	20:45:00	36.8	27.2
1141	12/07/2017	21:00:00	37.4	27.1
1142	12/07/2017	21:15:00	37.6	26.9
1143	12/07/2017	21:30:00	37.9	26.8
1144	12/07/2017	21:45:00	38.3	26.8
1145	12/07/2017	22:00:00	38.6	26.7
1146	12/07/2017	22:15:00	39.0	26.6
1147	12/07/2017	22:30:00	39.3	26.6
1148	12/07/2017	22:45:00	39.6	26.5
1149	12/07/2017	23:00:00	39.8	26.4
1150	12/07/2017	23:15:00	40.4	26.4
1151	12/07/2017	23:30:00	40.6	26.3
1152	12/07/2017	23:45:00	40.8	26.3
1153	13/07/2017	00:00:00	41.3	26.2
1154	13/07/2017	00:15:00	41.5	26.1
1155	13/07/2017	00:30:00	41.8	26.1

Index	Date	Time	%RH	°C
1156	13/07/2017	00:45:00	42.1	26.0
1157	13/07/2017	01:00:00	42.3	25.9
1158	13/07/2017	01:15:00	42.5	25.9
1159	13/07/2017	01:30:00	42.7	25.8
1160	13/07/2017	01:45:00	42.9	25.8
1161	13/07/2017	02:00:00	43.6	25.7
1162	13/07/2017	02:15:00	43.5	25.7
1163	13/07/2017	02:30:00	43.9	25.7
1164	13/07/2017	02:45:00	44.0	25.6
1165	13/07/2017	03:00:00	44.2	25.5
1166	13/07/2017	03:15:00	44.6	25.5
1167	13/07/2017	03:30:00	44.6	25.4
1168	13/07/2017	03:45:00	44.9	25.4
1169	13/07/2017	04:00:00	45.0	25.3
1170	13/07/2017	04:15:00	45.1	25.3
1171	13/07/2017	04:30:00	45.2	25.2
1172	13/07/2017	04:45:00	45.1	25.2
1173	13/07/2017	05:00:00	45.1	25.2
1174	13/07/2017	05:15:00	45.5	25.1
1175	13/07/2017	05:30:00	45.8	25.1
1176	13/07/2017	05:45:00	45.8	25.1
1177	13/07/2017	06:00:00	44.8	25.0
1178	13/07/2017	06:15:00	45.2	25.0
1179	13/07/2017	06:30:00	45.7	25.0
1180	13/07/2017	06:45:00	45.8	24.9
1181	13/07/2017	07:00:00	46.0	24.9
1182	13/07/2017	07:15:00	45.5	24.9
1183	13/07/2017	07:30:00	46.1	24.9
1184	13/07/2017	07:45:00	45.6	24.9
1185	13/07/2017	08:00:00	45.7	24.9
1186	13/07/2017	08:15:00	45.7	24.9
1187	13/07/2017	08:30:00	45.9	24.9
1188	13/07/2017	08:45:00	46.2	24.9
1189	13/07/2017	09:00:00	46.4	24.9
1190	13/07/2017	09:15:00	46.7	24.9
1191	13/07/2017	09:30:00	46.8	25.0
1192	13/07/2017	09:45:00	46.8	25.1
1193	13/07/2017	10:00:00	46.9	25.1
1194	13/07/2017	10:15:00	47.0	25.2
1195	13/07/2017	10:30:00	47.2	25.2
1196	13/07/2017	10:45:00	47.3	25.2
1197	13/07/2017	11:00:00	47.3	25.2
1198	13/07/2017	11:15:00	47.4	25.3
1199	13/07/2017	11:30:00	47.4	25.3
1200	13/07/2017	11:45:00	47.4	25.3
1201	13/07/2017	12:00:00	47.4	25.4
1202	13/07/2017	12:15:00	47.6	25.4
1203	13/07/2017	12:30:00	47.4	25.4
1204	13/07/2017	12:45:00	47.3	25.6
1205	13/07/2017	13:00:00	47.3	25.6
1206	13/07/2017	13:15:00	47.1	25.7
1207	13/07/2017	13:30:00	47.0	25.8
1208	13/07/2017	13:45:00	46.8	25.9
1209	13/07/2017	14:00:00	46.6	26.1
1210	13/07/2017	14:15:00	46.5	26.1
1211	13/07/2017	14:30:00	46.3	26.1
1212	13/07/2017	14:45:00	46.3	26.1
1213	13/07/2017	15:00:00	46.2	26.1
1214	13/07/2017	15:15:00	46.1	26.0
1215	13/07/2017	15:30:00	46.2	25.9
1216	13/07/2017	15:45:00	46.5	25.9
1217	13/07/2017	16:00:00	46.5	25.9
1218	13/07/2017	16:15:00	46.4	25.9
1219	13/07/2017	16:30:00	46.4	25.9
1220	13/07/2017	16:45:00	46.6	25.9
1221	13/07/2017	17:00:00	46.7	25.9
1222	13/07/2017	17:15:00	46.7	25.8
1223	13/07/2017	17:30:00	46.8	25.8
1224	13/07/2017	17:45:00	46.8	25.8
1225	13/07/2017	18:00:00	46.8	25.8
1226	13/07/2017	18:15:00	46.9	25.8
1227	13/07/2017	18:30:00	46.9	25.8
1228	13/07/2017	18:45:00	46.9	25.8
1229	13/07/2017	19:00:00	46.8	25.8
1230	13/07/2017	19:15:00	46.9	25.8
1231	13/07/2017	19:30:00	46.9	25.7
1232	13/07/2017	19:45:00	46.9	25.7

Index	Date	Time	%RH	°C
1233	13/07/2017	20:00:00	47.0	25.7
1234	13/07/2017	20:15:00	47.0	25.7
1235	13/07/2017	20:30:00	47.1	25.6
1236	13/07/2017	20:45:00	47.2	25.6
1237	13/07/2017	21:00:00	47.3	25.6
1238	13/07/2017	21:15:00	47.3	25.6
1239	13/07/2017	21:30:00	47.4	25.5
1240	13/07/2017	21:45:00	47.5	25.5
1241	13/07/2017	22:00:00	47.7	25.5
1242	13/07/2017	22:15:00	47.7	25.4
1243	13/07/2017	22:30:00	47.8	25.4
1244	13/07/2017	22:45:00	48.0	25.4
1245	13/07/2017	23:00:00	48.0	25.4
1246	13/07/2017	23:15:00	48.1	25.3
1247	13/07/2017	23:30:00	48.3	25.3
1248	13/07/2017	23:45:00	48.4	25.3
1249	14/07/2017	00:00:00	48.5	25.3
1250	14/07/2017	00:15:00	48.6	25.2
1251	14/07/2017	00:30:00	48.6	25.2
1252	14/07/2017	00:45:00	48.6	25.2
1253	14/07/2017	01:00:00	48.7	25.2
1254	14/07/2017	01:15:00	48.9	25.1
1255	14/07/2017	01:30:00	49.0	25.1
1256	14/07/2017	01:45:00	49.1	25.1
1257	14/07/2017	02:00:00	49.1	25.1
1258	14/07/2017	02:15:00	49.2	25.0
1259	14/07/2017	02:30:00	49.3	25.0
1260	14/07/2017	02:45:00	49.5	24.9
1261	14/07/2017	03:00:00	49.6	24.9
1262	14/07/2017	03:15:00	49.5	24.9
1263	14/07/2017	03:30:00	49.6	24.9
1264	14/07/2017	03:45:00	49.7	24.8
1265	14/07/2017	04:00:00	49.9	24.8
1266	14/07/2017	04:15:00	50.0	24.7
1267	14/07/2017	04:30:00	50.1	24.7
1268	14/07/2017	04:45:00	50.2	24.7
1269	14/07/2017	05:00:00	50.2	24.7
1270	14/07/2017	05:15:00	50.2	24.7
1271	14/07/2017	05:30:00	50.2	24.7
1272	14/07/2017	05:45:00	50.3	24.7
1273	14/07/2017	06:00:00	50.2	24.7
1274	14/07/2017	06:15:00	50.5	24.7
1275	14/07/2017	06:30:00	50.5	24.6
1276	14/07/2017	06:45:00	49.9	24.6
1277	14/07/2017	07:00:00	50.0	24.6
1278	14/07/2017	07:15:00	49.4	24.6
1279	14/07/2017	07:30:00	49.6	24.6
1280	14/07/2017	07:45:00	49.6	24.6
1281	14/07/2017	08:00:00	49.4	24.6
1282	14/07/2017	08:15:00	49.4	24.6
1283	14/07/2017	08:30:00	49.3	24.7
1284	14/07/2017	08:45:00	49.3	24.7
1285	14/07/2017	09:00:00	49.1	24.7
1286	14/07/2017	09:15:00	49.2	24.7
1287	14/07/2017	09:30:00	49.2	24.7
1288	14/07/2017	09:45:00	49.1	24.9
1289	14/07/2017	10:00:00	49.4	24.9
1290	14/07/2017	10:15:00	48.9	24.9
1291	14/07/2017	10:30:00	48.9	25.0
1292	14/07/2017	10:45:00	48.4	25.0
1293	14/07/2017	11:00:00	48.4	24.9
1294	14/07/2017	11:15:00	48.4	24.9
1295	14/07/2017	11:30:00	49.1	25.0
1296	14/07/2017	11:45:00	48.7	25.1
1297	14/07/2017	12:00:00	49.0	25.2
1298	14/07/2017	12:15:00	49.0	25.2
1299	14/07/2017	12:30:00	49.8	25.1
1300	14/07/2017	12:45:00	48.3	25.2
1301	14/07/2017	13:00:00	47.7	25.2
1302	14/07/2017	13:15:00	47.6	25.2
1303	14/07/2017	13:30:00	47.4	25.3
1304	14/07/2017	13:45:00	47.3	25.2
1305	14/07/2017	14:00:00	47.2	25.3
1306	14/07/2017	14:15:00	47.0	25.3
1307	14/07/2017	14:30:00	46.9	25.4
1308	14/07/2017	14:45:00	46.7	25.4
1309	14/07/2017	15:00:00	46.4	25.5

Index	Date	Time	%RH	°C
1310	14/07/2017	15:15:00	46.2	25.6
1311	14/07/2017	15:30:00	46.1	25.7
1312	14/07/2017	15:45:00	46.0	25.7
1313	14/07/2017	16:00:00	45.9	25.7
1314	14/07/2017	16:15:00	45.8	25.7
1315	14/07/2017	16:30:00	45.8	25.8
1316	14/07/2017	16:45:00	45.7	25.8
1317	14/07/2017	17:00:00	45.5	25.8
1318	14/07/2017	17:15:00	45.5	25.8
1319	14/07/2017	17:30:00	45.3	25.9
1320	14/07/2017	17:45:00	45.1	25.9
1321	14/07/2017	18:00:00	44.9	26.1
1322	14/07/2017	18:15:00	44.7	26.3
1323	14/07/2017	18:30:00	44.5	26.4
1324	14/07/2017	18:45:00	44.1	26.7
1325	14/07/2017	19:00:00	43.9	26.8
1326	14/07/2017	19:15:00	43.9	26.7
1327	14/07/2017	19:30:00	43.9	26.7
1328	14/07/2017	19:45:00	43.9	26.6
1329	14/07/2017	20:00:00	44.0	26.4
1330	14/07/2017	20:15:00	44.6	26.3
1331	14/07/2017	20:30:00	44.6	26.2
1332	14/07/2017	20:45:00	44.6	26.2
1333	14/07/2017	21:00:00	44.7	26.1
1334	14/07/2017	21:15:00	44.6	26.1
1335	14/07/2017	21:30:00	44.6	26.0
1336	14/07/2017	21:45:00	44.6	25.9
1337	14/07/2017	22:00:00	44.5	25.9
1338	14/07/2017	22:15:00	44.5	25.8
1339	14/07/2017	22:30:00	44.5	25.8
1340	14/07/2017	22:45:00	44.6	25.7
1341	14/07/2017	23:00:00	44.7	25.7
1342	14/07/2017	23:15:00	44.8	25.7
1343	14/07/2017	23:30:00	45.0	25.6
1344	14/07/2017	23:45:00	45.0	25.6
1345	15/07/2017	00:00:00	45.2	25.5
1346	15/07/2017	00:15:00	45.4	25.5
1347	15/07/2017	00:30:00	45.6	25.4
1348	15/07/2017	00:45:00	45.8	25.4
1349	15/07/2017	01:00:00	45.9	25.3
1350	15/07/2017	01:15:00	46.0	25.3
1351	15/07/2017	01:30:00	46.2	25.3
1352	15/07/2017	01:45:00	46.2	25.2
1353	15/07/2017	02:00:00	46.4	25.2
1354	15/07/2017	02:15:00	46.6	25.2
1355	15/07/2017	02:30:00	46.7	25.1
1356	15/07/2017	02:45:00	46.9	25.1
1357	15/07/2017	03:00:00	47.0	25.1
1358	15/07/2017	03:15:00	47.1	25.0
1359	15/07/2017	03:30:00	47.3	24.9
1360	15/07/2017	03:45:00	47.4	24.9
1361	15/07/2017	04:00:00	47.5	24.9
1362	15/07/2017	04:15:00	47.7	24.9
1363	15/07/2017	04:30:00	47.7	24.8
1364	15/07/2017	04:45:00	47.8	24.7
1365	15/07/2017	05:00:00	47.8	24.7
1366	15/07/2017	05:15:00	47.9	24.7
1367	15/07/2017	05:30:00	48.0	24.7
1368	15/07/2017	05:45:00	48.1	24.7
1369	15/07/2017	06:00:00	48.0	24.7
1370	15/07/2017	06:15:00	48.3	24.7
1371	15/07/2017	06:30:00	48.3	24.7
1372	15/07/2017	06:45:00	48.3	24.7
1373	15/07/2017	07:00:00	48.3	24.7
1374	15/07/2017	07:15:00	48.4	24.7
1375	15/07/2017	07:30:00	48.4	24.7
1376	15/07/2017	07:45:00	48.4	24.7
1377	15/07/2017	08:00:00	48.1	24.6
1378	15/07/2017	08:15:00	48.3	24.6
1379	15/07/2017	08:30:00	48.8	24.6
1380	15/07/2017	08:45:00	48.5	24.6
1381	15/07/2017	09:00:00	48.4	24.6
1382	15/07/2017	09:15:00	48.6	24.7
1383	15/07/2017	09:30:00	48.9	24.7
1384	15/07/2017	09:45:00	49.0	24.7
1385	15/07/2017	10:00:00	48.9	24.6
1386	15/07/2017	10:15:00	49.0	24.7

Index	Date	Time	%RH	°C
1387	15/07/2017	10:30:00	49.1	24.7
1388	15/07/2017	10:45:00	49.3	24.7
1389	15/07/2017	11:00:00	49.4	24.7
1390	15/07/2017	11:15:00	49.5	24.7
1391	15/07/2017	11:30:00	49.7	24.7
1392	15/07/2017	11:45:00	49.8	24.7
1393	15/07/2017	12:00:00	50.0	24.7
1394	15/07/2017	12:15:00	50.0	24.7
1395	15/07/2017	12:30:00	50.0	24.7
1396	15/07/2017	12:45:00	50.1	24.7
1397	15/07/2017	13:00:00	50.3	24.8
1398	15/07/2017	13:15:00	50.3	24.9
1399	15/07/2017	13:30:00	50.3	24.9
1400	15/07/2017	13:45:00	50.3	25.0
1401	15/07/2017	14:00:00	50.4	25.0
1402	15/07/2017	14:15:00	50.5	25.1
1403	15/07/2017	14:30:00	50.7	25.1
1404	15/07/2017	14:45:00	50.8	25.1
1405	15/07/2017	15:00:00	50.8	25.1
1406	15/07/2017	15:15:00	50.9	25.1
1407	15/07/2017	15:30:00	51.0	25.2
1408	15/07/2017	15:45:00	51.0	25.3
1409	15/07/2017	16:00:00	51.1	25.3
1410	15/07/2017	16:15:00	51.2	25.3
1411	15/07/2017	16:30:00	51.3	25.3
1412	15/07/2017	16:45:00	51.4	25.3
1413	15/07/2017	17:00:00	51.4	25.3
1414	15/07/2017	17:15:00	51.4	25.4
1415	15/07/2017	17:30:00	51.6	25.4
1416	15/07/2017	17:45:00	51.8	25.4
1417	15/07/2017	18:00:00	51.9	25.5
1418	15/07/2017	18:15:00	52.0	25.5
1419	15/07/2017	18:30:00	52.1	25.5
1420	15/07/2017	18:45:00	52.1	25.5
1421	15/07/2017	19:00:00	52.0	25.6
1422	15/07/2017	19:15:00	51.9	25.7
1423	15/07/2017	19:30:00	52.0	25.7
1424	15/07/2017	19:45:00	52.0	25.7
1425	15/07/2017	20:00:00	52.2	25.6
1426	15/07/2017	20:15:00	52.3	25.6
1427	15/07/2017	20:30:00	52.3	25.6
1428	15/07/2017	20:45:00	52.4	25.6
1429	15/07/2017	21:00:00	52.4	25.6
1430	15/07/2017	21:15:00	52.6	25.6
1431	15/07/2017	21:30:00	52.5	25.5
1432	15/07/2017	21:45:00	52.6	25.5
1433	15/07/2017	22:00:00	52.8	25.4
1434	15/07/2017	22:15:00	52.9	25.4
1435	15/07/2017	22:30:00	53.0	25.4
1436	15/07/2017	22:45:00	53.1	25.4
1437	15/07/2017	23:00:00	53.1	25.3
1438	15/07/2017	23:15:00	53.2	25.3
1439	15/07/2017	23:30:00	53.4	25.3
1440	15/07/2017	23:45:00	53.4	25.3
1441	16/07/2017	00:00:00	53.6	25.3
1442	16/07/2017	00:15:00	53.6	25.2
1443	16/07/2017	00:30:00	53.6	25.2
1444	16/07/2017	00:45:00	53.8	25.2
1445	16/07/2017	01:00:00	53.9	25.2
1446	16/07/2017	01:15:00	53.9	25.2
1447	16/07/2017	01:30:00	54.0	25.1
1448	16/07/2017	01:45:00	54.0	25.1
1449	16/07/2017	02:00:00	54.0	25.1
1450	16/07/2017	02:15:00	54.1	25.1
1451	16/07/2017	02:30:00	54.2	25.1
1452	16/07/2017	02:45:00	54.2	25.1
1453	16/07/2017	03:00:00	54.1	25.0
1454	16/07/2017	03:15:00	54.3	25.0
1455	16/07/2017	03:30:00	54.3	24.9
1456	16/07/2017	03:45:00	54.5	24.9
1457	16/07/2017	04:00:00	54.5	24.9
1458	16/07/2017	04:15:00	54.5	24.9
1459	16/07/2017	04:30:00	54.7	24.9
1460	16/07/2017	04:45:00	54.8	24.9
1461	16/07/2017	05:00:00	54.7	24.8
1462	16/07/2017	05:15:00	54.9	24.8
1463	16/07/2017	05:30:00	54.8	24.7

Index	Date	Time	%RH	°C
1464	16/07/2017	05:45:00	54.9	24.7
1465	16/07/2017	06:00:00	54.8	24.7
1466	16/07/2017	06:15:00	54.9	24.7
1467	16/07/2017	06:30:00	55.0	24.7
1468	16/07/2017	06:45:00	54.9	24.7
1469	16/07/2017	07:00:00	54.9	24.7
1470	16/07/2017	07:15:00	55.1	24.7
1471	16/07/2017	07:30:00	55.2	24.7
1472	16/07/2017	07:45:00	55.2	24.7
1473	16/07/2017	08:00:00	55.2	24.7
1474	16/07/2017	08:15:00	55.3	24.7
1475	16/07/2017	08:30:00	55.0	24.7
1476	16/07/2017	08:45:00	55.2	24.7
1477	16/07/2017	09:00:00	55.3	24.7
1478	16/07/2017	09:15:00	55.4	24.7
1479	16/07/2017	09:30:00	55.4	24.8
1480	16/07/2017	09:45:00	55.2	24.8
1481	16/07/2017	10:00:00	55.2	24.9
1482	16/07/2017	10:15:00	55.2	24.9
1483	16/07/2017	10:30:00	55.2	25.0
1484	16/07/2017	10:45:00	55.2	25.1
1485	16/07/2017	11:00:00	55.2	25.1
1486	16/07/2017	11:15:00	55.1	25.2
1487	16/07/2017	11:30:00	55.0	25.2
1488	16/07/2017	11:45:00	55.0	25.3
1489	16/07/2017	12:00:00	55.1	25.2
1490	16/07/2017	12:15:00	55.0	25.3
1491	16/07/2017	12:30:00	54.9	25.4
1492	16/07/2017	12:45:00	54.7	25.5
1493	16/07/2017	13:00:00	54.5	25.6
1494	16/07/2017	13:15:00	54.4	25.6
1495	16/07/2017	13:30:00	54.1	25.7
1496	16/07/2017	13:45:00	54.0	25.8
1497	16/07/2017	14:00:00	53.8	25.9
1498	16/07/2017	14:15:00	53.7	25.9
1499	16/07/2017	14:30:00	53.6	26.0
1500	16/07/2017	14:45:00	53.4	26.1
1501	16/07/2017	15:00:00	53.3	26.1
1502	16/07/2017	15:15:00	53.1	26.2
1503	16/07/2017	15:30:00	53.0	26.3
1504	16/07/2017	15:45:00	52.8	26.4
1505	16/07/2017	16:00:00	52.7	26.6
1506	16/07/2017	16:15:00	52.3	26.7
1507	16/07/2017	16:30:00	52.1	26.8
1508	16/07/2017	16:45:00	51.9	26.8
1509	16/07/2017	17:00:00	51.6	27.0
1510	16/07/2017	17:15:00	51.1	27.2
1511	16/07/2017	17:30:00	50.7	27.4
1512	16/07/2017	17:45:00	50.2	27.6
1513	16/07/2017	18:00:00	49.6	27.8
1514	16/07/2017	18:15:00	48.7	28.2
1515	16/07/2017	18:30:00	48.0	28.6
1516	16/07/2017	18:45:00	46.7	29.1
1517	16/07/2017	19:00:00	45.6	29.4
1518	16/07/2017	19:15:00	44.5	29.9
1519	16/07/2017	19:30:00	43.7	30.2
1520	16/07/2017	19:45:00	43.3	30.2
1521	16/07/2017	20:00:00	43.3	30.2
1522	16/07/2017	20:15:00	43.6	29.8
1523	16/07/2017	20:30:00	44.1	29.4
1524	16/07/2017	20:45:00	44.4	29.2
1525	16/07/2017	21:00:00	44.7	29.0
1526	16/07/2017	21:15:00	44.8	28.8
1527	16/07/2017	21:30:00	45.0	28.7
1528	16/07/2017	21:45:00	44.9	28.5
1529	16/07/2017	22:00:00	45.1	28.4
1530	16/07/2017	22:15:00	45.2	28.3
1531	16/07/2017	22:30:00	45.3	28.2
1532	16/07/2017	22:45:00	45.3	28.1
1533	16/07/2017	23:00:00	45.6	28.0
1534	16/07/2017	23:15:00	45.6	27.9
1535	16/07/2017	23:30:00	45.8	27.8
1536	16/07/2017	23:45:00	45.8	27.7
1537	17/07/2017	00:00:00	45.8	27.6
1538	17/07/2017	00:15:00	45.8	27.5
1539	17/07/2017	00:30:00	45.8	27.5
1540	17/07/2017	00:45:00	46.1	27.4

Index	Date	Time	%RH	°C
1541	17/07/2017	01:00:00	46.2	27.3
1542	17/07/2017	01:15:00	46.2	27.2
1543	17/07/2017	01:30:00	46.3	27.1
1544	17/07/2017	01:45:00	46.4	27.1
1545	17/07/2017	02:00:00	46.6	26.9
1546	17/07/2017	02:15:00	46.7	26.9
1547	17/07/2017	02:30:00	46.8	26.8
1548	17/07/2017	02:45:00	47.0	26.8
1549	17/07/2017	03:00:00	47.1	26.7
1550	17/07/2017	03:15:00	47.2	26.6
1551	17/07/2017	03:30:00	47.3	26.6
1552	17/07/2017	03:45:00	47.3	26.5
1553	17/07/2017	04:00:00	47.4	26.4
1554	17/07/2017	04:15:00	47.6	26.3
1555	17/07/2017	04:30:00	47.6	26.3
1556	17/07/2017	04:45:00	47.7	26.2
1557	17/07/2017	05:00:00	47.8	26.2
1558	17/07/2017	05:15:00	47.8	26.1
1559	17/07/2017	05:30:00	47.9	26.1
1560	17/07/2017	05:45:00	48.0	26.0
1561	17/07/2017	06:00:00	48.0	25.9
1562	17/07/2017	06:15:00	48.0	25.9
1563	17/07/2017	06:30:00	48.1	25.9
1564	17/07/2017	06:45:00	48.2	25.8
1565	17/07/2017	07:00:00	47.9	25.8
1566	17/07/2017	07:15:00	47.6	25.8
1567	17/07/2017	07:30:00	47.8	25.8
1568	17/07/2017	07:45:00	47.9	25.8
1569	17/07/2017	08:00:00	47.9	25.8
1570	17/07/2017	08:15:00	47.9	25.8
1571	17/07/2017	08:30:00	47.9	25.8
1572	17/07/2017	08:45:00	47.7	25.8
1573	17/07/2017	09:00:00	47.7	25.8
1574	17/07/2017	09:15:00	47.7	25.9
1575	17/07/2017	09:30:00	47.8	25.9
1576	17/07/2017	09:45:00	47.8	26.0
1577	17/07/2017	10:00:00	47.6	26.0
1578	17/07/2017	10:15:00	47.5	26.1
1579	17/07/2017	10:30:00	47.4	26.1
1580	17/07/2017	10:45:00	47.4	26.1
1581	17/07/2017	11:00:00	47.3	26.2
1582	17/07/2017	11:15:00	47.3	26.2
1583	17/07/2017	11:30:00	47.2	26.2
1584	17/07/2017	11:45:00	47.0	26.3
1585	17/07/2017	12:00:00	46.9	26.3
1586	17/07/2017	12:15:00	46.8	26.3
1587	17/07/2017	12:30:00	46.6	26.3
1588	17/07/2017	12:45:00	46.6	26.4
1589	17/07/2017	13:00:00	46.6	26.4
1590	17/07/2017	13:15:00	46.5	26.4
1591	17/07/2017	13:30:00	46.4	26.5
1592	17/07/2017	13:45:00	46.4	26.6
1593	17/07/2017	14:00:00	46.4	26.7
1594	17/07/2017	14:15:00	46.2	26.8
1595	17/07/2017	14:30:00	46.1	26.9
1596	17/07/2017	14:45:00	46.1	27.0
1597	17/07/2017	15:00:00	45.9	27.1
1598	17/07/2017	15:15:00	45.8	27.3
1599	17/07/2017	15:30:00	45.6	27.4
1600	17/07/2017	15:45:00	45.4	27.5
1601	17/07/2017	16:00:00	45.1	27.7
1602	17/07/2017	16:15:00	45.0	27.8
1603	17/07/2017	16:30:00	44.8	27.9
1604	17/07/2017	16:45:00	44.6	28.1
1605	17/07/2017	17:00:00	44.3	28.3
1606	17/07/2017	17:15:00	44.0	28.4
1607	17/07/2017	17:30:00	44.0	28.5
1608	17/07/2017	17:45:00	43.7	28.7
1609	17/07/2017	18:00:00	43.5	28.8
1610	17/07/2017	18:15:00	43.3	28.9
1611	17/07/2017	18:30:00	43.0	29.1
1612	17/07/2017	18:45:00	43.0	29.2
1613	17/07/2017	19:00:00	42.9	29.3
1614	17/07/2017	19:15:00	42.8	29.3
1615	17/07/2017	19:30:00	42.9	29.3
1616	17/07/2017	19:45:00	43.1	29.2
1617	17/07/2017	20:00:00	43.3	29.1

Index	Date	Time	%RH	°C
1618	17/07/2017	20:15:00	43.4	29.0
1619	17/07/2017	20:30:00	43.7	28.9
1620	17/07/2017	20:45:00	43.9	28.8
1621	17/07/2017	21:00:00	44.1	28.7
1622	17/07/2017	21:15:00	44.2	28.7
1623	17/07/2017	21:30:00	44.4	28.6
1624	17/07/2017	21:45:00	44.4	28.5
1625	17/07/2017	22:00:00	44.5	28.4
1626	17/07/2017	22:15:00	44.8	28.3
1627	17/07/2017	22:30:00	44.8	28.3
1628	17/07/2017	22:45:00	44.9	28.2
1629	17/07/2017	23:00:00	44.9	28.2
1630	17/07/2017	23:15:00	45.0	28.1
1631	17/07/2017	23:30:00	45.1	28.1
1632	17/07/2017	23:45:00	45.2	28.0
1633	18/07/2017	00:00:00	45.2	27.9
1634	18/07/2017	00:15:00	45.2	27.9
1635	18/07/2017	00:30:00	45.3	27.8
1636	18/07/2017	00:45:00	45.5	27.8
1637	18/07/2017	01:00:00	45.7	27.7
1638	18/07/2017	01:15:00	45.6	27.7
1639	18/07/2017	01:30:00	45.5	27.6
1640	18/07/2017	01:45:00	45.7	27.6
1641	18/07/2017	02:00:00	45.8	27.5
1642	18/07/2017	02:15:00	45.8	27.5
1643	18/07/2017	02:30:00	45.9	27.4
1644	18/07/2017	02:45:00	46.0	27.3
1645	18/07/2017	03:00:00	46.1	27.3
1646	18/07/2017	03:15:00	46.2	27.2
1647	18/07/2017	03:30:00	46.2	27.2
1648	18/07/2017	03:45:00	46.3	27.1
1649	18/07/2017	04:00:00	46.4	27.1
1650	18/07/2017	04:15:00	46.4	27.1
1651	18/07/2017	04:30:00	46.5	27.0
1652	18/07/2017	04:45:00	46.7	26.9
1653	18/07/2017	05:00:00	46.8	26.9
1654	18/07/2017	05:15:00	46.9	26.8
1655	18/07/2017	05:30:00	46.9	26.8
1656	18/07/2017	05:45:00	47.1	26.8
1657	18/07/2017	06:00:00	47.1	26.7
1658	18/07/2017	06:15:00	47.3	26.7
1659	18/07/2017	06:30:00	47.4	26.7
1660	18/07/2017	06:45:00	47.4	26.7
1661	18/07/2017	07:00:00	47.3	26.7
1662	18/07/2017	07:15:00	47.2	26.7
1663	18/07/2017	07:30:00	47.3	26.7
1664	18/07/2017	07:45:00	47.4	26.7
1665	18/07/2017	08:00:00	47.4	26.7
1666	18/07/2017	08:15:00	47.6	26.7
1667	18/07/2017	08:30:00	47.7	26.7
1668	18/07/2017	08:45:00	47.8	26.7
1669	18/07/2017	09:00:00	47.7	26.8
1670	18/07/2017	09:15:00	47.7	26.8
1671	18/07/2017	09:30:00	47.7	26.9
1672	18/07/2017	09:45:00	47.7	26.9
1673	18/07/2017	10:00:00	47.6	27.0
1674	18/07/2017	10:15:00	47.5	27.1
1675	18/07/2017	10:30:00	47.3	27.1
1676	18/07/2017	10:45:00	47.3	27.2
1677	18/07/2017	11:00:00	47.1	27.2
1678	18/07/2017	11:15:00	46.9	27.3
1679	18/07/2017	11:30:00	46.7	27.3
1680	18/07/2017	11:45:00	46.6	27.4
1681	18/07/2017	12:00:00	46.5	27.4
1682	18/07/2017	12:15:00	46.3	27.5
1683	18/07/2017	12:30:00	46.2	27.5
1684	18/07/2017	12:45:00	46.1	27.5
1685	18/07/2017	13:00:00	46.1	27.5
1686	18/07/2017	13:15:00	46.0	27.6
1687	18/07/2017	13:30:00	45.9	27.6
1688	18/07/2017	13:45:00	45.8	27.7
1689	18/07/2017	14:00:00	45.7	27.8
1690	18/07/2017	14:15:00	45.5	27.8
1691	18/07/2017	14:30:00	45.5	27.9
1692	18/07/2017	14:45:00	45.4	27.9
1693	18/07/2017	15:00:00	45.5	27.9
1694	18/07/2017	15:15:00	45.4	28.0

Index	Date	Time	%RH	°C
1695	18/07/2017	15:30:00	45.3	28.1
1696	18/07/2017	15:45:00	45.0	28.2
1697	18/07/2017	16:00:00	44.8	28.4
1698	18/07/2017	16:15:00	44.5	28.5
1699	18/07/2017	16:30:00	44.4	28.6
1700	18/07/2017	16:45:00	44.3	28.8
1701	18/07/2017	17:00:00	44.3	28.9
1702	18/07/2017	17:15:00	44.2	28.9
1703	18/07/2017	17:30:00	44.2	29.1
1704	18/07/2017	17:45:00	44.1	29.1
1705	18/07/2017	18:00:00	44.1	29.3
1706	18/07/2017	18:15:00	43.9	29.4
1707	18/07/2017	18:30:00	43.8	29.4
1708	18/07/2017	18:45:00	43.8	29.5
1709	18/07/2017	19:00:00	43.7	29.6
1710	18/07/2017	19:15:00	43.9	29.5
1711	18/07/2017	19:30:00	44.0	29.4
1712	18/07/2017	19:45:00	44.1	29.3
1713	18/07/2017	20:00:00	44.4	29.2
1714	18/07/2017	20:15:00	44.7	29.2
1715	18/07/2017	20:30:00	44.8	29.1
1716	18/07/2017	20:45:00	44.9	28.9
1717	18/07/2017	21:00:00	45.1	28.9
1718	18/07/2017	21:15:00	45.2	28.8
1719	18/07/2017	21:30:00	45.3	28.7
1720	18/07/2017	21:45:00	45.5	28.7
1721	18/07/2017	22:00:00	45.5	28.6
1722	18/07/2017	22:15:00	45.6	28.6
1723	18/07/2017	22:30:00	45.8	28.4
1724	18/07/2017	22:45:00	45.9	28.4
1725	18/07/2017	23:00:00	46.0	28.3
1726	18/07/2017	23:15:00	46.1	28.3
1727	18/07/2017	23:30:00	46.3	28.2
1728	18/07/2017	23:45:00	46.4	28.2
1729	19/07/2017	00:00:00	46.6	28.1
1730	19/07/2017	00:15:00	46.8	28.1
1731	19/07/2017	00:30:00	46.9	28.0
1732	19/07/2017	00:45:00	47.1	27.9
1733	19/07/2017	01:00:00	47.1	27.9
1734	19/07/2017	01:15:00	47.3	27.8
1735	19/07/2017	01:30:00	47.6	27.8
1736	19/07/2017	01:45:00	47.7	27.7
1737	19/07/2017	02:00:00	47.8	27.7
1738	19/07/2017	02:15:00	47.9	27.6
1739	19/07/2017	02:30:00	48.1	27.6
1740	19/07/2017	02:45:00	48.2	27.6
1741	19/07/2017	03:00:00	48.5	27.5
1742	19/07/2017	03:15:00	48.6	27.5
1743	19/07/2017	03:30:00	48.6	27.4
1744	19/07/2017	03:45:00	48.7	27.4
1745	19/07/2017	04:00:00	48.9	27.3
1746	19/07/2017	04:15:00	49.1	27.3
1747	19/07/2017	04:30:00	49.3	27.3
1748	19/07/2017	04:45:00	49.4	27.2
1749	19/07/2017	05:00:00	49.5	27.2
1750	19/07/2017	05:15:00	49.5	27.2
1751	19/07/2017	05:30:00	49.8	27.1
1752	19/07/2017	05:45:00	49.9	27.1
1753	19/07/2017	06:00:00	49.6	27.1
1754	19/07/2017	06:15:00	49.5	27.0
1755	19/07/2017	06:30:00	49.8	27.0
1756	19/07/2017	06:45:00	50.0	26.9
1757	19/07/2017	07:00:00	50.3	26.9
1758	19/07/2017	07:15:00	50.4	26.9
1759	19/07/2017	07:30:00	50.4	26.9
1760	19/07/2017	07:45:00	50.4	26.9
1761	19/07/2017	08:00:00	50.6	26.9
1762	19/07/2017	08:15:00	50.6	26.9
1763	19/07/2017	08:30:00	50.4	27.0
1764	19/07/2017	08:45:00	50.7	27.1
1765	19/07/2017	09:00:00	50.9	27.1
1766	19/07/2017	09:15:00	50.9	27.1
1767	19/07/2017	09:30:00	51.0	27.1
1768	19/07/2017	09:45:00	51.2	27.0
1769	19/07/2017	10:00:00	51.2	27.0
1770	19/07/2017	10:15:00	51.2	27.1
1771	19/07/2017	10:30:00	51.1	27.1

Index	Date	Time	%RH	°C
1772	19/07/2017	10:45:00	51.1	27.1
1773	19/07/2017	11:00:00	51.1	27.2
1774	19/07/2017	11:15:00	51.1	27.2
1775	19/07/2017	11:30:00	51.1	27.3
1776	19/07/2017	11:45:00	51.1	27.3
1777	19/07/2017	12:00:00	51.2	27.3
1778	19/07/2017	12:15:00	51.2	27.3
1779	19/07/2017	12:30:00	51.2	27.3
1780	19/07/2017	12:45:00	51.3	27.3
1781	19/07/2017	13:00:00	51.3	27.4
1782	19/07/2017	13:15:00	51.3	27.4
1783	19/07/2017	13:30:00	51.3	27.4
1784	19/07/2017	13:45:00	51.4	27.4
1785	19/07/2017	14:00:00	51.5	27.4
1786	19/07/2017	14:15:00	51.5	27.4
1787	19/07/2017	14:30:00	51.5	27.4
1788	19/07/2017	14:45:00	51.5	27.4
1789	19/07/2017	15:00:00	51.6	27.4
1790	19/07/2017	15:15:00	51.6	27.4
1791	19/07/2017	15:30:00	51.7	27.4
1792	19/07/2017	15:45:00	51.6	27.4
1793	19/07/2017	16:00:00	51.8	27.4
1794	19/07/2017	16:15:00	51.9	27.4
1795	19/07/2017	16:30:00	52.0	27.4
1796	19/07/2017	16:45:00	52.1	27.4
1797	19/07/2017	17:00:00	52.0	27.4
1798	19/07/2017	17:15:00	52.2	27.4
1799	19/07/2017	17:30:00	52.3	27.4
1800	19/07/2017	17:45:00	52.3	27.3
1801	19/07/2017	18:00:00	52.4	27.3
1802	19/07/2017	18:15:00	52.5	27.3
1803	19/07/2017	18:30:00	52.6	27.3
1804	19/07/2017	18:45:00	52.8	27.3
1805	19/07/2017	19:00:00	52.8	27.3
1806	19/07/2017	19:15:00	52.9	27.3
1807	19/07/2017	19:30:00	53.2	27.2
1808	19/07/2017	19:45:00	53.3	27.2
1809	19/07/2017	20:00:00	53.3	27.2
1810	19/07/2017	20:15:00	53.4	27.2
1811	19/07/2017	20:30:00	53.5	27.2
1812	19/07/2017	20:45:00	53.5	27.2
1813	19/07/2017	21:00:00	53.6	27.1
1814	19/07/2017	21:15:00	53.7	27.1
1815	19/07/2017	21:30:00	53.8	27.1
1816	19/07/2017	21:45:00	53.9	27.1
1817	19/07/2017	22:00:00	54.0	27.1
1818	19/07/2017	22:15:00	54.1	27.1
1819	19/07/2017	22:30:00	54.1	27.1
1820	19/07/2017	22:45:00	54.2	27.0
1821	19/07/2017	23:00:00	54.2	27.0
1822	19/07/2017	23:15:00	54.3	26.9
1823	19/07/2017	23:30:00	54.4	26.9
1824	19/07/2017	23:45:00	54.4	26.9
1825	20/07/2017	00:00:00	54.4	26.9
1826	20/07/2017	00:15:00	54.5	26.9
1827	20/07/2017	00:30:00	54.5	26.8
1828	20/07/2017	00:45:00	54.6	26.8
1829	20/07/2017	01:00:00	54.4	26.8
1830	20/07/2017	01:15:00	54.5	26.8
1831	20/07/2017	01:30:00	54.5	26.8
1832	20/07/2017	01:45:00	54.5	26.7
1833	20/07/2017	02:00:00	54.5	26.7
1834	20/07/2017	02:15:00	54.6	26.7
1835	20/07/2017	02:30:00	54.6	26.7
1836	20/07/2017	02:45:00	54.5	26.6
1837	20/07/2017	03:00:00	54.6	26.6
1838	20/07/2017	03:15:00	54.5	26.6
1839	20/07/2017	03:30:00	54.5	26.6
1840	20/07/2017	03:45:00	54.5	26.6
1841	20/07/2017	04:00:00	54.6	26.5
1842	20/07/2017	04:15:00	54.5	26.5
1843	20/07/2017	04:30:00	54.5	26.4
1844	20/07/2017	04:45:00	54.6	26.4
1845	20/07/2017	05:00:00	54.6	26.4
1846	20/07/2017	05:15:00	54.6	26.4
1847	20/07/2017	05:30:00	54.6	26.4
1848	20/07/2017	05:45:00	54.6	26.3

Index	Date	Time	%RH	°C
1849	20/07/2017	06:00:00	54.5	26.3
1850	20/07/2017	06:15:00	54.2	26.3
1851	20/07/2017	06:30:00	54.5	26.3
1852	20/07/2017	06:45:00	54.5	26.3
1853	20/07/2017	07:00:00	54.7	26.3
1854	20/07/2017	07:15:00	54.7	26.3
1855	20/07/2017	07:30:00	54.7	26.2
1856	20/07/2017	07:45:00	54.7	26.2
1857	20/07/2017	08:00:00	54.7	26.2
1858	20/07/2017	08:15:00	54.7	26.2
1859	20/07/2017	08:30:00	54.7	26.2
1860	20/07/2017	08:45:00	54.7	26.2
1861	20/07/2017	09:00:00	54.6	26.2
1862	20/07/2017	09:15:00	54.5	26.2
1863	20/07/2017	09:30:00	54.5	26.1
1864	20/07/2017	09:45:00	54.4	26.1
1865	20/07/2017	10:00:00	54.2	26.1
1866	20/07/2017	10:15:00	54.1	26.1
1867	20/07/2017	10:30:00	53.9	26.1
1868	20/07/2017	10:45:00	53.6	26.1
1869	20/07/2017	11:00:00	53.4	26.1
1870	20/07/2017	11:15:00	53.3	26.1
1871	20/07/2017	11:30:00	53.1	26.1
1872	20/07/2017	11:45:00	53.0	26.1
1873	20/07/2017	12:00:00	52.8	26.1
1874	20/07/2017	12:15:00	52.7	26.1
1875	20/07/2017	12:30:00	52.7	26.2
1876	20/07/2017	12:45:00	52.6	26.2
1877	20/07/2017	13:00:00	52.3	26.2
1878	20/07/2017	13:15:00	52.1	26.3
1879	20/07/2017	13:30:00	52.1	26.3
1880	20/07/2017	13:45:00	51.7	26.4
1881	20/07/2017	14:00:00	51.5	26.4
1882	20/07/2017	14:15:00	51.3	26.4
1883	20/07/2017	14:30:00	51.1	26.5
1884	20/07/2017	14:45:00	51.0	26.4
1885	20/07/2017	15:00:00	50.8	26.4
1886	20/07/2017	15:15:00	50.3	26.5
1887	20/07/2017	15:30:00	49.7	26.6
1888	20/07/2017	15:45:00	49.2	26.7
1889	20/07/2017	16:00:00	48.8	26.8
1890	20/07/2017	16:15:00	48.3	26.9
1891	20/07/2017	16:30:00	47.8	27.1
1892	20/07/2017	16:45:00	47.2	27.2
1893	20/07/2017	17:00:00	46.6	27.4
1894	20/07/2017	17:15:00	46.0	27.5
1895	20/07/2017	17:30:00	45.8	27.5
1896	20/07/2017	17:45:00	45.5	27.6
1897	20/07/2017	18:00:00	45.1	27.7
1898	20/07/2017	18:15:00	44.8	27.7
1899	20/07/2017	18:30:00	44.3	27.7
1900	20/07/2017	18:45:00	44.1	27.8
1901	20/07/2017	19:00:00	43.2	28.3
1902	20/07/2017	19:15:00	42.2	28.8
1903	20/07/2017	19:30:00	41.3	29.2
1904	20/07/2017	19:45:00	40.6	29.5
1905	20/07/2017	20:00:00	40.4	29.4
1906	20/07/2017	20:15:00	40.1	29.6
1907	20/07/2017	20:30:00	40.3	29.3
1908	20/07/2017	20:45:00	40.8	29.0
1909	20/07/2017	21:00:00	41.4	28.7
1910	20/07/2017	21:15:00	41.6	28.5
1911	20/07/2017	21:30:00	41.9	28.3
1912	20/07/2017	21:45:00	42.1	28.2
1913	20/07/2017	22:00:00	42.2	28.1
1914	20/07/2017	22:15:00	42.2	28.0
1915	20/07/2017	22:30:00	41.9	27.9
1916	20/07/2017	22:45:00	42.2	27.8
1917	20/07/2017	23:00:00	42.2	27.7
1918	20/07/2017	23:15:00	42.5	27.7
1919	20/07/2017	23:30:00	42.6	27.6
1920	20/07/2017	23:45:00	42.8	27.5
1921	21/07/2017	00:00:00	43.0	27.4
1922	21/07/2017	00:15:00	43.1	27.4
1923	21/07/2017	00:30:00	43.3	27.3
1924	21/07/2017	00:45:00	43.4	27.2
1925	21/07/2017	01:00:00	43.6	27.1

Index	Date	Time	%RH	°C
1926	21/07/2017	01:15:00	43.8	27.1
1927	21/07/2017	01:30:00	43.9	27.0
1928	21/07/2017	01:45:00	44.1	26.9
1929	21/07/2017	02:00:00	44.2	26.9
1930	21/07/2017	02:15:00	44.4	26.8
1931	21/07/2017	02:30:00	44.5	26.8
1932	21/07/2017	02:45:00	44.6	26.7
1933	21/07/2017	03:00:00	44.8	26.7
1934	21/07/2017	03:15:00	44.9	26.6
1935	21/07/2017	03:30:00	45.1	26.6
1936	21/07/2017	03:45:00	45.2	26.5
1937	21/07/2017	04:00:00	45.4	26.4
1938	21/07/2017	04:15:00	45.5	26.4
1939	21/07/2017	04:30:00	45.7	26.3
1940	21/07/2017	04:45:00	45.8	26.3
1941	21/07/2017	05:00:00	45.9	26.3
1942	21/07/2017	05:15:00	46.0	26.2
1943	21/07/2017	05:30:00	46.2	26.2
1944	21/07/2017	05:45:00	46.3	26.1
1945	21/07/2017	06:00:00	46.0	26.1
1946	21/07/2017	06:15:00	46.3	26.1
1947	21/07/2017	06:30:00	46.6	26.1
1948	21/07/2017	06:45:00	46.7	26.1
1949	21/07/2017	07:00:00	46.7	26.1
1950	21/07/2017	07:15:00	46.8	26.1
1951	21/07/2017	07:30:00	46.9	26.0
1952	21/07/2017	07:45:00	47.0	26.0
1953	21/07/2017	08:00:00	47.0	26.1
1954	21/07/2017	08:15:00	47.1	26.1
1955	21/07/2017	08:30:00	47.2	26.1
1956	21/07/2017	08:45:00	47.2	26.1
1957	21/07/2017	09:00:00	47.3	26.1
1958	21/07/2017	09:15:00	47.2	26.1
1959	21/07/2017	09:30:00	47.2	26.1
1960	21/07/2017	09:45:00	47.2	26.2
1961	21/07/2017	10:00:00	47.2	26.2
1962	21/07/2017	10:15:00	47.2	26.2
1963	21/07/2017	10:30:00	47.1	26.3
1964	21/07/2017	10:45:00	47.2	26.3
1965	21/07/2017	11:00:00	47.3	26.3
1966	21/07/2017	11:15:00	47.2	26.3
1967	21/07/2017	11:30:00	47.3	26.3
1968	21/07/2017	11:45:00	47.4	26.3
1969	21/07/2017	12:00:00	47.4	26.3
1970	21/07/2017	12:15:00	47.3	26.3
1971	21/07/2017	12:30:00	47.2	26.4
1972	21/07/2017	12:45:00	47.2	26.4
1973	21/07/2017	13:00:00	47.2	26.4
1974	21/07/2017	13:15:00	47.3	26.4
1975	21/07/2017	13:30:00	47.3	26.4
1976	21/07/2017	13:45:00	47.4	26.3
1977	21/07/2017	14:00:00	47.4	26.3
1978	21/07/2017	14:15:00	47.4	26.3
1979	21/07/2017	14:30:00	47.3	26.3
1980	21/07/2017	14:45:00	47.4	26.3
1981	21/07/2017	15:00:00	47.4	26.3
1982	21/07/2017	15:15:00	47.2	26.4
1983	21/07/2017	15:30:00	47.1	26.4
1984	21/07/2017	15:45:00	47.0	26.5
1985	21/07/2017	16:00:00	46.9	26.6
1986	21/07/2017	16:15:00	46.9	26.6
1987	21/07/2017	16:30:00	46.8	26.7
1988	21/07/2017	16:45:00	46.8	26.7
1989	21/07/2017	17:00:00	46.8	26.7
1990	21/07/2017	17:15:00	46.9	26.7
1991	21/07/2017	17:30:00	46.9	26.6
1992	21/07/2017	17:45:00	46.9	26.6
1993	21/07/2017	18:00:00	47.0	26.6
1994	21/07/2017	18:15:00	47.2	26.6
1995	21/07/2017	18:30:00	47.2	26.5
1996	21/07/2017	18:45:00	47.2	26.5
1997	21/07/2017	19:00:00	47.3	26.5
1998	21/07/2017	19:15:00	47.3	26.4
1999	21/07/2017	19:30:00	47.4	26.4
2000	21/07/2017	19:45:00	47.4	26.4
2001	21/07/2017	20:00:00	47.4	26.4
2002	21/07/2017	20:15:00	47.4	26.3

Index	Date	Time	%RH	°C
2003	21/07/2017	20:30:00	47.5	26.3
2004	21/07/2017	20:45:00	47.5	26.3
2005	21/07/2017	21:00:00	47.6	26.3
2006	21/07/2017	21:15:00	47.6	26.2
2007	21/07/2017	21:30:00	47.6	26.2
2008	21/07/2017	21:45:00	47.7	26.2
2009	21/07/2017	22:00:00	47.8	26.2
2010	21/07/2017	22:15:00	47.9	26.1
2011	21/07/2017	22:30:00	48.0	26.1
2012	21/07/2017	22:45:00	48.1	26.1
2013	21/07/2017	23:00:00	48.4	26.0
2014	21/07/2017	23:15:00	48.4	26.0
2015	21/07/2017	23:30:00	48.7	25.9
2016	21/07/2017	23:45:00	49.0	25.9
2017	22/07/2017	00:00:00	49.1	25.9
2018	22/07/2017	00:15:00	49.4	25.8
2019	22/07/2017	00:30:00	49.6	25.8
2020	22/07/2017	00:45:00	49.8	25.8
2021	22/07/2017	01:00:00	50.0	25.8
2022	22/07/2017	01:15:00	50.1	25.7
2023	22/07/2017	01:30:00	50.2	25.7
2024	22/07/2017	01:45:00	50.5	25.7
2025	22/07/2017	02:00:00	50.4	25.7
2026	22/07/2017	02:15:00	50.7	25.6
2027	22/07/2017	02:30:00	50.7	25.6
2028	22/07/2017	02:45:00	50.9	25.6
2029	22/07/2017	03:00:00	51.0	25.5
2030	22/07/2017	03:15:00	51.2	25.5
2031	22/07/2017	03:30:00	51.2	25.4
2032	22/07/2017	03:45:00	51.3	25.4
2033	22/07/2017	04:00:00	51.4	25.4
2034	22/07/2017	04:15:00	51.5	25.4
2035	22/07/2017	04:30:00	51.5	25.3
2036	22/07/2017	04:45:00	51.5	25.3
2037	22/07/2017	05:00:00	51.6	25.3
2038	22/07/2017	05:15:00	51.7	25.3
2039	22/07/2017	05:30:00	51.7	25.2
2040	22/07/2017	05:45:00	51.9	25.2
2041	22/07/2017	06:00:00	51.9	25.2
2042	22/07/2017	06:15:00	51.9	25.2
2043	22/07/2017	06:30:00	51.9	25.2
2044	22/07/2017	06:45:00	52.0	25.1
2045	22/07/2017	07:00:00	52.3	25.1
2046	22/07/2017	07:15:00	52.4	25.1
2047	22/07/2017	07:30:00	51.7	25.1
2048	22/07/2017	07:45:00	51.8	25.1
2049	22/07/2017	08:00:00	51.9	25.1
2050	22/07/2017	08:15:00	51.9	25.2
2051	22/07/2017	08:30:00	51.9	25.2
2052	22/07/2017	08:45:00	51.6	25.2
2053	22/07/2017	09:00:00	51.1	25.3
2054	22/07/2017	09:15:00	51.3	25.3
2055	22/07/2017	09:30:00	51.6	25.4
2056	22/07/2017	09:45:00	51.3	25.4
2057	22/07/2017	10:00:00	51.0	25.5
2058	22/07/2017	10:15:00	51.0	25.5
2059	22/07/2017	10:30:00	50.9	25.6
2060	22/07/2017	10:45:00	51.0	25.6
2061	22/07/2017	11:00:00	51.0	25.6
2062	22/07/2017	11:15:00	50.8	25.7
2063	22/07/2017	11:30:00	50.6	25.7
2064	22/07/2017	11:45:00	50.5	25.8
2065	22/07/2017	12:00:00	50.4	25.8
2066	22/07/2017	12:15:00	50.2	25.8
2067	22/07/2017	12:30:00	50.0	25.9
2068	22/07/2017	12:45:00	49.9	26.0
2069	22/07/2017	13:00:00	49.7	26.1
2070	22/07/2017	13:15:00	49.7	26.1
2071	22/07/2017	13:30:00	49.5	26.1
2072	22/07/2017	13:45:00	49.2	26.3
2073	22/07/2017	14:00:00	49.1	26.4
2074	22/07/2017	14:15:00	49.0	26.4
2075	22/07/2017	14:30:00	48.7	26.6
2076	22/07/2017	14:45:00	48.5	26.7
2077	22/07/2017	15:00:00	48.3	26.8
2078	22/07/2017	15:15:00	48.2	26.8
2079	22/07/2017	15:30:00	48.3	26.7

Index	Date	Time	%RH	°C
2080	22/07/2017	15:45:00	48.3	26.6
2081	22/07/2017	16:00:00	48.3	26.6
2082	22/07/2017	16:15:00	48.6	26.5
2083	22/07/2017	16:30:00	48.8	26.4
2084	22/07/2017	16:45:00	48.7	26.4
2085	22/07/2017	17:00:00	48.8	26.4
2086	22/07/2017	17:15:00	48.7	26.3
2087	22/07/2017	17:30:00	48.7	26.3
2088	22/07/2017	17:45:00	48.7	26.2
2089	22/07/2017	18:00:00	48.8	26.2
2090	22/07/2017	18:15:00	49.0	26.2
2091	22/07/2017	18:30:00	49.1	26.1
2092	22/07/2017	18:45:00	49.2	26.1
2093	22/07/2017	19:00:00	49.3	26.1
2094	22/07/2017	19:15:00	49.5	26.1
2095	22/07/2017	19:30:00	49.6	26.0
2096	22/07/2017	19:45:00	49.8	25.9
2097	22/07/2017	20:00:00	49.9	25.9
2098	22/07/2017	20:15:00	50.0	25.8
2099	22/07/2017	20:30:00	50.0	25.8
2100	22/07/2017	20:45:00	50.3	25.8
2101	22/07/2017	21:00:00	50.3	25.7
2102	22/07/2017	21:15:00	50.4	25.7
2103	22/07/2017	21:30:00	50.5	25.7
2104	22/07/2017	21:45:00	50.6	25.6
2105	22/07/2017	22:00:00	50.8	25.6
2106	22/07/2017	22:15:00	50.8	25.6
2107	22/07/2017	22:30:00	50.8	25.5
2108	22/07/2017	22:45:00	50.8	25.5
2109	22/07/2017	23:00:00	50.9	25.4
2110	22/07/2017	23:15:00	50.9	25.4
2111	22/07/2017	23:30:00	51.0	25.4
2112	22/07/2017	23:45:00	51.1	25.3
2113	23/07/2017	00:00:00	51.1	25.3
2114	23/07/2017	00:15:00	51.2	25.3
2115	23/07/2017	00:30:00	51.2	25.2
2116	23/07/2017	00:45:00	51.2	25.2
2117	23/07/2017	01:00:00	51.2	25.2
2118	23/07/2017	01:15:00	51.3	25.1
2119	23/07/2017	01:30:00	51.3	25.1
2120	23/07/2017	01:45:00	51.3	25.1
2121	23/07/2017	02:00:00	51.4	25.0
2122	23/07/2017	02:15:00	51.5	25.0
2123	23/07/2017	02:30:00	51.5	24.9
2124	23/07/2017	02:45:00	51.6	24.9
2125	23/07/2017	03:00:00	51.6	24.9
2126	23/07/2017	03:15:00	51.6	24.9
2127	23/07/2017	03:30:00	51.6	24.8
2128	23/07/2017	03:45:00	51.7	24.7
2129	23/07/2017	04:00:00	51.7	24.7
2130	23/07/2017	04:15:00	51.8	24.7
2131	23/07/2017	04:30:00	51.8	24.7
2132	23/07/2017	04:45:00	51.8	24.7
2133	23/07/2017	05:00:00	51.9	24.7
2134	23/07/2017	05:15:00	51.9	24.7
2135	23/07/2017	05:30:00	51.6	24.6
2136	23/07/2017	05:45:00	51.4	24.6
2137	23/07/2017	06:00:00	51.4	24.6
2138	23/07/2017	06:15:00	51.5	24.6
2139	23/07/2017	06:30:00	51.4	24.6
2140	23/07/2017	06:45:00	51.4	24.5
2141	23/07/2017	07:00:00	51.5	24.5
2142	23/07/2017	07:15:00	51.6	24.5
2143	23/07/2017	07:30:00	51.7	24.5
2144	23/07/2017	07:45:00	51.7	24.5
2145	23/07/2017	08:00:00	51.9	24.5
2146	23/07/2017	08:15:00	51.9	24.6
2147	23/07/2017	08:30:00	51.9	24.6
2148	23/07/2017	08:45:00	52.0	24.6
2149	23/07/2017	09:00:00	51.7	24.7
2150	23/07/2017	09:15:00	51.7	24.7
2151	23/07/2017	09:30:00	51.7	24.7
2152	23/07/2017	09:45:00	51.6	24.7
2153	23/07/2017	10:00:00	51.4	24.7
2154	23/07/2017	10:15:00	51.4	24.8
2155	23/07/2017	10:30:00	51.3	24.9
2156	23/07/2017	10:45:00	51.3	24.9

Index	Date	Time	%RH	°C
2157	23/07/2017	11:00:00	51.2	24.9
2158	23/07/2017	11:15:00	51.2	25.0
2159	23/07/2017	11:30:00	51.1	25.0
2160	23/07/2017	11:45:00	51.0	25.0
2161	23/07/2017	12:00:00	51.0	25.0
2162	23/07/2017	12:15:00	50.9	25.1
2163	23/07/2017	12:30:00	50.7	25.2
2164	23/07/2017	12:45:00	50.6	25.2
2165	23/07/2017	13:00:00	50.4	25.2
2166	23/07/2017	13:15:00	50.3	25.3
2167	23/07/2017	13:30:00	50.1	25.3
2168	23/07/2017	13:45:00	50.0	25.4
2169	23/07/2017	14:00:00	49.9	25.5
2170	23/07/2017	14:15:00	49.8	25.5
2171	23/07/2017	14:30:00	49.7	25.6
2172	23/07/2017	14:45:00	49.4	25.8
2173	23/07/2017	15:00:00	49.3	25.8
2174	23/07/2017	15:15:00	49.2	25.8
2175	23/07/2017	15:30:00	49.1	26.0
2176	23/07/2017	15:45:00	48.8	26.2
2177	23/07/2017	16:00:00	48.6	26.3
2178	23/07/2017	16:15:00	48.5	26.3
2179	23/07/2017	16:30:00	48.4	26.3
2180	23/07/2017	16:45:00	48.3	26.3
2181	23/07/2017	17:00:00	48.1	26.4
2182	23/07/2017	17:15:00	48.1	26.4
2183	23/07/2017	17:30:00	47.9	26.6
2184	23/07/2017	17:45:00	47.8	26.6
2185	23/07/2017	18:00:00	47.6	26.8
2186	23/07/2017	18:15:00	47.7	26.6
2187	23/07/2017	18:30:00	47.8	26.6
2188	23/07/2017	18:45:00	47.9	26.5
2189	23/07/2017	19:00:00	48.1	26.4
2190	23/07/2017	19:15:00	48.5	26.4
2191	23/07/2017	19:30:00	48.6	26.3
2192	23/07/2017	19:45:00	48.7	26.3
2193	23/07/2017	20:00:00	48.8	26.2
2194	23/07/2017	20:15:00	48.9	26.2
2195	23/07/2017	20:30:00	49.0	26.1
2196	23/07/2017	20:45:00	49.1	26.1
2197	23/07/2017	21:00:00	49.2	26.1
2198	23/07/2017	21:15:00	49.3	26.0
2199	23/07/2017	21:30:00	49.4	25.9
2200	23/07/2017	21:45:00	49.5	25.9
2201	23/07/2017	22:00:00	49.7	25.8
2202	23/07/2017	22:15:00	49.8	25.8
2203	23/07/2017	22:30:00	49.9	25.8
2204	23/07/2017	22:45:00	50.0	25.7
2205	23/07/2017	23:00:00	50.1	25.7
2206	23/07/2017	23:15:00	50.2	25.7
2207	23/07/2017	23:30:00	50.3	25.6
2208	23/07/2017	23:45:00	50.4	25.6
2209	24/07/2017	00:00:00	50.5	25.5
2210	24/07/2017	00:15:00	50.7	25.5
2211	24/07/2017	00:30:00	50.7	25.4
2212	24/07/2017	00:45:00	50.8	25.4
2213	24/07/2017	01:00:00	50.9	25.4
2214	24/07/2017	01:15:00	51.0	25.3
2215	24/07/2017	01:30:00	51.2	25.3
2216	24/07/2017	01:45:00	51.3	25.2
2217	24/07/2017	02:00:00	51.3	25.2
2218	24/07/2017	02:15:00	51.4	25.2
2219	24/07/2017	02:30:00	51.6	25.2
2220	24/07/2017	02:45:00	51.7	25.1
2221	24/07/2017	03:00:00	51.7	25.1
2222	24/07/2017	03:15:00	51.7	25.1
2223	24/07/2017	03:30:00	51.9	25.0
2224	24/07/2017	03:45:00	51.9	25.0
2225	24/07/2017	04:00:00	51.9	24.9
2226	24/07/2017	04:15:00	51.9	24.9
2227	24/07/2017	04:30:00	52.1	24.9
2228	24/07/2017	04:45:00	52.1	24.8
2229	24/07/2017	05:00:00	52.1	24.7
2230	24/07/2017	05:15:00	52.1	24.7
2231	24/07/2017	05:30:00	52.2	24.7
2232	24/07/2017	05:45:00	52.3	24.7
2233	24/07/2017	06:00:00	52.3	24.7

Index	Date	Time	%RH	°C
2234	24/07/2017	06:15:00	52.4	24.7
2235	24/07/2017	06:30:00	52.4	24.7
2236	24/07/2017	06:45:00	52.5	24.7
2237	24/07/2017	07:00:00	52.5	24.7
2238	24/07/2017	07:15:00	52.5	24.6
2239	24/07/2017	07:30:00	52.2	24.6
2240	24/07/2017	07:45:00	52.0	24.6
2241	24/07/2017	08:00:00	51.9	24.6
2242	24/07/2017	08:15:00	51.6	24.6
2243	24/07/2017	08:30:00	51.3	24.5
2244	24/07/2017	08:45:00	51.1	24.5
2245	24/07/2017	09:00:00	51.2	24.5
2246	24/07/2017	09:15:00	51.1	24.5
2247	24/07/2017	09:30:00	51.4	24.5
2248	24/07/2017	09:45:00	51.6	24.5
2249	24/07/2017	10:00:00	50.9	24.5
2250	24/07/2017	10:15:00	50.8	24.6
2251	24/07/2017	10:30:00	50.8	24.5
2252	24/07/2017	10:45:00	50.7	24.6
2253	24/07/2017	11:00:00	50.4	24.6
2254	24/07/2017	11:15:00	50.5	24.6
2255	24/07/2017	11:30:00	50.6	24.6
2256	24/07/2017	11:45:00	50.6	24.6
2257	24/07/2017	12:00:00	50.6	24.6
2258	24/07/2017	12:15:00	50.5	24.6
2259	24/07/2017	12:30:00	50.6	24.6
2260	24/07/2017	12:45:00	50.5	24.7
2261	24/07/2017	13:00:00	50.5	24.7
2262	24/07/2017	13:15:00	50.4	24.7
2263	24/07/2017	13:30:00	50.3	24.9
2264	24/07/2017	13:45:00	50.3	24.9
2265	24/07/2017	14:00:00	50.3	24.9
2266	24/07/2017	14:15:00	50.2	25.0
2267	24/07/2017	14:30:00	50.2	25.0
2268	24/07/2017	14:45:00	50.2	25.1
2269	24/07/2017	15:00:00	50.2	25.1
2270	24/07/2017	15:15:00	50.2	25.2
2271	24/07/2017	15:30:00	50.1	25.2
2272	24/07/2017	15:45:00	50.1	25.2
2273	24/07/2017	16:00:00	50.0	25.2
2274	24/07/2017	16:15:00	50.0	25.2
2275	24/07/2017	16:30:00	50.0	25.3
2276	24/07/2017	16:45:00	49.9	25.3
2277	24/07/2017	17:00:00	50.0	25.3
2278	24/07/2017	17:15:00	50.1	25.3
2279	24/07/2017	17:30:00	50.1	25.3
2280	24/07/2017	17:45:00	50.2	25.3
2281	24/07/2017	18:00:00	50.2	25.3
2282	24/07/2017	18:15:00	50.1	25.3
2283	24/07/2017	18:30:00	50.0	25.4
2284	24/07/2017	18:45:00	49.1	26.1
2285	24/07/2017	19:00:00	48.6	26.4
2286	24/07/2017	19:15:00	47.8	26.8
2287	24/07/2017	19:30:00	47.2	27.1
2288	24/07/2017	19:45:00	47.3	27.1
2289	24/07/2017	20:00:00	47.0	27.2
2290	24/07/2017	20:15:00	46.9	27.2
2291	24/07/2017	20:30:00	47.2	27.0
2292	24/07/2017	20:45:00	47.4	26.8
2293	24/07/2017	21:00:00	48.0	26.6
2294	24/07/2017	21:15:00	48.3	26.4
2295	24/07/2017	21:30:00	48.5	26.3
2296	24/07/2017	21:45:00	48.5	26.2
2297	24/07/2017	22:00:00	48.7	26.2
2298	24/07/2017	22:15:00	48.8	26.1
2299	24/07/2017	22:30:00	48.9	26.1
2300	24/07/2017	22:45:00	49.0	25.9
2301	24/07/2017	23:00:00	49.0	25.9
2302	24/07/2017	23:15:00	49.1	25.8
2303	24/07/2017	23:30:00	49.3	25.8
2304	24/07/2017	23:45:00	49.4	25.7
2305	25/07/2017	00:00:00	49.5	25.7
2306	25/07/2017	00:15:00	49.7	25.6
2307	25/07/2017	00:30:00	49.8	25.6
2308	25/07/2017	00:45:00	49.9	25.5
2309	25/07/2017	01:00:00	50.0	25.4
2310	25/07/2017	01:15:00	50.1	25.4

Index	Date	Time	%RH	°C
2311	25/07/2017	01:30:00	50.3	25.3
2312	25/07/2017	01:45:00	50.6	25.3
2313	25/07/2017	02:00:00	50.6	25.2
2314	25/07/2017	02:15:00	50.5	25.2
2315	25/07/2017	02:30:00	50.8	25.1
2316	25/07/2017	02:45:00	50.8	25.1
2317	25/07/2017	03:00:00	50.9	25.0
2318	25/07/2017	03:15:00	51.0	24.9
2319	25/07/2017	03:30:00	51.0	24.9
2320	25/07/2017	03:45:00	51.0	24.9
2321	25/07/2017	04:00:00	51.0	24.7
2322	25/07/2017	04:15:00	51.1	24.7
2323	25/07/2017	04:30:00	51.2	24.7
2324	25/07/2017	04:45:00	51.2	24.7
2325	25/07/2017	05:00:00	51.2	24.7
2326	25/07/2017	05:15:00	51.3	24.7
2327	25/07/2017	05:30:00	51.2	24.6
2328	25/07/2017	05:45:00	51.3	24.6
2329	25/07/2017	06:00:00	51.4	24.6
2330	25/07/2017	06:15:00	51.5	24.5
2331	25/07/2017	06:30:00	51.5	24.5
2332	25/07/2017	06:45:00	51.6	24.4
2333	25/07/2017	07:00:00	51.6	24.4
2334	25/07/2017	07:15:00	51.3	24.4
2335	25/07/2017	07:30:00	51.2	24.4
2336	25/07/2017	07:45:00	51.3	24.4
2337	25/07/2017	08:00:00	51.4	24.4
2338	25/07/2017	08:15:00	51.4	24.4
2339	25/07/2017	08:30:00	51.3	24.3
2340	25/07/2017	08:45:00	51.4	24.3
2341	25/07/2017	09:00:00	51.1	24.3
2342	25/07/2017	09:15:00	51.0	24.3
2343	25/07/2017	09:30:00	50.9	24.4
2344	25/07/2017	09:45:00	50.9	24.4
2345	25/07/2017	10:00:00	50.8	24.4
2346	25/07/2017	10:15:00	50.7	24.5
2347	25/07/2017	10:30:00	50.7	24.6
2348	25/07/2017	10:45:00	50.6	24.6
2349	25/07/2017	11:00:00	50.6	24.7
2350	25/07/2017	11:15:00	50.2	24.7
2351	25/07/2017	11:30:00	47.9	24.7
2352	25/07/2017	11:45:00	48.5	24.7
2353	25/07/2017	12:00:00	49.5	24.7
2354	25/07/2017	12:15:00	47.1	24.7
2355	25/07/2017	12:30:00	46.9	24.7
2356	25/07/2017	12:45:00	46.9	24.7
2357	25/07/2017	13:00:00	46.7	24.7
2358	25/07/2017	13:15:00	46.7	24.7
2359	25/07/2017	13:30:00	47.0	24.7
2360	25/07/2017	13:45:00	47.5	24.8
2361	25/07/2017	14:00:00	47.7	24.9
2362	25/07/2017	14:15:00	47.2	24.9
2363	25/07/2017	14:30:00	46.6	24.8
2364	25/07/2017	14:45:00	46.4	24.9
2365	25/07/2017	15:00:00	46.8	24.9
2366	25/07/2017	15:15:00	47.7	24.9
2367	25/07/2017	15:30:00	47.6	25.1
2368	25/07/2017	15:45:00	47.7	25.1
2369	25/07/2017	16:00:00	47.7	25.2
2370	25/07/2017	16:15:00	47.7	25.3
2371	25/07/2017	16:30:00	47.7	25.4
2372	25/07/2017	16:45:00	47.6	25.6
2373	25/07/2017	17:00:00	47.2	25.8
2374	25/07/2017	17:15:00	47.0	26.0
2375	25/07/2017	17:30:00	46.8	26.2
2376	25/07/2017	17:45:00	46.6	26.4
2377	25/07/2017	18:00:00	46.1	26.7
2378	25/07/2017	18:15:00	45.4	26.8
2379	25/07/2017	18:30:00	43.1	27.1
2380	25/07/2017	18:45:00	43.0	27.3
2381	25/07/2017	19:00:00	42.6	27.1
2382	25/07/2017	19:15:00	44.0	26.9
2383	25/07/2017	19:30:00	44.6	26.7
2384	25/07/2017	19:45:00	44.6	26.7
2385	25/07/2017	20:00:00	44.6	26.5
2386	25/07/2017	20:15:00	45.1	26.4
2387	25/07/2017	20:30:00	46.3	26.2
2388	25/07/2017	20:45:00	46.2	26.1
2389	25/07/2017	21:00:00	46.6	26.0
2390	25/07/2017	21:15:00	46.9	26.0
2391	25/07/2017	21:30:00	47.0	25.9
2392	25/07/2017	21:45:00	47.1	25.9
2393	25/07/2017	22:00:00	47.3	25.8
2394	25/07/2017	22:15:00	47.5	25.8
2395	25/07/2017	22:30:00	47.7	25.8
2396	25/07/2017	22:45:00	47.9	25.7
2397	25/07/2017	23:00:00	48.2	25.7
2398	25/07/2017	23:15:00	48.4	25.6
2399	25/07/2017	23:30:00	48.6	25.6
2400	25/07/2017	23:45:00	48.7	25.6
2401	26/07/2017	00:00:00	48.9	25.5
2402	26/07/2017	00:15:00	49.1	25.4
2403	26/07/2017	00:30:00	49.2	25.4
2404	26/07/2017	00:45:00	49.5	25.4
2405	26/07/2017	01:00:00	49.6	25.3
2406	26/07/2017	01:15:00	49.8	25.3
2407	26/07/2017	01:30:00	49.9	25.3
2408	26/07/2017	01:45:00	50.1	25.2
2409	26/07/2017	02:00:00	50.2	25.2
2410	26/07/2017	02:15:00	50.5	25.2
2411	26/07/2017	02:30:00	50.6	25.1
2412	26/07/2017	02:45:00	50.8	25.1
2413	26/07/2017	03:00:00	50.9	25.0
2414	26/07/2017	03:15:00	51.2	25.0
2415	26/07/2017	03:30:00	51.0	24.9
2416	26/07/2017	03:45:00	51.3	24.9
2417	26/07/2017	04:00:00	51.3	24.9
2418	26/07/2017	04:15:00	51.5	24.7
2419	26/07/2017	04:30:00	51.7	24.7
2420	26/07/2017	04:45:00	51.8	24.7
2421	26/07/2017	05:00:00	51.7	24.7
2422	26/07/2017	05:15:00	52.0	24.7
2423	26/07/2017	05:30:00	52.0	24.7
2424	26/07/2017	05:45:00	52.0	24.7
2425	26/07/2017	06:00:00	52.0	24.6
2426	26/07/2017	06:15:00	51.5	24.6
2427	26/07/2017	06:30:00	51.6	24.6
2428	26/07/2017	06:45:00	51.9	24.6
2429	26/07/2017	07:00:00	51.9	24.6
2430	26/07/2017	07:15:00	52.0	24.6
2431	26/07/2017	07:30:00	52.0	24.6
2432	26/07/2017	07:45:00	52.1	24.6
2433	26/07/2017	08:00:00	51.6	24.5
2434	26/07/2017	08:15:00	51.3	24.6
2435	26/07/2017	08:30:00	51.3	24.6
2436	26/07/2017	08:45:00	51.2	24.6
2437	26/07/2017	09:00:00	51.2	24.6
2438	26/07/2017	09:15:00	51.2	24.6
2439	26/07/2017	09:30:00	51.3	24.6
2440	26/07/2017	09:45:00	51.5	24.6
2441	26/07/2017	10:00:00	51.7	24.6
2442	26/07/2017	10:15:00	51.8	24.6
2443	26/07/2017	10:30:00	52.0	24.6
2444	26/07/2017	10:45:00	52.1	24.6
2445	26/07/2017	11:00:00	53.7	24.5

Summary

Log Tag ID	**1010095587**	
User ID	**5587**	
Log Tag battery	**OK**	
Non alert range	**0.0 to 100.0 %RH**	**-18.9 to -13.9 °C**
Time zone	**UTC +00:00, daylight time**	
Number of readings	**2445**	
Reading interval	**15 Minutes**	
Number of starts	**1**	
First reading	**01/07/2017 00:00:00**	
Last reading	**26/07/2017 11:00:00**	
Elapsed Time	**25 Days, 11 Hours**	
Reading range	**34.7 to 56.5 %RH**	**22.3 to 30.2 °C**
Average reading	**48.8 %RH**	**26.0 °C**
Standard Deviation (S)	**3.3 %RH**	**1.4 °C**
Degree Minutes below lower alert	**0.00 %RH-Minutes**	**0.00 °C-Minutes**
Degree Minutes above upper alert	**0.00 %RH-Minutes**	**1,464,921.00 °C-Minutes**
Mean Kinetic Temperature		**26.14 °C**
Time below lower alert	**None**	**None**
Time above upper alert	**None**	**25 Days, 11 Hours**
Time not in alert	**25 Days, 11 Hours**	**None**

Appendix B: Thermography Results

Infrared thermography survey of the clubhouse was carried out in the summer of 2019 to see the extent at which the deficiencies have increased. The survey was done on the 10th of April 2019 during the day. Results revealed that more internal cracks have surfaced in the building hence increasing the infiltration levels, which in turns increases the air changes per hour.

The images of the cracks and other deficiencies are presented in this section of the appendices. The images have been divided into main-lounge and changing rooms images.

Appendix B1: Main- Lounge Survey

In the main-lounge, it was observed that there was no new deficiency other than the deficiencies noted in the first thermography survey. However, the cracks on the external wall and joints have increased (see below).

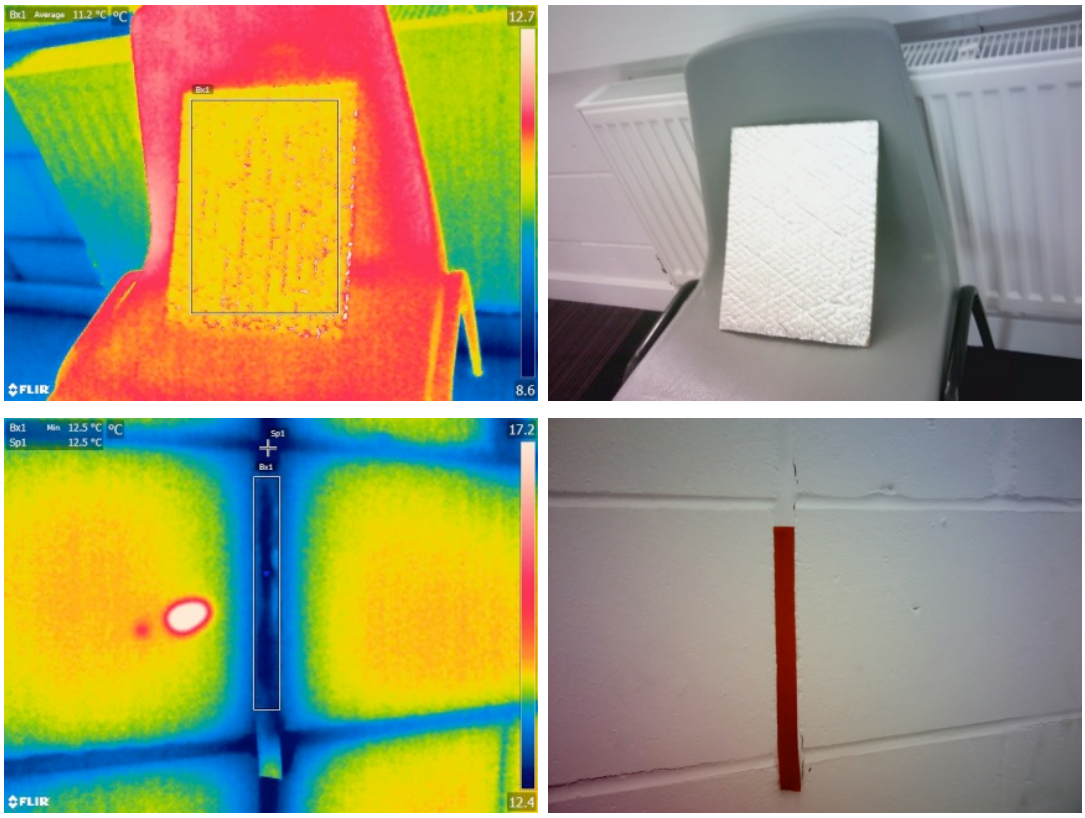

Figure B-0-1: Determination of effective temperature and emissivity using a thermal camera

Figure B-0-1 shows the methods used to obtain the reflective temperature using a crunched aluminium foil (top) and emissivity using a material with known emissivity, in this case, an electrical tape.

Figure B-0-2: Thermal images and digital images of the external wall in main-lounge

The figure below shows the locations of each of the steel frame cramps along each of the five windows. The steel cramps are a major source of heat loss from within the room.

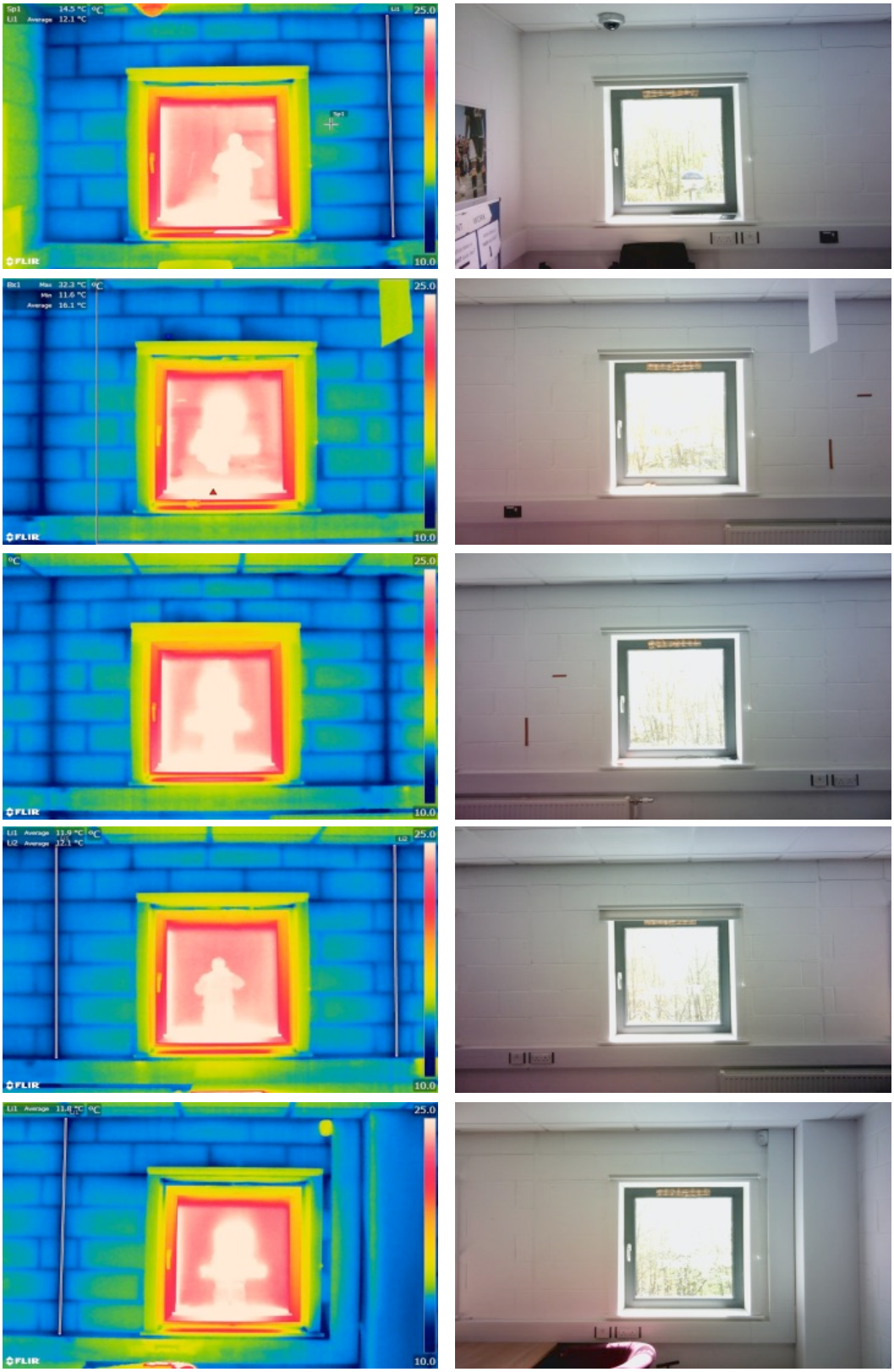

Figure B-0-3: Steel cramp location on the window (thermal and digital images)

Appendix B2: Changing Rooms Survey

In the changing rooms, new deficiencies have been observed in comparison with the survey conducted during the winter period. The deficiencies are mostly cracking in the internal wall, which increases infiltration and air changes per hour; hence, an increase in energy use to keep the rooms at the desired temperature. Below are thermal images with their corresponding digital images to show the deficiencies encountered during the survey.

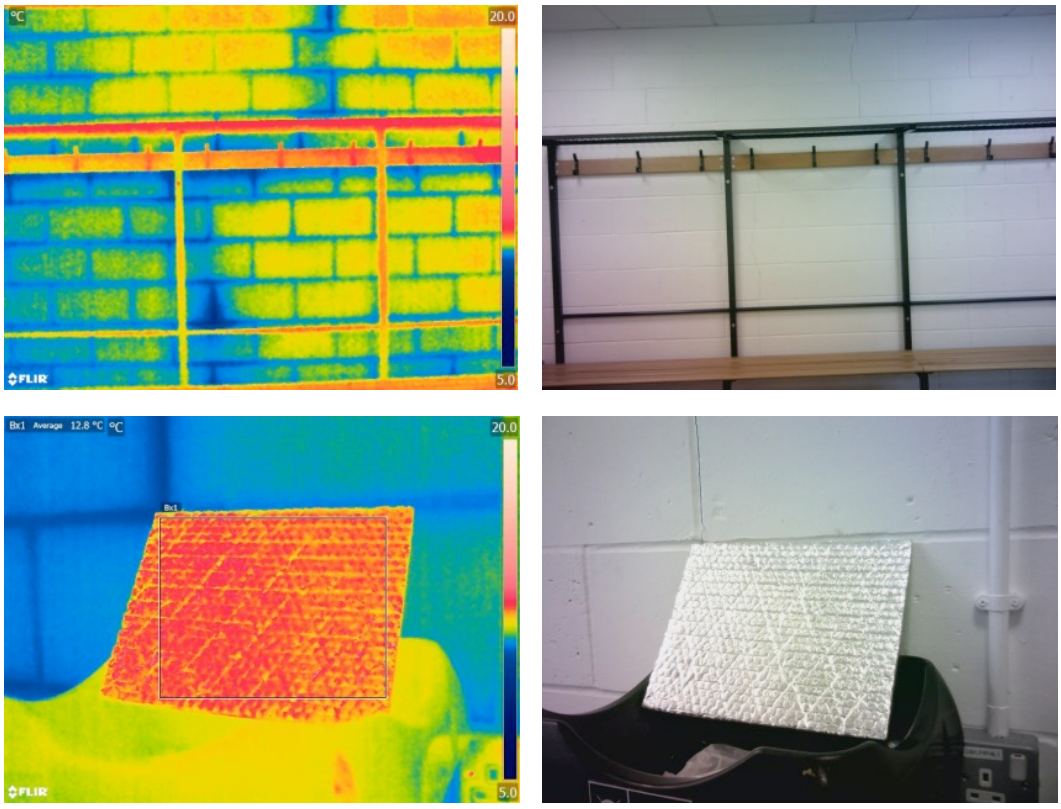

Figure B-0-4: Thermal image and a digital image of a crack in the internal wall (top) and reflective temperature measurement (bottom)

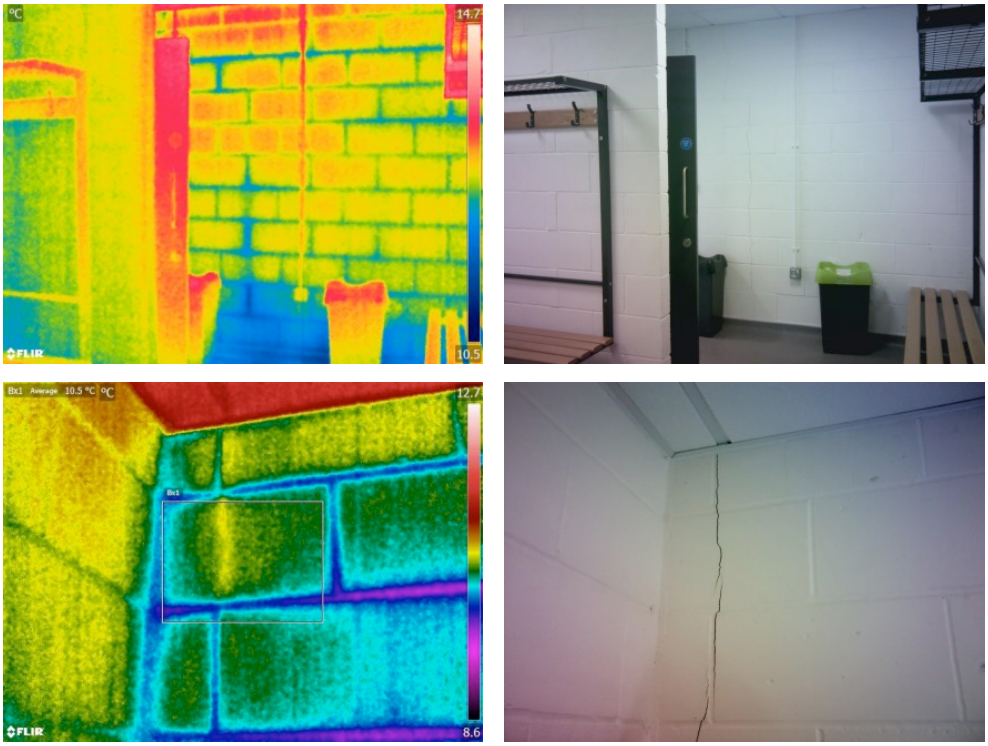

Figure B-0-5: Thermal images and digital images of cracks in the internal wall (changing room 3)

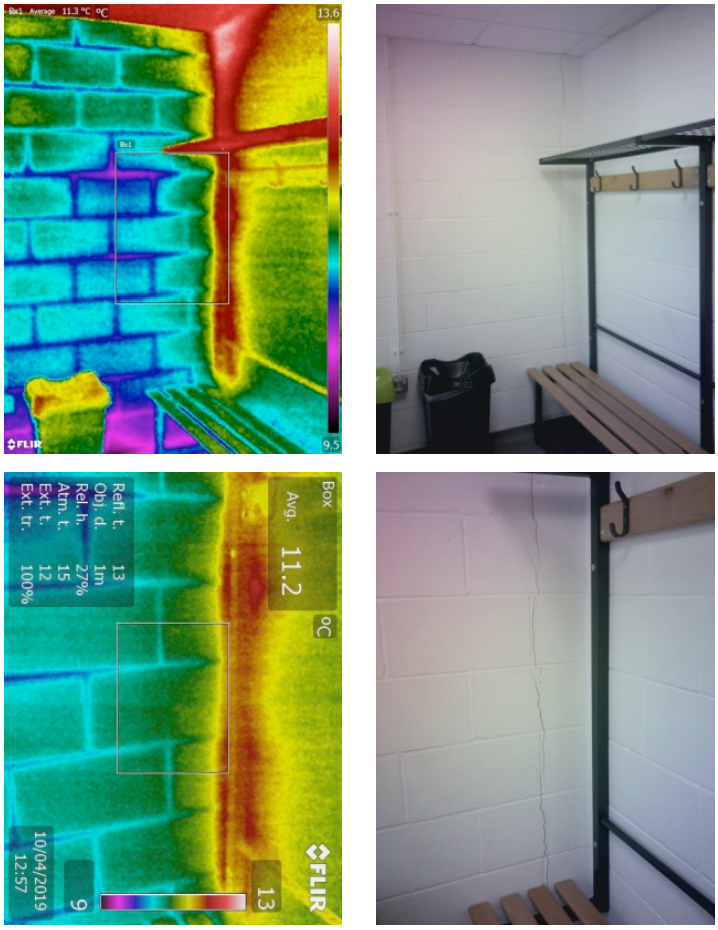

Figure B-0-6: Thermal images and digital images of cracks in the internal wall (changing room 2)

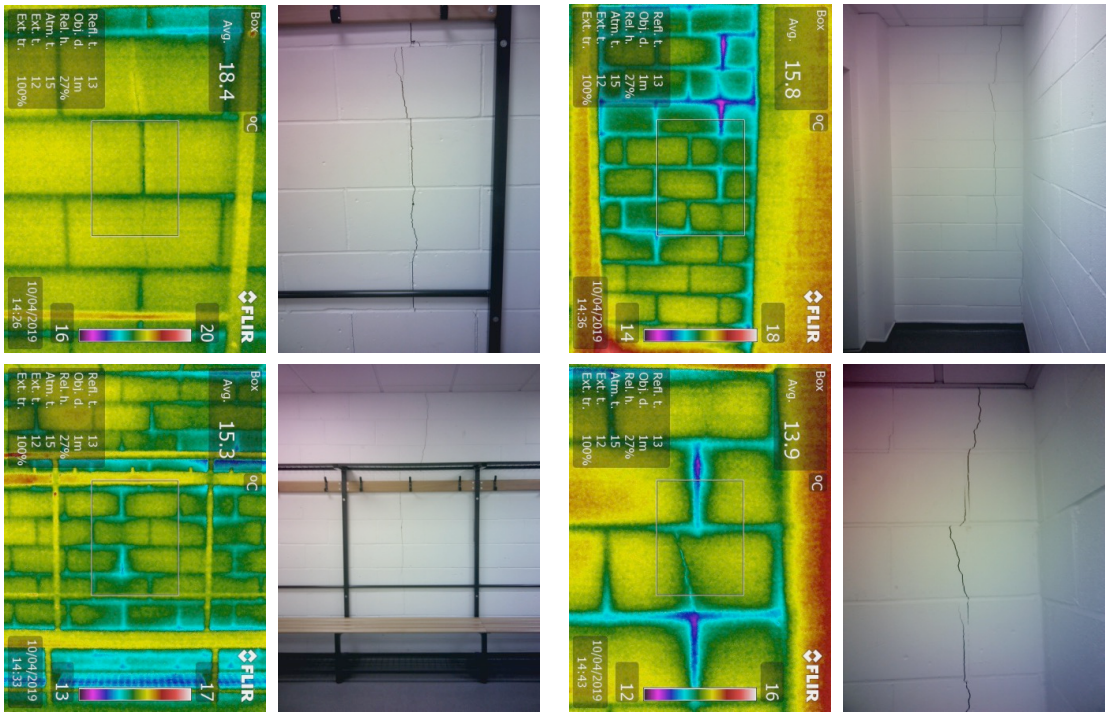

Figure B-0-7: Thermal images and digital images of cracks in the internal wall (changing room 5)

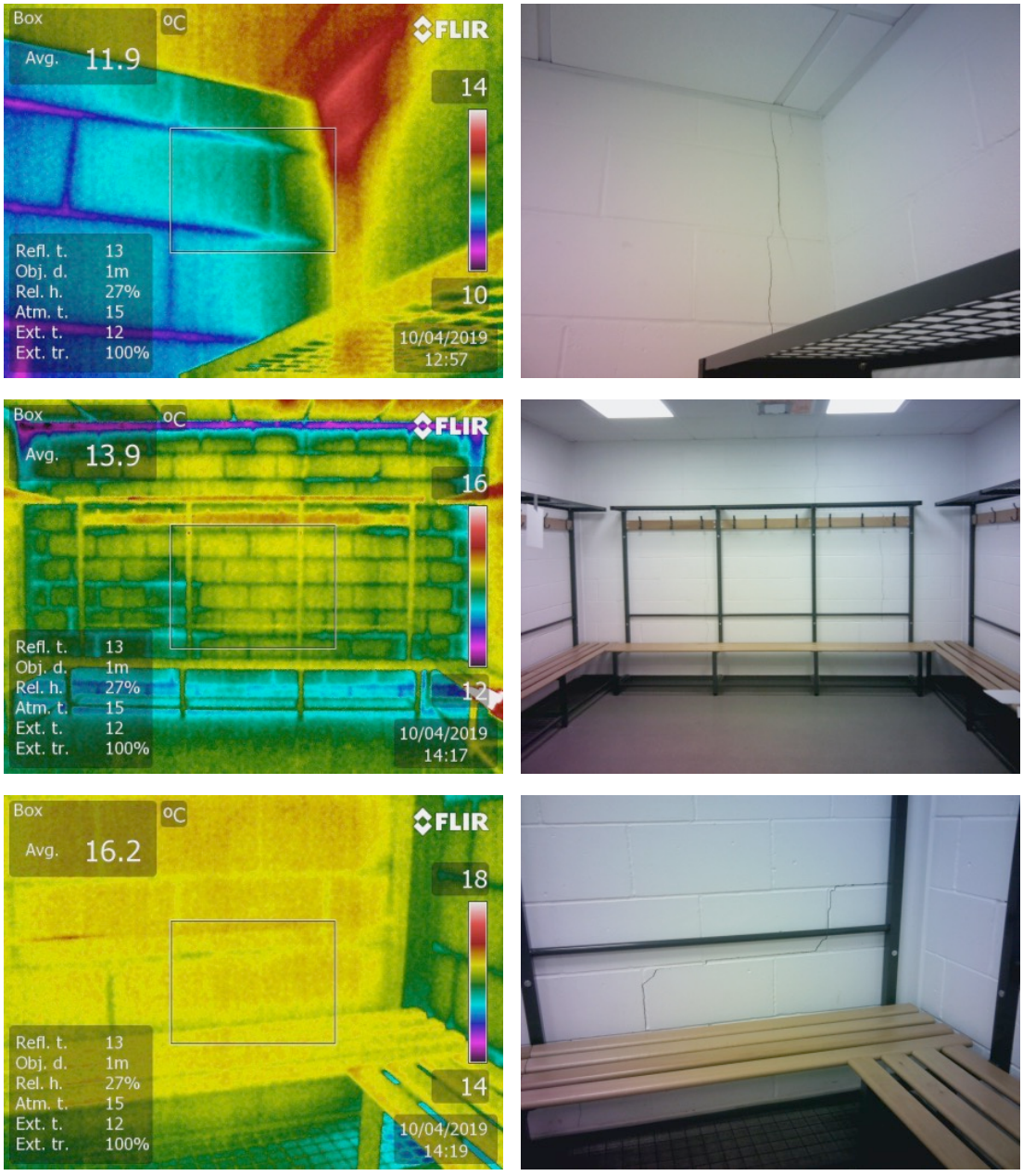

Figure B-0-8: Thermal images and digital images of cracks in the internal wall (changing room 6)

Appendix C: Computer Simulation

DesignBuilder displays the results from EnergyPlus output files in the form of graphs (which can be exported as images), grid (which can be exported as a .csv file) and graph and table (which can be exported as images). For ease of comparison between EnergyPlus results and monitored results, the results were exported as a .csv result and imported into MATLAB for analysis.

In this section, the results from EnergyPlus are displayed in the form of images downloaded from the DesignBuilder software. The results are divided into two sections, the year 2017 and the year 2018 which corresponds to the time of monitoring.

Appendix C1: Energy Results of 2017

As mentioned in Section 5.4.2, the weather data used to simulate the Clifton Clubhouse was obtained from the UK Met Office. The requested data were for the monitoring period of July 2017 to July 2018. The data was processed into EnergyPlus readable weather data (.epw) using software called Elements. Figure C1-0-1 below shows the processed data in DesignBuilder for the period of June 2017 to December 2017.

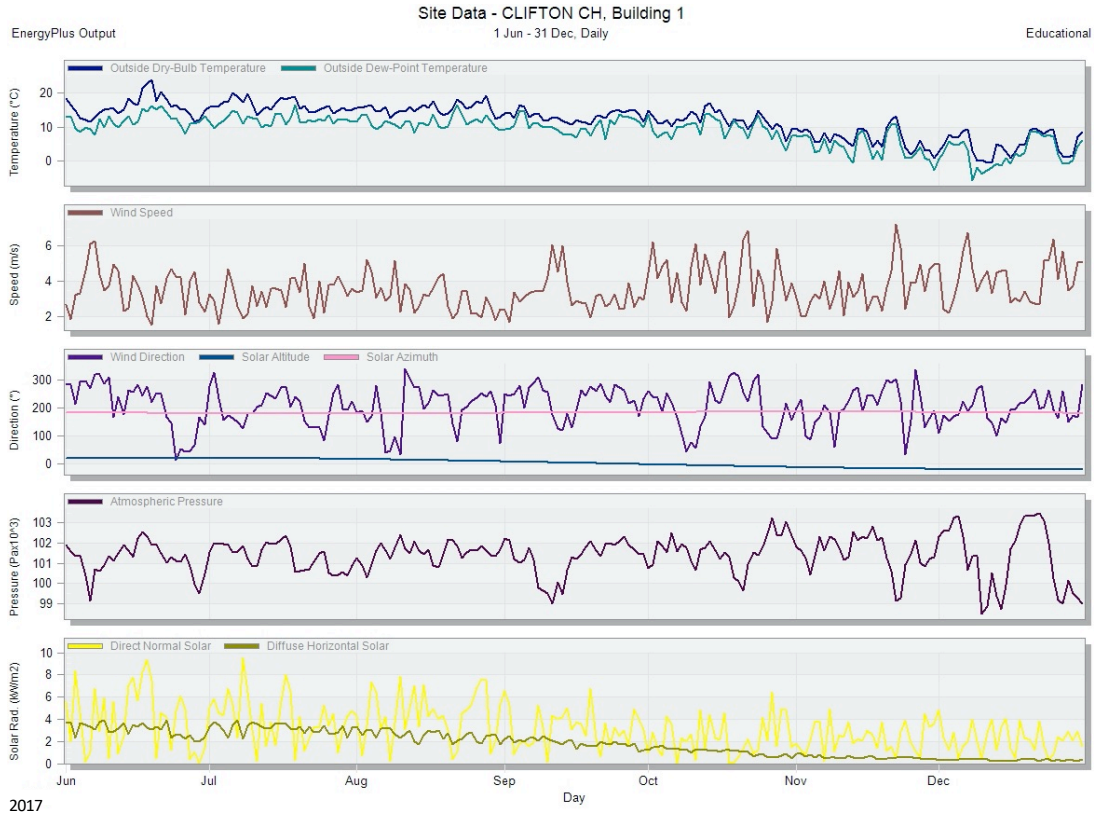

Figure C1-0-1: Site Data year 2017

The comfort temperatures (see Figure C1-0-2), which are air, radiant and operative temperatures were observed to have an average reading of 20.02°C, 20.61°C and 20.31°C respectively. The average outside dry bulb temperature has an average reading of 12.16°C. Relative humidity within the facility was observed to be 53.79% while thermal comfort using Fanger PMV index was revealed to be -0.66, which translates into the neutral comfort zone.

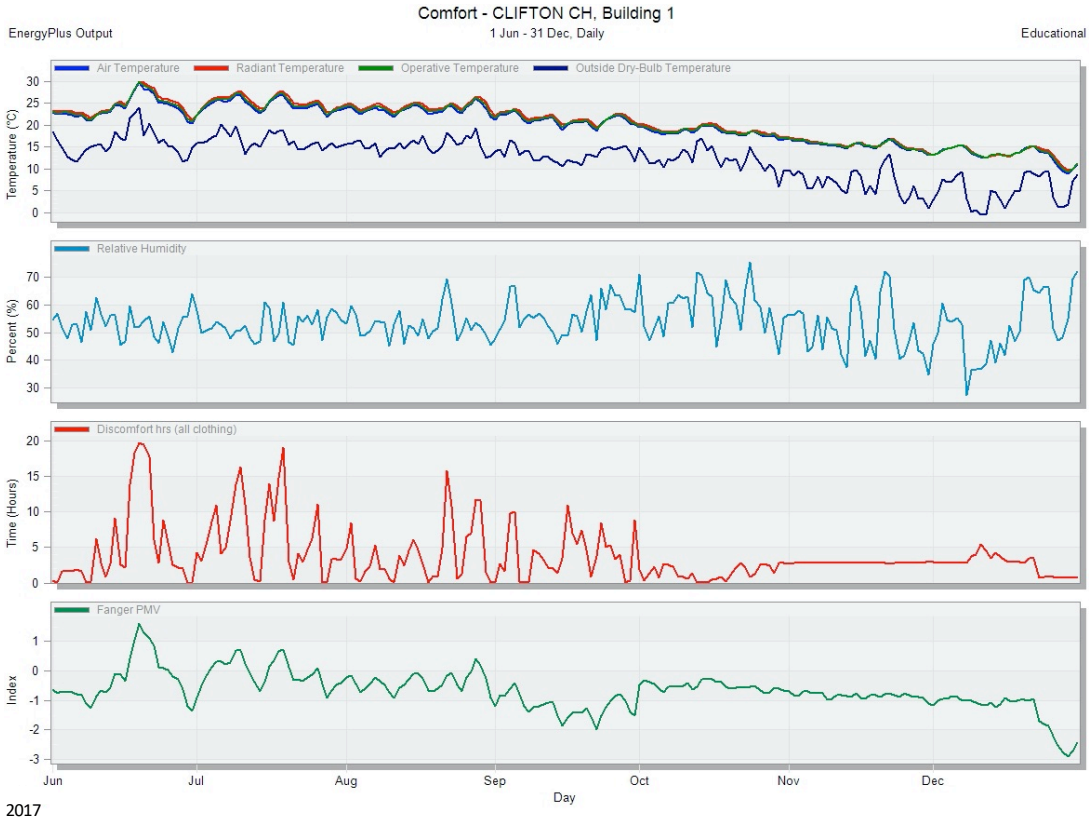

Figure C1-0-2: Comfort results year 2017

External walls, internal floors, roofs, external ventilation and infiltration were observed to have been the main contributors of heat loss within the Clifton clubhouse. The average air changes per hour in the facility due to mechanical ventilation, natural ventilation and infiltration were observed to be 1.45. The daily averages of the heat losses and gains and air changes per hour of the facility are shown in Figure C1-0-3

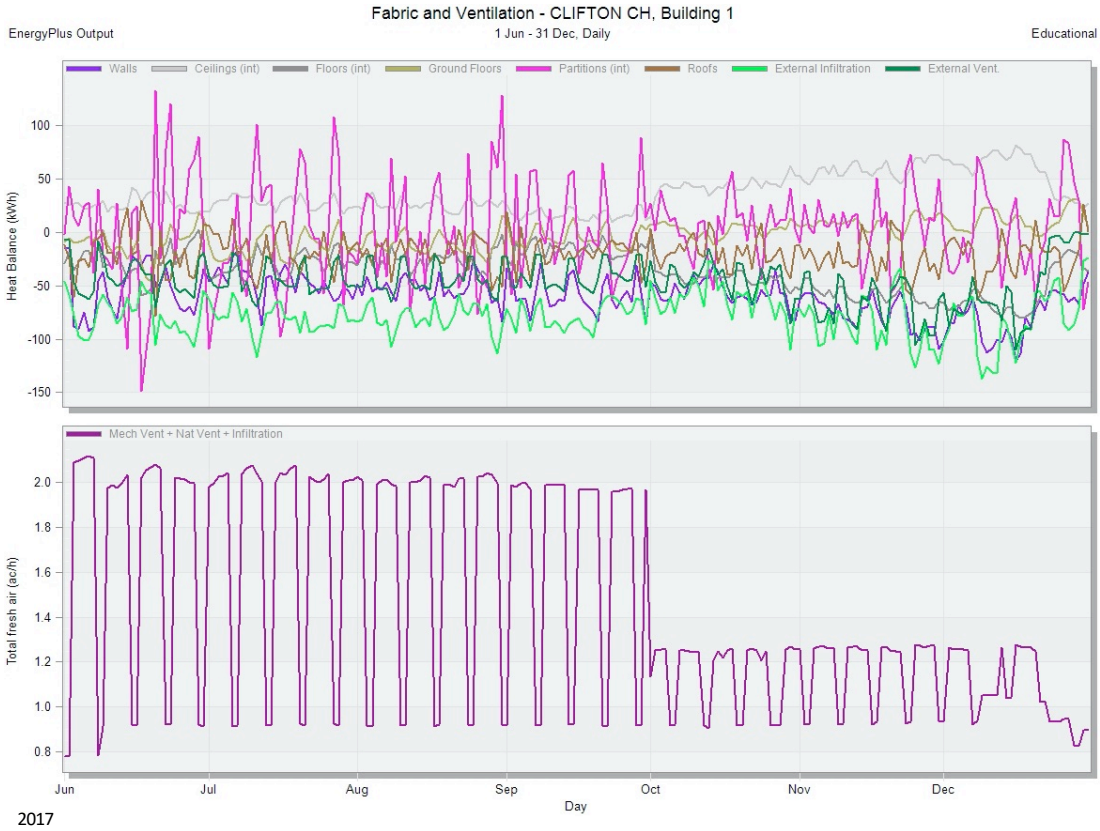

Figure C1-0-3: Fabric and Ventilation results year 2017

The fuel usage of the Clifton clubhouse was also calculated using EnergyPlus. Results (shown in Figure C1-0-4) revealed that the main usage of electricity comes from the room electricity (which is used for appliances) and that of natural gas is heating. The total natural gas used within June 2017 and December 2017 was 14236.61 (kWh) while the total electricity used was 23967.58 (kWh). However, due to the availability of photovoltaic panels, the clubhouse generated a total 17475.03 (kWh) of electricity. From the generated electricity, the highest share of electricity was generated in the summer months of June, July, August and September with readings of 4007.31 (kWh), 4137.27(kWh), 3705.28 (kWh) and 2.499.13 (kWh) respectively. Due to the electricity generated in the clubhouse, the CO2 production was observed to be low during the summer months with a minimum production value of 113.53 (kg) in June and a maximum of 1943.11 (kg) in December.

Figure C1-0-4: Fuel breakdown results 2017

Appendix C2: Energy Results of 2018

The site data for the year 2018 (Jan 2018 to Jul 2018) is shown below (see Figure C2-0-5). The outside dry temperature has an annual average of 10.08°C with the highest temperature of 19.30°C occurring in July and the lowest temperature of 2.47°C occurring in February. The average wind speed recorded within that period was 3.76(m/s) with an average direction of 200.19°. Solar Altitude and azimuth had an average reading of 4.79° and 179.45° respectively. The atmospheric pressure within that period has an average reading of 101.34 (kPa), while direct solar and diffuse horizontal solar has a reading of 698.42 (kWh) and 426.42 (kWh) respectively.

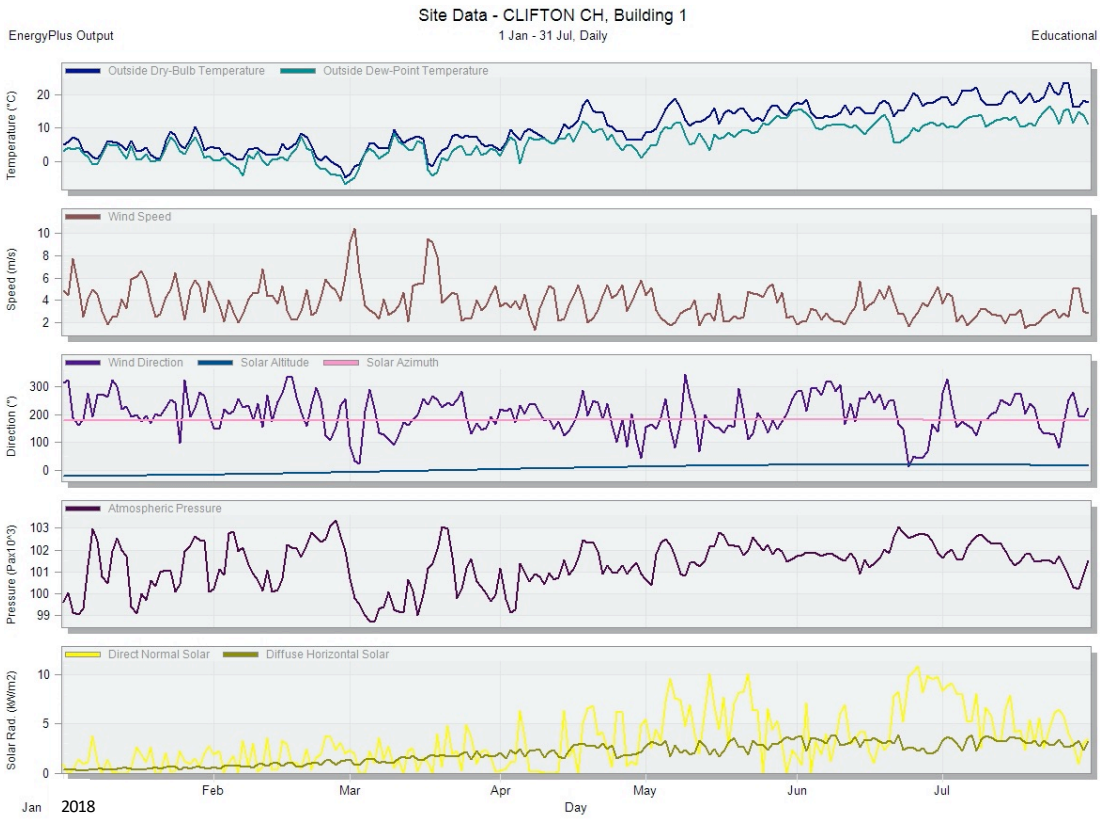

Figure C2-0-5: Site data from the UK Met office processed in DesignBuilder for the year 2018 (Jan - Jul)

For comfort results (see Figure C2-0-6), the air, radiant and operative temperature within the building had an average reading of 17.94°C, 18.59°C and 18.26°C respectively. Relative humidity in the facility ranges from 47.24% to 56.74%. Using the Fanger PMV scale, the average thermal comfort reading was -1.05, which means that the occupants felt slightly cool

within that period. However, during the summer period, the Fanger PMV result was neutral with a reading of 0.73.

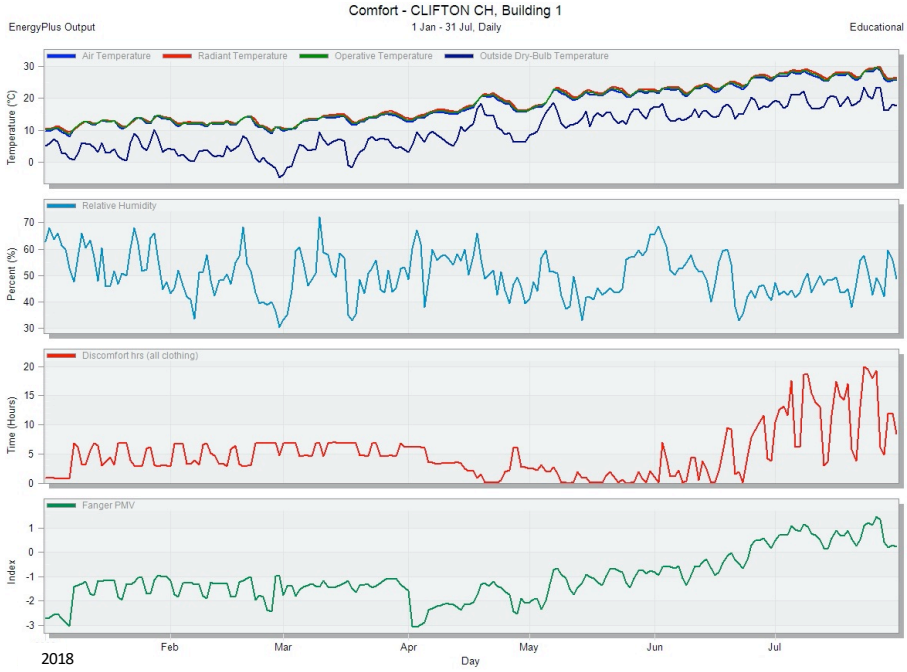

Figure C2-0-6: Comfort results for the year 2018

In terms of heat losses and gains due to fabric and ventilation (see Figure C2-0-7). The Clifton clubhouse had heat losses mainly due to external walls, internal floors, external infiltration and external vents which were the main contributors. The roof and internal partitions also played a part in the heat losses in the facility. Due to the presence of heat recovery units, the mechanical ventilation together with the natural ventilation and infiltration were calculated to have an average reading of 1.40 air changes per hour.

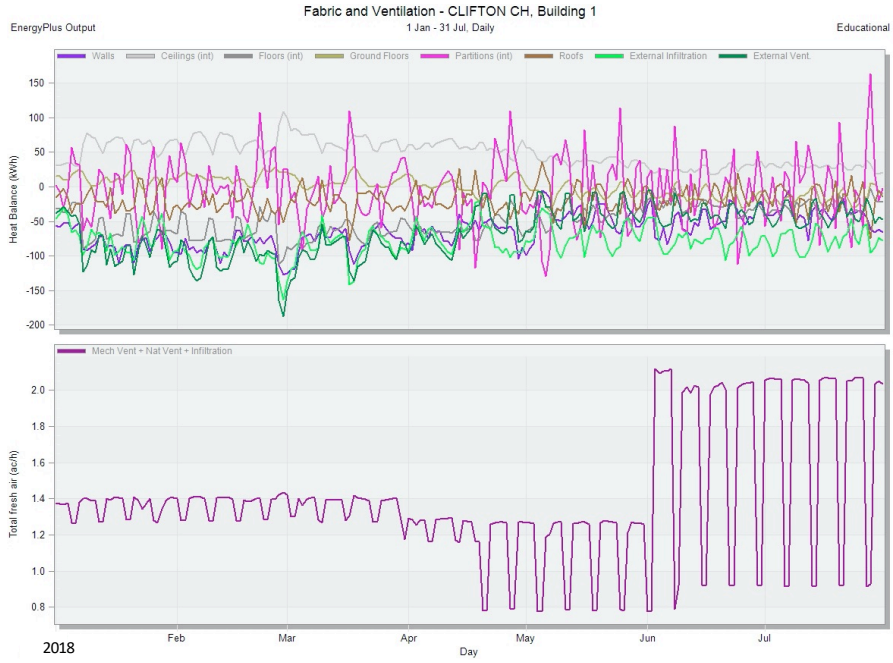

Figure C2-0-7: Fabric and ventilation results for the year 2018

The breakdown of fuel consumption was calculated, and the results are shown in Figure C2-0-8 below. Room electricity and natural gas for heating had the highest share of the fuel in the clubhouse. The room electricity which is for appliances has a total reading of 19905 (kWh) while natural gas for heating and domestic hot water had a combined total of 19107.23 (kWh). The PV panels generated total energy of 21327.79 (kWh) in which the highest share of the energy was generated during May, June and July with readings of 4909.30 (kWh), 4848.64 (kWh) and 5142.61 (kWh) respectively.

Figure C2-0-8: Fuel breakdown results for the year 2018

Due to the share of energy used during the winter periods, the CO2 production results (Figure C2-0-9) revealed that the highest production of CO2 occurs during the winter periods with the highest reading being 2285.66 (kg) in January. However, due to the production of electricity during the summer periods, the CO2 production results become negative as from May with a reading of -410.34 (kg).

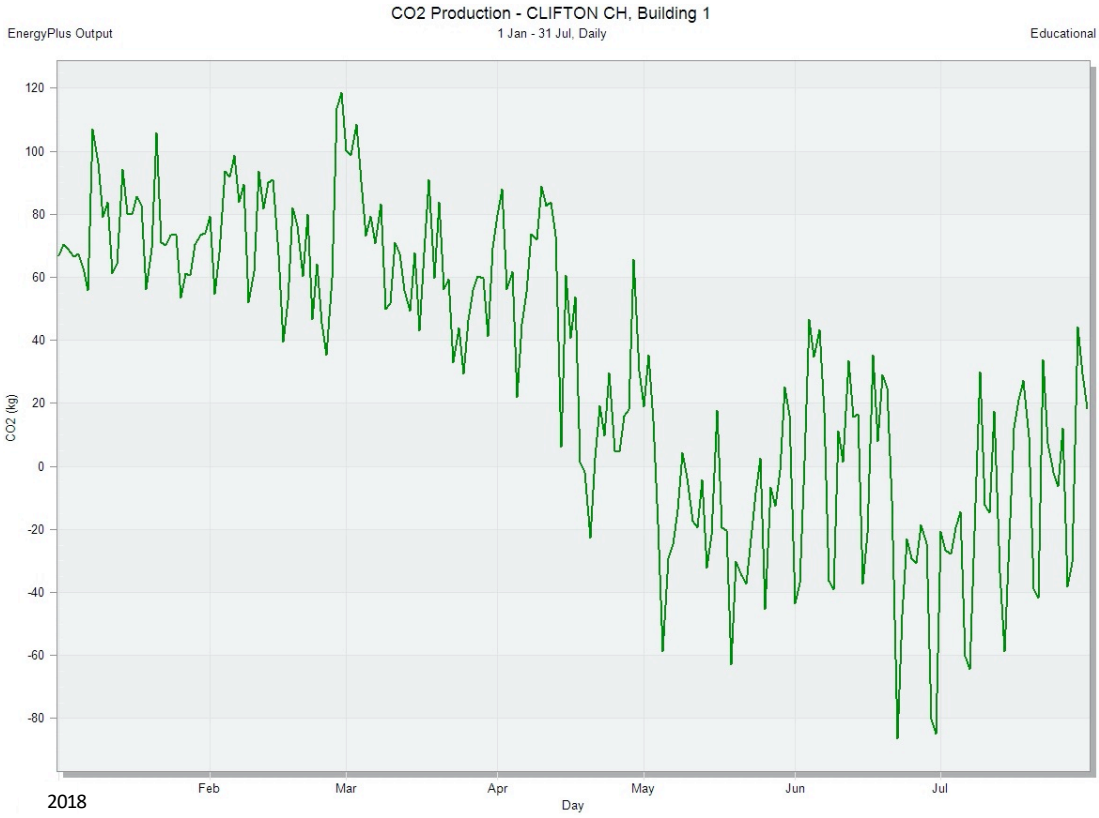

Figure C2-0-9: CO2 Production for the year 2018

Bibliography

Papers Presented by the author

- Galadanci, A. S., Ianakiev, A., Kromanis, R., & Robinson, J. (2020). Energy investigation framework: understanding buildings from an energy perspective view. *Journal of Building Engineering, 28.* https://doi.org/10.1016/j.jobe.2019.101046

Conferences Attended and Presented

- Galadanci, A.S. et al. (2018) 'Building Energy Investigation: Understanding buildings from an energy perspective view', *4th International Conference on Smart Energy Systems and 4th Generation District Heating (4DH)*, Aalborg, Denmark, 13th – 14th November 2018
- Energy Systems Conference 19th – 20th June 2018: Poster Presentation titled The Risk of Overheating in Buildings (A case study Clifton clubhouse)
- Nottingham Trent University, School of Architecture Design and Built Environment (ADBE) 2018 Conference:

Journal of Building Engineering 28 (2020) 101046

Contents lists available at ScienceDirect

Journal of Building Engineering

journal homepage: http://www.elsevier.com/locate/jobe

Energy investigation framework: Understanding buildings from an energy perspective view

Ahmad Said Galadanci [a,b,*], Anton Ianakiev [a], Rolands Kromanis [a,c], Julian Robinson [a]

[a] Nottingham Trent University, United Kingdom
[b] Bayero University Kano, Nigeria
[c] University of Twente, The Netherlands

ABSTRACT

A careful design and construction of energy efficient buildings is essential to reduce both the global energy consumption and carbon dioxide emissions. The desired outcome can be achieved by increasing the construction of low energy buildings, which are designed to sustain desired indoor temperature with a minimal energy input, and by improving the energy performance of existing buildings. Some buildings underperform by gaining or losing more heat than needed. This study introduces a framework for investigating building energy performance. Thermography investigation, building modelling, characterization of thermal bridges and future prediction for overheating are encapsulated in the proposed framework. A sport changing facility, which was designed as a low energy building, serves as a demonstrator for the application of the framework. The energy investigation framework revealed that the facility is underperforming. According to the building model, the main reason for the poor building performance is thermal bridging (presence of steel members), which increases gas consumption and wall heat-loss by 18% and 11%, respectively. Other contributors to heat lose/gain are cracks in the building envelop, weak mortar joints and uninsulated hot water pipes. Furthermore, the future temperature data, which is input to the building model, suggests that the entire facility is under the risk of overheating.

1. Introduction

According to the United Nations Global Status Report 2017, buildings and construction account for 36% of the global energy use and 39% of energy related carbon dioxide emissions [1]. The need to reduce greenhouse gas emissions and increase energy efficiency of buildings has grown in recent years. Effects of climate change can be observed with recent events such as wild fires in Greece and USA, record heat waves around the globe and a four week summer period in the United Kingdom without rain [2]. Researchers have argued that recent heatwaves may evince that the Earth is becoming very sensitive to warming [3]. Since the establishment of the climate change act in 2008, building regulations across the world have imposed restrictions for the thermal performance of building envelope. This has led to buildings being designed as low energy buildings, in which minimal energy input is required to sustain desired indoor temperature.

Low carbon policies and increasing costs of energy make society aware of the need for low energy solutions [4]. Around a third of the total energy demand comes from the domestic sector which is also responsible for 27% of all carbon emissions in the United Kingdom [4]. Clark [5] states that it is not an overstatement that designs of new buildings should be improved to reduce the energy consumption by 50–75%. High performance buildings would reduce significantly our nation's energy bill, contribute substantially to the environmental impact and climate change mitigations, and improve building indoor thermal conditions.

Well-designed building envelopes protect the inner space from harsh outdoor climatic conditions, both hot and cold, and provide the necessary thermal comfort for the building occupants. This is not necessarily the case in most buildings at present. Some buildings lose heat or gain unwanted energy from the envelope through thermal bridges in the structure. According to EN ISO 10211, a thermal bridge is a discontinuity regarding the thermal physical properties of the building envelop, with reference to the thermal resistance, due to material, thickness or shape variation. Thermal bridges are critical parts of a buildings overall structure or envelope. They are areas where the heat losses are usually higher than through external walls [6]. A thermal bridge is a discontinuity in thermophysical properties of the building envelope due to changes in the thermal resistance due to material thickness or variations of shape [7,8]. These are created in building envelopes by repetitive structural members and junctions between different building envelope components for example steel structural members in a brick clad building [9]. Al-Sanea and Zedan [10] stated that thermal bridges pose the highest threat to almost all measures taken by designers to reduce

* Corresponding author. Nottingham Trent University, United Kingdom.
E-mail address: ahmad.galadanci2013@my.ntu.ac.uk (A.S. Galadanci).

https://doi.org/10.1016/j.jobe.2019.101046
Received 13 June 2019; Received in revised form 29 October 2019; Accepted 31 October 2019
Available online 5 November 2019
2352-7102/